A STUDY OF THE USE OF COMBINED THERMAL AND MICROWAVE MODELLING OF BODY REGIONS FOR MICROWAVE THERMOGRAPHY.

Margaret Black Kelso, BSc,
Department of Physics & Astronomy,
University of Glasgow.

Presented for the degree of Doctor of Philosophy
to the University of Glasgow.

August 1995.

TABLE OF CONTENTS

page number

LIST OF FIGURES

LIST OF TABLES

ACKNOWLEDGEMENTS

This work was carried out whilst I was a student in the Department of Physics & Astronomy, University of Glasgow.

Firstly and most importantly, I would like to thank my parents for their long lasting financial support throughout the last 3 years, also Dr. D. V. Land for his help, advice and encouragement.

I would also like to thank the following people who have assisted me, Mr. A. Seath; Andrew and Gavin; Dr. Neil Abbot; Dr. Paul Harness; nursing staff and patients of wards 14/15 & the Rheumatology Clinic, Glasgow Royal Infirmary; Prof. Sturrock, Glasgow Royal Infirmary; and all the "volunteers" who have assisted throughout this period of research.

Last but not least, I would like to thank Eddie for all his help and encouragement.

Declaration.

This thesis has been composed by the undersigned. It has not been accepted in any previous application for a degree. The work of which it is a record has been done by myself, unless otherwise indicated in the text.

Margaret B. Kelso.

ABSTRACT

In medical applications of microwave thermography an apparent microwave temperature is obtained from a sample of the thermal radiation flux generated in body tissues and measured at the body's surface. The temperature variation over the human body reflects the effects of blood perfusion, metabolism and environmental temperature, therefore any disease which causes changes in the physiological properties of the human body also changes the measured microwave temperature and can be investigated using microwave thermography.

The Glasgow radiometer operates at a frequency of 3GHz where tissues are relatively transparent to electromagnetic radiation. The choice of measurement frequency strongly influences the lateral spatial resolution and depth of penetration of radiation. The equipment consists of three basic parts, a microwave antenna designed for operation in contact with the skin where it feeds the tissue thermal radiation signal to a measuring radio receiver. The received signal is passed through a signal processor to produce output information calibrated in degrees Celsius.

The tissue temperature distribution, T_t is assumed to be determined by a heat supply due to arterial blood perfusion, ω_b at T_{art}, and metabolic activity, Q, in total $\omega_b(T_{art} - T_t) + Q$, the tissue thermal conductivity and the region thermal boundary conditions. This tissue temperature distribution with the microwave propagation properties of the tissues determines the microwave radiation temperatures measured at the skin surface. By measuring the infra-red surface and microwave temperatures it is then possible to make estimates of the physiological heat supply to a volume of tissue.

Microwave thermography has been used for the objective assessment of inflammation in the knee joints and wrist and finger joints of patients suffering with rheumatoid arthritis by comparison with similar information obtained from a control group of subjects. Combined microwave and thermal modelling has been used to estimate the effective blood supply to the anterior intra-articular region of the patella, and the perfusion of the quadriceps muscle in both groups. 2-D numerical modelling was compared with results obtained using 1-D modelling.

Microwave thermography has also been used for the detection of breast cancer. However, problems such as high false positive detection rates have occurred due to natural cyclical breast temperature changes. The thermal behaviour of the normal breast throughout the menstrual cycle has been investigated and it is shown that microwave thermography is capable of detecting temperature variations in the female breast corresponding to the ovulatory and luteal phase of the menstrual cycle. Combined microwave and thermal modelling estimated the effective perfusion of the normal breast to be in the range $0.2 - \sim 2$ kg $m^{-3}s^{-1}$. This is consistent with previous work.

Microwave thermography is a quick, simple technique which clinicians can easily use. It is non-invasive, passive and causes the patient no distress. By using combined microwave and thermal modelling it is possible to estimate tissue blood perfusions and water contents and compare them with expected values. The technique has many potential applications and will hopefully find a secure niche in clinical medicine.

CHAPTER 1.0 GENERAL INTRODUCTION.

1.0 Introduction.

In general, detection and definition of medical conditions (diagnosis) requires the clinician to use his experience to bring together various disparate pieces of information - some subjective (pain, etc), some quasi-objective (history of symptoms), some objective (biochemical test, X-ray images). He will often have to make a differential diagnosis on the basis of incomplete or uncertain pieces of information. Therefore, there is clearly a need for more reliable clinical information in order to provide a greater chance of correct diagnosis. Objective measures giving clear information are the most useful.

An obvious aim should be to make maximum use of the information provided naturally by the body, thereby reducing the need for invasive techniques, which may have undesirable side effects (e.g. injection/ingestion of radio-active material). Body tissue temperature behaviour is "naturally" available information; is it possible to measure it non-invasively? Yes, by using infra-red and microwave thermography techniques, thermal images can be obtained. Thermal imaging can provide the clinician with an inherently safe, well tolerated, objective assessment technique.

Over the last 20 years thermal imaging techniques have proven to be useful in clinical medicine. The measurement of naturally emitted heat energy from the body is a non-invasive and inherently safe technique. Extensive studies have been performed on infra-red imaging techniques (Collins et al, 1974). However, this technique has a number of drawbacks

because the measurement of infra-red wavelength thermal radiation, emitted from essentially the skin surface, requires that for reproducible results, the environmental conditions must be very closely controlled. In comparison microwave radiation thermography uses a wavelength of approximately 10cm, so microwaves having a greater penetration depth than infra-red radiation, therefore information about internal body temperatures can be obtained.

Microwave thermography obtains information about the temperature of internal body tissues by a spectral measurement of the intensity of the natural thermally generated radiation emitted by body tissues. At lower microwave frequencies microwave radiation is able to pass through medically useful thicknesses of human tissue , up to a few centimetres, and therefore the subcutaneous temperature may be measured non-invasively. (Fig. 1.0) The temperature variation over the human body reflects the effects of blood perfusion, metabolism and environmental temperature therefore any disease which causes changes in physiological properties may be investigated using microwave thermography.

Microwave thermography is both an objective and a quantitative measure, it provides the possibility of assessing the degree or severity of disease activity, and monitoring of therapeutic intervention.

Throughout the last 10 - 15 years clinical studies using microwave thermography have included osteo-articular diseases, vascular disorders, diseases of the abdomen and cancers of the breast, thyroid and brain (Brown, 1989). A review of clinical microwave thermography is given in 1.5.

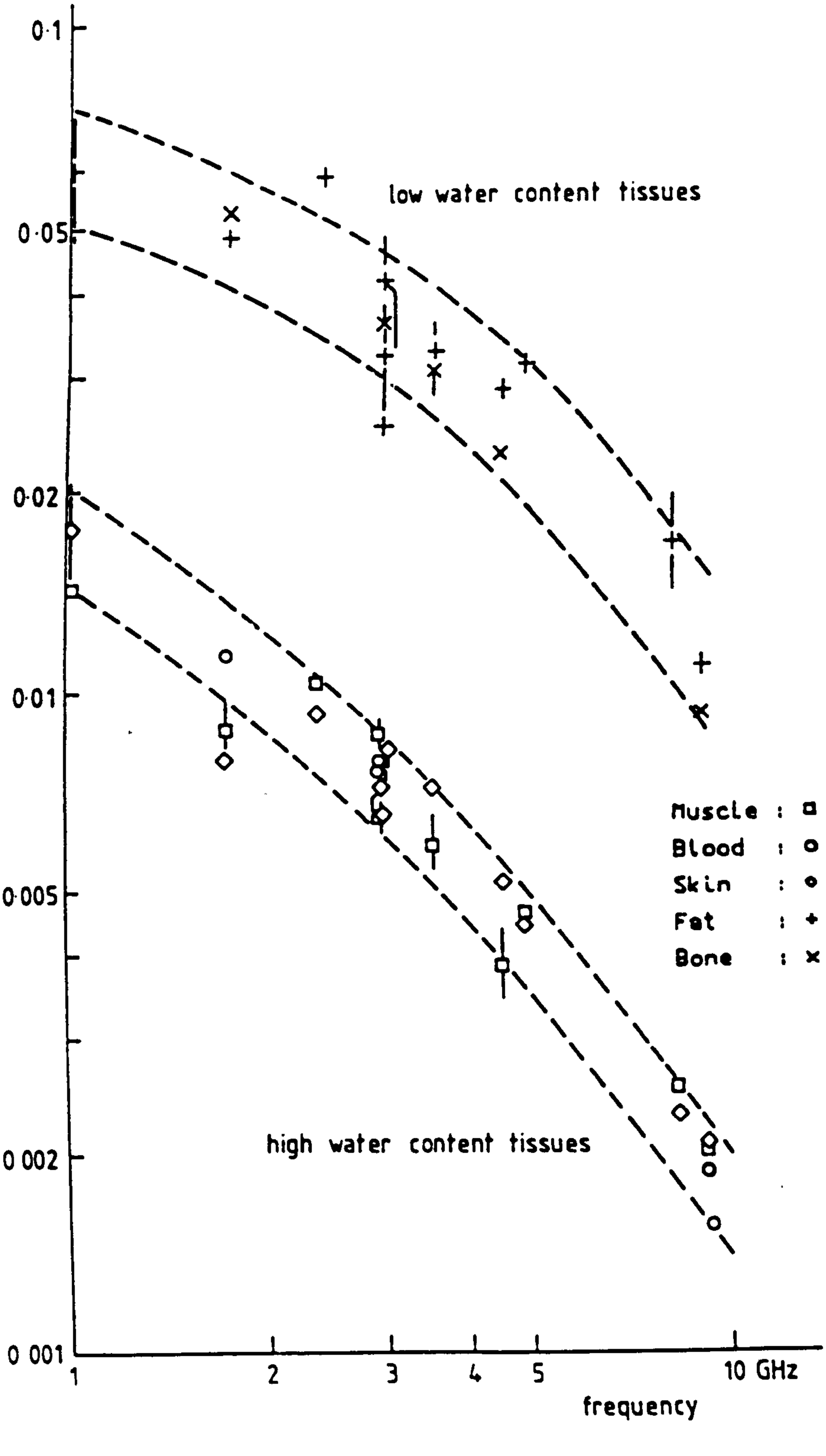

Fig. 1.0 Transmission of microwave radiation through body tissues.

The aim of this research was to determine the usefulness of using microwave thermography in a clinical environment on various body parts, and its ability to provide clinicians with useful information. The object of the knee work was to show that simple combined thermal and microwave radiation modelling may give a useful estimate of the blood supply to the anterior intra-articular region of the patella and the quadriceps muscle of both normal controls and in patients suffering from rheumatoid arthritis (RA). The increase in temperature over the knee joint has been shown to be due primarily to an increase in blood perfusion to the affected area. A 2-dimensional numerical modelling technique was developed by Dr. Paul Harness (UMIST, 1994), this model was compared with the 1 dimensional analytical and numerical models used previously. A pilot study was carried out at the Centre for Rheumatic Diseases, Glasgow Royal Infirmary, to assess the usefulness of microwave thermography for the monitoring and assessment of disease activity in the hand and finger joints of patients suffering from rheumatoid arthritis.

Finally the application of microwave thermography to the study of breast disease was considered. Variations in thermal and microwave properties in the breast during the menstrual cycle were investigated as this knowledge is essential if changes in the breast due to disease are to be detected. Combined thermal heat transport and microwave radiation modelling was used to estimate the effective perfusion in breasts.

This thesis is structured as follows. Chapter 1 gives an introduction to microwave thermography and discusses other imaging techniques. Basic principles behind microwave thermography are explained in Chapter 2.

Chapter 3 looks at tissue properties which affect microwave thermographic measurements. The microwave radiometer used in this work is described in Chapter 4. This is followed by a discussion of temperature distributions in the human body and combined modelling in Chapter 5. Chapters 6 & 7 look at the application of microwave thermography to the study of joint and breast disease and finally conclusions are considered in Chapter 8.

1.1 Introduction to blackbody radiation.

At all temperatures above absolute zero objects radiate energy in the form of electromagnetic waves by virtue of the thermal vibration of the electrical charges of the object material. This is "thermal radiation". Since a good absorber of radiation is a good emitter, it follows that the best emitter is a surface that is the best absorber. A surface which absorbs all the incident energy falling on it at all wavelengths is called a "black body" surface.

The intensity of the radiation from a black body is governed by Planck's radiation law, which is

$$B = \frac{2h\nu^3}{c^2} \frac{1}{e^{h\nu/KT} - 1} \qquad 1.1.1$$

where B is the intensity of radiation per unit wavelength, T is the absolute temperature and ν is the frequency of the radiation, h is Planck's constant, K is Boltzmann's constant and c is the velocity of light. Figure 1.1 shows that maximum emission of radiation occurs at around 10^{13} Hz for a surface at 300K.

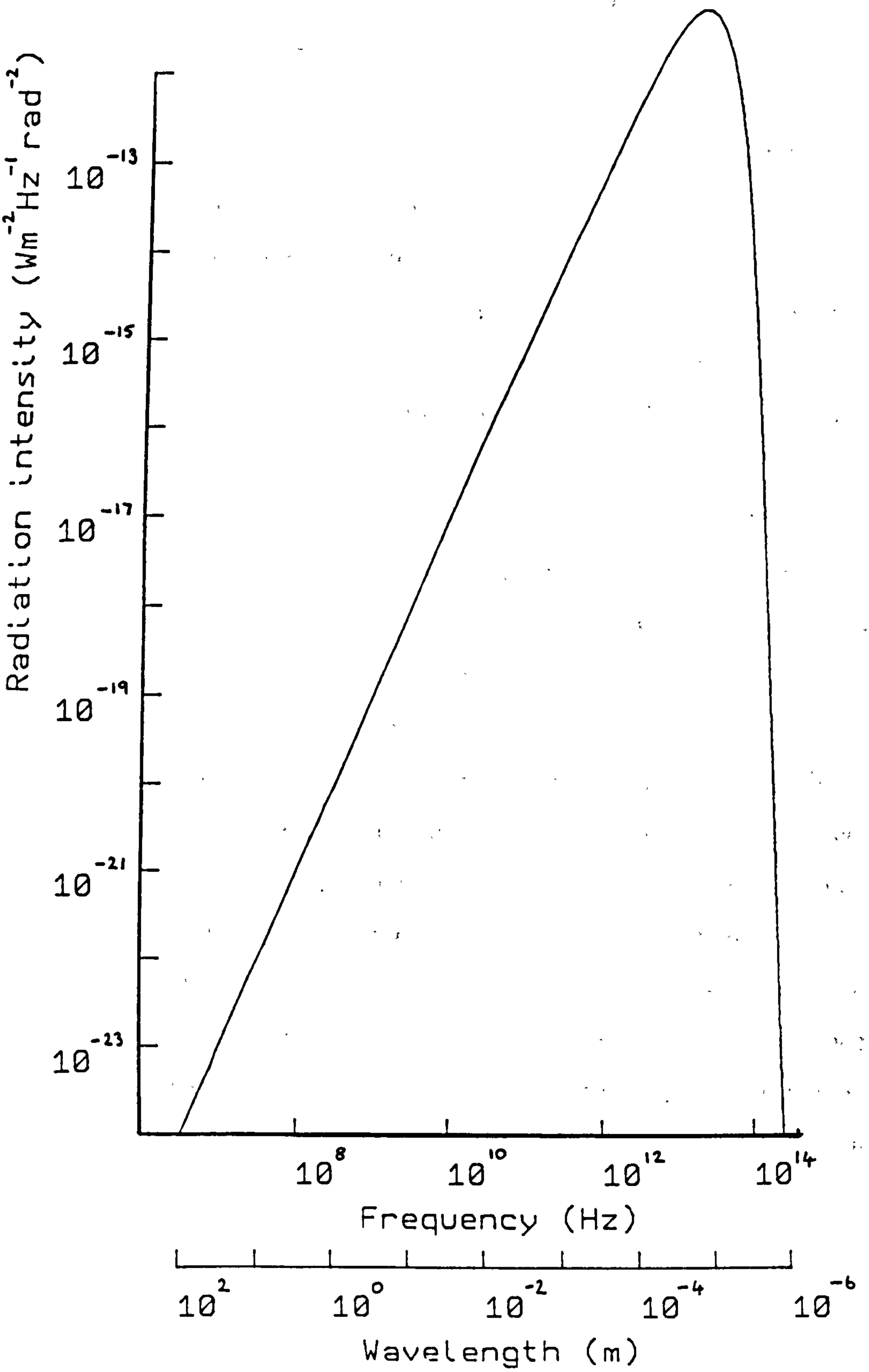

Fig. 1.1 Intensity spectrum of a black body at a temperature of 300K.

No surfaces are ideal black bodies, however the human body is an excellent radiator, therefore it follows that it must be a good absorber of radiation. Human skin has an emmissivity of ~ 0.98 (Mitchell, 1967). It can be assumed that the human body behaves very close to a black body in the wavelength range of (0.2 - 20)μm.

If the infra-red absorption of radiation takes place over a depth of tissue of the order of 0.1mm, so the emission of infra-red radiation is from this superficial layer of tissue, i.e. infra-red measurements give a surface temperature, which may or may not, through internal heat conduction, reflect body interior temperatures.

In contrast, the longer centimetric microwaves are absorbed over a depth of a few centimetres, and so are emitted from tissues extending in from the skin surface of a similar distance, i.e body tissues can be thought of as being modestly transparent to centimetric microwave radiation, so that some of the microwave component of the thermal radiation, generated by internal tissues, reaches the surface where it can be measured. The body can be considered to have a "microwave temperature" at the skin surface, and through the partial transparency of the tissues this will provide some information about internal, as distinct from superficial tissue temperatures.

Human tissue properties are such that for medical applications the optimum measurement frequency is approximately 3GHz, 10cm free space wavelength, at which frequency temperature pattern information can be obtained for tissues at clinically useful depths of several centimetres within the body and a thermal pattern resolution at the surface of 1 - 2 cm. Figure

1.0 shows the general form of the transmission of microwave radiation through body tissues.

The tissue attenuation constant for the microwave radiation gives the measure of the depth within the body from which useful temperature information can be obtained. The attenuation constant is defined as the thickness of tissue which will absorb e^{-1} or 37% of the power incident plane wave radiation. Because of the resonant absorption of microwave radiation by the polar water molecule at about 26GHz, tissue water content determines the radiation attenuation constant. Fat and bone have a low water content and so have a lower power attenuation constant, whereas , high water content tissue such as muscle and skin have a higher attenuation constant.

1.2 Microwave thermography equipment.

The radiometer used in this study operates at a frequency of 3GHz where tissues are relatively transparent to electromagnetic radiation. As mentioned above the spatial resolution is about 10mm to 20mm, and tissue radiation transmission distances are about 10mm to 40mm. These values are well suited to the examination of major articulations and breasts, but are larger than optimum for the smaller dimensions of the finger. This will be discussed further in Chapter 6. The equipment consists of three basic parts;a microwave antenna designed for operation in contact with the skin which feeds a tissue thermal radiation signal to a measuring radio receiver. The received signal which is a result of the summation of the emitted radiation at all interior points reduced by a weighting factor taking into

account the tissue microwave attenuation is then passed through a signal processor to produce output "microwave temperatures" calibrated in degrees Celsius. Skin surface temperature measurements were made using a commercial pyroelectric element infra-red thermometer. Measurement data was recorded using a small computer.

1.3 Background of thermometry.

The correlation between disease and an increase in body temperature was accepted as for back as 400 a.c when Hippocrate used his hand as a thermometer when assessing patients. In 1595 Gallilei in Pisa devised the thermometer but it was not widely used until 1612. Fahrenheit's scale of temperature was adopted in 1708 followed by the centigrade scale in 1742. Throughout the 1800's the thermometer was used for many studies and by 1870 it was an accepted measure in medical circles.(Solonsa et al, 1978)

Skin temperature is a reflection of the state of the vascular system, so diseases of the vascular system often result in regional or local temperature changes. The diseases under investigation in this thesis being rheumatoid arthritis and breast disease. Both of these conditions resulting in an increase in temperature over the affected area. The remainder of this chapter will look at various clinical imaging techniques currently in use throughout the medical world at present and a review of microwave thermography will be given in 1.5.

1.4 Imaging techniques.

The following techniques are probably the most widely used in clinical medicine.

- Infra-red thermography

Infra-red thermography detects the infra-red radiation being emitted from the skin, and can be used to quantify changes in blood flow and inflammation in limbs and joints. This technique is also used to evaluate and monitor disease activity.

- Conventional X-ray imaging

When a beam of X-rays pass through the human body, the X-rays are differentially attenuated according to the physical nature of the material. The X-ray beam is altered in two ways as it passes through the body. Energy is absorbed from the beam into the tissue of the subject. The beam is then differentially attenuated according to the thickness, atomic number and density of the material in its path. The radiation interacts with the body tissue by photoelectric absorption and Compton scattering.

Possible hazardous effects of radiation on living tissue however means that it is essential to obtain the required information with the lowest X-ray dose possible.

- X-ray computed tomography

The change in tissue density and hence absorption of the X-rays can provide a technique with an estimated resolution of 1C. (Fallone et al, 1982)

- Ultra-sound-coded doppler imaging

Ultrasound is used to obtain information from within the body about the movement of structures and about the flow of blood. A shift in frequency is observed by a receiving transducer when a moving target scatters or reflects ultrasound from an isonifying beam. The doppler shifted information associated with a specific location can be detected and displayed as an image.(Duck, F.A, 1989)

- Nuclear magnetic relaxation imaging

In nuclear magnetic relaxation imaging the tissue temperature depends on the nuclear magnetic relaxation mechanism for moments in a static magnetic field involving thermal interactions with the surrounding environment.

- Multiple Gamma ray imaging

The spatial distribution in the body of gamma-ray emitting injected or ingested radionuclides can be measured by an array of radiation detectors forming a "gamma camera". Modern gamma cameras are provided with two or three energy channels so that simultaneous images of different radio nuclides can be obtained. A problem however is the withdrawal, manipulation and re-injection of blood components involve hazards to both the patient and the radio pharmacist. The spatial resolution of the technique is relatively poor.

- Microwave thermography

Microwave thermography is the technique of observing the natural thermal radiation emitted from body tissues at centimetric wavelengths to obtain

information about internal body temperatures. The technique will be discussed further in the following chapters.

1.5 Review of Microwave radiometry for medical applications.

Research into the clinical use of microwave radiometry began 20 years ago when Enander and Larsen (1974) measured temperatures regions of the abdominal cavity inside the human body using a system which operated in the frequency band 0.9 - 1.2 GHz. A loop contact antenna was used for this application. They concluded that "measurements of this type may have applications in medicine for diagnostic purposes". Approximately 4 years later Ludeke, Schiek and Kohler (1978) published a paper describing an improved radiometer that they had developed which was capable of measuring physical microwave temperature independently of any mismatch between the radiation emitting object and receiving antenna. Also in 1978, Edrich and Smyth were investigating the new technique of remote sensing at centimetre and millimetre wavelengths. This solid state scanner operated at 68GHz and had a temperature resolution of 0.25C. They concluded that this system was capable of distinguishing between normal knees and knees affected with rheumatoid arthritis and that it could be used to monitor the effectiveness of drug treatments that patients were receiving. In 1980, Edrich, Jobe et al published findings from research carried out on the use of the remote scanning system for the detection of breast cancer, arthritis and scanning of the head and neck region. They suggested that the long wavelength

thermography may be suited for the detection of thermally active brain tumours.

Barret, Myers and Sadowsky (1980) performed a breast cancer detection study of approximately 5000 patients using microwave thermography. The equipment operated at wavelengths of 23cm and 9.1cm and was used to examine 1000 and 4000 patients respectively. In addition each patient underwent infra-red thermography, mammography and clinical examinations. By using statistical analysis techniques they decided that the most effective detection criteria was to determine the maximum temperature difference between symmetrically opposite points on the right and left breast. Unfortunately at a wavelength of 23cm they discovered that this detection criteria was ineffective. The performance of the above systems indicated that microwave thermography at a wavelength of 23cm has true-positive and true-negative detection rates of 0.8 and 0.6 respectively for this application and detection criteria. This result is similar to infra-red thermography (0.7), but is less than xeromammography (0.9). They also noted that the microwave and infra-red imaging techniques disagreed in 41% of the cancer cases.

In 1983, Mamouni, Leroy, Van de Velde and Bellarbi proposed a new microwave technique known as correlation microwave thermography. This technique will be briefly described. Two identical radiometer channels and antennas are used. Both antennas viewing a common volume of tissue inside the body. Now since the signal in each channel is composed of two components, one from the common region and the other from the rest of the antennas field of view it is possible to separate the

common component out. The radiometric signal received will then be due to a signal originating at a depth inside the body. It is possible to change the depth viewed inside the tissue by altering the relative orientation of the antennas. Using this technique they hoped to improve the processes of localisation of the thermal gradients in living tissues.

Iskander and Durney (1983) decided to investigate the use of microwaves in measuring changes in lung water content as techniques available to measure such changes lacked either the reliability or sensitivity to monitor early changes in water content. The techniques they stated were also "elaborate, expensive and impractical for clinical use". They looked at two methods. The first was based on measuring changes in the phase of an active microwave signal transmitted through the thorax- the frequency band being 700MHz - 1.5GHz. The second technique being based on measuring the natural radiation emitted by the body. They constructed a 1GHz Dicke radiometer and made measurements on phantoms to further demonstrate the usefulness of the radiometer for measuring changes in lung water content.

In 1987, Abdul Razzack and colleagues built a scanning microwave thermograph operating in the frequency band, 9 - 10 GHz. This system produces a video display of the variations in the emission temperature of the human body. To assess the clinical usefulness of the system studies were carried out at St. James Hospital, Leeds in the Vascular Surgery Department. It was concluded that the technique is accurate in the detection of occlusive vascular disease and may provide useful information

in the investigation of patients with occlusive disease and especially in the prediction of amputation levels.

Also in 1987 Fraser, Land and Sturrock carried out an investigation into the use of microwave thermography as an index of inflammatory joint disease in patients suffering with rheumatoid arthritis. Fifty-two knees affected were scanned and a microwave thermographic index was calculated for each knee. A strong correlation was found between the microwave thermographic index and the clinical and laboratory parameters measured.

Marr, 1992, carried out an investigation to determine whether microwave thermography could be used for the investigation of injury of the superficial digital flexor tendon in the horse. The microwave radiometer used in this investigation was developed by Land (1987). Microwave profiles were recorded from 77 normal horses. These profiles could be separated in specific profile types. In 48 horses with acute injury of the superficial digital flexor tendon and 12 horses with acute injury of the soft tissues of the palmar meta-carpal region, it was found that an elevation of temperature was present over the injured areas.

Another use of microwave thermography was investigated by al-Alousi et al, 1994 in which they used the system to estimate the time after death. Using the microwave radiometer they were able to measure temperatures of internal organs of the body by placing the antenna on the skin, therefore estimating the time of death. This method provides an ethical, non-invasive technique for determining such a measurement.

McDonald et al, 1994, carried out a study to determine the usefulness of microwave thermography as a non-invasive assessment of disease activity in inflammatory arthritis. The equipment used was again developed by Land(1987). This study confirmed previous work suggesting that microwave thermography may well be a useful tool for the assessment of local joint disease.

Clinical studies of the application of microwave thermography continue at several centres in the UK and other European countries. The microwave thermography group at the University of Glasgow continues to carry out clinical investigations to consider the usefulness of microwave thermography in rheumatology, oncology, gastro-enterology as a diagnostic aid for heat producing disease. However, microwave thermography "has yet to find a secure niche in the medical world".(Foster and Cheever, 1992).

CHAPTER 2.0 BASIC CONCEPTS OF RADIATION THEORY.

2.0 Introduction.

This chapter discusses the basic principles on which the technique of microwave thermography is based.

2.1 Definition of terms.

The amount of radiant power, dW, in a specified frequency window or bandwidth, $d\nu$ which is transported across an element of surface area, $d\sigma$ and in directions confined to an element of solid angle $d\Omega$ is given below. The specific intensity, I_ν, is related to this radiant power, dW by

$$dW = I_\nu Cos\theta d\Omega d\sigma d\nu \qquad 2.1.1$$

where θ is the angle between normal to $d\sigma$ and $d\Omega$.

Radiation is commonly defined in terms of spectral intensity, I, or specific intensity, I_ν. Specific intensity refers to the combined radiation emitted at all frequencies whereas spectral intensity refers to radiation emitted in a specified radiation window. Quite often the term "brightness" is used instead of intensity.

In microwave thermography it is the spectral intensity in a limited range of frequencies of the microwave region of the electromagnetic spectrum which is important.

2.2 Black body radiation.

As previously explained in Chapter 1, at temperatures above absolute zero all objects radiate energy in the form of electromagnetic waves. In 1859 Kirchoff showed that a good absorber of radiation is also a good emitter. Absorption occurs when there is a transfer of energy to matter from radiation passing through matter. The process of a body losing energy to its surroundings by radiation is known as emission. A perfect absorber is known as a blackbody, and so it must also be a perfect emitter. A black body is one which absorbs completely any radiation reaching it and reflects none. It remains in equilibrium with the radiation reaching and leaving it, and at a given steady temperature emits radiation with a flux density and spectral energy distribution which are characteristic of that temperature and is described by Plank's radiation formula.

$$B_\nu(T) = \frac{2h\nu^3}{c^2}\frac{1}{e^{h\nu/KT} - 1} \qquad 2.2.1$$

where $B_\nu(T)$ is the power per unit frequency emitted per unit area of radiating surface at absolute temperature T, (brightness), normal to that surface, ν is the frequency, h is Planks constant, K is boltzmanns constant and c is the velocity of light.

At frequencies $\frac{h\nu}{KT} << 1$, the plank function can be simplified to the Rayleigh -Jeans relation

$$B = \frac{2h\nu^3}{c^2}\frac{KT}{h\nu} = \frac{2KT\nu^2}{c^2} = \frac{2KT}{\lambda^2} \qquad 2.2.2$$

So according to the Rayleigh-Jeans radiation law, the Intensity varies inversely as the square of the wavelength.

2.3 Radiative transfer.

If the specific intensity, I_ν changes, it can do this only by the absorption or emittance of radiation. This change of specific intensity is described by the *equation of transfer*, Eqn. 2.4.5.

2.3.1 Absorption.

If a pencil of radiation passes through a material it will be reduced by its interaction with the matter. It follows that the specific intensity, I_ν becomes $I_\nu + dI_\nu$, after passing through a distance dz of the material therefore

$$dI_\nu = -k_\nu \rho I_\nu dz \qquad 2.3.1.1$$

where ρ is the density of the material, k_ν is the mass absorption coefficient for radiation at a frequency, ν.

2.3.2 Emission.

The amount of radiant energy emitted by an element of mass, dm in directions confined to an element of solid angle $d\Omega$, in the frequency interval ν to $\nu + d\nu$ in a time dt is given by

$$j_\nu dm d\Omega d\nu dt \qquad 2.3.2.1$$

where j_ν is the emission coefficient.

2.4 Equation of transfer.

In order to develop the equation of transfer the source function must be defined as the ratio of the emission to absorption coefficients

$$S_\nu = \frac{j_\nu}{k_\nu} \qquad 2.4.1$$

The equation of transfer governs the loss of intensity due to absorption and the gain in intensity from emission.

Considering a small cylindrical element of cross section $d\sigma$, length dz which has a radiation intensity I_ν incident in the z-direction on one face and $I_\nu + dI_\nu$ emerging from the second face in the same normal direction. It follows that both faces will absorb and emit part of the incident radiation.

The amount of radiation absorbed is given by

$$k_\nu \rho dz I_\nu d\nu d\sigma d\Omega dt \qquad 2.4.2$$

and the amount emitted is

$$j_\nu \rho d\sigma dz d\nu d\Omega dt \qquad 2.4.3$$

So the total change in the radiation during its traversal of the cylinder is given by

$$\frac{dI_\nu}{dz} = -k_\nu \rho I_\nu + j_\nu \rho \qquad 2.4.4$$

Using Eqn. 2.4.1, the above equation becomes

$$-\frac{1}{k_\nu \rho}\frac{dI_\nu}{dz} = I_\nu - S_\nu \qquad 2.4.5$$

This is the *equation of radiative transfer*.

2.5 Formal solution to the equation of transfer.

The formal solution to Eqn. 2.4.5 is given as

$$I(z) = I(0)e^{-\tau(z,0)} + \int_0^z S_\nu(z')e^{-\tau(z,z')}k_\nu \rho dz' \qquad 2.5.1$$

where $\tau(z,z')$ is known as the optical thickness of the material between the points z and z' and is given by

$$\tau(z,z') = \int_z^{z'} k_\nu \rho dz \qquad 2.5.2$$

From Eqn. 2.5.1 it follows that the intensity at any point in a given direction is the summation of the emitted radiation at all anterior points, z',

reduced by a factor $e^{-\tau(z,z')}$, which allows for absorption by the intervening material.

2.6 Equation of radiative transfer in relation to the human body.

In relation to the human tissue, Eqn. 2.5.2 can be rewritten as

$$\tau(z,z') = k_{,}\rho(z-z') \qquad 2.6.1$$

due to the uniform density of tissue.

It follows that Eqn. 2.5.1 can be written as

$$I(z) = I(0)e^{-k_{,}\rho z} + \int_0^z S_{,}(z')e^{-k_{,}\rho z'}k_{,}\rho dz' \qquad 2.6.2$$

By comparing Eqn 2.6.2 with the solution to the wave equation obtained for a wave propagating in a material with conduction or dielectric absorption losses, Eqn. 3.2.1.5, it is clear that

$$k_{,}\rho = 2\alpha \qquad 2.6.3$$

where 2α is the radiation power attenuation constant determined by the dielectric properties of tissue.

By considering the human body to be in thermal equilibrium when at rest in a room at constant temperature, it can be assumed that *Kirchoffs law* holds

$$\frac{j_\nu}{k_\nu} = S_\nu = B_\nu(T) \qquad 2.6.4$$

where $B_\nu(T)$ is the Plank function, Eqn. 2.2.1, and S_ν is the source function, Eqn. 2.4.1.

However, as shown earlier the Planck function simplifies to the Rayleigh-Jeans relation, Eqn. 2.2.2, at microwave frequencies, so Eqn. 2.6.2 becomes

$$I(z) = I(0)e^{-2\alpha z} + \frac{2\nu^2 K}{c^2}\int_0^z 2\alpha T(z')e^{-2\alpha z'}dz' \qquad 2.6.5$$

The physical meaning of Eqn. 2.6.5 is that the microwave temperature observed on the skin surface is a result of the summation of the emitted radiation at all interior points reduced by a weighting factor of the form $e^{-2\alpha z}$ which takes into account the tissue microwave attenuation factor. However, it should be noted that Eqn. 2.6.5 is for a single material region and does not include surface emissivity, due to material discontinuity.

The resultant intensity from several different regions e.g. skin, muscle and fat can be calculated by a simple extension of Eqn. 2.6.5 taking into account the inter-regional reflections due to impedance changes and signal attenuation across different tissue regions giving

$$I(z) = \frac{2\nu^2 K}{c_1^2}\int_0^{t_1} 2\alpha_1 T(z)e^{(-2\alpha_1 z)}dz + \frac{2\nu^2 K}{c_2^2}e^{-2\alpha_1 t_1}\int_{t_1}^{t_1+t_2} 2\alpha_2 T(z)e^{-2\alpha_2 z}dz + \cdots\cdots$$

2.6.6

where α_1, α_2 are power attenuation constants. Theoretical modelling of radiometer antenna spatial response shows a more complex behaviour than Eqn. 2.6.6 close to the antenna, but experimental measurements have shown that the dominant features of the response are of this form, (Land, 1987 & Mamouni, 1988).

If the temperature, T, is uniform throughout the material the intensity emitted by a homogeneous piece of thickness, d is given from Eqn. 2.6.6 to be

$$\frac{2\nu^2 KT}{c^2}(1-e^{-2\alpha z}) \qquad 2.6.7$$

Now if the optical depth is large (αz is large), If follows that the intensity emitted is approximately equal to that emitted by a black body at the same temperature (Eqn. 2.2.2). On the other hand if $\alpha z << 1$, the intensity emitted is of the approximate form

$$\frac{2\nu^2 KT}{c^2}2\alpha z \qquad 2.6.8$$

and is less than that emitted by a black body at the same temperature.(Brown, 1989)

2.7 Antenna response function.

In 1928 Nyquist showed that the noise power per unit bandwidth at the terminals of a resistor, R, and temperature, T, is given by

$$W=KT \qquad 2.7.1$$

where W is the spectral power per unit bandwidth, K is boltzmanns constant and T is the absolute temperature of the resistor.

If the resistor is replaced by a lossless antenna of radiation resistance, R, in contact with a lossy material of the same impedance and is connected to a terminating resistor of a lossless transmission line then the terminating load radiates an average power of KT watts per unit bandwidth through the transmission line and into the lossy material if the system is in thermal equilibrium. If this condition holds then the antenna must also receive KT watts per unit bandwidth from the lossy material. However if the antenna, transmission line and load are not in thermal equilibrium with the lossy medium the antenna must still receive the same power per unit bandwidth. The power per unit bandwidth, P, received by the antenna can be expressed as

$$P=\frac{1}{2}\int_V I_v(\underline{r})P_n(\underline{r})dV \qquad 2.7.2$$

where $I_v(\underline{r})$ is the intensity of radiation at a position $\underline{r}$, with origin at the position of the antenna. $P_n(\underline{r})$ is the normalised power response pattern of the antenna given by

$$P_n(\underline{r})=\frac{P(\underline{r})}{P(\underline{r})_{\max}} \qquad 2.7.3$$

where $P(\underline{r})$ is the relative antenna power pattern and $P(\underline{r})_{max}$ represents the maximum power response pattern of the antenna (Kraus, 1961).

Any antenna is responsive to only one polarisation component, so since thermal radiation is of an incoherent, unpolarized nature, only half of the total incident power is present in Eqn. 2.7.2.

For a radiating antenna, the propagation power density of the wave is given by

$$P = \frac{1}{2}\frac{E_0^2}{\varsigma} \qquad 2.7.4$$

where E_0 is the electric field strength and ς is the intrinsic wave impedance.

The noise power per unit band width received by the antenna is then given by

$$p = \frac{\nu^2 K}{c^2} A \int_V 2\alpha T(\underline{r}) |E(\underline{r})|^2 dV \qquad 2.7.5$$

for an impedance matched, uniform material.

The reciprocity theorem (Slater, 1942) provides a way of measuring the normalised power response pattern. The theorem states "that if there is a four terminal network, which may include radiation as part of its elements, and a given voltage impressed on two of the terminals produces a given current at the other two, then the same voltage impressed on the second set of terminals will produce the same current on the first set. When

discussing a system of two antennas, each with its two terminals, the theorem is used to compare the radiation from the first antenna toward the second, and the radiation from the second toward the first." Following the above argument the transmitting and receiving power patterns of an antenna must be identical. Therefore the power dissipated in an element when an antenna is radiating into the lossy medium is proportional to the power received from that element when the antenna is receiving. The power dissipation density is thus given by

$$P = \frac{1}{2}\sigma E_0^2(\underline{r}) \qquad 2.7.6$$

where σ is the conductivity ($\Omega^{-1}m^{-1}$) and $\underline{E} = \underline{E}_0 e^{i\omega t}$ is the electric field.

So by reciprocity the power response pattern must be proportional to the power dissipation density, Eqn. 2.7.6 which gives

$$P_n(\underline{r}) = A|\underline{E}(\underline{r})|^2 \qquad 2.7.7$$

where A is a constant of proportionality.

Considering Eqn. 2.6.8 the intensity of radiation emitted by a small thickness, dz of homogeneous material is given by

$$I_\nu(\underline{r}) = \frac{2\nu^2 KT(\underline{r})}{c^2} 2\alpha dz \qquad 2.7.8$$

By substituting Eqns. 2.7.7 and 2.7.8 into Eqn. 2.7.2, the power per unit bandwidth received by the antenna can be expressed as (Eqn 2.7.5)

$$p = \frac{v^2 K}{c^2} A \int_V 2\alpha T(\underline{r}) |E(\underline{r})|^2 dV \qquad 2.7.5$$

for an impedance matched, uniform material.

From thermodynamical considerations the power received per unit bandwidth is equal to KT thus Eqn 2.7.5 can be written as

$$\frac{v^2 2\alpha}{c^2} A \int_V |E(\underline{r})^2| dV = 1 \qquad 2.7.9$$

In general for a lossy material, it is difficult to determine theoretically the distribution of $E(\underline{r})$. However, the antenna pattern may be described approximately by an exponential variation in the direction of the central axis of the antenna in a single region of tissue. The effect of the varying lateral response, over an area slightly greater than that of the antenna, is often removed by considering the viewed temperature pattern to be uniform over this area.

Because of the above reciprocity relationship, "active" field measuring techniques can be used to find the weighting functions of practical antennas:

1. by field sensing with a very small probe, essentially a small antenna (Mamouni, 1988).

and

2. by field perturbation by small conducting or dielectric objects (Land, 1988).

Both these techniques have been used to measure dielectric phantom materials with properties simulating body tissues. A further discussion of the antenna response function is given in Chapter 4, section 4.5.2.

CHAPTER 3.0 DIELECTRIC PROPERTIES OF BIOLOGICAL TISSUE.

3.0 Introduction.

In this chapter a brief outline of the processes which give rise to the absorption of energy from microwave radiation propagated in biological materials will be given. In the microwave region of the electromagnetic spectrum body tissues behave as lossy dielectric material. However biological tissue is a complex mixture of water, ions and membranes, so prior to the discussion of tissue dielectric properties, tissue structure and composition will be discussed.

3.1 Biological tissue structure.

Within the human body, biological tissues consist of cells which have undergone various developments in order to perform different functions. Cells consist of a mass of protoplasm which contains proteins, polysaccharides, nucleic acids and lipids which are bound by a delicate membrane. Molecules of the protoplasm are suspended in intra-cellular electrolyte. Cells are suspended in an aqueous environment of intercellular electrolyte. Intracellular water contributes approximately 67% of the body total water content, intercellular fluid 25%, and the remaining 8% is accounted for by plasma (extra cellular). These fluids are basically electrolytic solutions. However, the fluids differ in that plasma and intercellular water may be treated as 0.9% sodium chloride, NaCl, solution, where as the intracellular water has a high concentration of potassium ions. In contrast to fat and protein,

water has strong dielectric properties and thus dominates the dielectric behaviour of tissues.

3.2 Behaviour of electromagnetic radiation in lossy dielectric material.

The behaviour of electromagnetic radiation in a dielectric depends on the electrical conductivity, σ (Sm^{-1}), and the dielectric constant, ε (Fm^{-1}). The permittivity or "dielectric constant" of a material is a measure of the extent to which the electric charge distribution in the material can be 'distorted' or polarized by the application of an electric field. The displacement of charges within the atoms or molecules of a dielectric makes each atom or molecule a dipole with a particular moment, $\underline{p}$. If $\underline{p}$ is the average dielectric dipole moment per molecule in a small volume, τ and N is the number of molecules per unit volume, then

$$\underline{P} = N\underline{p} \qquad 3.2.1$$

In other words, the electric polarization , $\underline{P}$, is the dipole moment per unit volume at a given point (Corson & Lorrain). At radio/microwave frequencies the use of a complex dielectric constant is common as in this frequency band a phase lag between the field and the dipole orientation develops, and energy is drawn from the electrical source by the material and is dissipated as heat. This is dielectric loss. The complex dielectric constant can be written in terms of real and imaginary parts

$$\varepsilon = \varepsilon' - i\varepsilon'' \qquad 3.2.2$$

where $\varepsilon^{'}$ is the "relative permittivity" and $\varepsilon^{''}$ the loss factor.

The loss tangent of a dielectric material is defined to be

$$\tan\delta = \frac{\varepsilon^{'}}{\varepsilon^{''}} = \frac{\sigma}{\omega\varepsilon} \qquad 3.2.3$$

where σ is taken to be the equivalent conductivity for all loss forms.

At electrolyte concentrations found in body tissues, the equivalent conductivity for dielectric power loss in water by the Debye relaxation process is similar to the electrolytic ionic conductivity at the lower microwave frequencies . (Land, 1987). The water dielectric constant is nearly constant close to its low frequency value and so a pronounced minimum occurs of the electrolyte loss tangent at about 3GHz for electrolyte temperatures of 35 - 37C. In body tissue, since conductivity and dielectric constant tend to show similar variations with water content, tissue loss tangents can be expected to show a similar minimum. Fig. 3.0 shows the variation of loss tangent of human tissue at 37C at microwave frequencies. From this figure a pronounced minimum in the loss tangent at 3GHz can be seen.

3.2.1 Wave propagation in a lossy dielectric.

By considering a time harmonic plane-wave propagating along the z-axis in an infinite, homogeneous, isotropic, linear medium a wave equation can be deduced using Maxwell's equations. In a material with dielectric losses, $\sigma > 0$ and so Joule heating occurs and the wave energy decreases. To obtain the wave equation the following Maxwell Equations are used:

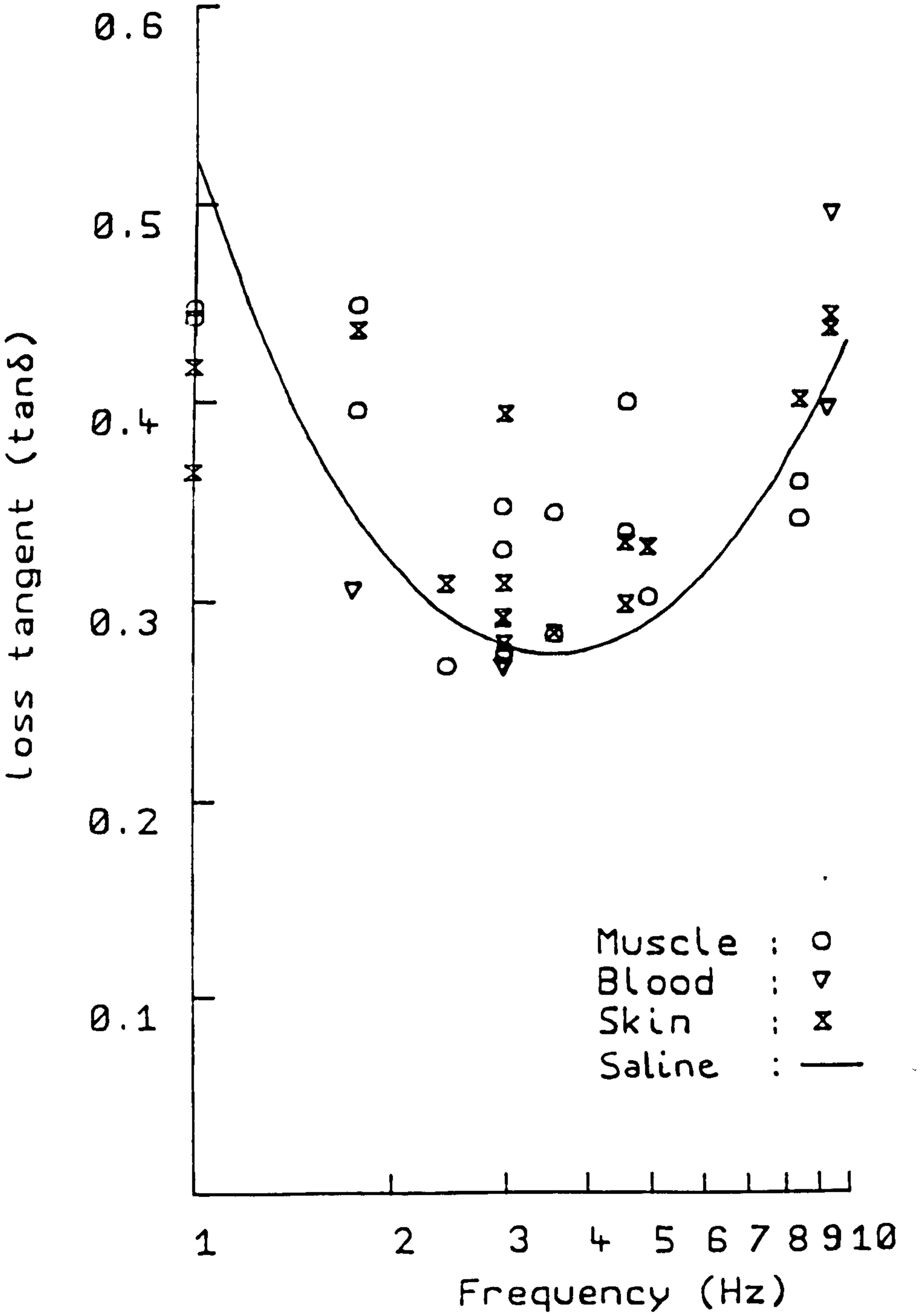

Fig. 3.0 Variation of loss tangent of human tissues at microwave frequencies at 37C (from Brown, 1989).

Maxwell 3:

$$Curl\underline{E} = -i\omega\mu_0\underline{H} \qquad 3.2.1.1$$

Maxwell 4:

$$Curl\underline{H} = \sigma\underline{E} + i\omega\varepsilon\underline{E} \qquad 3.2.1.2$$

This gives the Helmholtz wave equation

$$\nabla^2\underline{E} = \mu_0\sigma\frac{\partial\underline{E}}{\partial t} + \mu_0\varepsilon\frac{\partial^2\underline{E}}{\partial t^2} \qquad 3.2.1.3$$

where the first term on the left hand side is the damping term of the power loss to the material (Corson & Lorrain). The solution to Eqn 3.2.1.3, split into its real and imaginary parts, can be written as

$$\gamma = \frac{\omega\sqrt{\mu\varepsilon}}{\sqrt{2}}\left[\sqrt{1+\left(\frac{\sigma}{\omega\varepsilon}\right)^2}+1\right]^{1/2} \qquad 3.2.1.4$$

with the imaginary part, α given by

$$\alpha = \frac{\omega\sqrt{\mu\varepsilon}}{\sqrt{2}}\left[\sqrt{1+\left(\frac{\sigma}{\omega\varepsilon}\right)^2}-1\right]^{1/2} \qquad 3.2.1.5$$

The imaginary part is the field attenuation constant mentioned in section 2.6.3 and is related to the power penetration depth by Eqn 4.5.2.1. In a perfect dielectric $\sigma = 0$, so there is no attenuation of the wave. The real part is then equal to $2\pi/\lambda$ where λ is the wavelength in the material.

Considering the dielectric properties of tissues at the frequencies of interest, Eqn. 3.2.1.5, can be approximated to by

$$2\alpha = \frac{Z_0 \sigma}{\sqrt{\varepsilon_r'}} \qquad 3.2.1.6$$

where 2α is the wave power attenuation coefficient and $Z_0 = \sqrt{\frac{\mu_0}{\varepsilon_0}}$, is the vacuum wave impedance. The wave power attenuation coefficient can also be written as

$$2\alpha \approx \frac{2\pi}{\lambda_0}\sqrt{\varepsilon_r'}\tan\delta \qquad 3.2.1.7$$

where λ_0 is the vacuum wavelength.

3.3 Dielectric loss mechanisms of water and electrolytes.

In order to determine the plane wave power penetration at a given frequency it is essential to know the dielectric properties ε, σ of the tissue at that frequency. The frequency dependent dielectric behaviour is characterised by the presence of 4 dispersions, Fig 3.1, covering the audio to infra-red frequency range. The dispersions being labelled α, β, δ, γ.

The α - dispersion is most probably due to counterion polarization around the cell membrane and is important over the 100Hz to 100KHz range.

The β - dispersion is a result of the non-homogeneity of biological material which causes charge accumulation at interfaces between media

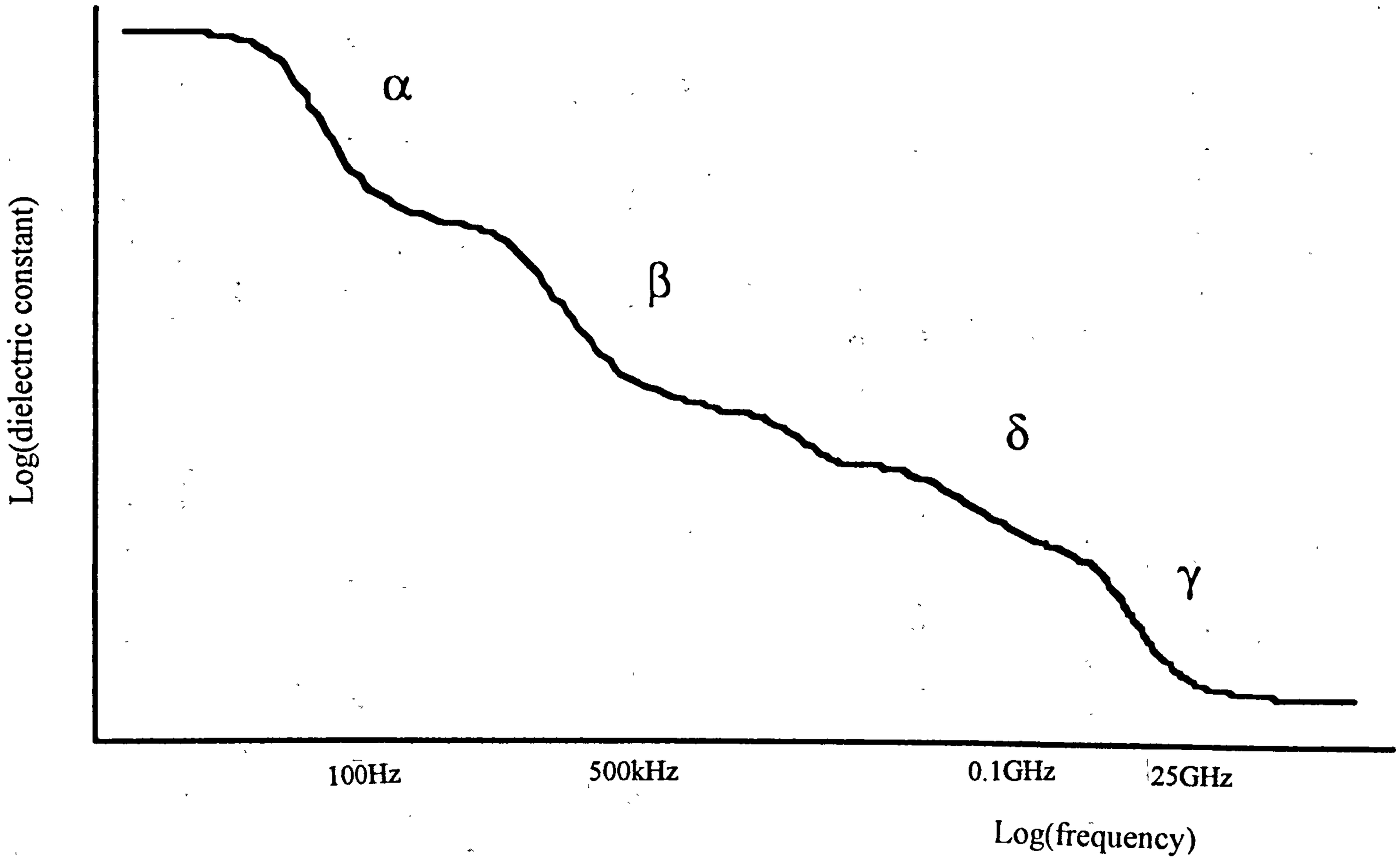

Fig. 3.1 Variation with frequency of dielectric constant, ε', for biological tissue.

of differing dielectric properties. This dispersion occurs in the megahertz range.

The δ - dispersion is a small dispersion which takes place between 0.1 to 1 GHz and is due to relaxation of bound water, rotational relaxation of polar side chains and contributions from small polar molecules.

Finally the γ - dispersion occurs at approximately 26GHz and is a result of the dipole relaxation of the water component of plasma, and intracellular and interstitial fluids in tissues.

From the above description of the relaxation processes which occur it can be assumed that in the microwave frequency range it is the water dependent processes which are important i.e. the δ and γ dispersions.

3.3.1 Losses in electrolytic solutions.

Two main power loss mechanisms may be applied to describe the frequency dependent nature of the dielectric properties of polar fluids. These are the Debye or polarization loss and the ionic conductivity of intercellular fluids.

The Debye polarization loss can be described as the transfer of energy when polarizing the molecules to align them with the radiation electric field, then the transfer of this energy to thermal vibration of the molecules as they "relax" from alignment. The simple Debye relaxation theory has been extended by Cole-Cole. In this formulation a spread of relaxation times for the polar molecules is allowed for, compared to only a discrete relaxation time in the Debye Theory. However, since in water the spread of relaxation times is small, the Debye Theory can be used to give an adequate description of the dielectric properties of water. (Hasted).

The Debye equations describing the dielectric behaviour at angular frequency, ω, are commonly given as

$$\varepsilon_r^{'} = \varepsilon_\infty + \left(\frac{\varepsilon_s - \varepsilon_\infty}{1 + \omega^2 \tau^2} \right) \qquad 3.3.1.1$$

and

$$\varepsilon_r^{''} = \left(\frac{(\varepsilon_s - \varepsilon_\infty)\omega\tau}{(1 + \omega^2 \tau^2)} \right) \qquad 3.3.1.2$$

where ε_∞ is a high frequency limit of the dielectric constant at millimetre wavelengths, ε_s is the static or low frequency value of the dielectric constant, and τ is the characteristic relaxation time.

Now if τ is the characteristic time for the relaxation process, determined by temperature and the viscosity acting on the molecules, the energy transfer is most efficient when $f = 1/\tau$. From Fig 3.2, the Debye dielectric dispersion of water, it is clear that over a range of radio frequencies the complex dielectric constant reduces considerably from its static value, ε_S, to its high frequency value, ε_∞. For water the characteristic frequency of rotation , $1/\tau$ is approximately 26GHz at 37C and the high frequency dielectric constant is about 4.5. The static dielectric constant is approximately 78. (Hasted). Over the lower microwave frequencies of interest for microwave imaging ~ 1-6GHz, the water dielectric constant changes very little from its large static value.

As mentioned previously in 3.1 the body's fluids can be considered to be basically electrolytic solutions. These intercellular fluids are close to 0.9 % saline solution. The ohmic heating loss of form $\frac{1}{2}\sigma E^2$ (=

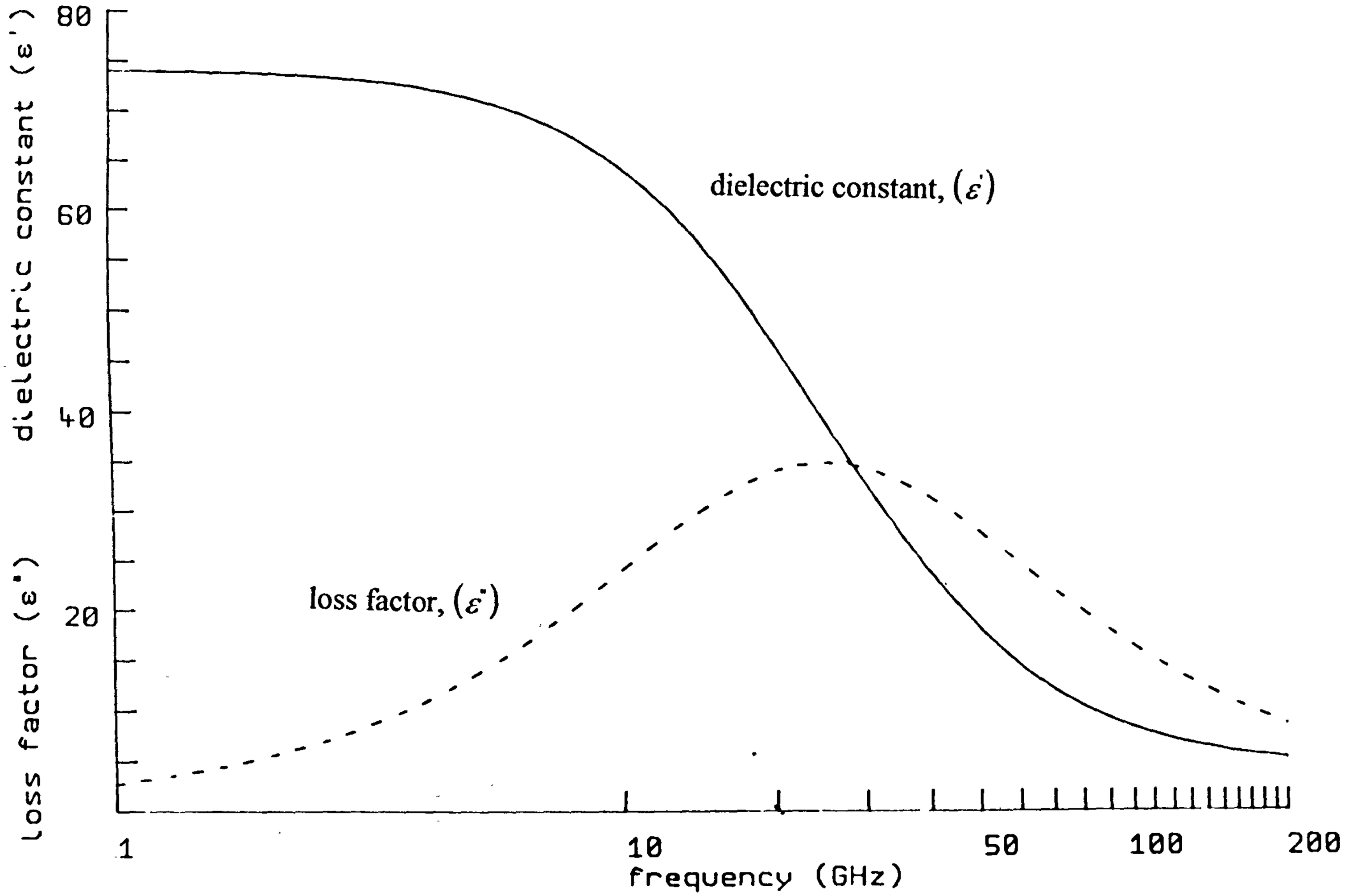

Fig. 3.2 Debye dielectric dispersion of water at 37C.

density of power dissipation) where E is the wave field amplitude, is due to ionic conductivity of the ions and must be added to the pure water loss factor due to Debye relaxation. So the total effective conductivity is of the form

$$\sigma_e = \sigma_{electrolytes} + \sigma_{relaxation\,loss}$$
$$where \quad \sigma_{\text{relaxation loss}} = \omega\varepsilon_r'' \qquad 3.3.1.3$$

which covers the basic types of loss.

3.4 Behaviour of the dielectric properties of tissues at 3GHz.

A considerable amount of research has been performed looking at the dielectric behaviour of tissue and its relation to its water content. The actual relationship between the water content and dielectric properties is in some cases difficult to define, possibly as a result of some of the water being 'bound'. It is also uncertain as to whether 'bound' and 'free' water molecules in tissue have the same characteristic frequency of rotation and high and low frequency limits of dielectric constant.

As explained in section 3.2 the water content of tissues is the dominant factor in determining the dielectric properties of tissues at 3GHz. However, water in biological systems is present in both 'bound' forms and as 'free' water depending on its proximity to membranes or interfaces, 'bound' water is associated with biological substrate e.g. protein, DNA. The 'bound' water compartment is a relatively fixed size and contains water which is structured by individual binding sites in tissue. This 'bound' water is unable to rotate freely in an alternating electric field.(Kuntz & Cooke, 1974) In comparison the free water

compartment contains the less strongly held water and is thought to be present as a result of a dipolar interaction.

Mixture equations have been developed (e.g. Maxwell 1881, Fricke 1924, Bruggeman 1935) which attempt to describe the dielectric properties of suspensions of particles in terms of the suspended and the suspending mediums, and the relative volumes of the two mediums present (Brown, 1989 & Campbell, 1990).

Maxwell, 1881, was first to derive a mixture equation for the thermal conductivity of a dilute suspension of identical spheres. Maxwell's form of mixtures for dielectric media can be expressed as

$$\frac{\varepsilon_s - \varepsilon_{2s}}{\varepsilon_s + 2\varepsilon_{2s}} = \frac{\varepsilon_{1s} - \varepsilon_{2s}}{\varepsilon_{1s} + 2\varepsilon_{2s}}\theta \qquad 3.4.1$$

where ε_{2s} is the medium of static dielectric constant in which spherical particles of static dielectric constant ε_{1s} and radius ai randomly fill a spherical volume of radius R. θ is the volume fraction of medium 1. The Maxwell form of the mixture equations could be applied to a tissue model to be a suspension of spherical particles in physiological saline solution. It is assumed that the suspended particles have no effect on each other.

Fricke, 1924, introduced a geometrical form factor x which allowed the particles to be oblate or prolate spheroids. Fricke's equation can be written as

$$\frac{\varepsilon_s - \varepsilon_{2s}}{\varepsilon_s + x\varepsilon_{2s}} = \frac{\varepsilon_{1s} - \varepsilon_{2s}}{\varepsilon_{1s} + x\varepsilon_{2s}}\theta \qquad 3.4.2$$

where x is a function of the axial ratio of the ellipsoids and the ratio of the static dielectric constants of the two phases.

In more concentrated dispersions the electrical interactions among particles are not negligible. Bruggeman, 1935, devised an integral procedure which consisted of building up the spherical dispersion system by successive additions of infinitesimal amounts of the disperse phase. The Brugemann equation is written as

$$\left[\frac{\varepsilon_{1s}-\varepsilon_{2s}}{\varepsilon_{1s}-\varepsilon_{s}}\right]^{3}\frac{\varepsilon_{s}}{\varepsilon_{2s}}=\frac{1}{(1-\theta)^{3}} \qquad 3.4.3$$

Most biological materials cannot be categorised as simple two-phase mixtures, so therefore predictions from the mixture theories must only be considered as a qualitative guide. However, mixture theory has been applied successfully to describe the dielectric behaviour of blood and suspensions of proteins (Cook).

For this study the biological tissues of interest are muscle, skin, and fat. Table 3.0 gives the water content of these tissues. It is clear from the table that biological tissues can be separated into three groups from their water content as follows

Water content	Type
low water content (0-30)%	Fat, bone
medium " " (30-60)%	Skin, some breast tissue
high water content (60-100)%	Muscle, blood.

Tissue	Water content (% weight)
Whole blood	78.5
Blood plasma	91
Blood corpuscles	68 - 72
Muscle	70 - 80
Skin	62 - 76
Fat	5 - 20

Table 3.0 Water contents of human organs and tissues.
(Compiled from Brown, 1989).

Fig 1.0 in Chapter 1 shows that tissue properties are such that for many applications the optimum measurement frequency is near 3GHz. At this frequency temperature pattern information can be obtained for tissues at clinically useful depths of several centimetres within the body (Land, 1989). It is clear from this graph that the transmission of radiation through tissue varies depending on the tissue water content. Low water content tissue has a higher penetration depth than high water content tissue.

Dielectric properties of fat, bone, bone marrow, muscle, whole blood and skin are given in Table 3.1 (Compiled from Brown, 1989). Again there is a distinct difference between the dielectric properties of high and low water content tissues. A summary of the information given in Table 3.1 is given in Table 3.2.

The variation of the dielectric constant at 3GHz with water content for body tissues is shown in Fig 3.3 (Land, 1987). A clear relationship between dielectric constant and water content is shown.

The effective conductivity, σ_e or loss factor, $\varepsilon_r^{\cdot}$, for power loss will, through the mixture relations, have a similar dependence on water content to the dielectric constant, $\varepsilon_r^{'}$. This is well shown by Fig. 3.4. This relationship will be discussed further in Chapter 5.0.

Tissue type	Dielectric constant	Loss factor	Power penetration depth(cm)	Reference
Fat	3.9-7.2	0.67-1.36	2.3-6.2	Herrick
	4.92	1.46	2.4	Cook
	3.94	0.87	3.7	Cook
	7.0	1.75	2.4	Cook
	11.6	2.25	2.4	Cook
	5.2	1.5	2.4	England
	7.2	1.7	2.5	England
Bone	7.5	1.0	4.3	Herrick
	8.35	1.32	3.4	Cook
Bone Marrow	4.2-5.8	0.7-1.35	2.4-5.6	Herrick
Muscle	45-48	13-14	0.77-0.85	Herrick
	50	17.1	0.67	Cook
	51	18	0.64	Cook
	52	18.9	0.62	Cook
Whole blood	55-56	15-18.6	0.65-0.80	Herrick
	56	15.9	0.76	Cook
	53	15	0.78	England

Table 3.1 Dielectric properties of human tissues at a frequency of 3GHz and at 37C (Compiled from Brown, 1989).

Tissue type	Dielectric constant	Loss factor	Power penetra-tion depth(cm)	Reference
Skin	40	13.1	0.80	Cook
	42.4	13.1	0.80	Cook
	51.1	15.2	0.76	Cook
	40.9	16.8	0.62	England
	50.2	14.8	0.77	England
	52.2	17	0.68	England

Table 3.1(contd) Dielectric properties of human tissues at a frequency of 3GHz and at 37C (Compiled from Brown, 1989).

Tissue type	Water content	Range dielectric constant, ε_r'	Range loss factor, ε_r''	Range power penetration depth(cm)
Fat	0-30	3.9-11.6	.67-2.25	2.3-6.2
Bone	0-30	7.5-8.35	1.0-1.32	3.4-4.3
Skin	30-60	40-52.2	13.1-17.0	.62-.80
Muscle	60-100	45-52	13-18.9	.62-.85
Blood	60-100	53-56	15-18.6	.65-.80

Table 3.2 Summary of dielectric properties of human tissue taken at a frequency of 3GHz at 37C

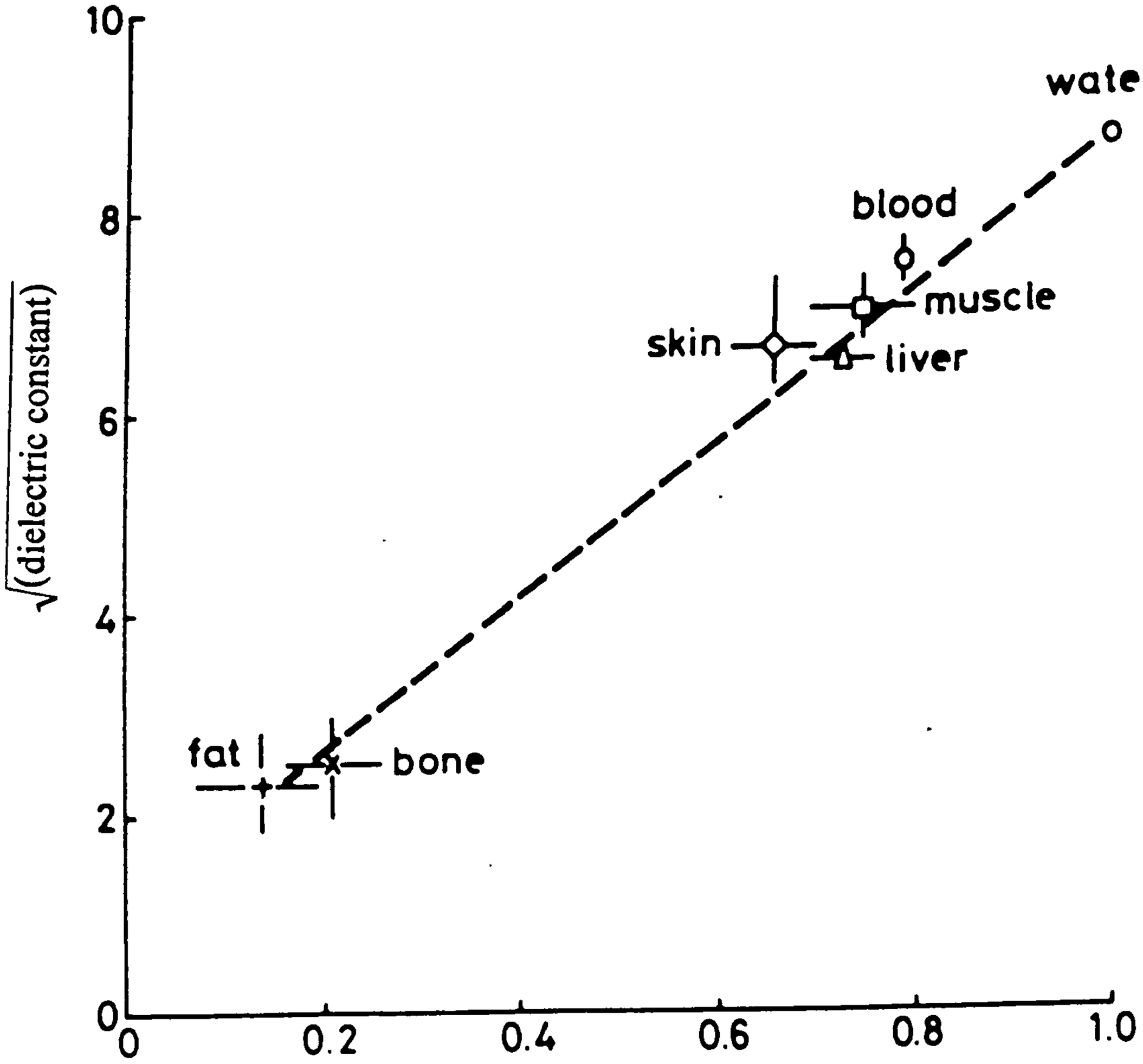

Fig. 3.3 Variation of dielectric constant at 3GHz with water content for body tissues.

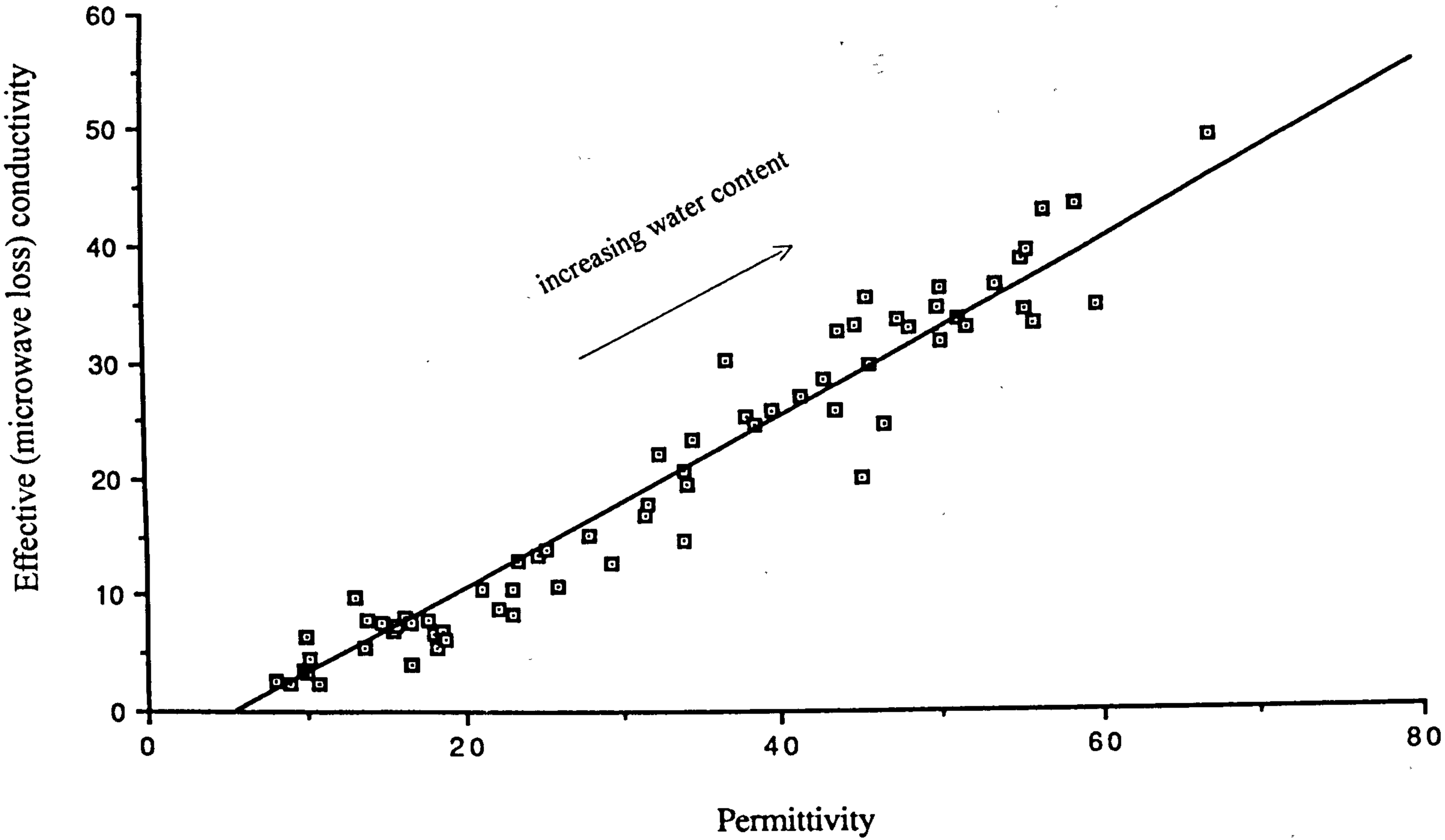

Fig. 3.4 Variation of conductivity with permittivity (from Campbell)

CHAPTER 4.0 MICROWAVE THERMOGRAPHY.

4.0 Introduction.

Microwave thermography is the technique of observing the naturally emitted thermal radiation from body tissues at centimetric wavelengths. This method of body temperature measurement using the natural thermal radiation from the tissues of the body to obtain information about internal temperatures is attractive to clinicians since the technique is passive, non-invasive and safe.

The intensity of the natural microwave radiation from the body is very small, giving a signal at the input of the receiver of only about 10^{-12} Watts. The noise power at the same wavelength from most surroundings and from the measuring equipment itself is of a similar order, therefore, detection of the signal is difficult. These problems have been overcome by using techniques originally developed for radio astronomy.

4.1 Basic elements of a microwave thermography system.

In order to provide medically useful information the following points must be considered when designing a microwave thermography system:

- temperature resolution
- lateral spatial resolution
- tissue penetration depth
- system response time

Experience has shown that to be of any use to clinicians the equipment must have a temperature resolution of approximately 0.1C. The spatial resolution should be 10mm to 20mm and the tissue penetration depth 10mm to 40mm. Both of these spatial parameters are dependent upon the frequency at which the measurements are taken. Finally, the system response time should be as short as possible, though for simple investigations it can be comparable to that for convenient hand measurements.

To meet these requirements, a Dicke type comparison radiometer receiver is used, in which the radiation signal being measured is compared with the thermal noise signal from a resistive source of known temperature close to the tissue temperature.

The remainder of this chapter will consider the optimum measurement frequency, factors which affect temperature resolution, the Glasgow design of microwave radiometer and some aspects of antenna design. Fig. 4.0 shows the basic thermography system.

4.2 Choice of optimum measurement frequency.

The choice of measurement frequency is almost independent of tissue type. As mentioned in Chapter 3, tissue water content varies from about 8 - 26% for fat and bone (low water content) to 62 - 80% for muscle and skin (high water content). Also, the majority of tissue water is present as 0.9% NaCl solution.

As previously mentioned the spatial resolution and penetration depth are both highly dependent on the measurement frequency. So it follows that the radiation attenuation constant, α and tissue wavelength, λ_T are important quantities when choosing an optimum measurement

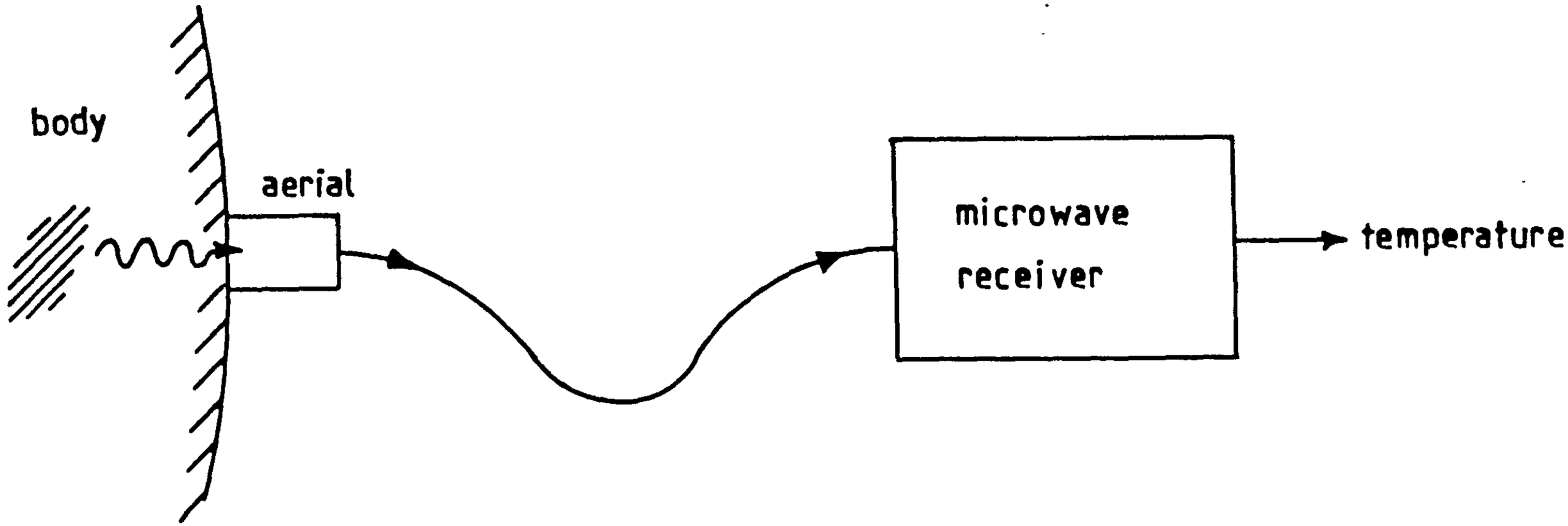

Fig. 4.0 Basic microwave thermography system.

frequency. The spatial resolution is of the order of 1/2 the wavelength in the tissue, λ_T and is given by

$$\frac{\lambda_T}{2} = \frac{\lambda_0}{2\sqrt{\varepsilon_r'}} \qquad 4.2.1$$

where λ_0 is the free-space wavelength and ε_r' is the relative dielectric constant. So it is clear that as the operating frequency increases, λ_T decreases and as a result the attainable spatial resolution of the source temperature patterns improves. However, in Chapter 1 it can be seen from Fig 1.0, that the transmission of radiation decreases as frequency increases, and for the measurements to provide clinically useful information the penetration depth must be of the order of 10mm to 40mm. It was shown in Chapter 3 that for electromagnetic radiation travelling through tissues, the complex propagation constant is used. For practical purposes, α, the wave field attenuation constant is given by

$$\alpha = \frac{\pi}{\lambda_0}\sqrt{\varepsilon_r'}\tan\delta \qquad 4.2.2$$

where $\tan\delta$, is the tissue loss tangent and is defined by Eqn. 3.2.3.

and $$\beta = \frac{2\pi}{\lambda_T} \qquad 4.2.3$$

is the phase constant with λ_T the wavelength in tissue.

Now the product of equations 4.2.1 and 4.2.2 varies as tanδ. This is essentially the product of the spatial resolution and the inverse of the attenuation length. Therefore it can be assumed that an optimum measurement frequency occurs at a minimum of the loss tangent. As a result of the dielectric behaviour of physiological saline, discussed in Chapter 3.0, there is a pronounced minimum at around 3GHz.(Fig. 3.0). It follows that the optimum measurement frequency should be around 3GHz for many potential medical applications. (Land, 1983).

4.3 Factors which affect the temperature resolution.

The two factors which affect the temperature resolution are the randomly fluctuating nature of the measured noise signals and gain fluctuations of the measuring radiometer.

4.3.1 Thermal signals.

A radiometer is used to detect a window of frequencies of randomly fluctuating thermal electromagnetic signals. The temperature resolution achievable by a radiometer is given by the Gabor relationship,

$$\Delta T_{rms} = KT'_{system}\sqrt{B_d/B} \qquad 4.3.1.1$$

where ΔT_{rms} is the root mean square fluctuation of the mean measured temperature signal, K is the radiometer constant, approximately 2, T_{system} is the system noise temperature at the antenna terminals where

$$T_{system} = T_{source} + T_{radiometer} \qquad 4.3.1.2$$

T_{source} is the source temperature at the antenna and $T_{radiometer}$ is the effective noise temperature at the input of the receiver and includes the effect of antenna and input circuit losses. B_d and B are the post and pre-detection bandwidths of the radiometer.

To obtain optimum combinations of temperature resolution and system response time, $T_{radiometer}$ must be minimised and B, - pre-detection bandwidth, maximised. However, since the source noise temperature, T_{source} at the input of the receiver is close to 310K there is little to be gained by reducing $T_{radiometer}$ below about 300K. Pre-detection bandwidth, B is set by technical requirements such as antenna impedance matching and so it cannot be increased beyond about 20 % of the operating frequency. (Land, 1983)

4.3.2 Gain fluctuations.

The gain, G, varies significantly with amplifier ambient temperature and supply voltage changes. The effect of supply voltage changes is easily overcome by providing a stabilised supply voltage. However variations in the gain, G, due to active device temperatures can be only approximately compensated.

The effect of gain fluctuations can be greatly reduced by using a Dicke comparator radiometer as shown in Fig 4.1, in which the receiver produces an output at the input switching frequency that is proportional to the difference between T_{source} and the temperature of an internal reference load, T_{ref} . If the reference temperature is close to the noise temperature, the difference signal is relatively small and the effect of receiver gain fluctuations is reduced. Fig 4.1a shows how the size of the post-detection square wave signal at the switching frequency

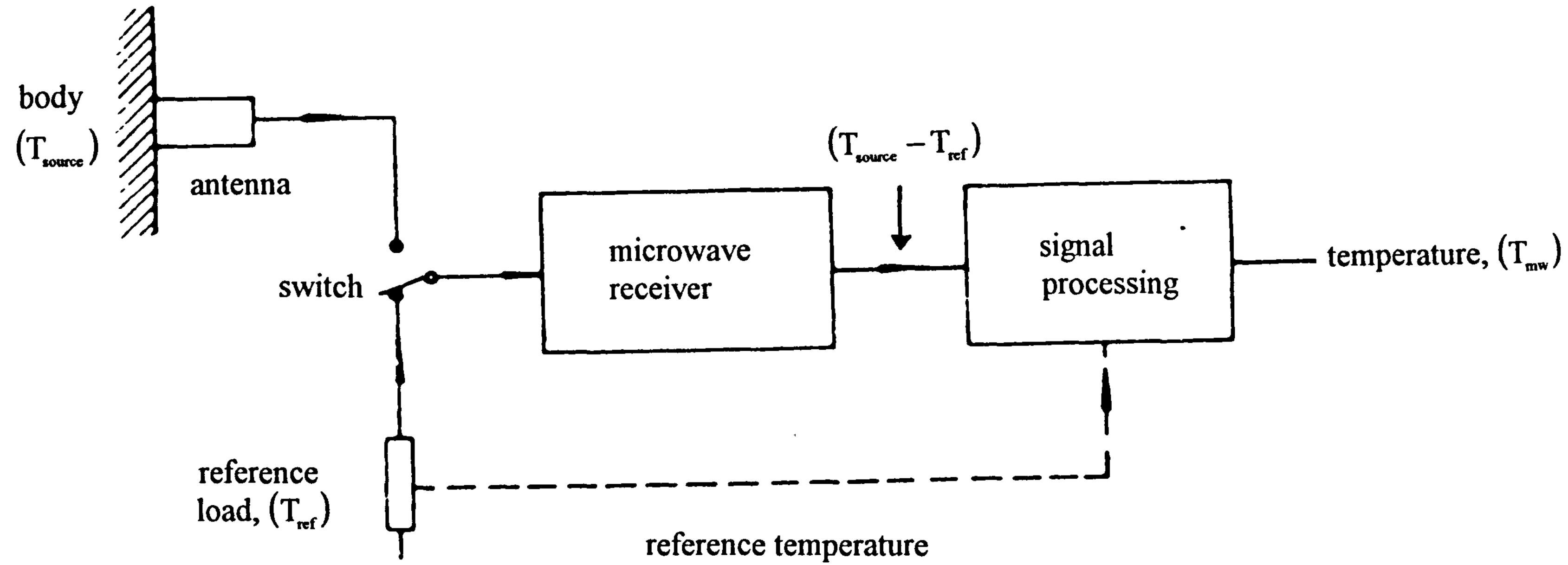

Fig. 4.1 Dicke radiometer configuration.

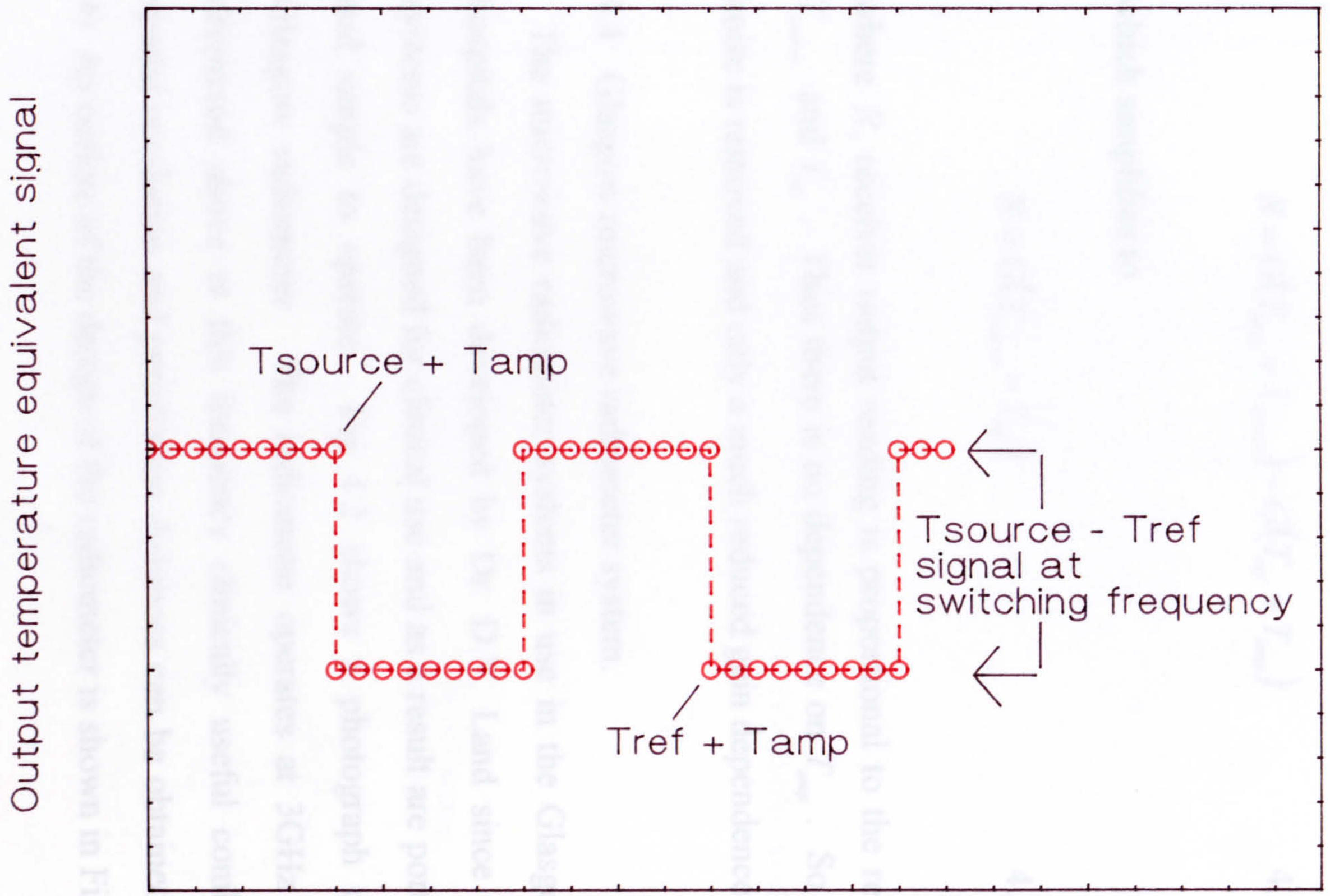

Fig. 4.1a Dicke radiometer operation

represents the difference in magnitude between the signal from the antenna and the reference source. A synchronous detector is used to measure this signal and give an output which is directly proportional to the difference in magnitude between the temperatures.(Brown, 1989)

It is shown in Fig 4.1a that

$$R = G\left(T_{amp} + T_{source}\right) - G\left(T_{ref} + T_{amp}\right) \qquad 4.3.2.1$$

which simplifies to

$$R = G\left(T_{source} - T_{ref}\right) \qquad 4.3.2.2$$

where R, receiver output reading is proportional to the receiver gain, T_{source} and T_{ref} . Thus there is no dependence on T_{amp} . So the average noise is removed and only a much reduced gain dependence remains.

4.4 Glasgow microwave radiometer system.

The microwave radiometer systems in use in the Glasgow teaching hospitals have been developed by Dr. D.V. Land since 1981. The systems are designed for clinical use and as a result are portable, robust and simple to operate. Fig 4.2 shows a photograph of a typical Glasgow radiometer. The radiometer operates at 3GHz because as discussed above at this frequency clinically useful combinations of spatial resolution and penetration distances can be obtained. (Chs. 3 & 4) An outline of the design of the radiometer is shown in Fig 4.4.

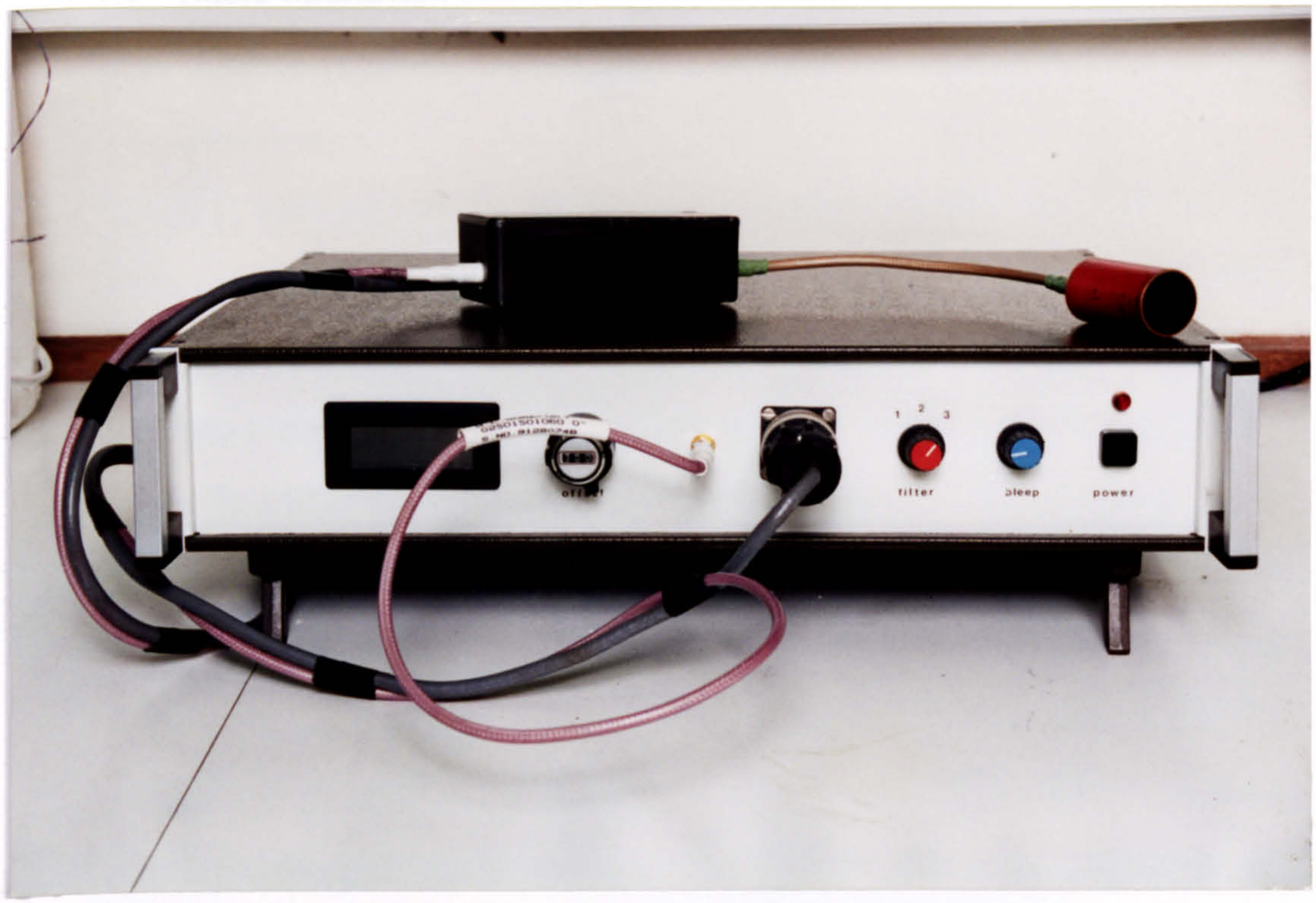

Fig. 4.2 Glasgow clinical microwave thermography system.

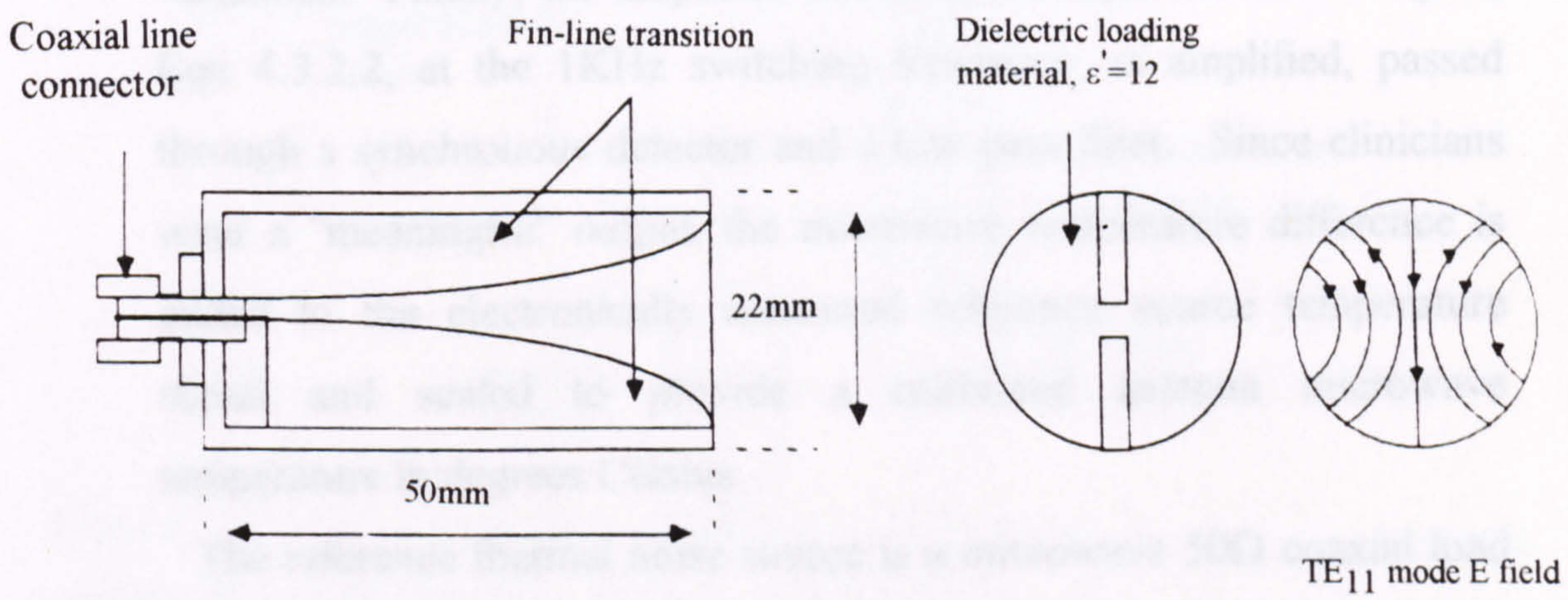

Fig. 4.3 Glasgow antenna design.

4.4.1 Basic operation.

This section will give a brief description of the operation of the Glasgow system.

Through the use of a Dicke switch between the antenna and a reference source, the radiation signal being measured is compared with a thermally generated signal from a source of known temperature. The signal from the source cannot pass directly into the radio-frequency detector because its equivalent noise temperature is too high, so it is necessary to perform "low-noise" microwave amplification between the antenna and the detector. By referring to Fig 4.4 it is seen that the signal is passed through a low-noise GAs FET pre-amplifier for the measurement frequency range (3.0 - 3.5)GHz. The signal is then frequency changed by a mixer and local oscillator at 3GHz to an intermediate frequency band of (20-500)MHz for further amplification before detection. The above method is known as a "super-heterodyne" system. Detection is by a "back-diode" semiconductor diode which is a form of tunnel diode which has low resistance for good matching to the preceding amplifier and low sensitivity to ambient temperature variations. Finally, the amplified and detected input difference signal, Eqn 4.3.2.2, at the 1KHz switching frequency, is amplified, passed through a synchronous detector and a low pass filter. Since clinicians want a "meaningful" output, the microwave temperature difference is added to the electronically measured reference source temperature signal and scaled to provide a calibrated antenna microwave temperature in degrees Celsius.

The reference thermal noise source is a microwave 50Ω coaxial load heated to approximately 40C. This temperature is measured using a

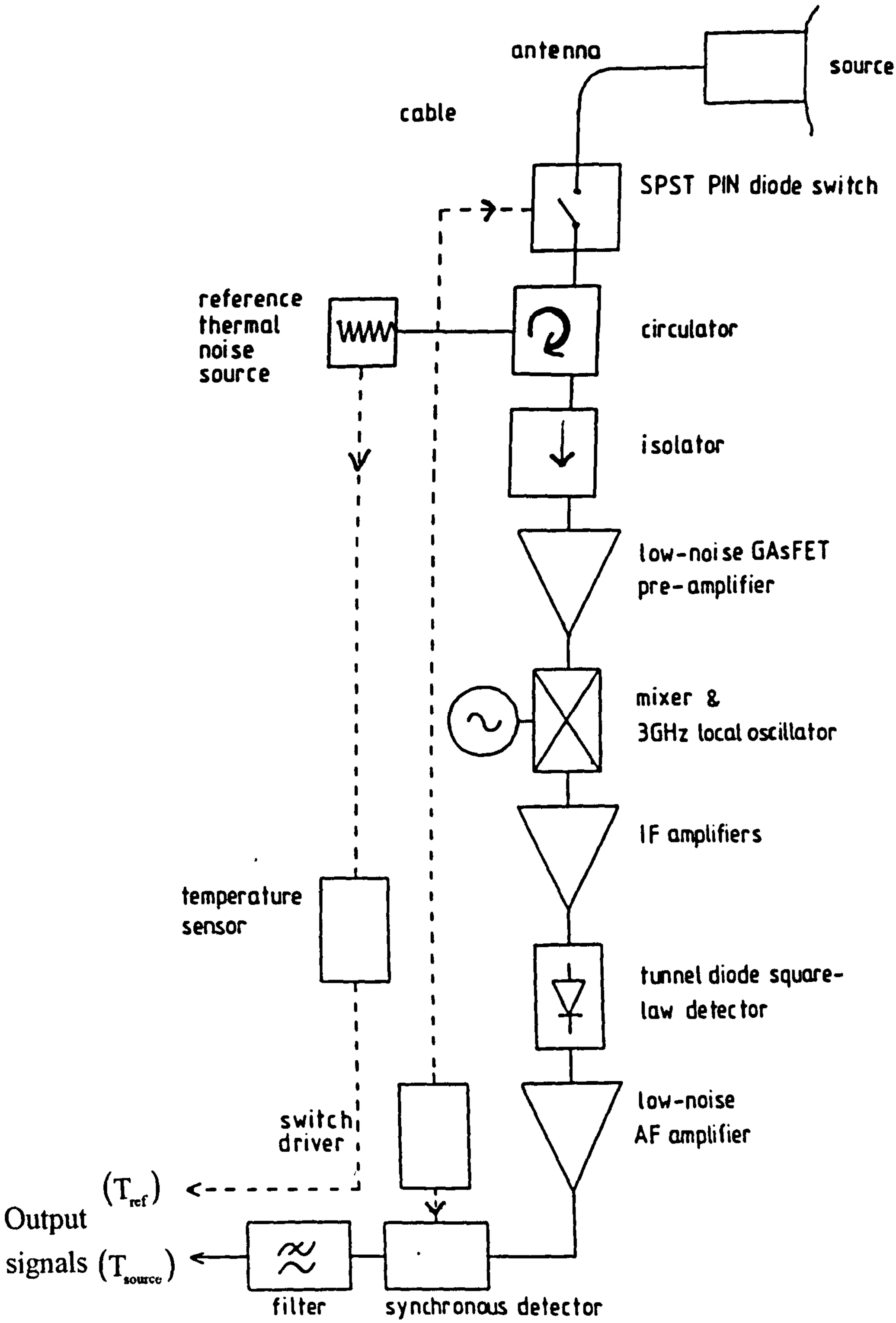

Fig. 4.4 Glasgow microwave radiometer outline.

semi conductor temperature sensor. When the Dicke switch is on the antenna position, the noise from the reference source is directed to the antenna by the microwave circulator (Fig 4.5). When the noise signal from the reference is directed to the antenna by the circulator some of the signal is reflected at the antenna-skin boundary back into the receiver. This partially compensates for the radiation reflected internally into the tissue. This is shown schematically in Fig 4.5 . The accuracy of this system is dependent on how close the reference and source temperatures are to one and other. The effective reference source temperature at the Dicke switch is reduced by the loss in the circulator and the switch, and attenuation between the circulator and reference load introduced to balance the input circuits for ambient temperature variation. The effective temperature difference between source and reference is usually less than 3C.(Land, Electronic Letters, 1983)

4.4.2 Radiometer sensitivity.

As stated in section 4.3.1, the temperature resolution or sensitivity achievable by a radiometer is governed by Eqn 4.3.1.1

$$\Delta T_{rms} = K T_{system} \sqrt{B_d / B} \qquad 4.3.1.1$$

where $$T_{system} = T_{source} + T_{radiometer} \qquad 4.3.1.2$$

With reference to the Glasgow system, K is 2 and T_{source} is 310K (approximately equal to the temperature of the human body). $T_{radiometer}$ is the effective noise temperature at the input of the receiver and

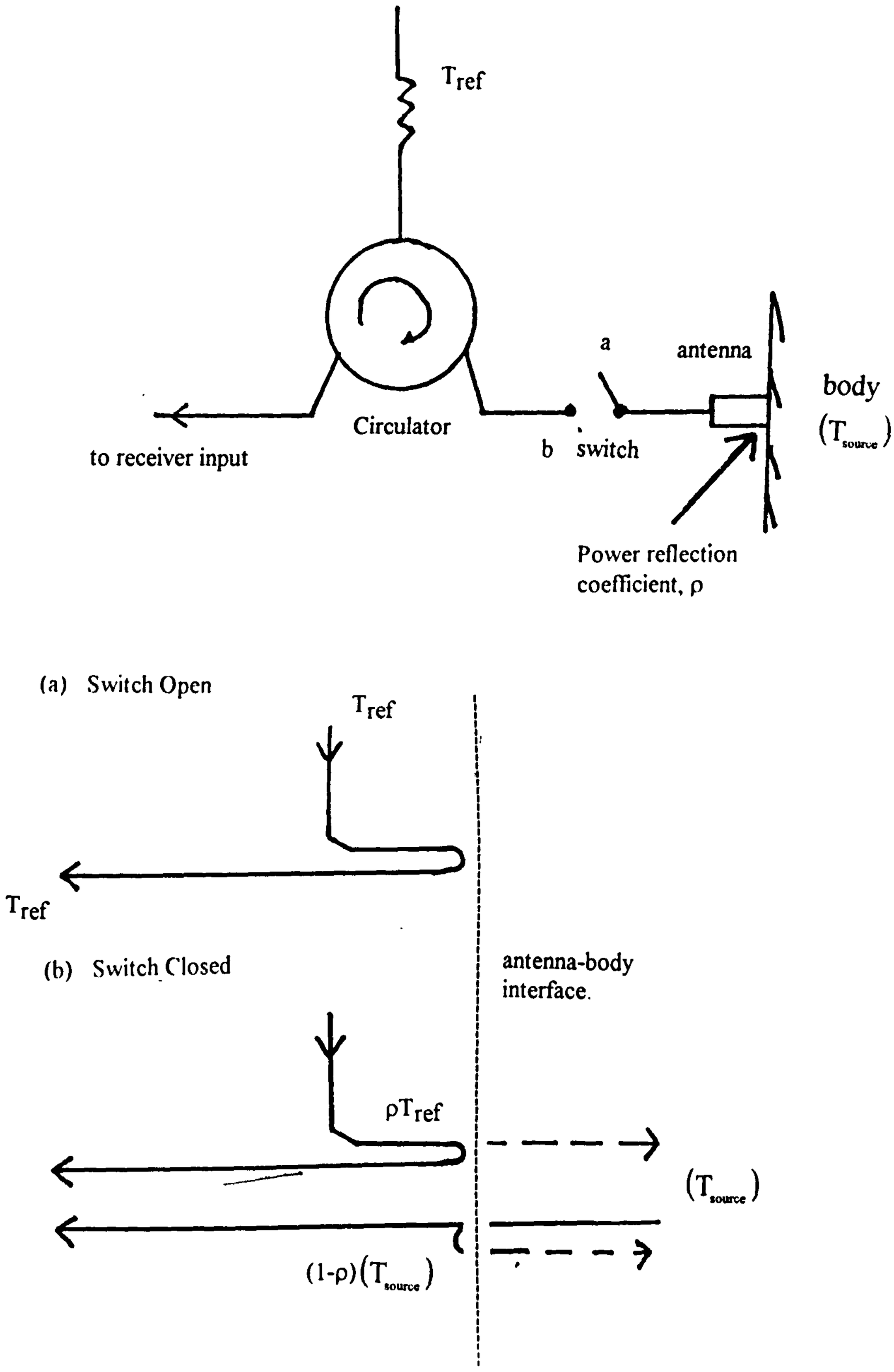

Fig. 4.5 Microwave Dicke switch and circulator operation

includes the effects of input circuit losses (antenna, switch, cables and circulator) and the GAs FET amplifier and is approximately 400K - 600K for the various Glasgow systems. The system response time is determined by the post-detection to pre-detection pass band ratio. This response time is optimised by using a critically or slightly under-damped filter response. As noted above, 4.3.1, B is determined by the need for reasonable antenna to 50Ω coaxial cable matching over the measurement bandwidth, as well as the avoidance of possible interference signals. If the fluctuations of the output signal have an approximately Gaussian distribution, for 95 % of the time the signal will be in a range of equivalent temperature width 3.92 ΔT_{rms} . This value is considered a reasonable measure of the temperature resolution of the system (Land, 1983). Using the information given in this and previous sections the following summary information about the Glasgow radiometer can be given:

- temperature resolution - 0.1C - 0.2 C
- spatial resolution - 10mm - 20 mm
- tissue penetration - 10mm - 40mm
- system response time - 1s - 3s

This concludes the sections on radiometer design and sensitivity. The following sections will cover some aspects of antenna design.

4.5 Antenna design.

A wide range of microwave antennas have been designed for use in direct contact with the skin at frequencies above 200MHz for both

radiometry and hyperthermia induction. The most commonly used contact antennas are dielectric loaded rectangular wave guides, with the dominant mode in the aperture of the antenna being the TE_{10} mode. The loading of the wave guide with a dielectric material allows a reduction in the linear dimensions of the antenna since it reduces the wavelength by a factor of $\sqrt{\varepsilon_r}$ in the dielectric, and lowers the wave impedance by the same factor. Typical loading dielectrics have relative permittivities in the range 10 - 20.

4.5.1 Glasgow antenna.

The antenna currently being used in the Glasgow Microwave Thermography systems is a cylindrical wave-guide antenna with dimensions of 22mm diameter × 50mm length. It is loaded with a low-loss dielectric material (Emerson and Cummings, Eccoflo HiK dielectric powder, $\varepsilon_r = 12$) to achieve good coupling to the body tissues. Fig 4.3 shows how the antenna uses a tapered fin-line type wave-guide to coaxial line transition. The allowed propagation modes in the operating bandwidth of 3.0 - 3.5 GHz are TE_{11} and TM_{01} with the cut-off frequency for these propagation modes being 2.3GHz and 3.0GHz respectively. However, the finline transition will only couple to the former propagation mode, TE_{11}. (Mimi, 1990). As mentioned in sec.4.5, the most commonly used contact antennas for clinical measurements are rectangular wave guides with the dominant propagation mode , TE_{10}. Commonly used rectangular wave-guide antennas (e.g Mamouni, Lille) have 2:1 side ratio. This leads to a greater spreading of the antenna response in the E-plane (narrow aperture direction) and reduces response with depth. The circular

aperture TE_{11} mode antenna has a nearly circular symmetric response and a much smaller field discontinuity at the aperture than the rectangular section antenna. This gives it the best of all response with depth of any antenna. In practice, layering of tissues has a much larger effect than the variations between reasonable antennas forms.

4.5.2 Measured properties of antennas.

The microwave radiometer antenna response pattern determines the contribution of a small volume element of the tissue to the total signal. However, the antenna pattern is highly dependent on the operating frequency, dimensions and geometry of the guide, dielectric loading of the guide, dielectric properties of the observed tissue and tissue geometry. The antenna response pattern can be determined in two ways:

1. theoretically
2. experimentally

It is very difficult to calculate the response pattern theoretically. In order to theoretically calculate the pattern, numerical methods are used, in which the tissue geometry is assumed to be in planar layers. Theoretical/computational modelling of antenna response patterns is being developed by the microwave radiometry research groups at the University of Lille (Leroy, Mamouni & Borquet) and University of Rome (Bardati). These models are at the stage of being compared with experimentally measured response patterns. They appear to show that tissue layering has a strong influence on the response patterns.

Experimental determination of the pattern is performed using "phantom" materials which simulate the dielectric properties of the tissue.

The antenna pattern reduces the effective penetration depth of the microwave radiation from that of the plane wave penetration depth. It should be noted that δ, the effective power penetration depth is related to the effective field attenuation constant , α' by

$$\delta = \frac{1}{2\alpha'} \qquad 4.5.2.1$$

The effective power penetration depth must always be less than the plane wave power penetration depth, Fig 4.6, and it is important to realise that the plane wave power penetration depth in tissue indicates the maximum performance of a radiometer system. For practical microwave thermographic measurement, the radiometer antenna must produce a large plane wave far-field zone with a minimal near field zone to give maximum signal contribution with depth in the viewed material.

The microwave radiometer antenna response is generated as shown in Figs. 4.7, 4.8 & 4.9. Fig 4.7 represents the configuration of the near and far field zones. It is clearly shown that the response pattern of the near-field zone differs from the far-field zone where the field is perpendicular to the antenna axis. Fig 4.8 shows the behaviour of the microwave signal inside the body tissue. It is clear from the figure that if an element , dz, of body tissue is considered, the microwave signal will be generated from that element and the microwave signal in the region between dz element and the antenna is attenuated by the factor

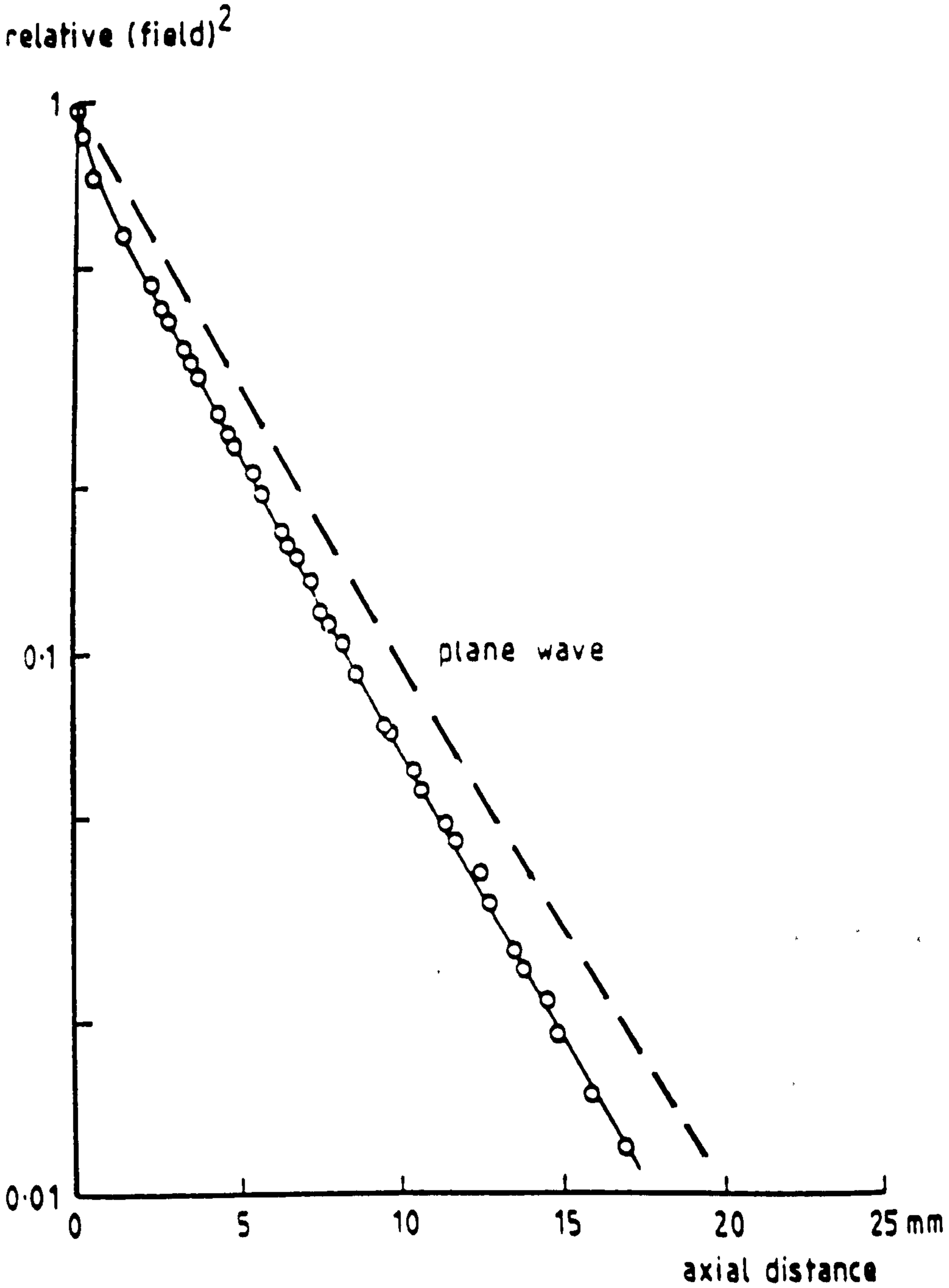

Fig. 4.6 Cylindrical radiometer response to signals integrated over the plane normal to the axis.

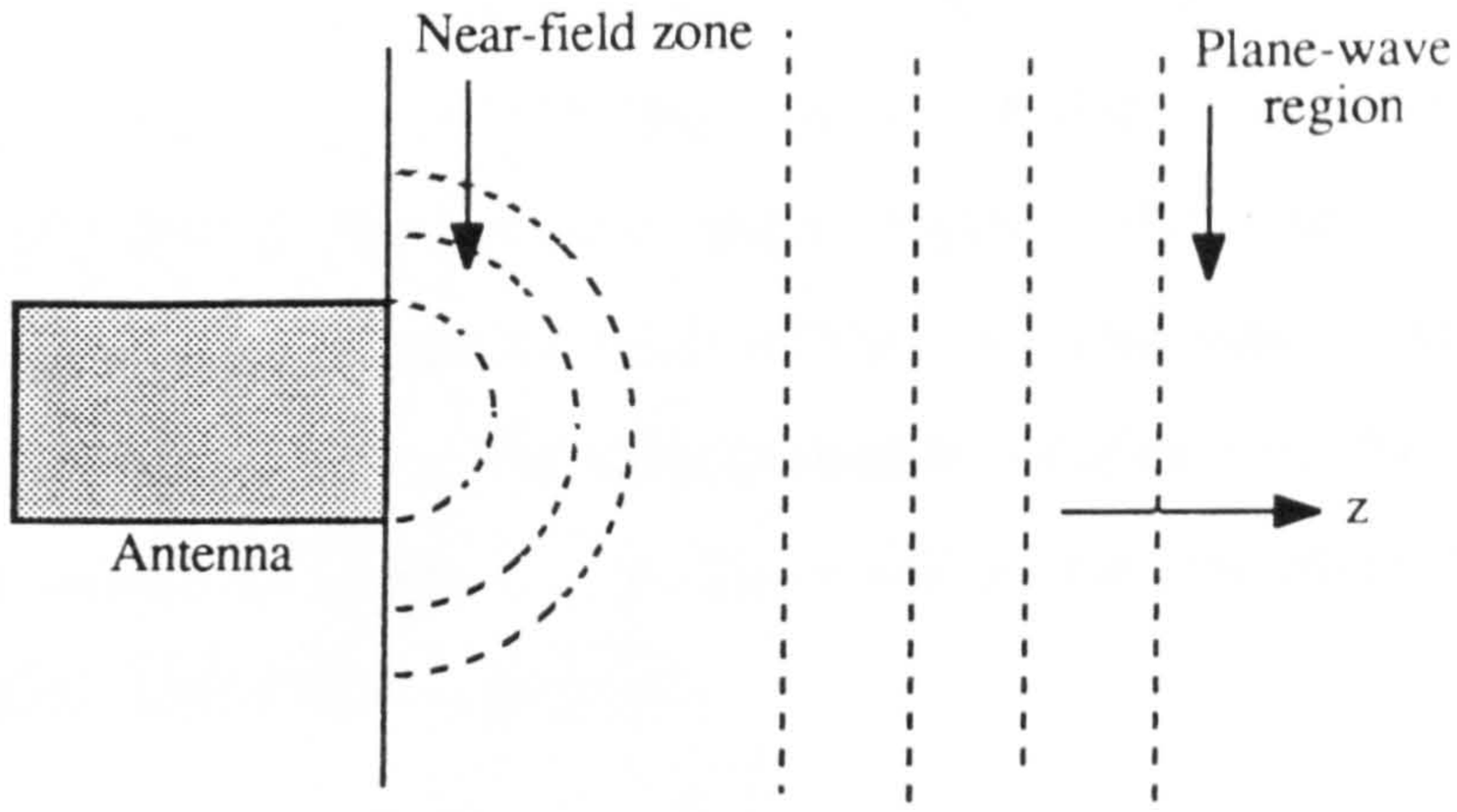

Fig. 4.7 Configuration of the near- and far- field zones.

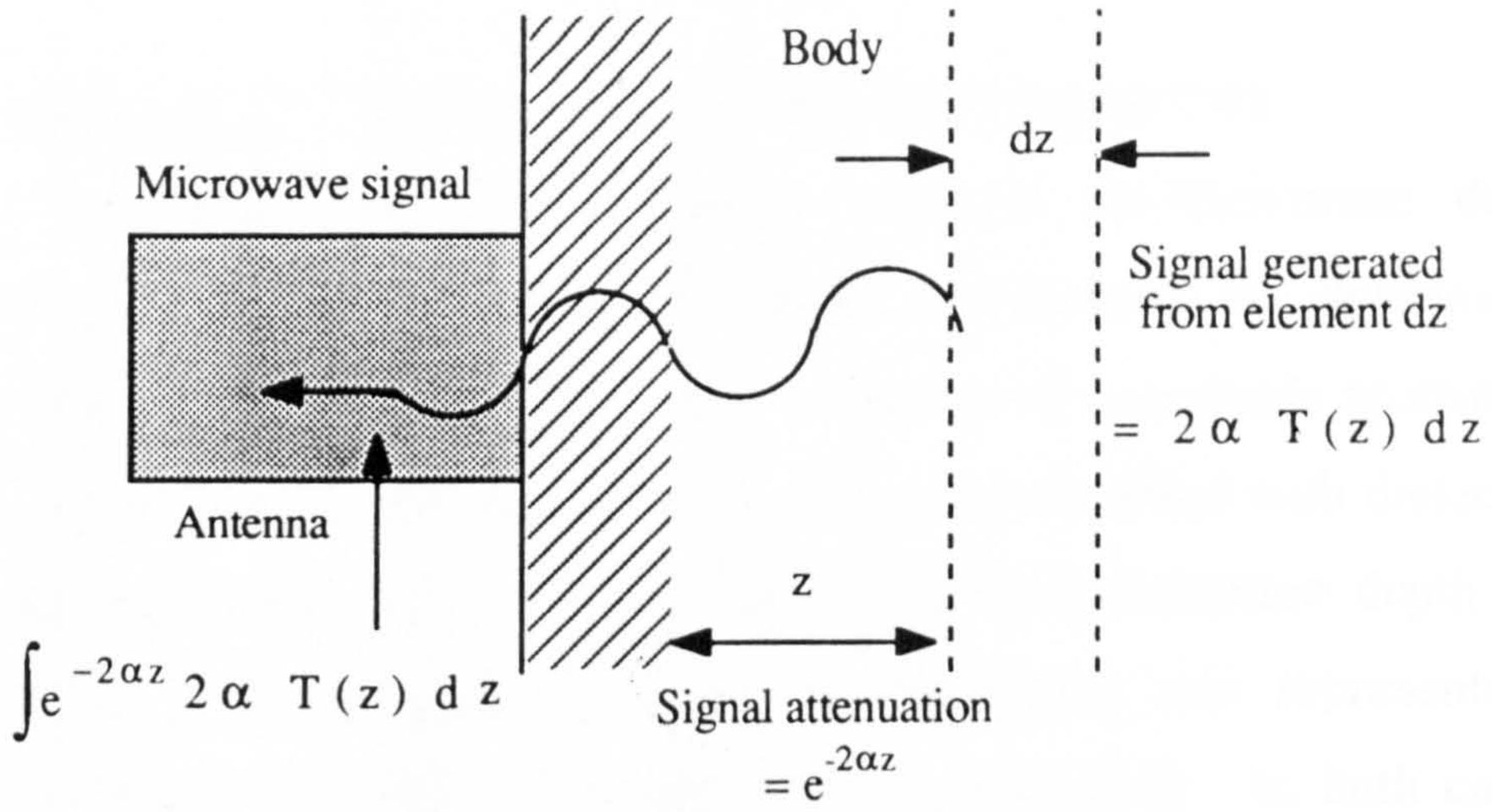

Fig. 4.8 Behaviour of the microwave signal inside body tissue.

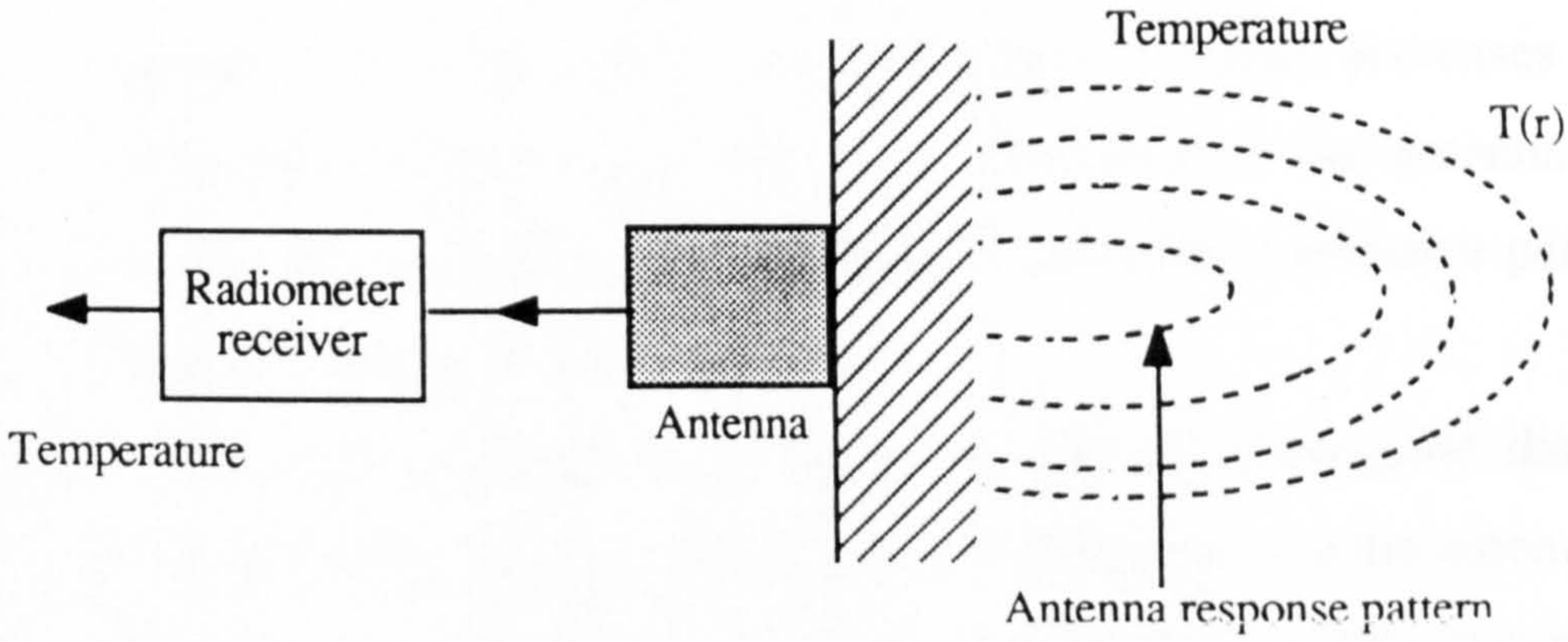

Fig. 4.9 The microwave radiometer antenna configuration into the body tissue.

$e^{-2\alpha z}$, where α is the attenuation constant of the region z. The microwave signal received by the antenna is then the integral of the signal from the dz element over the z region. The antenna response pattern inside body tissue is shown in Fig 4.9. The radiometer receiver gives the temperature of the viewed region weighted by the complete antenna response pattern. So the total power obtained from the microwave radiometer is given by

$$2\alpha \int_V w(z) e^{-2\alpha z} e^{-2\alpha z} T(z) dz \qquad 4.5.2.2$$

where w(z) is the weighting function (ref. Chapter 2.0)

The Microwave Thermography Group at the Universite' de Lille, France have performed numerical calculations to determine the effective penetration depth from a number of waveguide aperture sizes operating at frequencies of 1, 3 and 9 GHz and filled with dielectrics of dielectric constant 1 to 25. The effective penetration depth in two types of homogeneous tissue was calculated; one representing the dielectric properties of muscle and the second fat. In both cases the effective penetration depth was reduced by decreasing the width of the guide. These results are to be expected as diffraction effects increase as the ratio of the aperture size to wavelength in tissue decreases. Larger diffraction effects widen the lateral response of the antenna and so reduce the on-axial response causing a decrease in effective penetration depth.(Mamouni, Lille)

The dielectric loading of the guide and the waveguide dimensions also determine the wave impedance of the guide. At the antenna-tissue boundary, an impedance mismatch occurs which results in a reflection

of the radiation signal from the tissue. Ideally this reflection should be kept to a minimum. It should be noted however that although closer values of the dielectric constant of the guide and tissue reduce the reflection, the reflection coefficient will be less than 0.2 if the ratio of dielectric constant of the guide to tissue ratio is between 0.5 and 5. (Nguyen et al, 1980)

The response pattern of the cylindrical antenna used in this research has been experimentally measured using a non-resonant perturbation technique. Non-resonant perturbation is a simple technique which can be used to measure electromagnetic fields in a lossy material close to an antenna. It has been used to measure the effective penetration depths in several different dielectric materials with properties simulating body tissues (Land, 1988). This technique has the advantage that it gives a direct measurement of the square of the electric field (E^2) distribution in the material coupled to the applicator.

The previous discussion has mentioned the dependence of the antenna pattern on the operating frequency, dimensions and geometry of the guide and the dielectric loading of the guide. The last point to be mentioned in this chapter is the effect of the observed tissue on the antenna pattern. In 1980 Edenhofer computed the near-field characteristics of a rectangular wave-guide antenna in contact with planar layers of tissue. His tissue model consisted of a surface layer of skin 2mm thick over a 5mm layer of fat followed by an infinite layer of muscle. The guide was loaded with a dielectric material with dielectric constant, 10 and its dimensions were 6.2 × 3.1 cm at 1GHz and 2.3 × 1.1 cm at 3GHz. He found that at 3GHz only about 13 % of the signal originated in the muscle layer (power was attenuated by e^{-2} by 0.67cm

of tissue). At 1GHz the same attenuation required 1.9cm of tissue. However, the electrically effective lateral area of tissue which contributed to the signal was 11cm^2, compared with 1.25cm^2 at 3GHz. This shows that there is a marked decrease in spatial resolution which accompanies an improved penetration depth at lower frequencies.

CHAPTER 5.0 COMBINED THERMAL HEAT TRANSPORT AND MICROWAVE RADIATION ANALYTICAL MODELLING.

5.0 Introduction.

It has been shown that combining thermal heat transport and microwave radiation analytical models of body tissue regions allows an equivalent physiological heat supply to the tissues to be estimated from temperature measurement data (Brown, 1989). This chapter will consider thermal and microwave modelling, why combined modelling is possible, the heat loss processes at the skin surface and the relationship of thermal conductivity of tissues to their water content.

5.1 Thermal heat transport modelling.

For the anatomical structures considered in this research, thermal modelling to determine $T(z)$, the temperature at a depth z into tissue, using appropriate tissue thermal conductivities, surface heat loss mechanisms to the surrounding environment, and assuming heat supply to the tissues from arterial blood and metabolic activity is well described by the 1-dimensional equilibrium Fourier equation for $T(z)$,

$$\frac{d^2T(Z)}{dz^2}+\frac{\omega_b c_b}{K}(T_{art}-(T(z)))+Q=0 \qquad 5.1.1$$

where c_b is the specific heat of blood, $(J\,kg^{-1}K^{-1})$

ω_b is the rate of supply of arterial blood at temperature, T_{art} to the tissue, $(\mathrm{kg}\,m^{-3}s^{-1})$

K is the tissue thermal conductivity, $(Wm^{-1}K^{-1})$

and Q is the metabolic heat production in the tissue, (Wm^{-3}).

The first term of Eqn. 5.1.1 represents the conduction of heat through the tissue, the second term represents the energy transfer to tissue by blood perfusion and the third term is the energy supplied by metabolic heat generated in the tissue itself. It should be noted that a number of assumptions must be made to ensure the validity of Eqn. 5.1.1. These assumptions are

1. The exchange of heat between the blood and tissue takes place entirely in the capillary bed and that this exchange is complete resulting in the tissue and the blood reaching the same temperature.

2. Heat exchanges between large blood vessels and the surrounding tissue and artery-vein pairs are neglected.

and, finally,

3. There is no net directionality involved in the capillary blood flow.

The most important of these assumptions is that the exchange of heat between blood and tissue takes place entirely in the capillary bed.

At the skin surface boundary, Newtonian cooling of the form

$$E(T_s - T_{amb}) \qquad 5.1.2$$

can be assumed, where T_S is the surface temperature and T_{amb} is the temperature of the surrounding environment. The heat loss processes of radiation, convection and evaporation determine the cooling coefficient, E. Of these radiation and convection are the dominant

processes. Evaporative cooling is known to be of the order of only a few percent of the total heat loss for the resting body at normal room temperature.(Draper & Boag, 1971).

The following subsections will determine the cooling coefficient, E, where

$$E = E_{radn} + E_{conv} + E_{evap} \qquad 5.1.3$$

The above terms in Eqn. 5.1.3 correspond to the processes just listed.

5.2 Heat loss by radiation.

The net rate of heat loss per unit surface area of a body with a surface temperature, T_s, surrounded by walls at a temperature, T_{amb}, is given by the Stefan-Boltzmann Law to be

$$e_{radn} = \sigma_s e(T_s^4 - T_{amb}^4) \qquad 5.2.1$$

where σ_s is stefans constant $(5.67 \times 10^{-8}\ \mathrm{W}m^{-2}K^{-4})$ and e is the emissivity of the skin surface which is close to 1, since skin behaves very similarly to a black body.(Chapter 1.0).

In a stable environment the temperature difference $(T_s - T_{amb})$ will be small compared to the mean absolute temperature, where

$$T_{mean} = \frac{1}{2}(T_s - T_{amb}) \qquad 5.2.2$$

and Eqn. 5.2.1 can be put in the approximate form

$$e_{radn} = 4\sigma_s e T_{mean}^3 (T_s - T_{amb}) \qquad 5.2.3$$

The radiative heat transfer coefficient is then defined to be

$$E_{radn} = 4\sigma_s e T_{mean}^3 \qquad 5.2.4$$

This gives an estimated radiative heat transfer coefficient of $6.0 Wm^{-2}C^{-1}$. (Draper & Boag, 1971).

5.2.1 Heat loss by convection.

Heat loss by convection is due to the transport of heat away from the skin surface by the movement of air surrounding the body. The rate of convection heat transfer is governed by a number of factors including humidity, air density, viscosity , specific heat capacity, thermal conductivity and temperature coefficient of expansion. These variables may grouped into dimensionless quantities which each describe a particular aspect of the air behaviour important in convection.(Brown) When the skin to ambient temperature difference is small the rate of convective heat flux per unit surface area can be expressed in the form

$$e_{conv} = E_{conv}(T_s - T_{amb}) \qquad 5.2.1.1$$

where E_{conv} is calculated using engineering formulae since the body can be approximated to by cylinders of different sizes. For this study, the coefficient of convective heat transfer was calculated using the following (Mcadams, Heat Transmission)

$$E_{conv} = 0.38(T_s - T_{amb})^{.25} \qquad 5.2.1.2$$

This gives an estimated heat transfer coefficient of approximately $4.0 Wm^{-2}C^{-1}$, also Draper & Boag, 1971.

5.2.2 Heat loss by evaporation.

This is the removal of heat from the body surface by water leaving the surface. Water leaves human skin by two processes, diffusion and sweating. However, in most normal clinical environments no sweating should occur and so heat loss will be due only to diffusion. This diffusion is in the form of insensible perspiration (Buettner, 1953). The approximate value of the heat transfer coefficient can be taken as $0.8 Wm^{-2}C^{-1}$. This heat loss does not obey Newton's Law but is very small compared to radiative and convective losses (Draper & Boag, 1971).

5.2.3 Total heat loss.

By summing the heat transfer coefficients for radiation, convection and evaporation the total estimated heat loss at the skin surface is approximately $11 Wm^{-2}C^{-1}$ for the skin to ambient temperature differences of about 10C applicable for the studies undertaken.

Variation of this coefficient with surface curvature is estimated to be of the order of only about 5% for the measurement situations applicable to this work. The variation in heat loss due to local ambient temperature variations around the body will be of a similar order.

5.3 Microwave radiation analytical modelling.

As previously discussed in Chapter 2.0, the microwave temperature signal observed on the skin surface is a result of the summation of the emitted radiation at all interior points reduced by a weighting factor of the approximate form, $e^{-2\alpha z}$, which takes into account the microwave attenuation factor, α of the tissue. For a region of uniform material, depth d, the microwave temperature is then

$$S = 2\alpha \int_0^d T(z) e^{-2\alpha z} dz \qquad 5.3.1$$

It should be noted that the α values will be the effective attenuation factors discussed for antenna modelling measurements. The resultant intensity from several different tissue regions such as skin, muscle and fat can be calculated by an extension of Eqn. 5.3.1, taking into, account the inter-regional reflections due to impedance changes and signal attenuation across different tissue regions gives a temperature of

$$S = 2\alpha_1 t_{01} \int_0^{d_1} T(z) e^{-2\alpha_1 z} dz + 2\alpha_2 t_{12} \int_{d_1}^{d_2} T(z) e^{-2\alpha_2 z} dz + \cdots\cdots 5.3.2$$

where α_1, α_2 etc are power attenuation constants and $t_{01,}$ t_{12} are the transmission coefficients. Theoretical modelling of the radiometer antenna spatial response shows a more complex behaviour than the above close to the antenna, but experimental measurements have shown that the dominant features of the response are of the form given above. With the attenuation coefficients α_1, α_2 etc, appropriate to the tissue antenna combination used.

Now if microwave thermography measurements are to accurately detect internal body patterns, the contribution from the skin which is essentially of the form

$$\left(1-e^{-2\alpha z}\right) \qquad 5.3.3$$

must be a small fraction of the total thermal signal (Land, 1987). Fig. 5.0 shows the variation of this skin contribution to the total temperature signal between 1 and 10GHz for skin tissue thicknesses of 1mm and 2.5mm. It is seen that the fraction of the total signal due to skin is approximately 0.12 and 0.29 at skin thicknesses of 1mm and 2.5mm respectively at 3GHz. This illustrates the importance of measuring at the lowest possible frequencies consistent with adequate spatial resolution.

5.4 Is combined modelling possible?

In the previous sections thermal heat transport and microwave radiation analytical models have been considered. The important question to be asked is - is there any relationship between the two models ? Fig. 5.1 shows the connection between the thermal and microwave models. There is a common dependence on geometry, anatomy, and tissue distribution, and both models must share the same temperature pattern. Provided it is possible to relate uniquely the tissue microwave and thermal properties, realistic combined microwave and thermal models can be used to estimate internal tissue thermal behaviour from temperature measurements made at the body surface.

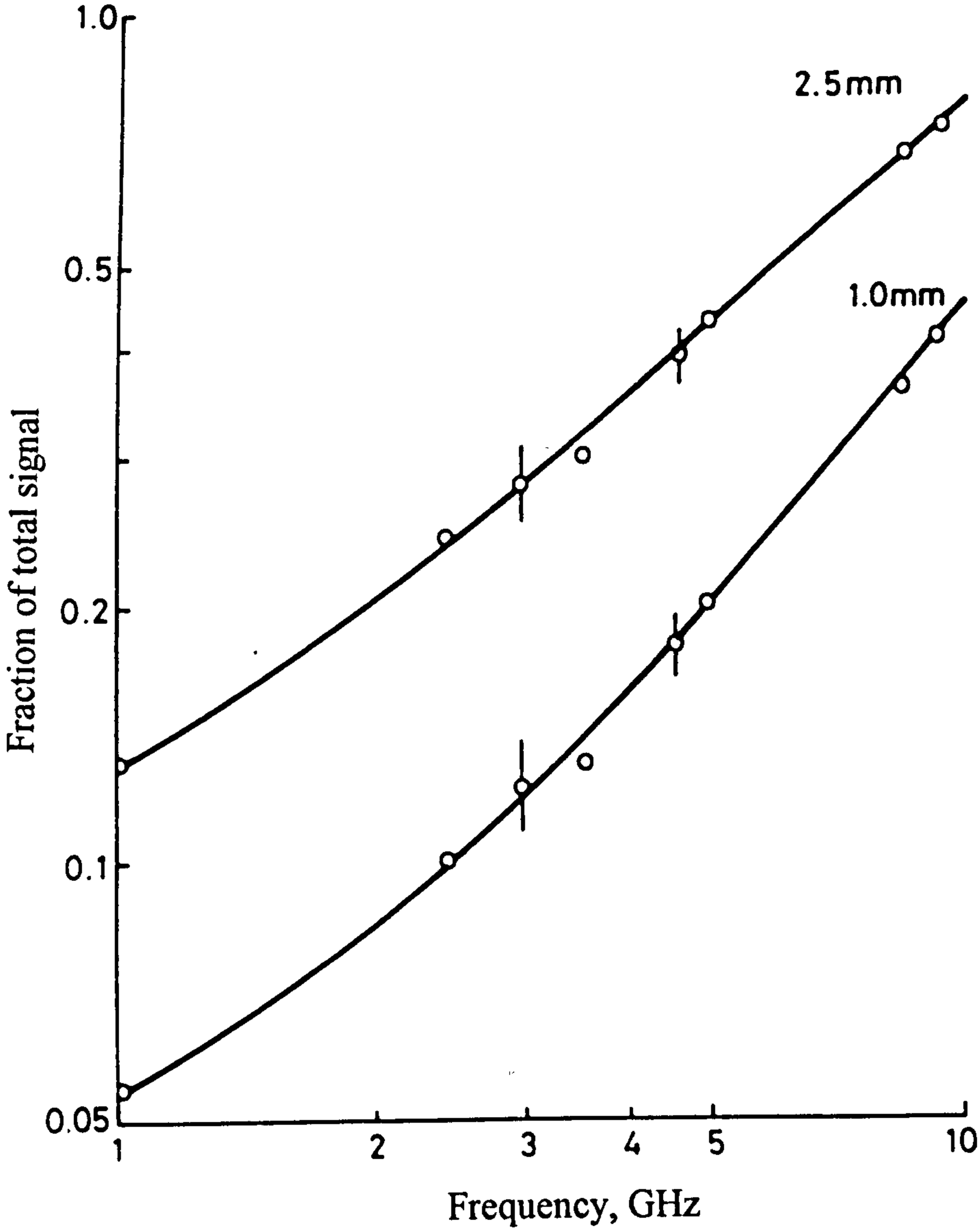

Fig. 5.0 Skin contribution to total microwave thermal radiation signal for skin thickness of 1mm and 2.5mm.

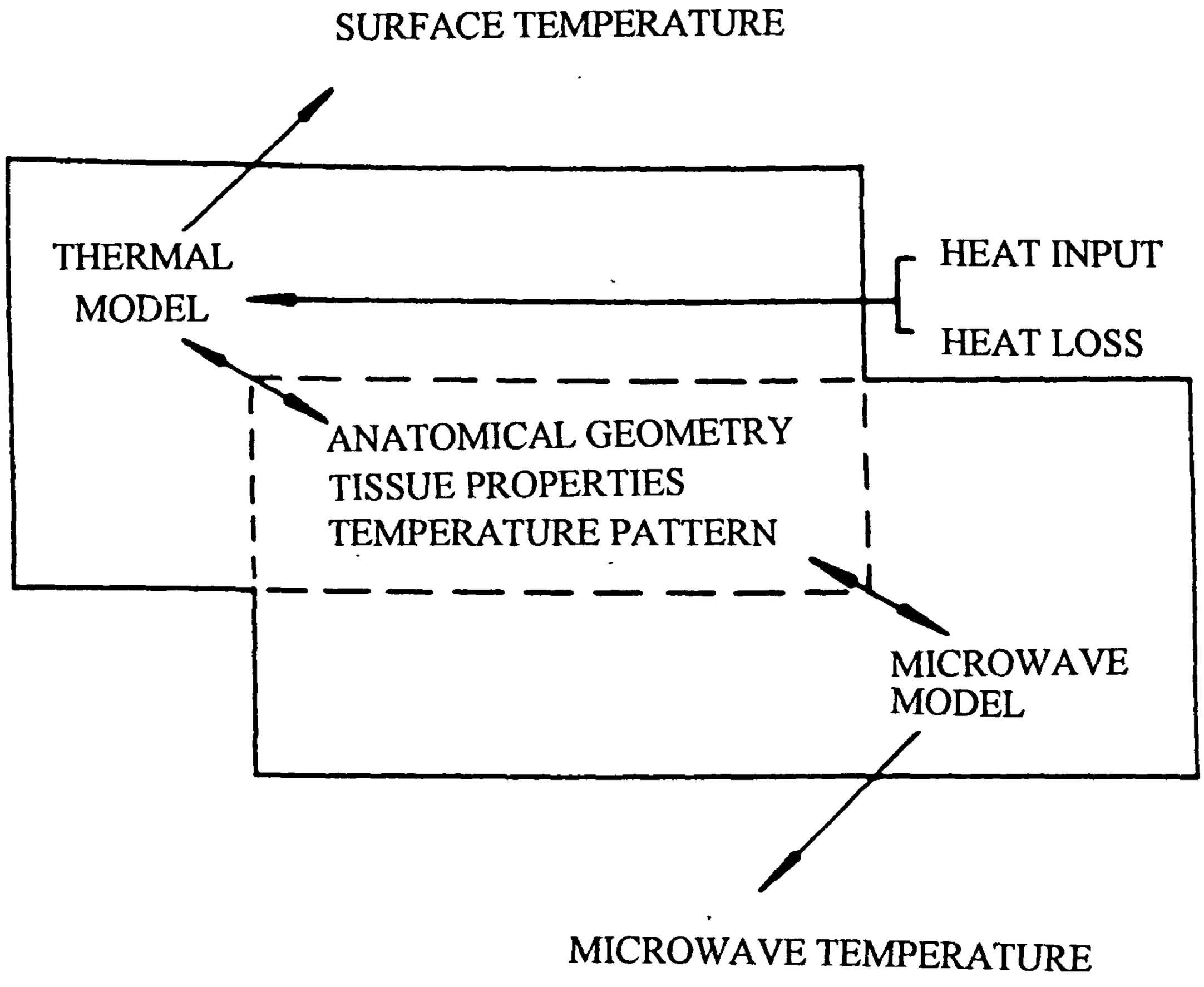

Fig. 5.1 Relationship of the microwave and thermal components of the body tissue modelling.

5.5 Tissue thermal conductivity.

As shown in Chapter 3, the water content of tissue determines the dielectric properties. All "conduction" type properties can be expected to follow similar mixture equation behaviour, so, it is therefore expected that the water content of tissues will determine the thermal conductivity in a similar manner. Water has the highest thermal conductivity of soft biological tissue components, 0.623 $Wm^{-1}K^{-1}$ at 37C. Table 5.0 shows values of the thermal conductivity of tissues important to this research. Fig. 5.2 illustrates these measured thermal conductivities as a function of water content. The high thermal conductivity of bone is due to its mineral content. The low dielectric loss of bone is due to its water content.

5.6 Tissue microwave and thermal behaviour.

Table 5.1 gives measured thermal and microwave properties for various biological tissues. A possible relationship between tissue microwave and thermal behaviour is shown in Fig. 5.3. There has been a limited amount of research into this relationship and so the only conclusion which can be reached from Fig. 5.3 is that there is likely to be a general trend between the microwave attenuation and thermal conductivity.

All "conduction" type properties of a solid mixture of materials can be expected to show the same general form of variation of the conduction properties with the variation of the relative properties of the materials mixture components. Possible forms of the variation have been considered and compared with observed behaviour for the microwave properties (Campbell, 1992). For both microwave and thermal

Tissue	Thermal conductivity ($Wm^{-1}K^{-1}$)	Reference	Year
Whole blood	0.51	Spells	1960
Muscle	0.41	Lipkin	1954
	0.44	Hatfield	1953
Skin	0.39(living)	Lipkin	1954
	0.32(excised)	Lipkin	1954
Fat	0.22	Lipkin	1954
	0.20	Hatfield	1953
Bone	0.8	Kirkland	1967
Water	0.62	CRC Handbook	1977

Table 5.0 Thermal conductivities of human tissue at 37C.

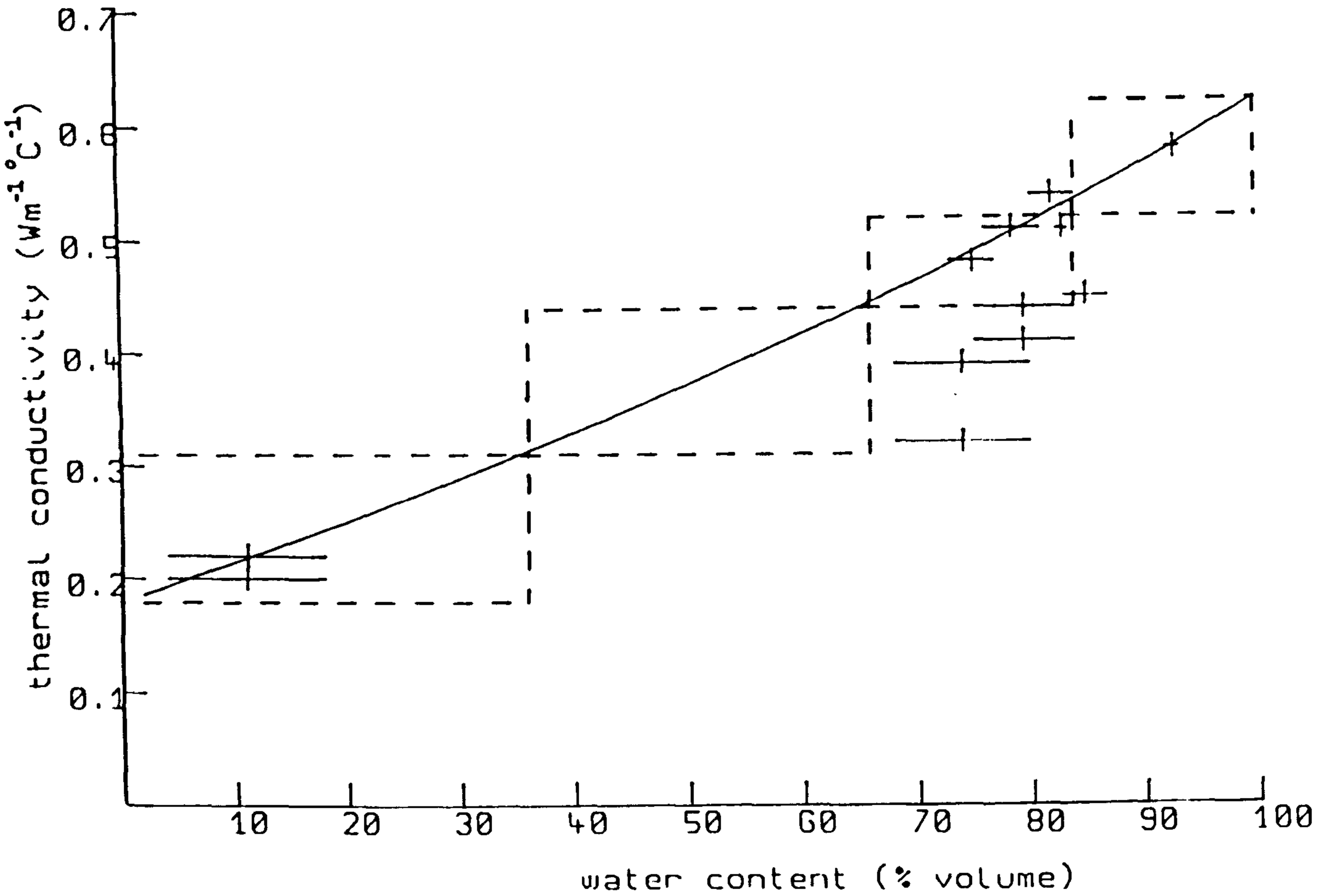

Fig. 5.2 Variation of thermal conductivity with water content for human tissues at 37C (from Brown, 1989).

Tissue	Thermal conductivity ($Wm^{-1}K^{-1}$)	Dielectric constant, ε_r'
Water	0.62	77
Blood	0.51	53 - 56
Muscle	0.41 - 0.44	45 - 52
Fat	0.20 - 0.22	3.9 - 11.6
Bone	0.8	7.5 - 8.35

Table 5.1 Comparison between tissue thermal and microwave properties.

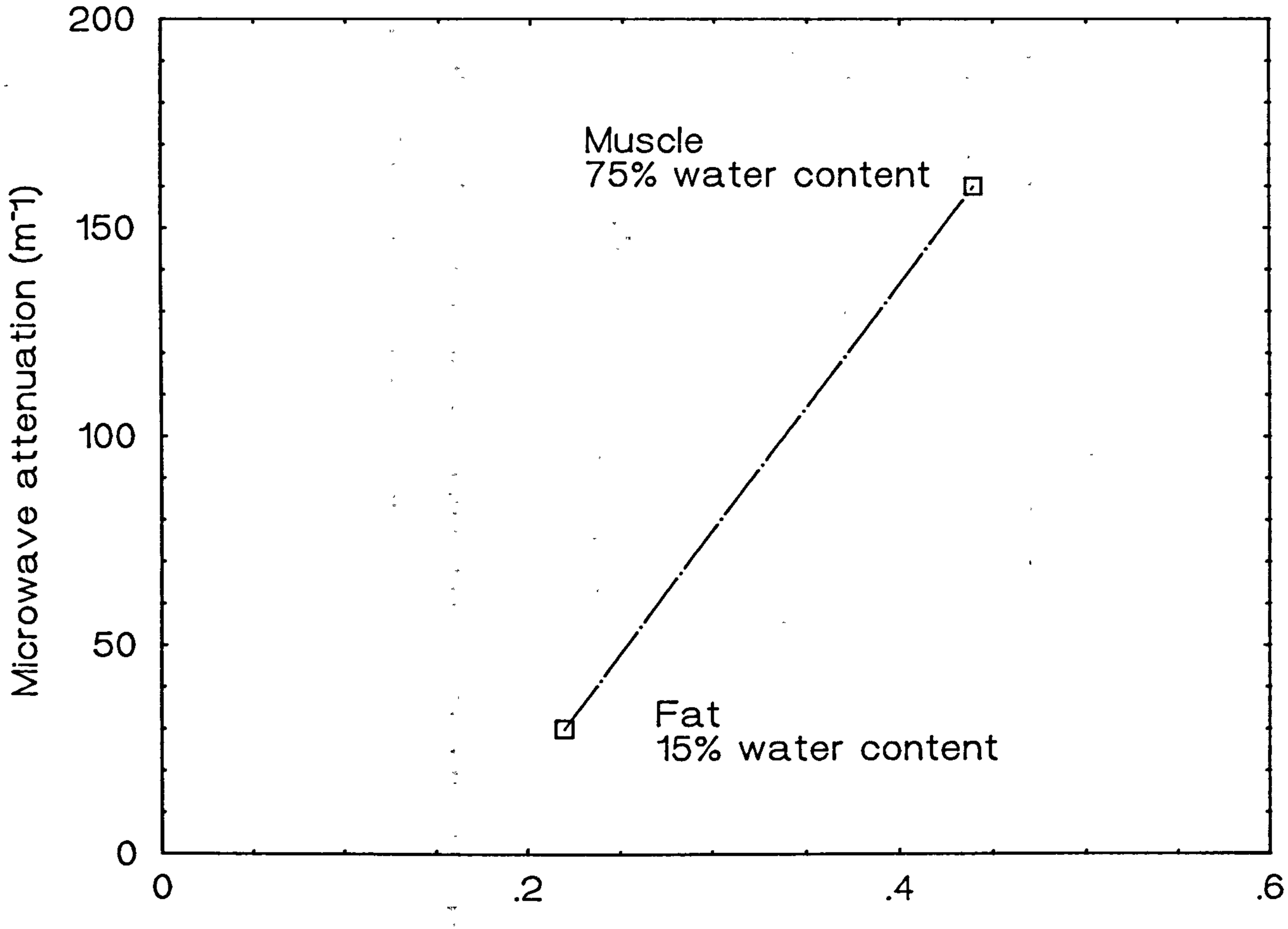

Fig. 5.3 Tissue microwave and thermal behaviour.

properties the variation with tissue water content will dominate in soft tissues through the high relative permittivity/loss factor and thermal conductivity of water in comparison with tissue fat and protein components.

Translating the microwave complex permittivity variation into the equivalent radiation attenuation coefficient at 3GHz gives Fig. 5.4.

Bone appears to have distinctly different behaviour. The water content is low, but the mineral content has a high thermal conductivity and a low microwave attenuation. Again, however, there is reasonably defined, related microwave and thermal behaviour (Land, unpublished measurements).

5.7 Solution to the one -dimensional Fourier Equation.

The solution to Eqn. 5.1.1, assuming a boundary equation at the surface given by

$$K\frac{dT}{dz} = E(T_s - T_{amb}) \qquad \text{at} \quad z=0 \qquad 5.7.1$$

and the condition that the temperature tends to be a finite value as the depth in the tissue increases is given by

$$T(z) = \left[\frac{(T_{amb} - T_c)}{\left(1+\left(\frac{K\beta}{E}\right)\right)}\right] e^{-\beta z} + T_c \qquad 5.7.2$$

where $$T_c = T_{art} + \frac{Q}{\omega_b c_b} \qquad 5.7.3$$

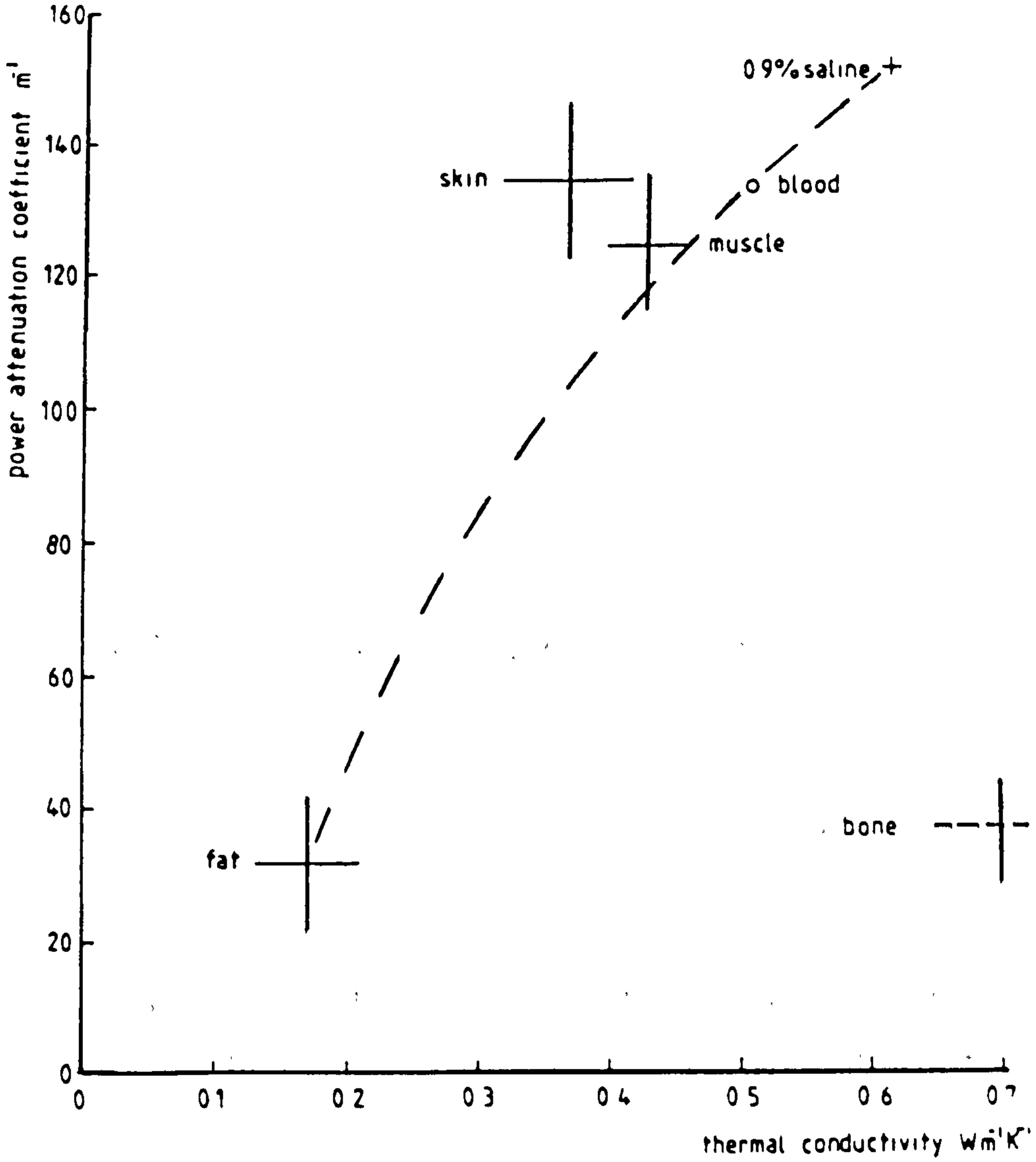

Fig. 5.4 The variation of microwave attenuation and thermal conductivity for soft tissues due to the common dependence on tissue water content.

is the core temperature and

$$\beta = \sqrt{\frac{\omega_b c_b}{K}} \qquad 5.7.4$$

This equation describes the temperature distribution in the tissue and from this the measured microwave temperature may be determined. Similarly, the surface temperature is given by

$$T_s = \frac{(T_{amb} - T_c)}{(1 + {}^{K\beta}/_{E})} + T_c \qquad 5.7.5$$

for a single region of tissue.

It is clear from Eqn. 5.7.5, that the surface temperature is dependent on $(T_{amb} - T_c)$, the effective thermal resistance of the perfused tissue, Z_t, where

$$Z_t = \frac{1}{K\beta} = \frac{1}{\sqrt{\omega_b c_b K}} \qquad 5.7.6$$

and, in series with this, the thermal resistance between the skin and the environment given by the inverse of the heat transfer coefficient, E. There is an elevation of skin surface temperature as the effective thermal resistance is decreased, which occurs with increasing thermal conductivity and/or perfusion.

The above descriptions, though simplified, can provide useful measures of the body's behaviour of *thermal resistance* and *effective perfusion.* The reasonably known surface heat loss coefficient is

providing a thermal resistance standard which allows the measures to be estimated.

5.8 Microwave temperatures at the surface of a single region.

The operation of the radiometer and its antenna is assumed to be such as to make a true measure of the microwave radiation temperatures at the skin surface.

For a single region this will be given by

$$T_{mw} = \int_0^\infty 2\alpha T(z) e^{-2\alpha z} dz \qquad 5.8.1$$

as stated in section 5.3.1.

If the temperature variation is of the form

$$T(z) = T_c - (T_c - T_s)(1 - e^{-\beta z}) \qquad 5.8.2$$

where T_c is the deep core tissue temperature and T_s the surface temperature, then

$$T_{mw} = 2\alpha T_c \int_0^\infty e^{-2\alpha z} dz - 2\alpha (T_c - T_s) \int_0^\infty (1 - e^{-2\beta z}) e^{-2\alpha z} dz$$

5.8.3

which simplifies to

$$T_{mw} = T_c - \left(\frac{1}{1 + \beta/2\alpha} \right) (T_c - T_s) \qquad 5.8.4$$

This immediately indicates that if β and 2α are roughly similar, the microwave temperature should lie about mid-way between the core and surface temperatures.

Using the relationships of 5.7, Eqn. 5.8.4 can be rearranged to give

$$2\alpha K = E\left(\frac{T_c - T_{mw}}{T_{mw} - T_s}\right)\left(\frac{T_s - T_{amb}}{T_c - T_s}\right) \qquad 5.8.5$$

which is essentially, through the attenuation - thermal conductivity relation, a measure of the tissue water content.

With the water content estimated it is then possible to estimate the tissue arterial blood perfusion, since

$$\omega_b = \frac{E^2}{Kc_b}\left(\frac{T_s - T_{amb}}{T_c - T_s}\right)^2 \qquad 5.8.6$$

In practice it has proved most convenient to compute the variation of surface temperatures with microwave temperatures, using the assumed thermal-microwave tissue behaviour, for various ambient/core temperatures and plot them in the form of a grid covering the different water contents and perfusion values, Fig.6.7. Plots of subject's measured surface and microwave temperatures can then be overlaid with the grid and estimated effective tissue water contents and perfusions read off. The modelling has also been used to estimate the dependence of surface and microwave temperatures on ambient and subject core temperature changes.

The single region modelling has been compared with similar two-region analytical and numerical models and 2-dimensional finite-

difference computational modelling. For the tissue regions of most interest for these studies (limbs and breasts), the difference between the models were similar to or smaller than the uncertainties due to the present limited information about tissue thermal conductivity and the thermal-microwave behaviour relation (Land, Pers. comm.). The single region model based on estimates of tissue properties is therefore considered to be both reasonable and useful measures given the present knowledge of tissue properties.

CHAPTER 6.0 MICROWAVE THERMOGRAPHY IN RHEUMATOLOGY.

6.0 Introduction.

The aim of this chapter is to show the potential role of microwave thermography in the assessment and monitoring of disease activity in Rheumatology.

Rheumatology encompasses a broad spectrum of diseases including osteoarthritis, ankylosing spondylitis, rheumatoid arthritis and gout. This chapter applies to the study of patients with rheumatoid arthritis. Fig. 6.0 shows the distribution of affected joints in rheumatoid arthritis.

Objective assessment in rheumatology is a long standing problem. Assessment methods currently in use are described in 6.1 below.

In the rheumatology investigations microwave thermography has been used for the objective assessment of inflammation in the knee joints and wrist and finger joints of patients with rheumatoid arthritis (RA) by comparison with similar information obtained from a group of control subjects, assumed to be disease free.

With measured environmental, oral, microwave and infra-red surface temperatures, combined microwave and thermal modelling has been used to estimate an equivalent physiological heat supply to tissues.

6.1 Disease assessment in rheumatology.

Rheumatoid arthritis (RA) is a common inflammatory disease of joints. The affected areas are hot, swollen and painful at rest and show restricted painful movement (Deighton, C). In an inflamed area the blood flow

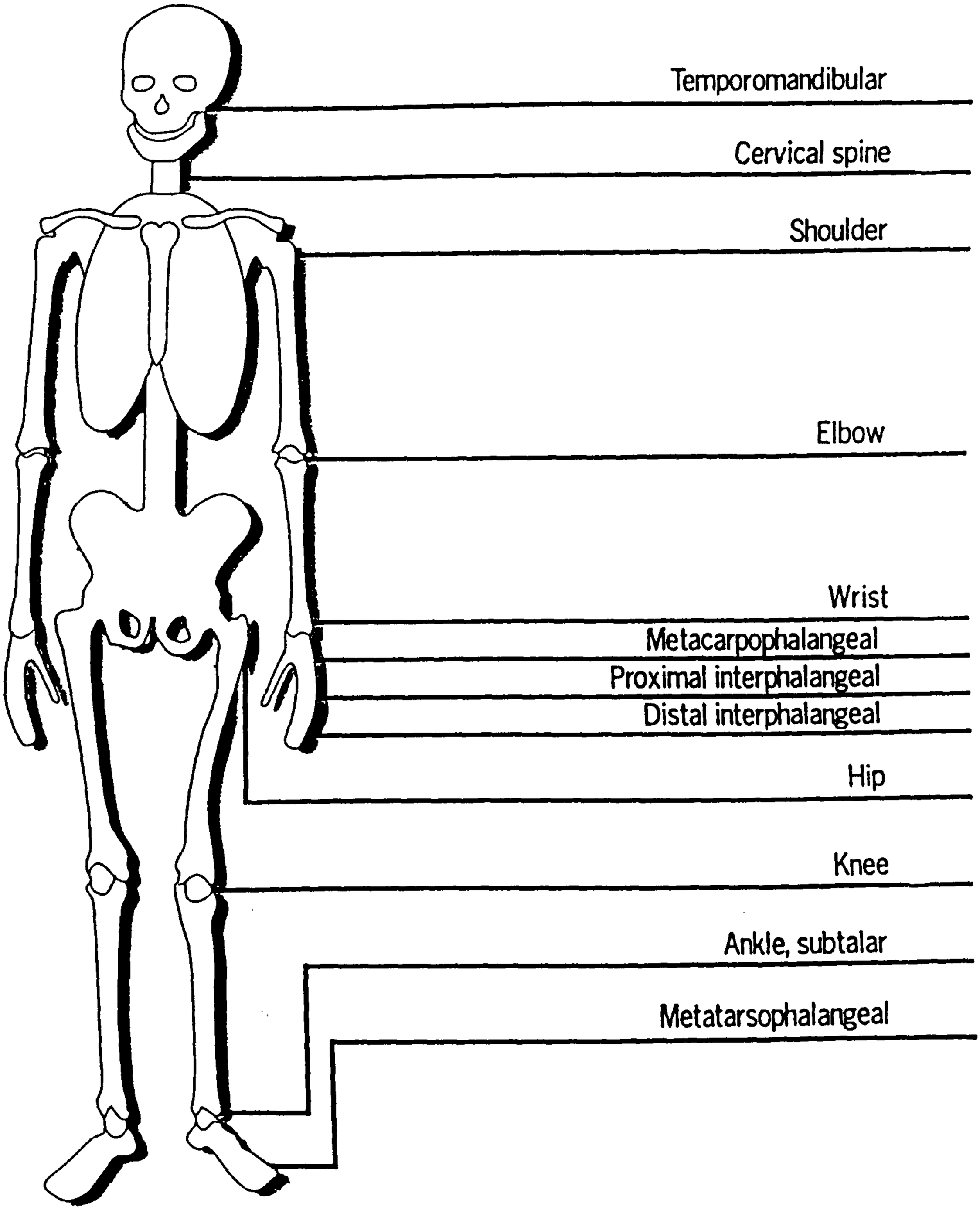

Fig. 6.0 Distribution of affected joints in rheumatoid arthritis.

increases resulting in heat and redness; fluid and cells leak into the tissue causing swelling. Therefore, the objective measurement of joint inflammation presents a problem due to "inflammation" involving multiple factors. As a result many methods have been developed for the accurate measurement of disease activity. These include clinical assessment, infra-red thermography skin temperature measurements and radio-nuclide measurements.

Simple measurements such as ringsize, grip strength, pain analogue scales and swollen/tender joint count have been used in an attempt to satisfy the criterion of an independent, reproducible, measure of inflammation.

However, the accuracy of clinical measurements are dependent on minimal inter- and intra- observer variation. They can be affected by other factors such as the time of day when the measurements are taken (Fraser, Land, 1987). Although clinical measurements may easily detect major changes in disease activity they are unsatisfactory for the detection of small changes in inflammatory activity.

Skin temperature patterns can be seen with infra-red thermography, so that diseases which affect superficial blood circulation produce clear changes which are usually shown by thermography. Infra-red thermography has been used for the last 20 years to measure skin temperature over inflamed joints. (Cosh & Ring, 1970). This technique is also used to monitor the patients response to drug treatments.(Collins & Cosh, 1970) However, difficulties in maintaining a stable environment

and physiological changes of skin temperature have limited the usefulness of this technique. (Salisbury et al, 1983).

Haimovici, 1982, developed an invasive method to directly obtain the intra-articular joint temperature. Basically the technique involved a thermocouple being inserted into the affected/normal joint. He showed that by obtaining a single temperature measurement from the intra-articular joint he was able to differentiate between a normal and diseased joint. This is, however, clearly an invasive technique causing the patient pain and/or stress, and requiring significant clinical skill to avoid infection and tissue damage.

Radio nuclide scanning is used as an index of inflammatory activity as it is able to give an independent, reproducible measure of disease activity (Pinals, 1983). Of the several different isotopes that are available the ^{99}-*Tc* uptake technique is most commonly used. (Dick et al, 1970; Patterson et al, 1978). A number of research groups have compared the technetium uptake technique with clinical assessment. Huskisson et al, 1973, found no correlation between the two techniques, but a number of groups did find a correlation.(Paterson et al, 1978; Dick and Grennan, 1976; Haataja et al, 1975 and De Silva et al, 1986).

6.2 Clinical investigations.

Recent clinical assessments of microwave thermography have been carried out at the Centre for Rheumatic Diseases, Glasgow Royal Infirmary. The studies have looked at knee, wrist and finger joints affected by inflammatory rheumatoid arthritis. Infra-red surface temperatures and

microwave temperature profiles were recorded across 88 "normal" resting knees and 60 resting knees of patients suffering from RA. Similar scans were taken across 48 "normal" hands/fingers and 48 hands/fingers of patients suffering from RA. The microwave antenna was held in contact with the skin surface and moved at a rate of 1cm/2.5secs. The skin surface temperature measurements were made using a commercial pyroelectric element infra-red thermometer. Oral and ambient temperatures were measured with thermistor and thermocouple thermometers. All thermometers were intercalibrated over the working temperature range using combined microwave - infra-red - contact calibration sources. Temperature measurement resolution was 0.1C or better. Inter-modal temperature intercalibration was approximately 0.2C or better.

Typical microwave temperature profiles for the knees and hand - fingers are shown in Figs. 6.1 and 6.2 respectively. Fig. 6.1 shows how an initial reference point at the centre of the patella was marked and a scaled line drawn to 16cm above the patella (Quadriceps muscle) and 8cm below the patella (Tibia). The fairly uniform temperature zone over the quadriceps muscle is used to provide a local, subject specific temperature reference with which the patella region temperature is compared. This comparison yields a "Microwave Thermographic Index" for the joint, which is proving to be a useful indicator of disease activity (Fraser, Land & Sturrock, 1987; MacDonald, 1994). Similarly, Fig. 6.2 shows how for the hand - fingers the scan is taken down the lateral surface of the forearm over the

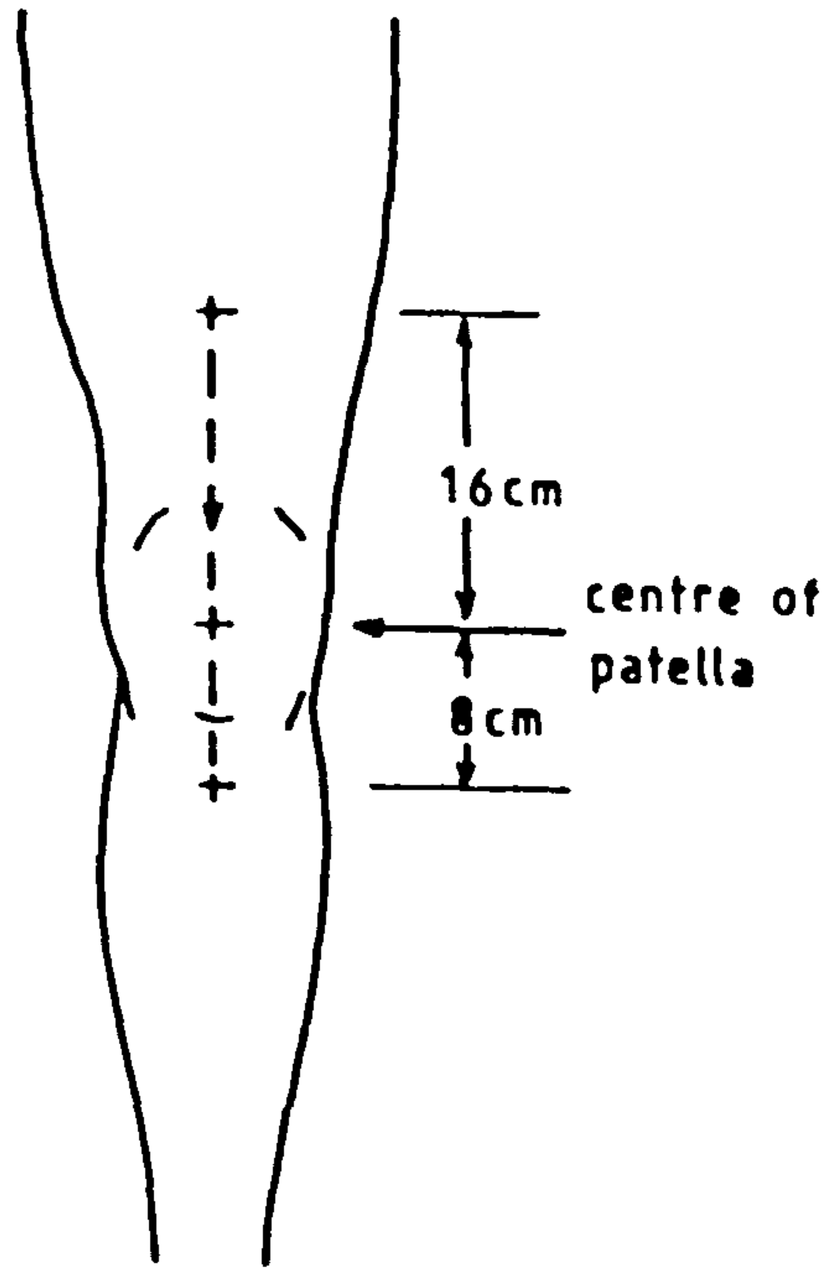

Knee scan outline

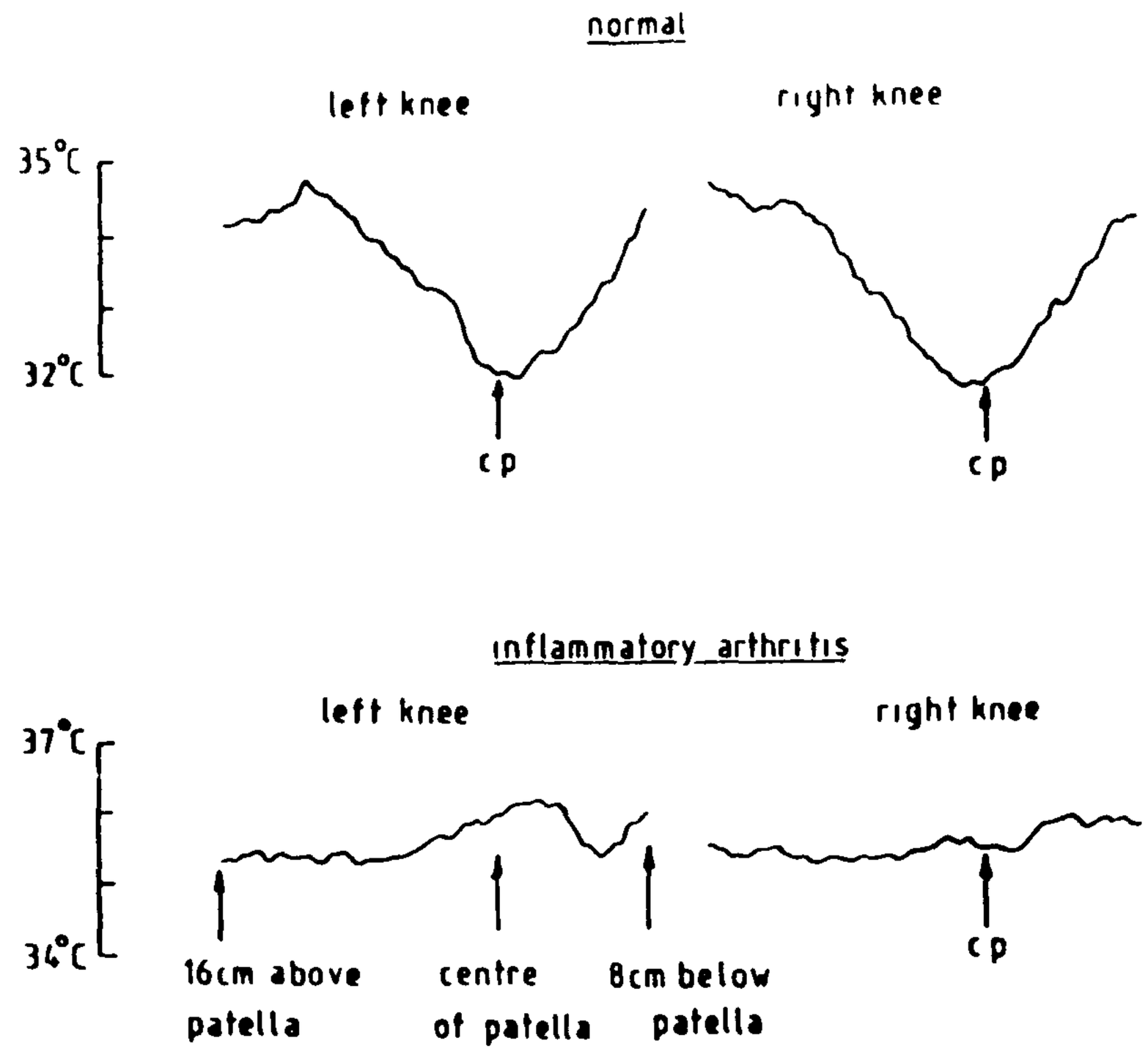

Fig. 6.1 Microwave temperature profiles taken across normal knees and knees affected by rheumatoid arthritis.

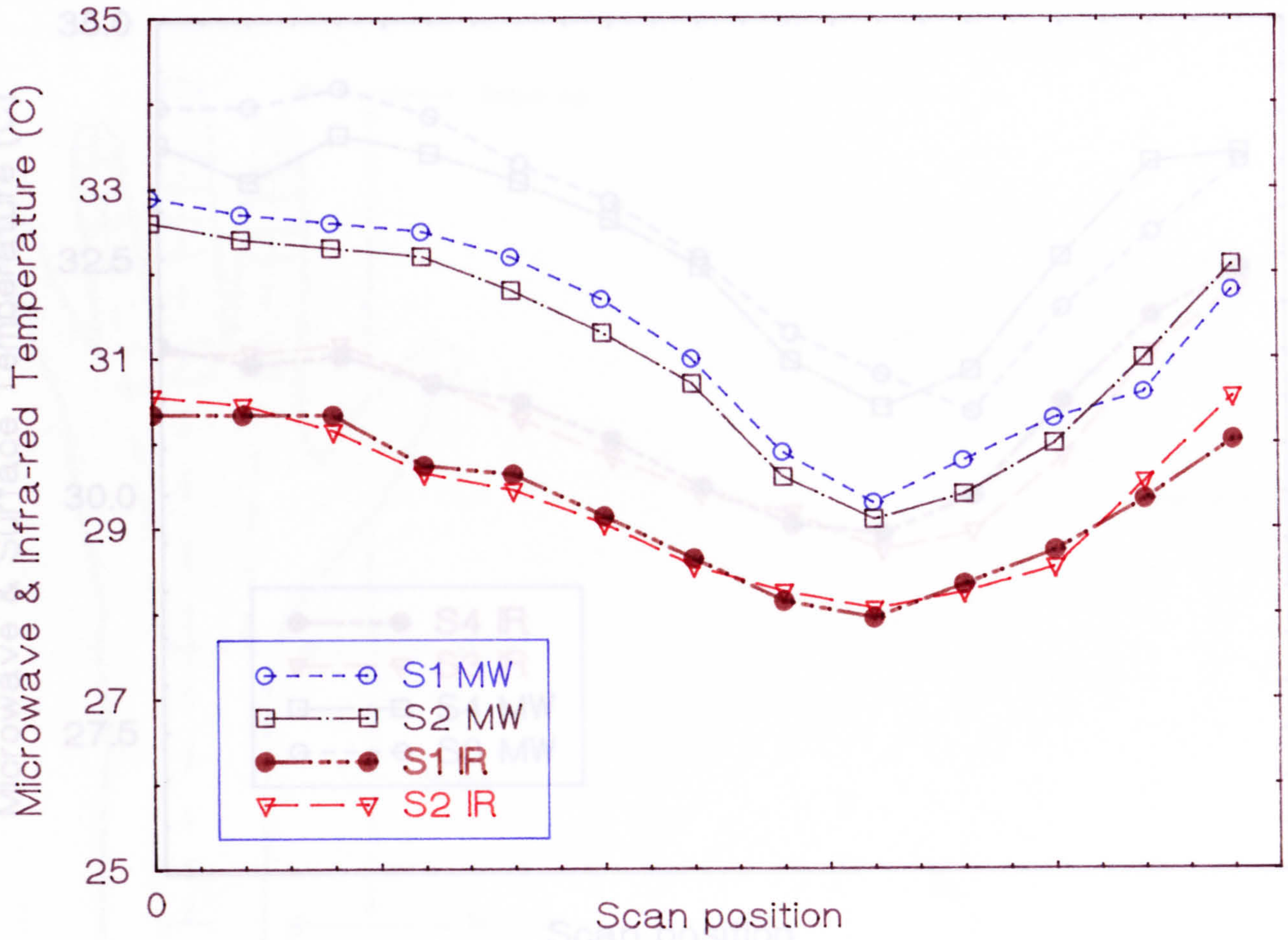

Fig. 6.1A Reproducibility of Quadriceps/Patella scan

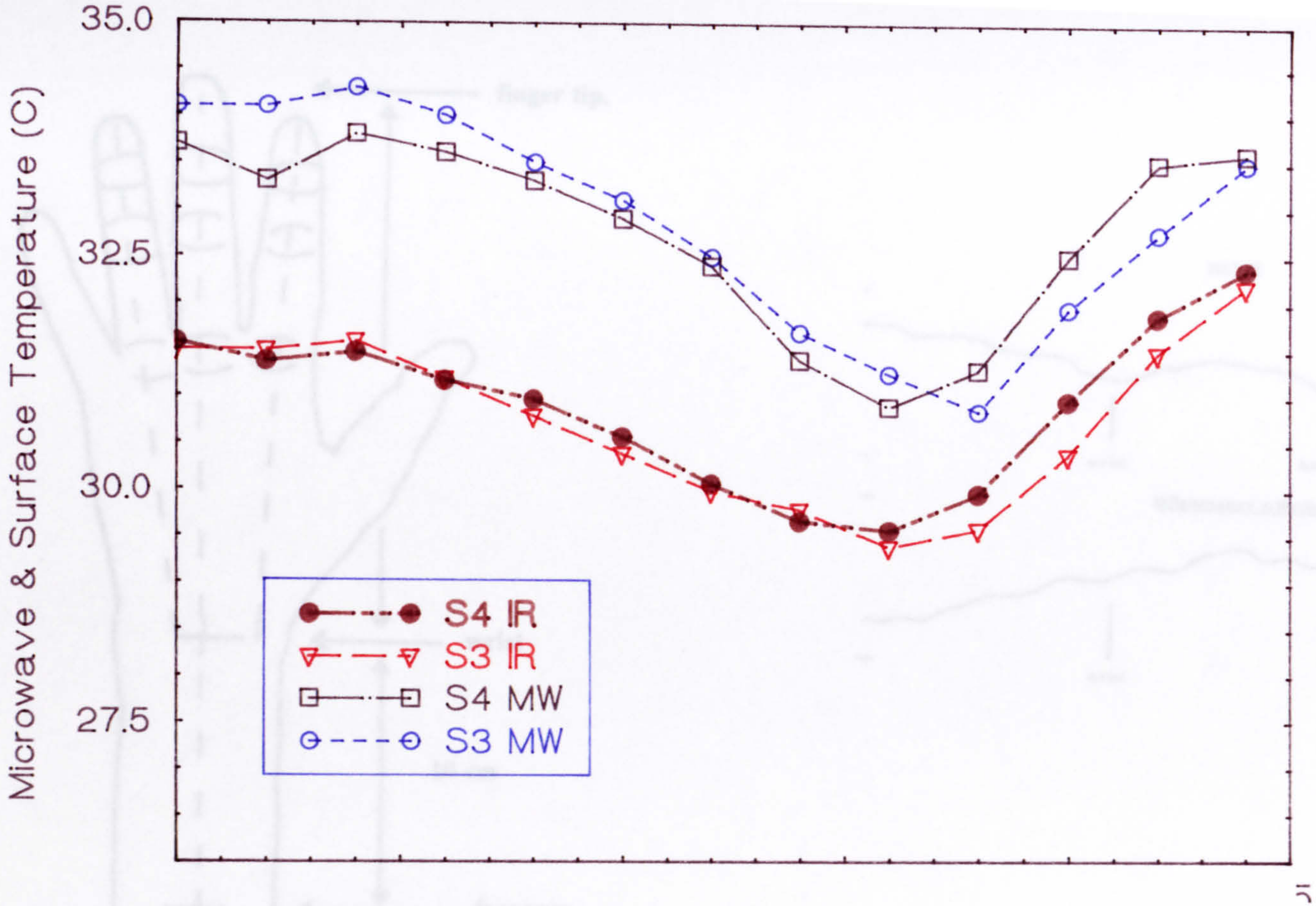

Fig 6.1B Reproducibility of Quadriceps/Patella scan

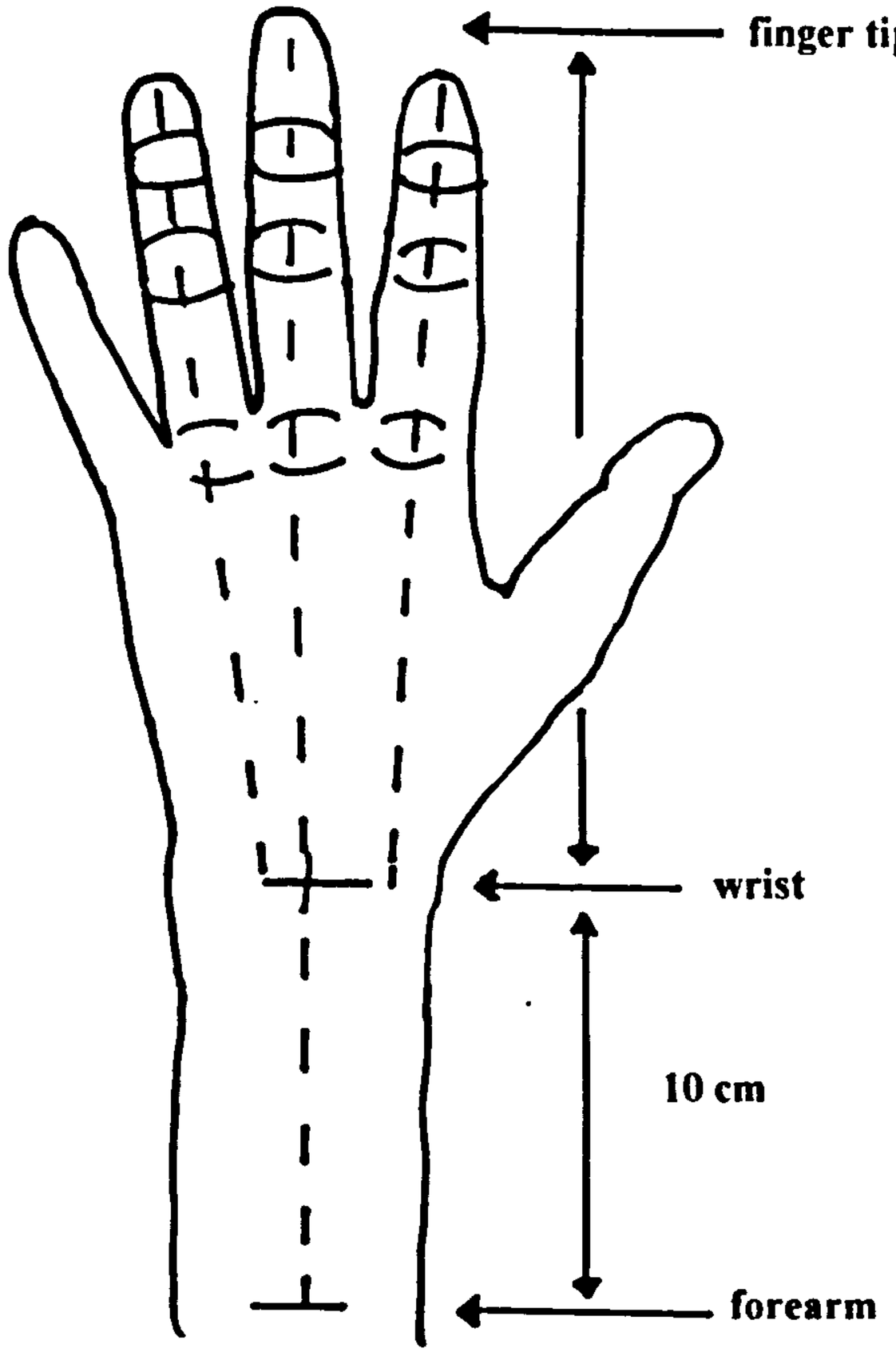

Hand/finger scan outline

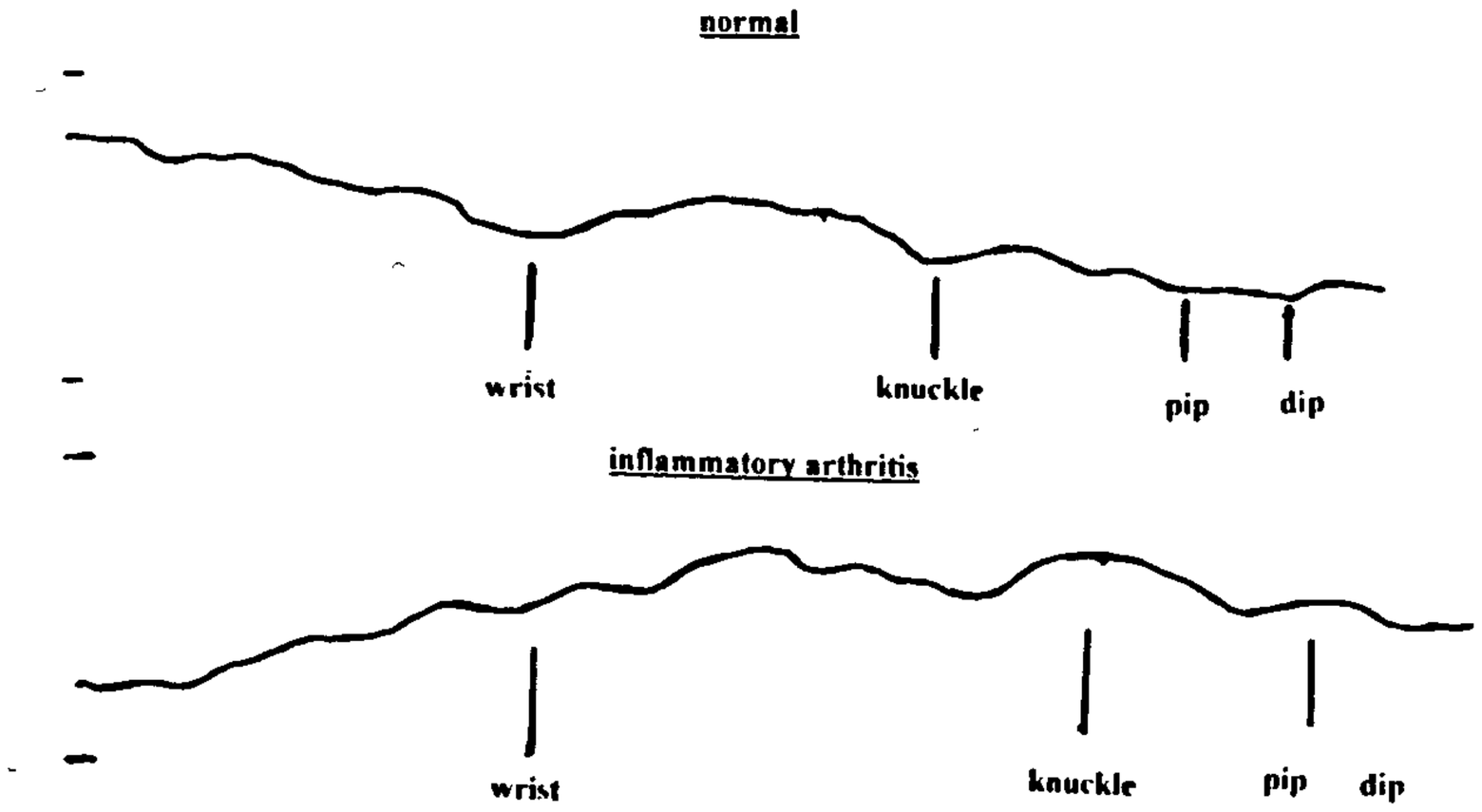

Fig. 6.2 Microwave temperature profiles taken across normal hands and hands affected by rheumatoid arthritis.

articulation of the wrist and down over the three central fingers, Index, Middle and Ring, in turn.

6.3 Estimation of equivalent physiological heat supply to the quadriceps and patella.

It has been shown in Chapter 5.0 that combining thermal heat transport and microwave radiation models of tissue regions allows an estimate of the physiological heat supply to tissues to be estimated from temperature measurement data.

The tissue temperature, T_t is assumed to be determined by a heat supply due to arterial blood perfusion, ω_b at T_{art}, and metabolic activity, Q, in total

$$\omega_b(T_{art} - T_t) + Q \qquad 6.3.1$$

with the tissue thermal conductivity and the region boundary conditions. This tissue temperature distribution with the microwave propagation properties of the tissues determines the microwave radiation temperatures measured at the skin surface. By measuring the surface and microwave temperatures and using the thermal and microwave modelling it is possible to make estimates of the heat supply to a volume of tissue. Changes in this heat supply are considered to be a good measure of inflammatory disease activity in that part of the body. Fig. 6.1 shows there is an elevation in temperature over the patella region in patients suffering from RA. Cosh and Ring, 1970 also noted an elevation of temperature over

inflamed joints using Infra-red thermography. Fraser et al, 1987 and MacDonald et al, 1994 also concluded that microwave thermography can measure inflammatory activity in the knee joints of patients suffering with RA. This increase in temperature over the patella region is probably due to an increase in both blood perfusion and metabolic heat production. However, the maximum temperature increase which can be caused by increased reasonable levels of metabolic heat production alone is estimated to be rather less than the microwave temperature increases seen. Also, no cases were observed where tissue temperature is driven above the arterial blood temperature which could occur if metabolic heat production were a dominant effect. So it can be deduced that the increase in microwave temperature over the inflamed joints is predominantly due to an increase in perfusion.

It is also likely that there is some degree of interdependence of metabolic heat production and tissue perfusion, so the heat deposition and production within a tissue region can then be reasonably expressed in terms of an "effective perfusion". It is considered that this increase in effective perfusion may provide a clinically useful measure of disease activity.(Land, 1987; Kelso et al, 1995)

6.4 Estimation of effective perfusion.

With measured environmental, oral, microwave and infra-red surface temperatures, combined microwave and thermal modelling has been used to estimate the effective blood supply to the quadriceps muscle and the anterior intra-articular region of the patella, in both "normal" knee joints

and knee joints affected by RA. In the modelling, the metabolic heat term, Q of Eqn. 6.3.1 is assumed to be part of a total heat supply represented by an effective perfusion term $\omega_b c_b (T_{art} - T_t)$. 1- dimensional analytical and 1- and 2- dimensional numerical models have been used based on the relations given in Chapter 5.0.

6.4.1 Results.

As mentioned in 6.3 infra-red surface temperatures and microwave temperature profiles were recorded across 80 "normal" resting knees and 60 resting knees of patients suffering from RA. An example of a typical microwave temperature profile taken longitudinally down the quadriceps muscle and over the patella is given in Fig. 6.1. The measured values of microwave and infra-red surface temperatures recorded over the quadriceps muscle for both "normal" subjects and patients suffering with RA are given in Figs. 6.3 and 6.4 respectively. It was initially expected that the microwave and surface temperatures over the quadriceps region of both groups would be similar, however by comparing Figs 6.3 and 6.4 it is clear that higher surface and microwave temperatures were recorded over the RA subjects quadriceps. It is thought that this may be due to an increase in upper limb perfusion as a result of the severe joint inflammation. Figs. 6.5 and 6.6 show the measured values of microwave and surface temperatures over the centre of the patella for both "normal" subjects and patients with RA. Fig. 6.6 shows that for patients with RA the microwave and surface temperatures are greater. This is most

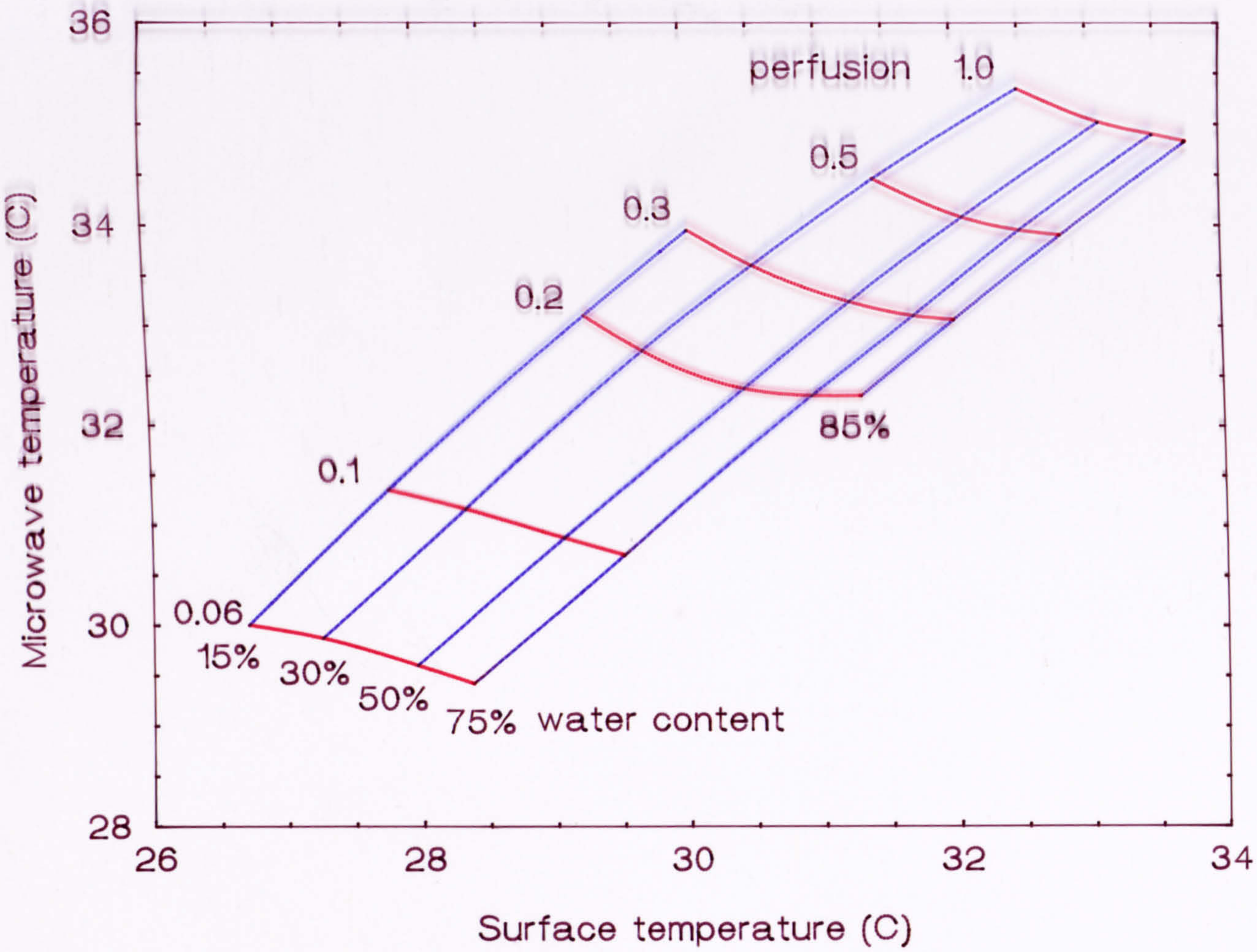
36
34
32
30
28
26
28
30
32
34
perfusion
1.0
0.5
0.3
0.2
0.1
0.06
85%
15%
30%
50%
75% water content
Microwave temperature (C)
Surface temperature (C)

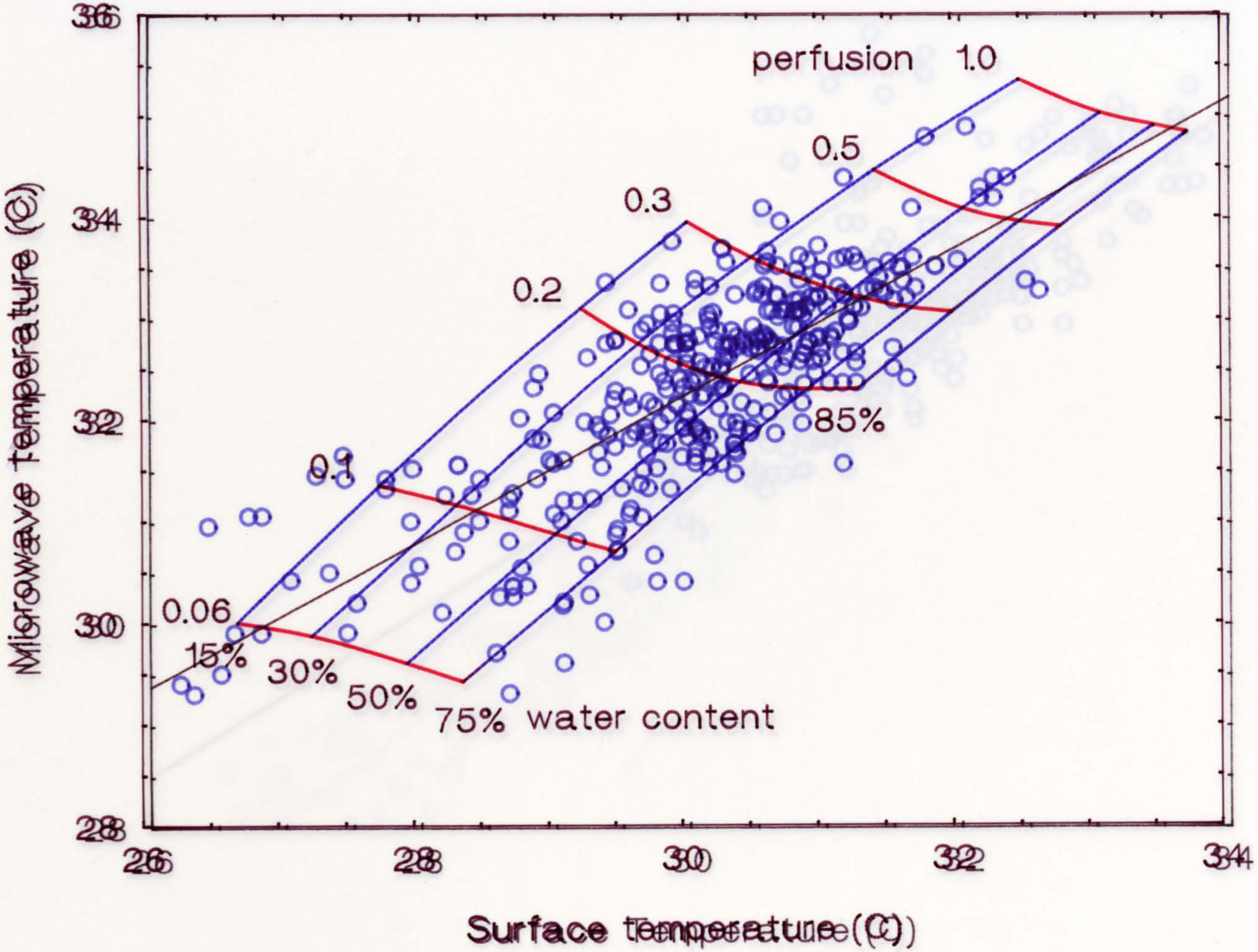

Fig. 6.3 Measured values of microwave and surface temperatures over the quadriceps muscle of normal subjects.

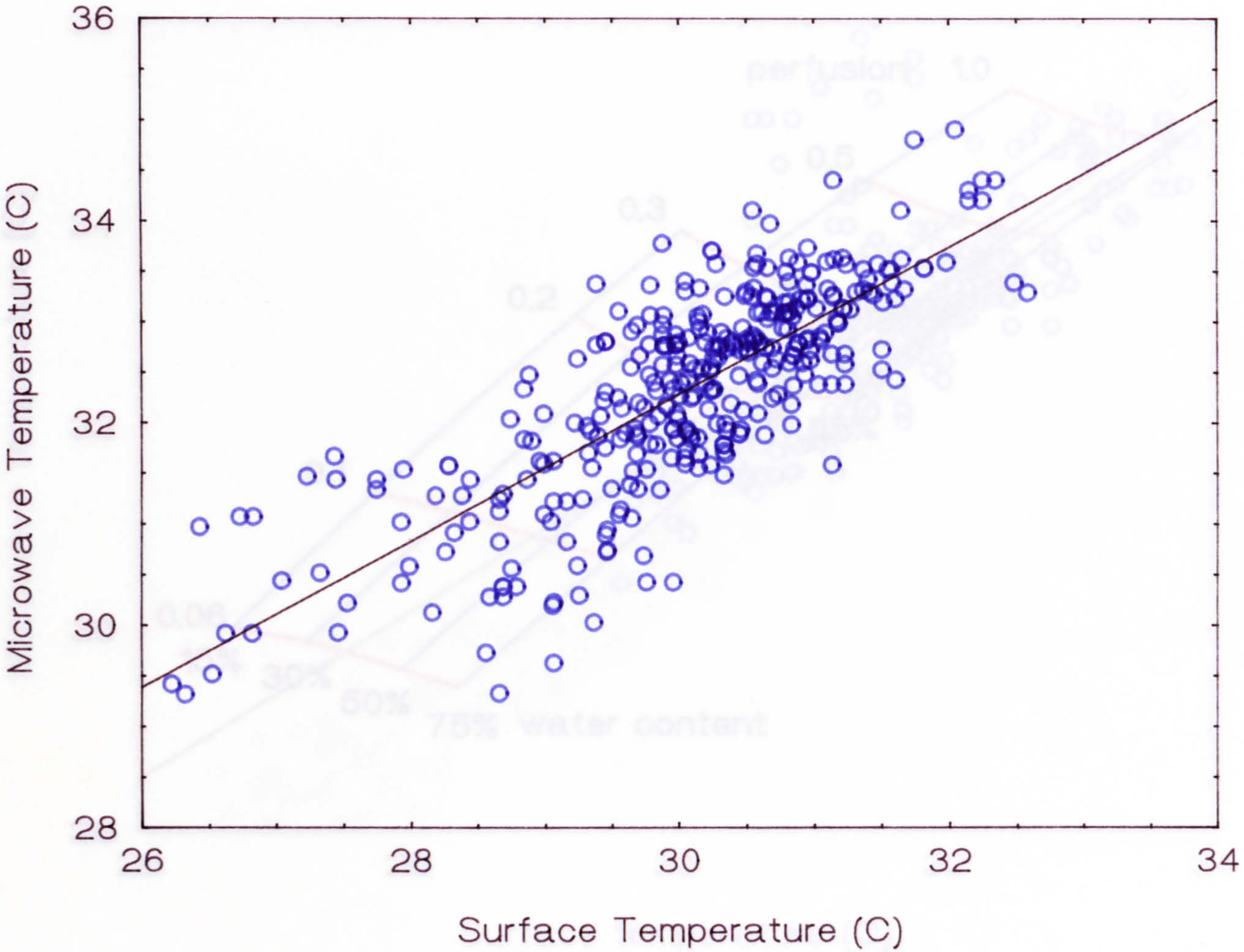

Fig. 6.3 Measured values of microwave and surface temperatures over the quadriceps muscle of normal subjects.

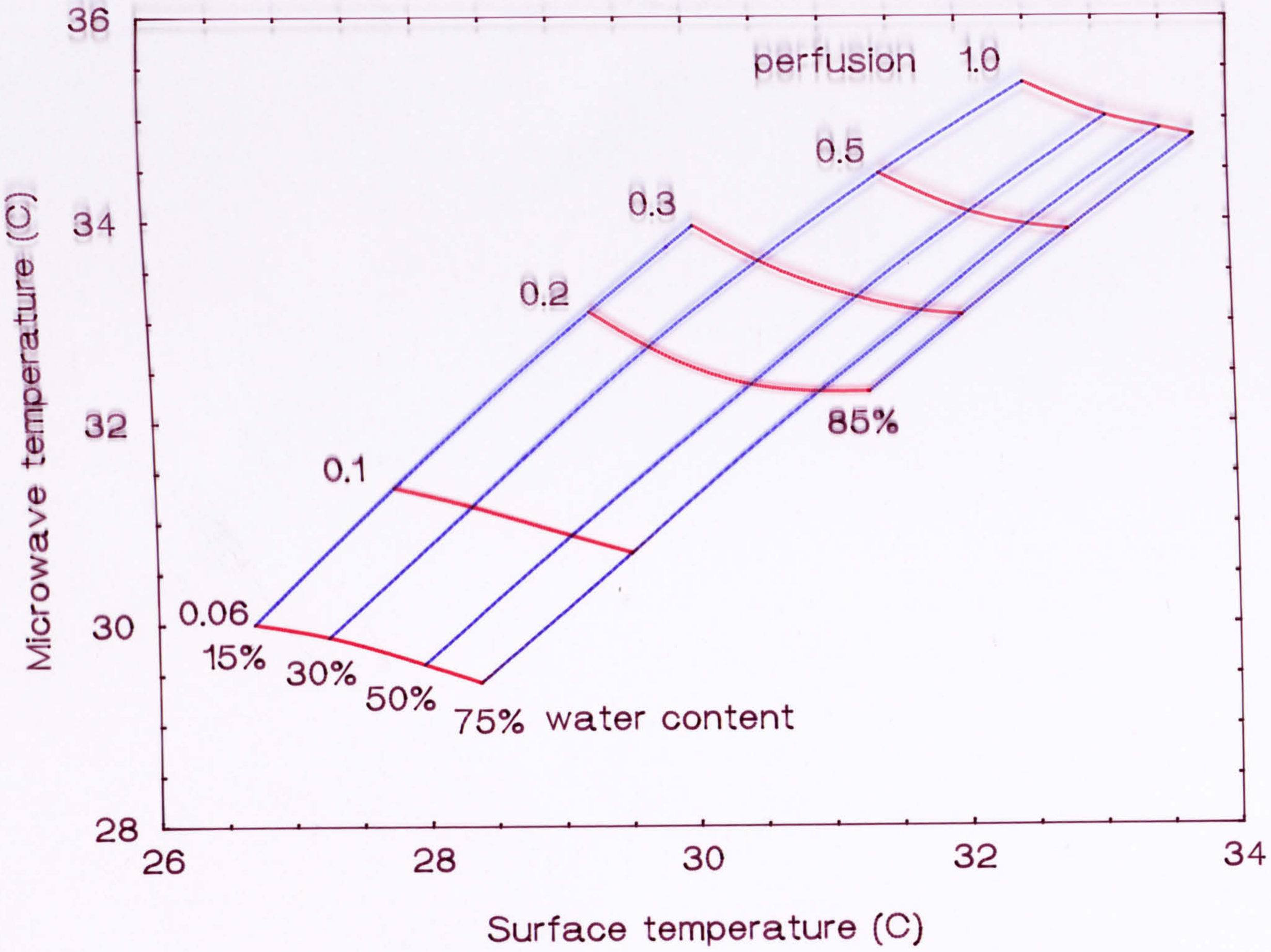
36
34
32
30
28
26
28
30
32
34
perfusion
1.0
0.5
0.3
0.2
0.1
0.06
85%
15%
30%
50%
75% water content
Microwave temperature (C)
Surface temperature (C)

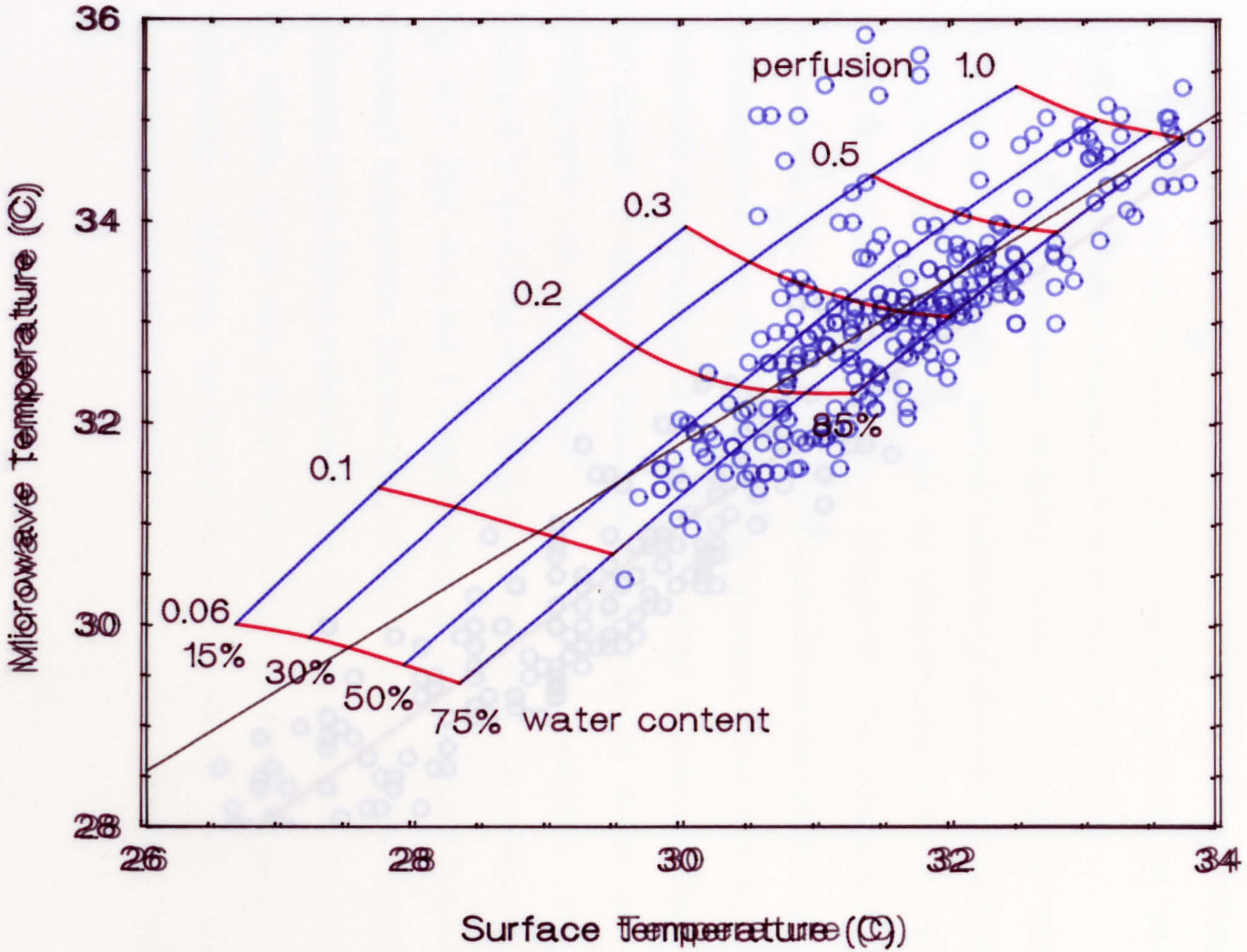

Fig. 6.4 Measured values of microwave and surface temperatures over the quadriceps muscle of patients suffering from rheumatoid arthritis.

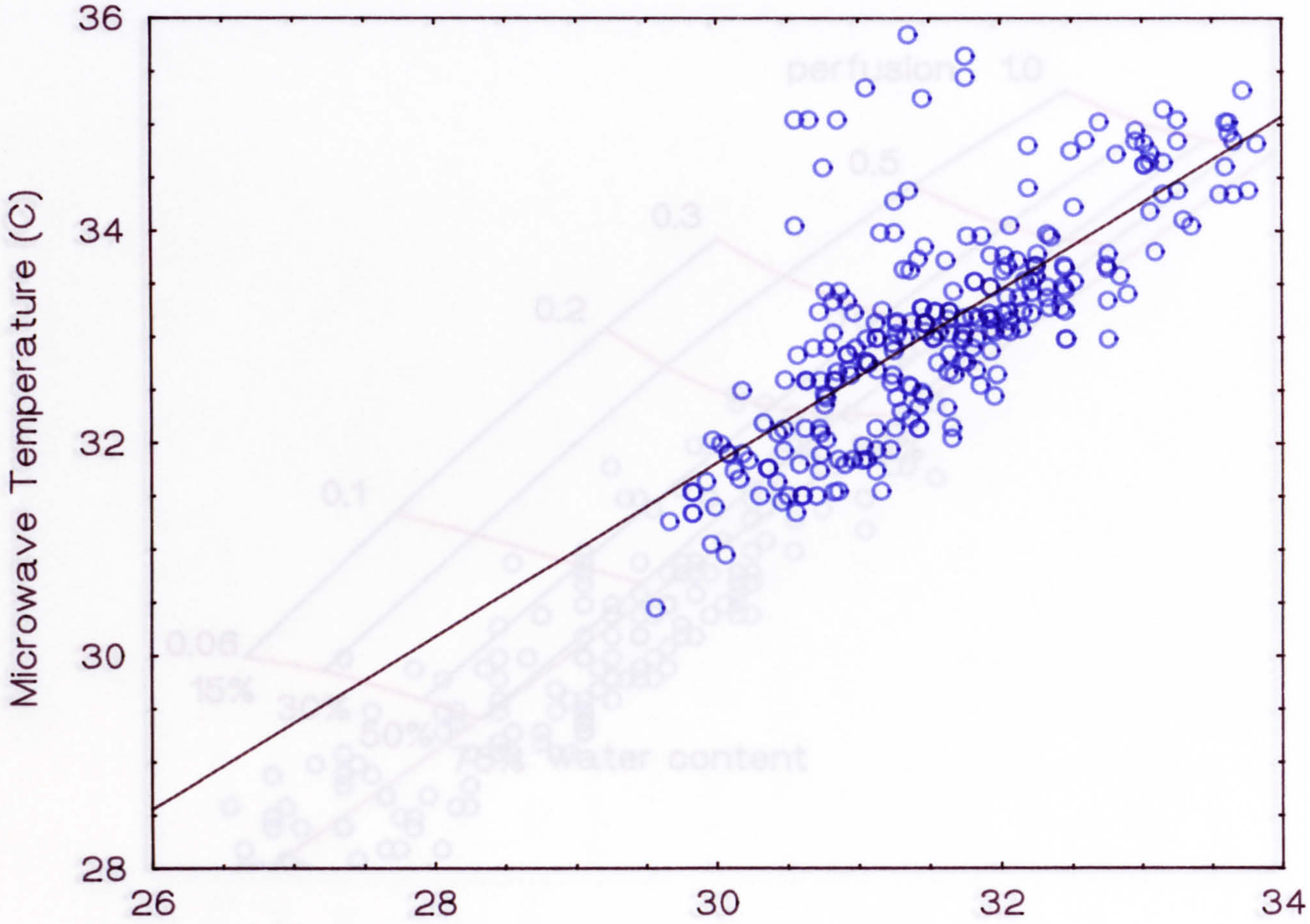

Fig. 6.4 Measured values of microwave and surface temperatures over the quadriceps muscle of patients suffering from rheumatoid arthritis.

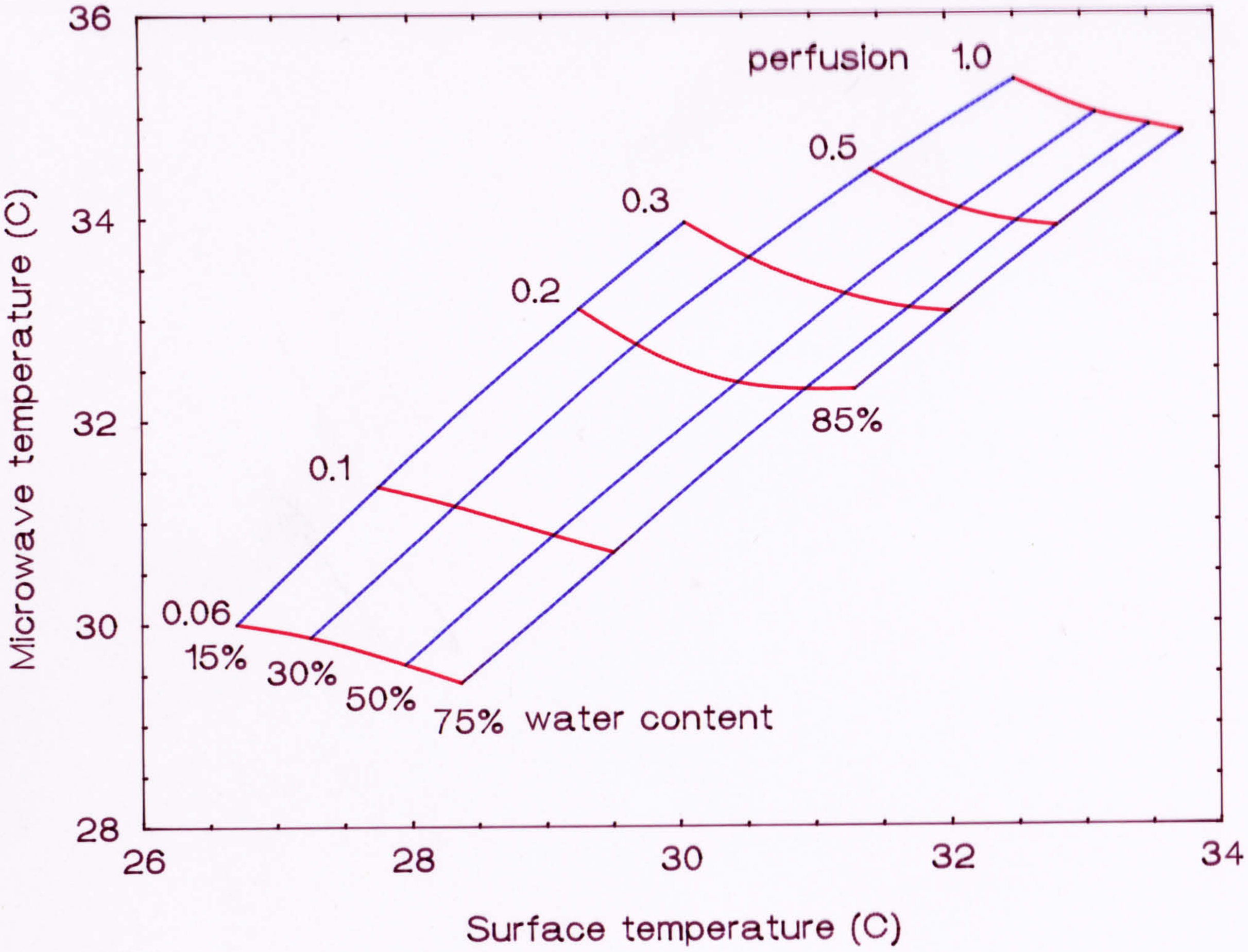
36
34
32
30
28
26
28
30
32
34
Microwave temperature (C)
Surface temperature (C)
perfusion 1.0
0.5
0.3
0.2
0.1
0.06
85%
15%
30%
50%
75% water content

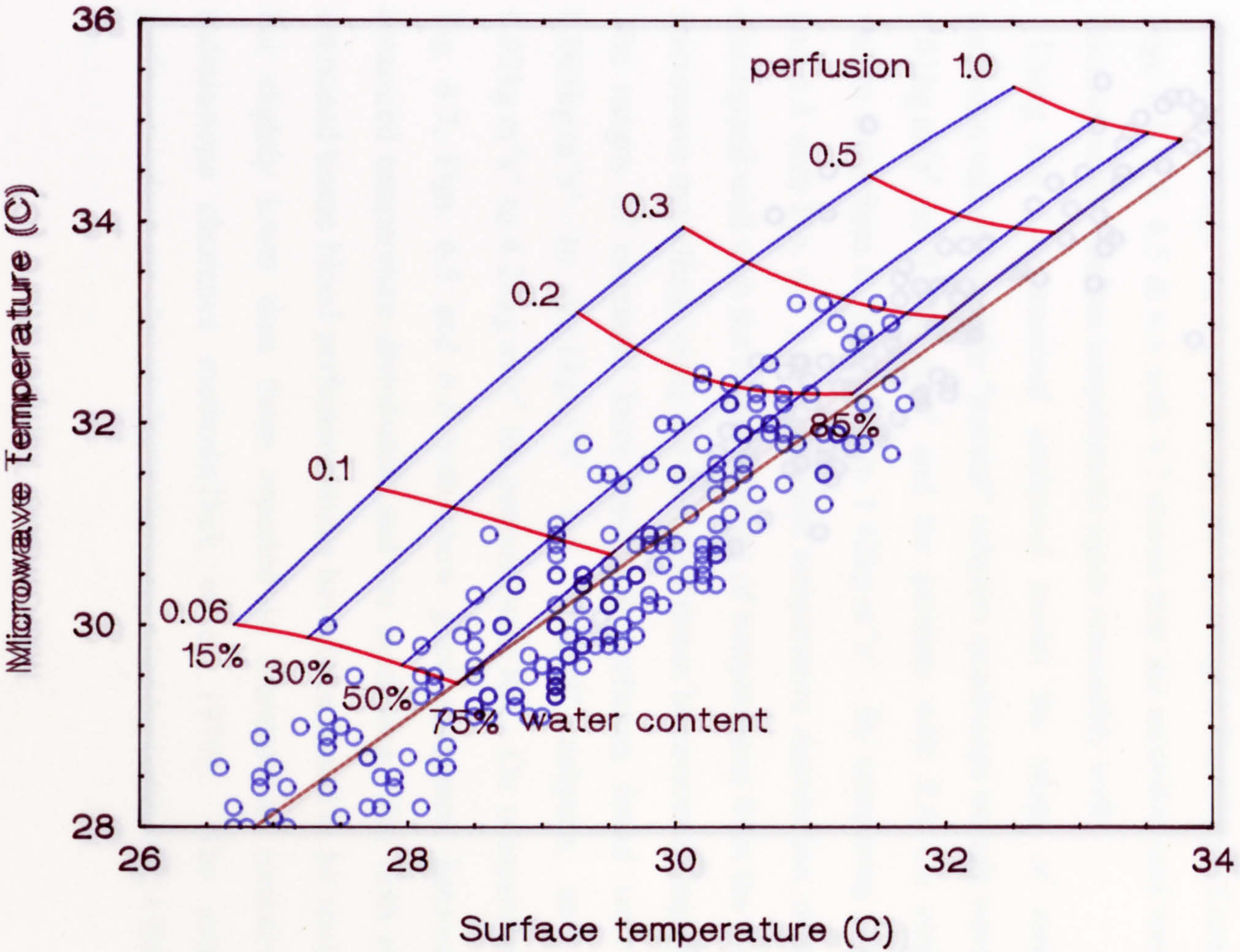

Fig. 6.5 Measured values of microwave and surface temperatures over the centre of the patella of normal subjects.

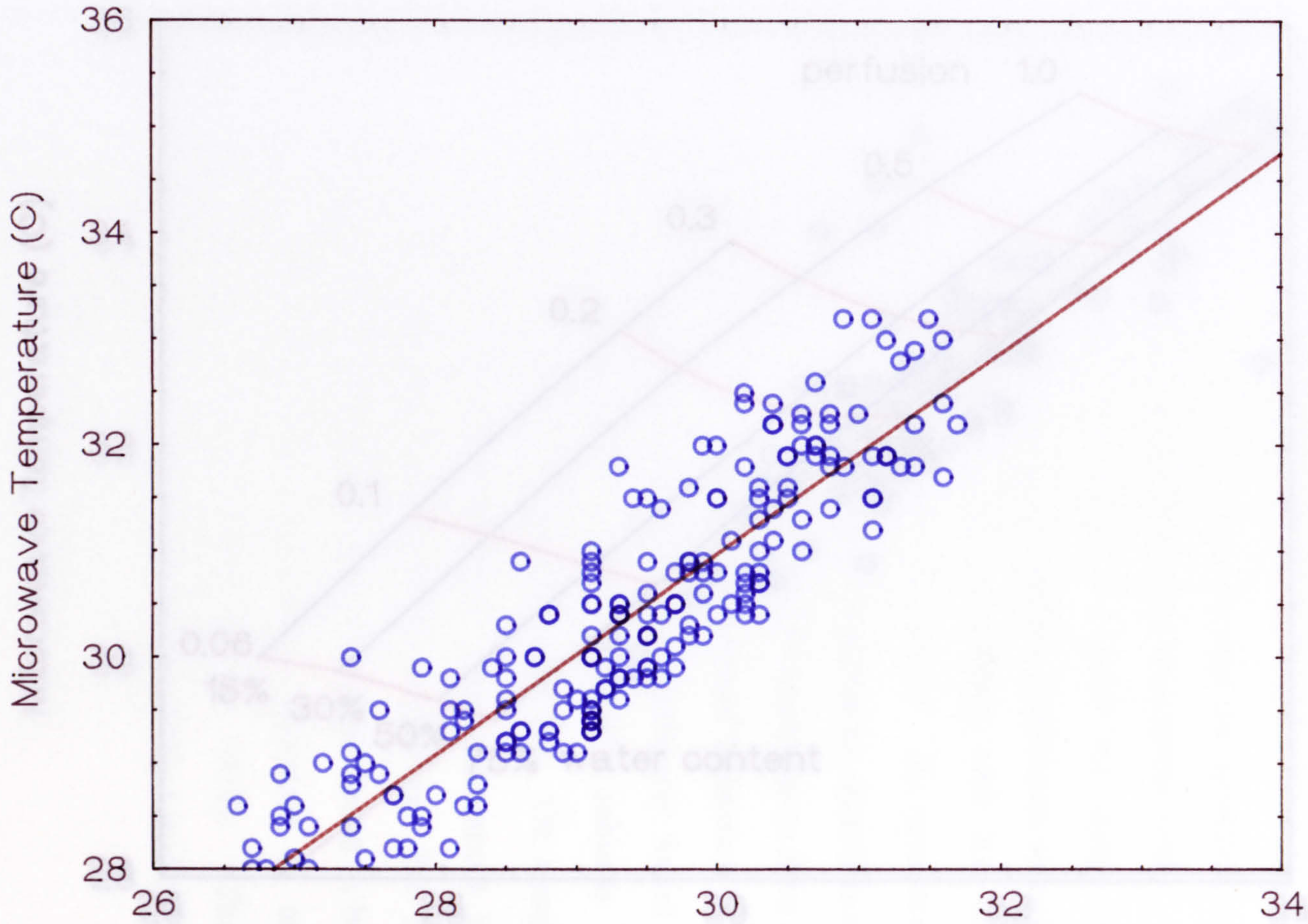

Fig. 6.5 Measured values of microwave and surface temperatures over the centre of the patella of normal subjects.

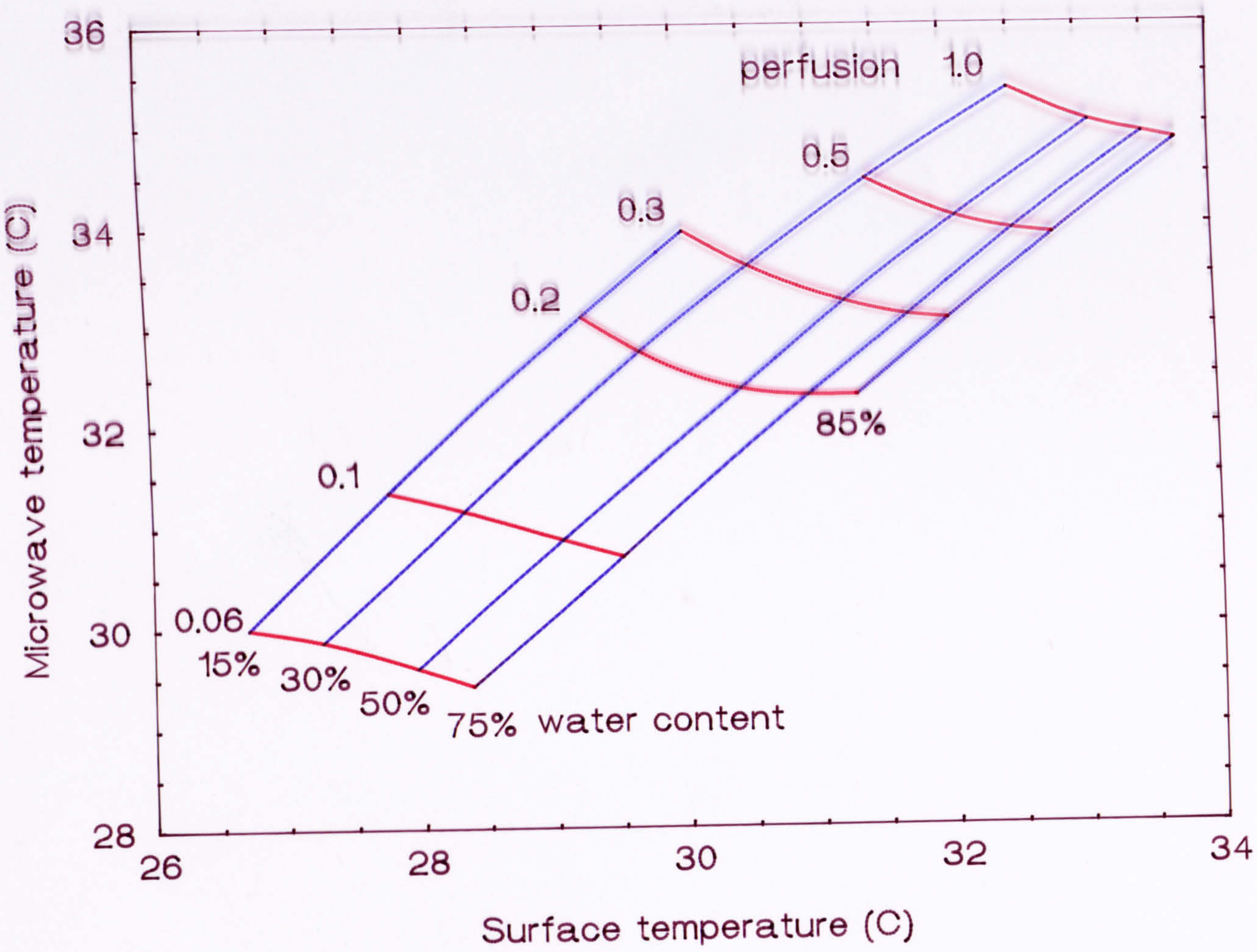
36
34
32
30
28
26
28
30
32
34
perfusion
1.0
0.5
0.3
0.2
0.1
85%
0.06
15%
30%
50%
75% water content
Microwave temperature (C)
Surface temperature (C)

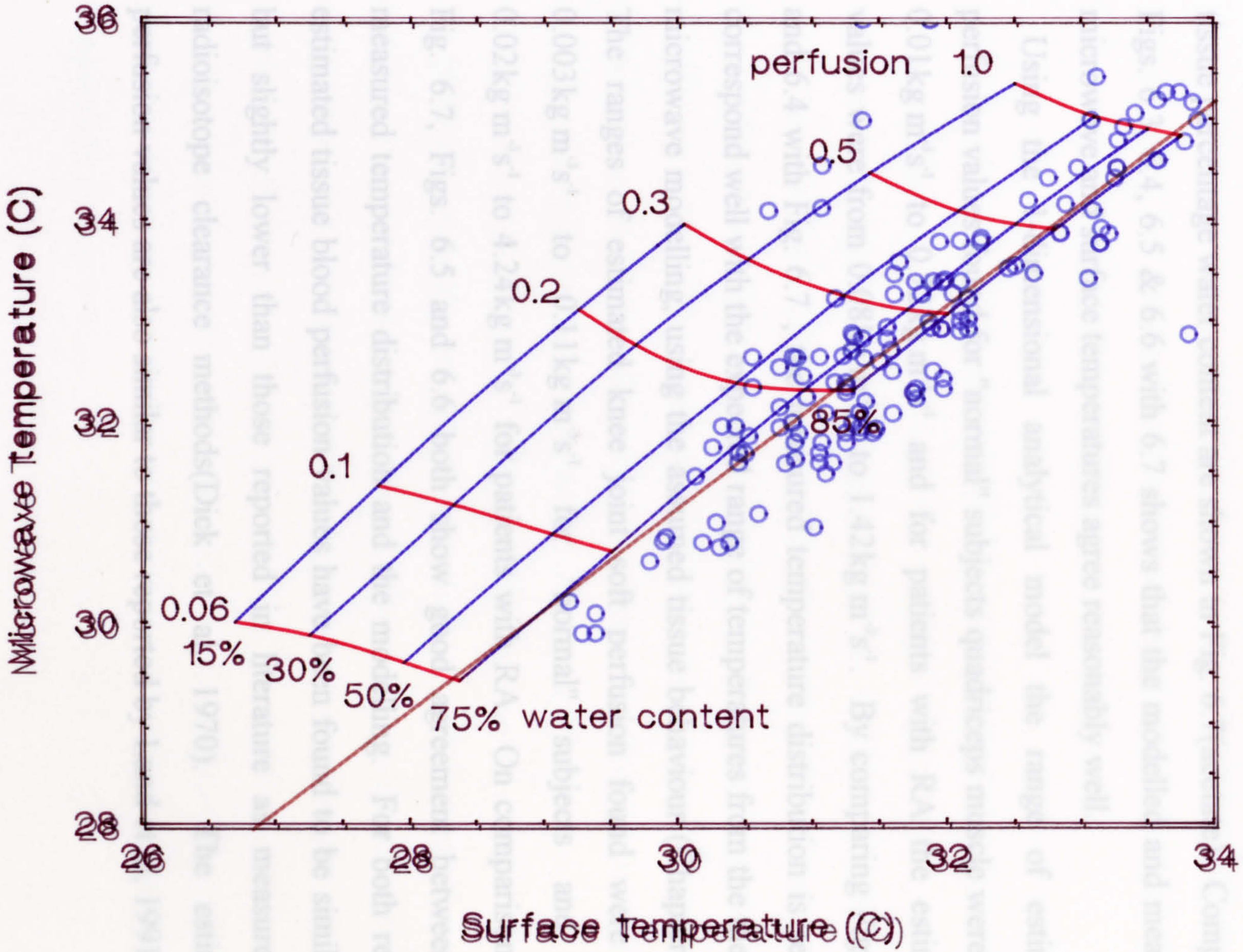

Fig. 6.6 Measured values of microwave and surface temperatures over the centre of the patella of patients suffering from rheumatoid arthritis.

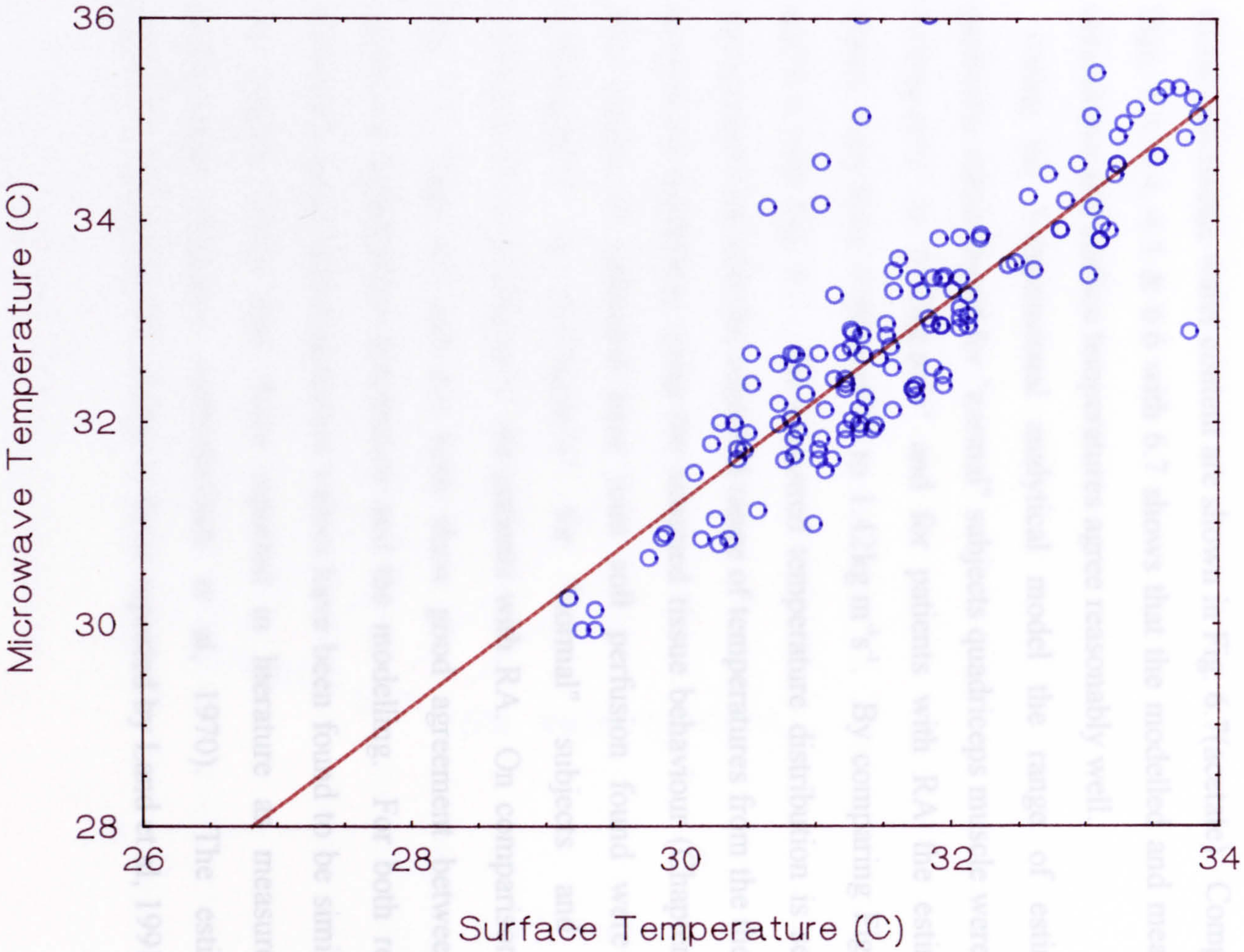

Fig. 6.6 Measured values of microwave and surface temperatures over the centre of the patella of patients suffering from rheumatoid arthritis.

probably due to an increase in blood flow through skin removing excess heat from the inflamed joint.

6.5 Use of 1-dimensional modelling for estimation of effective perfusion.

Modelled values of microwave and surface temperatures, perfusions and tissue percentage water content are shown in Fig. 6.7(acetate). Comparing Figs. 6.3, 6.4, 6.5 & 6.6 with 6.7 shows that the modelled and measured microwave and surface temperatures agree reasonably well.

Using the 1-dimensional analytical model the range of estimated perfusion values found for "normal" subjects quadriceps muscle were from $0.01 kg\,m^{-3}s^{-1}$ to $0.72 kg\,m^{-3}s^{-1}$ and for patients with RA the estimated values were from $0.08 kg\,m^{-3}s^{-1}$ to $1.42 kg\,m^{-3}s^{-1}$. By comparing Figs. 6.3 and 6.4 with Fig. 6.7 , the measured temperature distribution is seen to correspond well with the expected range of temperatures from the thermal-microwave modelling, using the assumed tissue behaviour (Chapter 5.0). The ranges of estimated knee joint soft perfusion found were from $0.003 kg\,m^{-3}s^{-1}$ to $0.11 kg\,m^{-3}s^{-1}$ for "normal" subjects and from $0.02 kg\,m^{-3}s^{-1}$ to $4.24 kg\,m^{-3}s^{-1}$ for patients with RA. On comparison with Fig. 6.7, Figs. 6.5 and 6.6 both show good agreement between the measured temperature distribution and the modelling. For both regions estimated tissue blood perfusion values have been found to be similar to, but slightly lower than those reported in literature as measured by radioisotope clearance methods(Dick et al, 1970). The estimated perfusion values are also similar to those reported by Land et al, 1991.

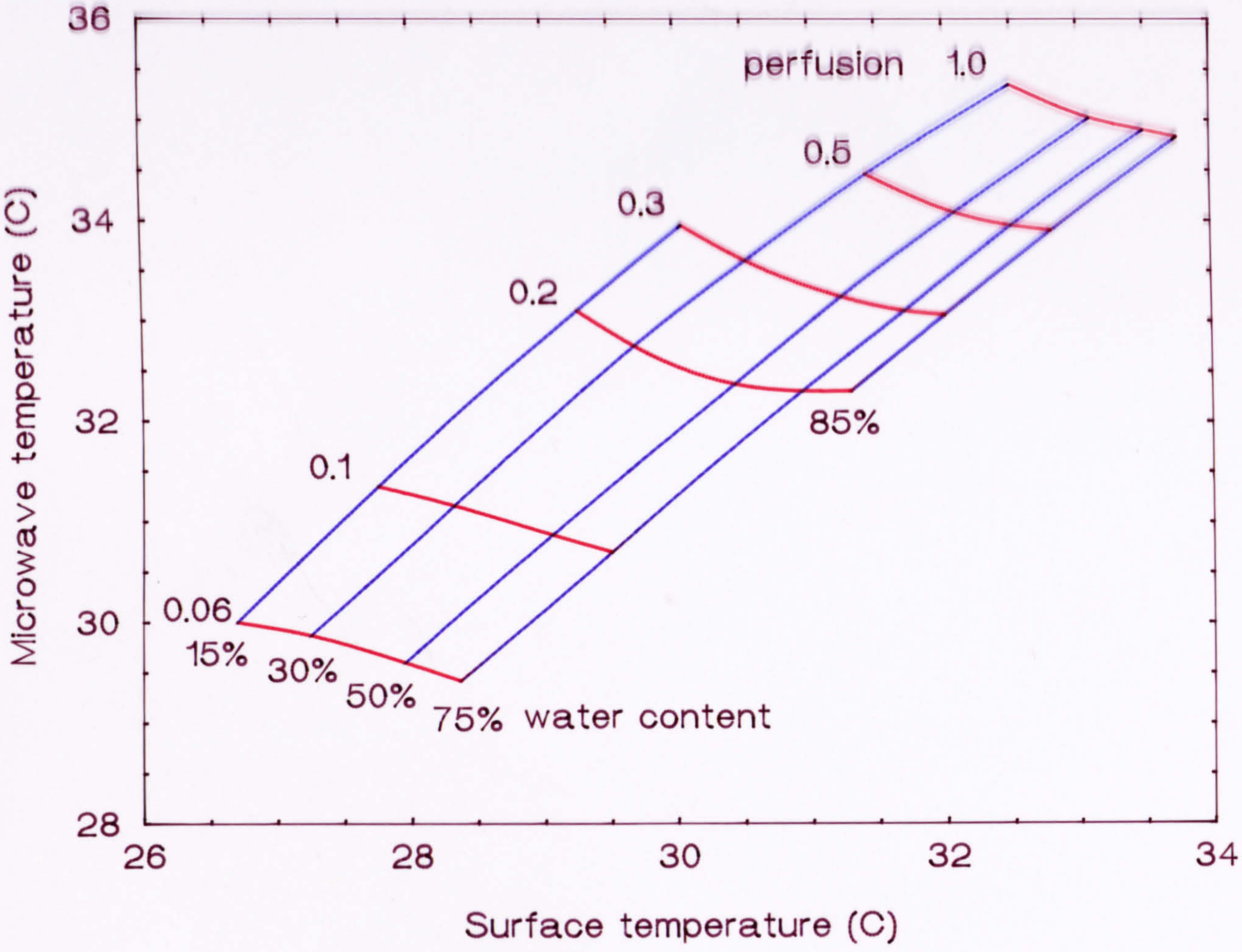

Fig. 6.7 Single region numerical model

Fig. 6.8 shows the estimated power attenuation constants for both "normal" subjects and RA patients. The average 2α values in both cases are similar to those estimated by Land, Brown & Fraser, 1991 and those measured at 3GHz as given in Fig. 1.0. This supports the use of the relationship between thermal and microwave tissue properties discussed in Chapter 5.0. The slightly higher tissue attenuation coefficient for the RA group would be consistent with higher water content tissue in the inflammed joint tissue of these subjects.

6.6 Use of a 2-dimensional model of the quadriceps region in RA disease assessment.

Finite element models were developed by Dr. P. Harness (UMIST) to allow the calculation of the temperature distribution of the human body. The models use the Galerkin approach to solve the weak form of the heat transfer equation. Two-dimensional meshes have been constructed of cross-sections of the leg (about the quadriceps muscle). The models can use experimental microwave data in one of two ways:

1. Use experimentally estimated values of blood perfusion coupled with Newtonian surface boundary conditions. The resulting calculated skin temperatures can then be compared with experimental infra-red measurements.

2. Use experimental skin temperature values as the boundary conditions and vary perfusion coefficients to determine their effect on the internal temperature distribution.

Fig. 6.8 Estimated power attenuation coefficients (m^{-1}) for normal subjects and patients with RA. Data type

finally, an arterial temperature of 37.1SC and temperature of 21C were used for modelling purposes. The initial calculation was performed using the measured cooling coefficient and muscle perfusion rate. Using this measured cooling coefficient value the measured and modelled microwave temperatures did not correlate very well. By reducing the cooling coefficient the measured and modelled microwave temperatures start to correlate. Examples of this finding are given in Table 6.5. It is clear that this method of modelling is extremely sensitive to the cooling coefficient[E]. This is not an ideal

In either case the microwave temperature can be calculated from the resulting temperature distribution.

Applying the convection boundary condition the following conditions were used

In either case the microwave temperature can be calculated from the resulting temperature distribution.

Applying the convection boundary condition the following conditions were used:

Quadricep diameter	16.5cm
Skin layer	0.3cm
Fat layer	1.1cm
Muscle layer	3 - 4cm
Bone diameter	6.8cm

The perfusion rates used in the model being (Harness P & Land, D.V)

Skin	0.5kg $m^{-3}s^{-1}$
Fat	0.05kg $m^{-3}s^{-1}$
Bone	0.05kg $m^{-3}s^{-1}$

Finally, an arterial temperature of 37.15C and temperature of 21C were used for modelling purposes.

The initial calculation was performed using the measured cooling coefficient and muscle perfusion rate. Using this measured cooling coeffic nt value the measured and modelled microwave temperatures did not correlate very well. By reducing the cooling coefficient, the measured and modelled microwave temperatures start to correlate. Examples of this finding are given in Table 6.0. It is clear that this method of modelling is extremely sensitive to the cooling coefficient, E. This is not an ideal

2 - Dimensional modelling
CONVECTION BOUNDARY CONDITION

$T_{core} = 37.15C$
$T_{amb} = 21.0C$

Measured $T_{mw.}$ (C)	Measured T_{sur}(C)	Estimated perfusion kg $m^{-3}s^{-1}$	Measured cooling coeff., E	Modelled T_{mw}, (C)	Modelled T_{sur}, (C)
32.8	31.0	.138	10.196	31.56	29.05
32.8	31.0	.138	8.0	32.34	30.04
32.8	31.0	.138	7.0	32.59	30.47
32.8	31.0	.138	6.0	33.06	31.17
32.8	31.0	.138	6.3	32.85	30.98
32.8	31.0	.138	6.2	32.88	31.04
32.0	29.9	.062	9.97	30.45	28.46
32.0	29.9	.062	6.45	31.76	30.24
32.0	29.9	.062	6.35	31.82	30.3
32.0	29.9	.062	6.25	31.87	30.36
33.9	31.2	.255	10.42	32.55	29.48
33.9	31.2	.255	7.0	33.41	31.06
33.9	31.2	.255	6.0	33.74	31.63
33.9	31.2	.255	5.5	33.93	31.95
33.5	32.0	.325	10.41	32.89	29.66
33.5	32.0	.325	7.5	33.61	30.96
33.5	32.0	.325	6.5	33.85	31.51
33.4	31.3	.205	10.31	32.08	29.34
33.4	31.3	.205	6.0	33.42	31.48
33.8	32.0	.250	10.42	32.33	29.46
33.8	32.0	.250	8.0	33.13	30.52
33.8	32.0	.250	7.0	33.39	31.04
33.8	32.0	.250	6.0	33.76	31.62

Table 6.0 Comparison between measured and modelled microwave and surface temperatures

modelling situation and so modelling using the second fixed boundary condition was investigated.

By using measured infra-red skin temperatures as the boundary conditions and varying perfusion rates to determine the effect on the internal temperature distribution, the modelled microwave temperatures were found to compare favourably with measured microwave temperatures. Table 6.1 gives examples of comparisons between measured and modelled microwave temperatures.

Fig. 6.9 shows the modelled temperatures obtained from the numerical model for different values of blood perfusion. By superimposing Fig. 6.9 onto Fig. 6.3, it is shown that there is excellent agreement between the measured and modelled microwave and surface temperatures, Fig. 6.10. The muscle blood perfusion range used from $0.1 kg\, m^{-3}s^{-1}$ to $0.7 kg\, m^{-3}s^{-1}$. Similarly, by superimposing Fig. 6.9 onto Fig. 6.4, measured microwave and surface temperatures over the quadriceps muscle of RA patients gives similar agreement.(Fig. 6.11)

Unfortunately, it was not possible at the time of these studies to investigate the factors which could cause lateral shifting of the T_{mw}/T_{sur} line obtained. These factors include quadriceps dimensions and thermal conductivity.

6.7 Hand and finger pilot study.

As mentioned previously, section 6.2, the microwave temperature increases over joints affected with RA. Comparing Figs 6.1 and 6.2 shows that the increase in microwave temperature over hand and finger joints

2 - Dimensional modelling

FIXED TEMPERATURE BOUNDARY CONDITION

T_{core} = 37.15C
T_{amb} = 21.0C

Measured T_{mw} (C)	Measured T_{sur} (C)	Estimated perfusion kg $m^{-3}s^{-1}$	Modelled T_{mw} (C)
30.0	27.3	0.011	28.50
31.4	28.1	.044	29.81
32.0	29.9	.062	31.52
32.8	31.0	.138	32.91
32.7	31.2	.184	33.09
33.4	31.3	.205	33.25
34.1	32.5	.248	34.23
33.9	31.2	.270	33.39
34.1	32.8	.326	34.54
34.9	33.3	.647	35.06

Table 6.1 Comparison between measured and modelled microwave temperaures.

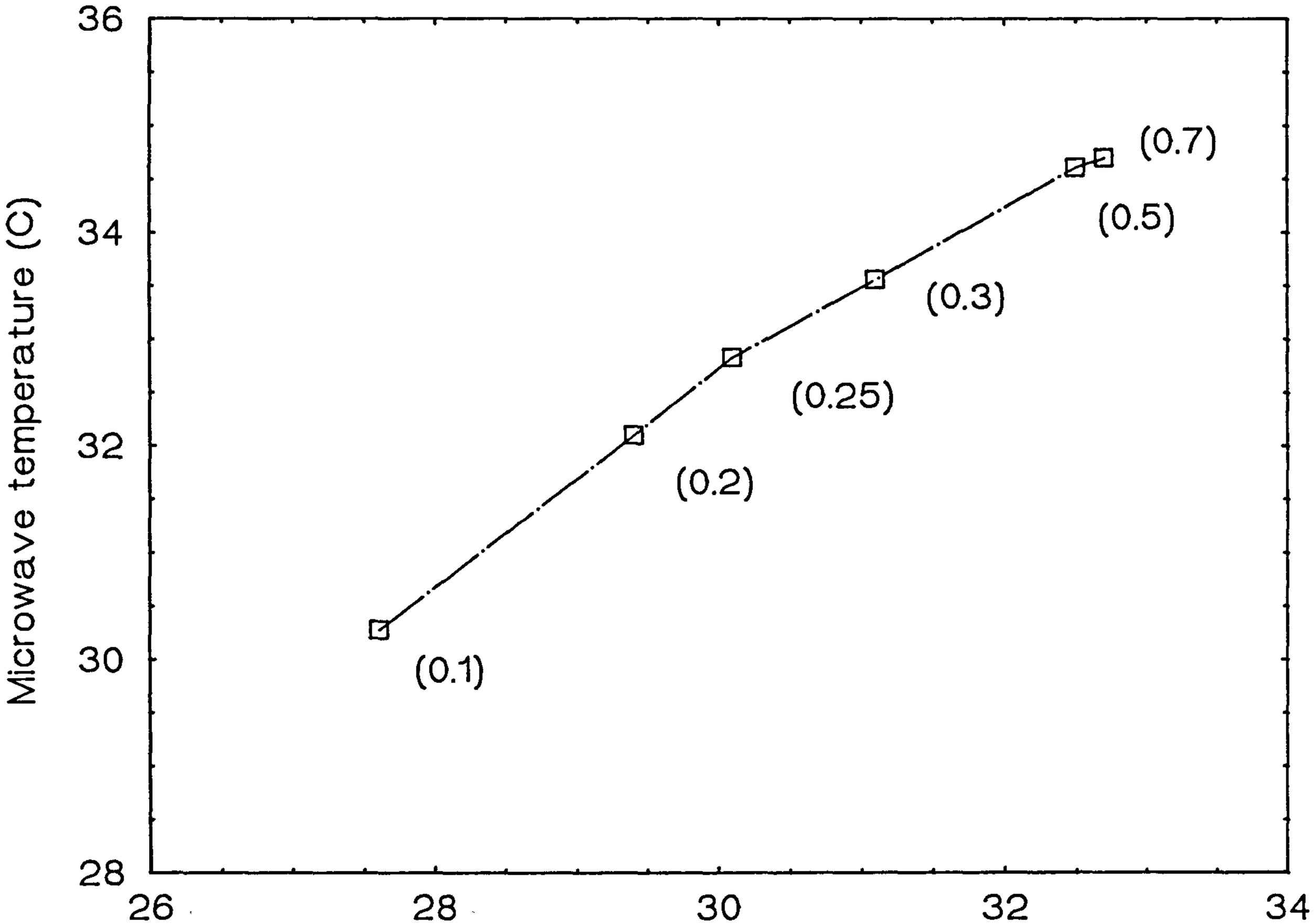

Fig. 6.9 Modelled surface and microwave temperatures obtained using the 2-D modellimg. () indicate blood perfusion.

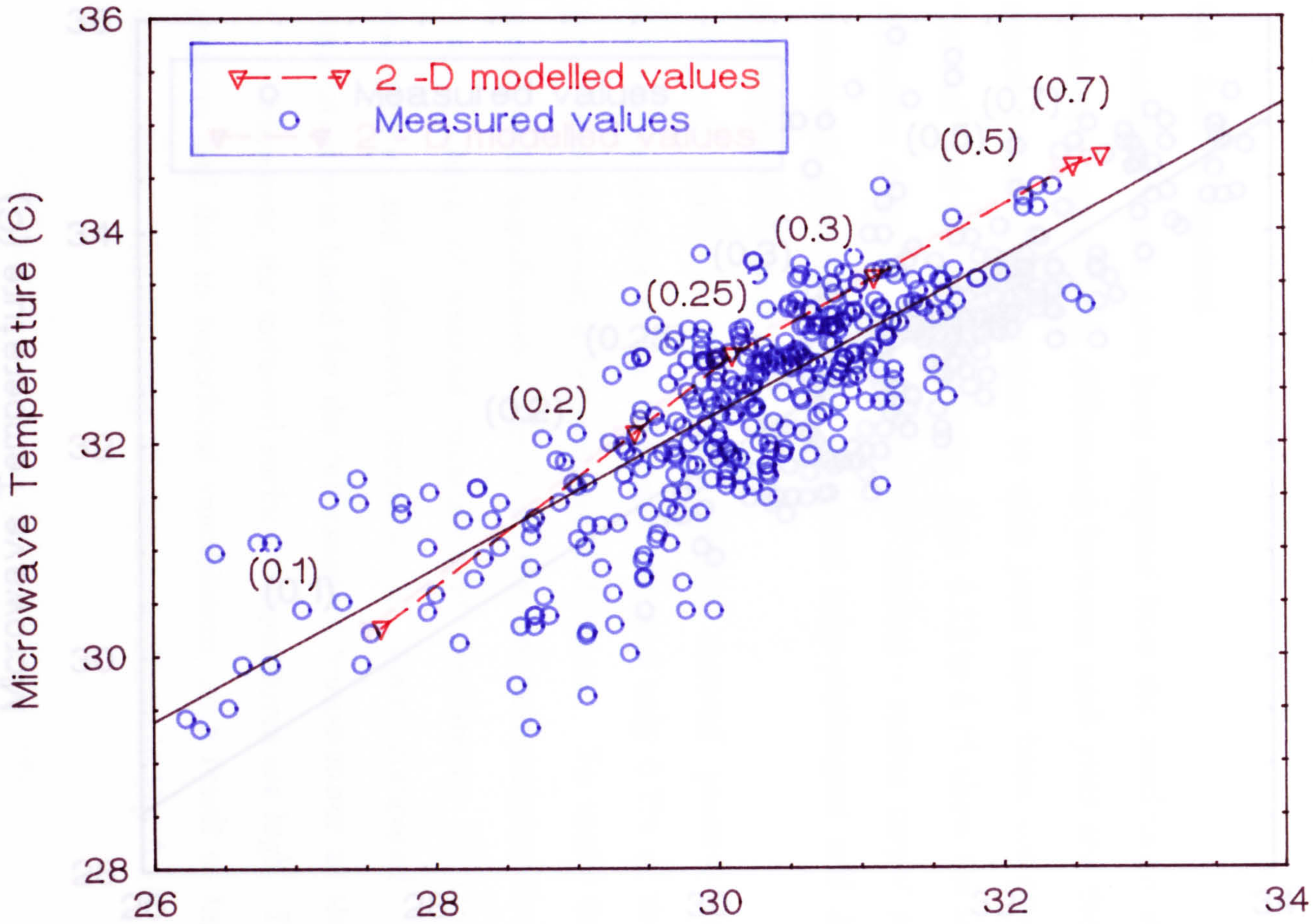

Fig. 6.10 Comparison between measured and 2-D modelled microwave and surface temperatures over the quadriceps muscle of normal subjects.

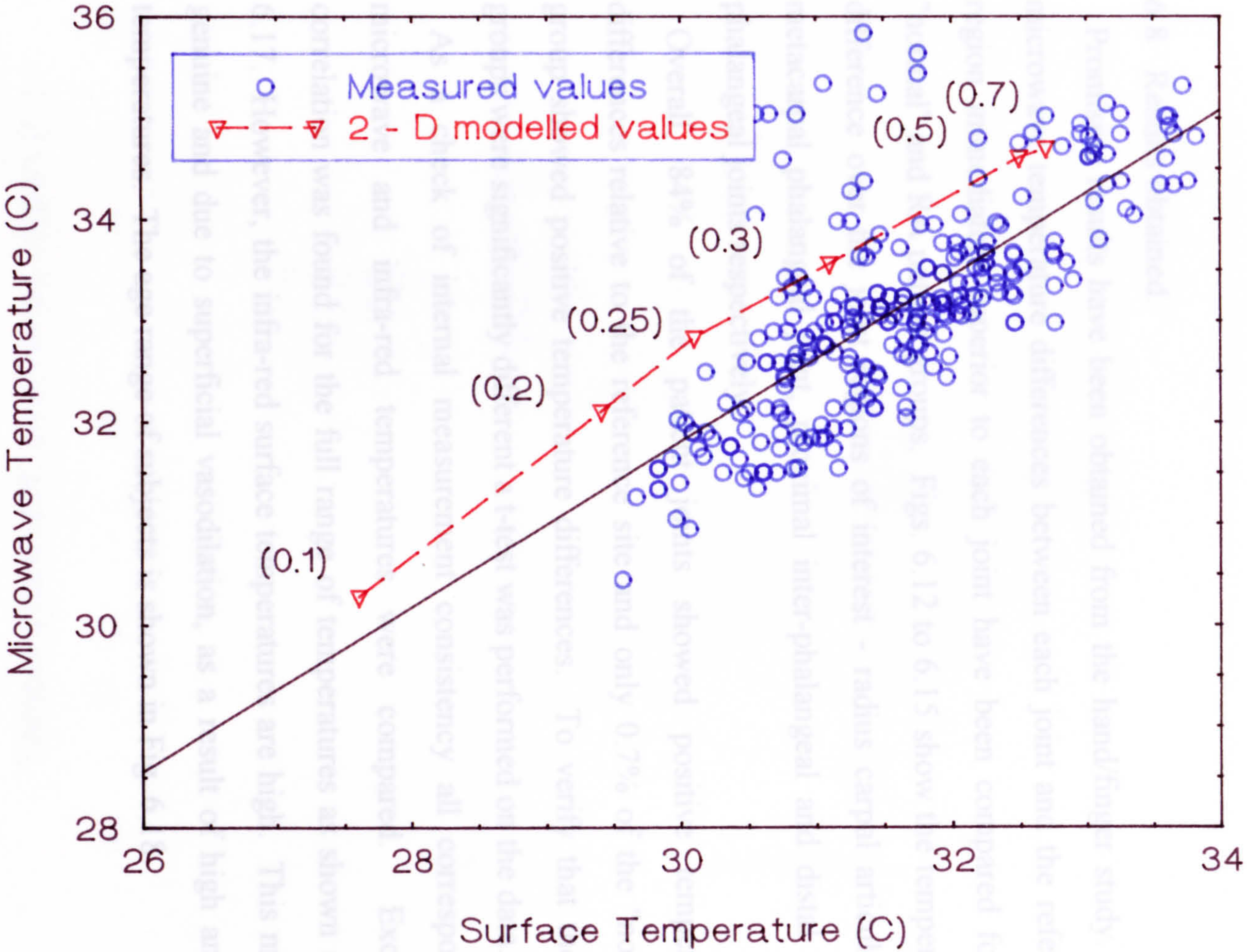

Fig. 6.11 Comparison between measured and 2-D modelled microwave and surface temperatures over the quadriceps muscle of patients suffering from rheumatoid arthritis.

affected with RA is significantly less than the increase in temperature over affected knee joints. This is to be expected because of the larger surface area to tissue volume, and the tendency for the peripheral blood supply to be lower in the fingers. It should be noted that higher than usual ambient temperatures had to be accepted for this group of measurements, (24-27C).

6.8 Results obtained.

Promising results have been obtained from the hand/finger study. The microwave temperature differences between each joint and the reference region immediately superior to each joint have been compared for the "normal" and RA patient groups. Figs. 6.12 to 6.15 show the temperature difference over the joint regions of interest - radius carpal articulation, metacarpal phalangeal joint, proximal inter-phalangeal and distal inter-phalangeal joints respectively.

Overall, 84% of the patient joints showed positive temperature differences relative to the reference site and only 0.7% of the "normal" group showed positive temperature differences. To verify that the two groups were significantly different a t-test was performed on the data.

As a check of internal measurement consistency all corresponding microwave and infra-red temperatures were compared. Excellent correlation was found for the full range of temperatures as shown in Fig 6.17. However, the infra-red surface temperatures are high. This may be genuine and due to superficial vasodilation, as a result of high ambient temperatures. The age range of subjects is shown in Fig. 6.18.

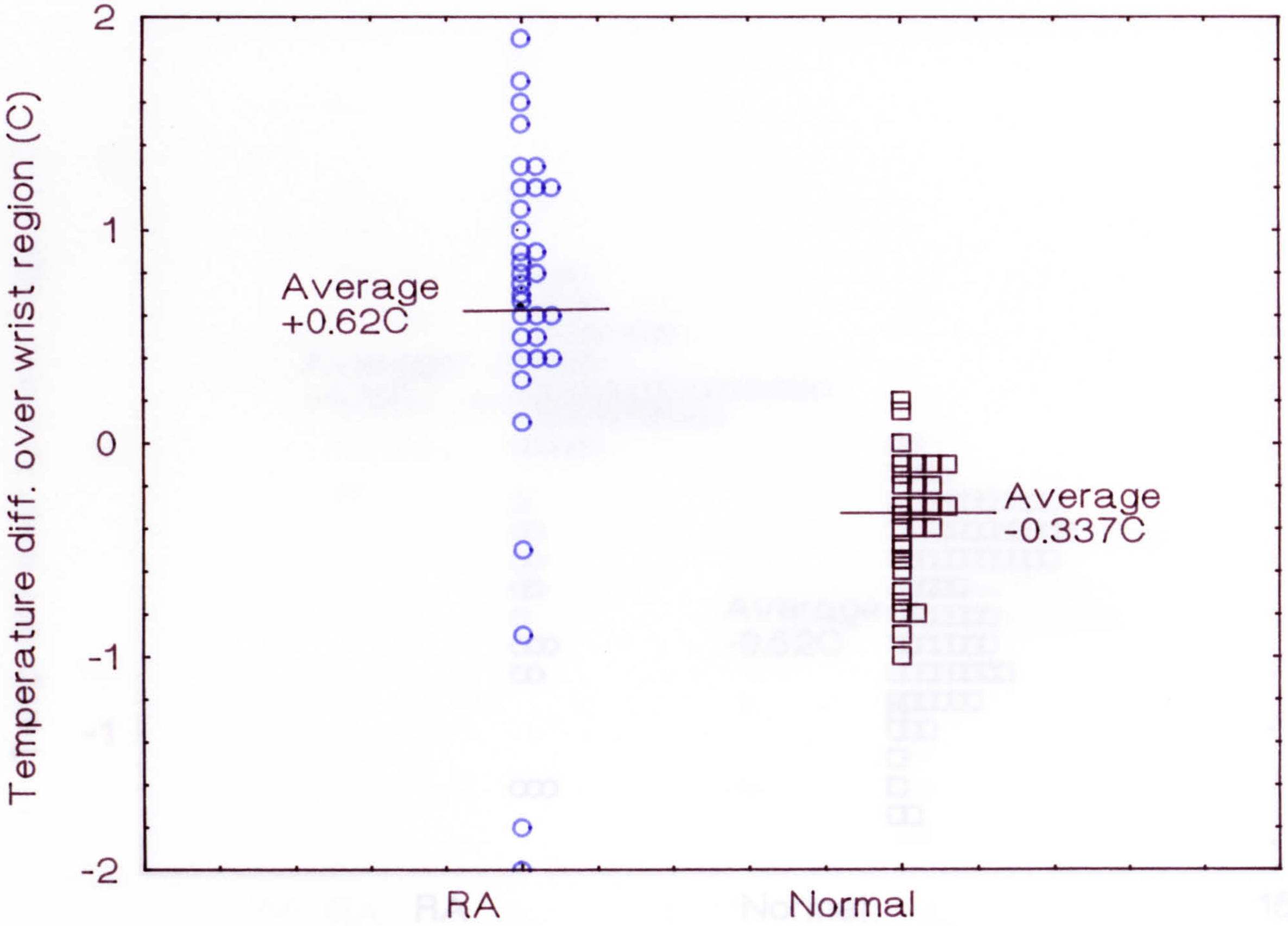

Fig. 6.12 Microwave temperature difference over the radius carpal articulation in both normal and patient groups.

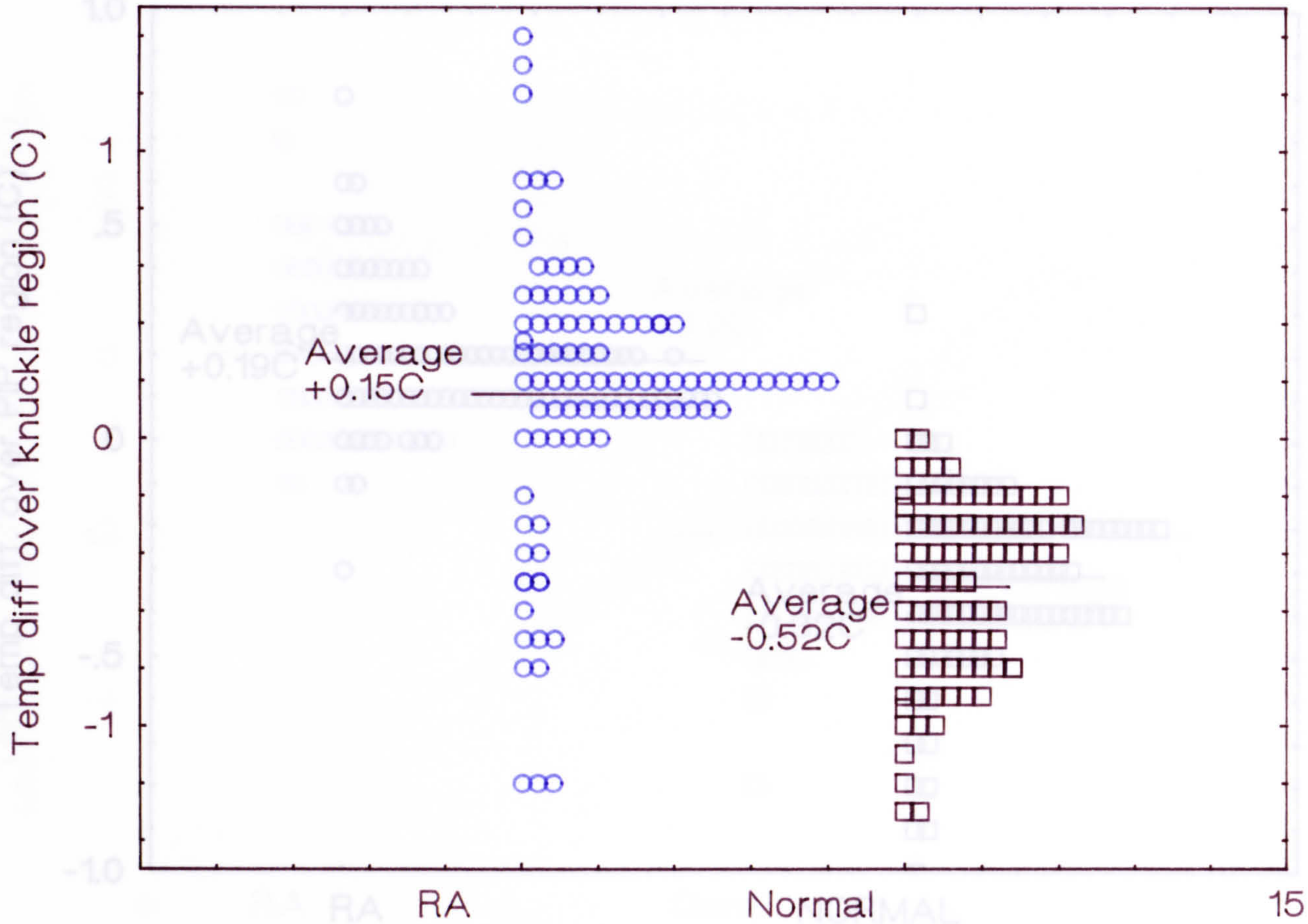

Fig. 6.13 Microwave temperature difference over the metacarpal phalangeal joint in both normal and patient groups.

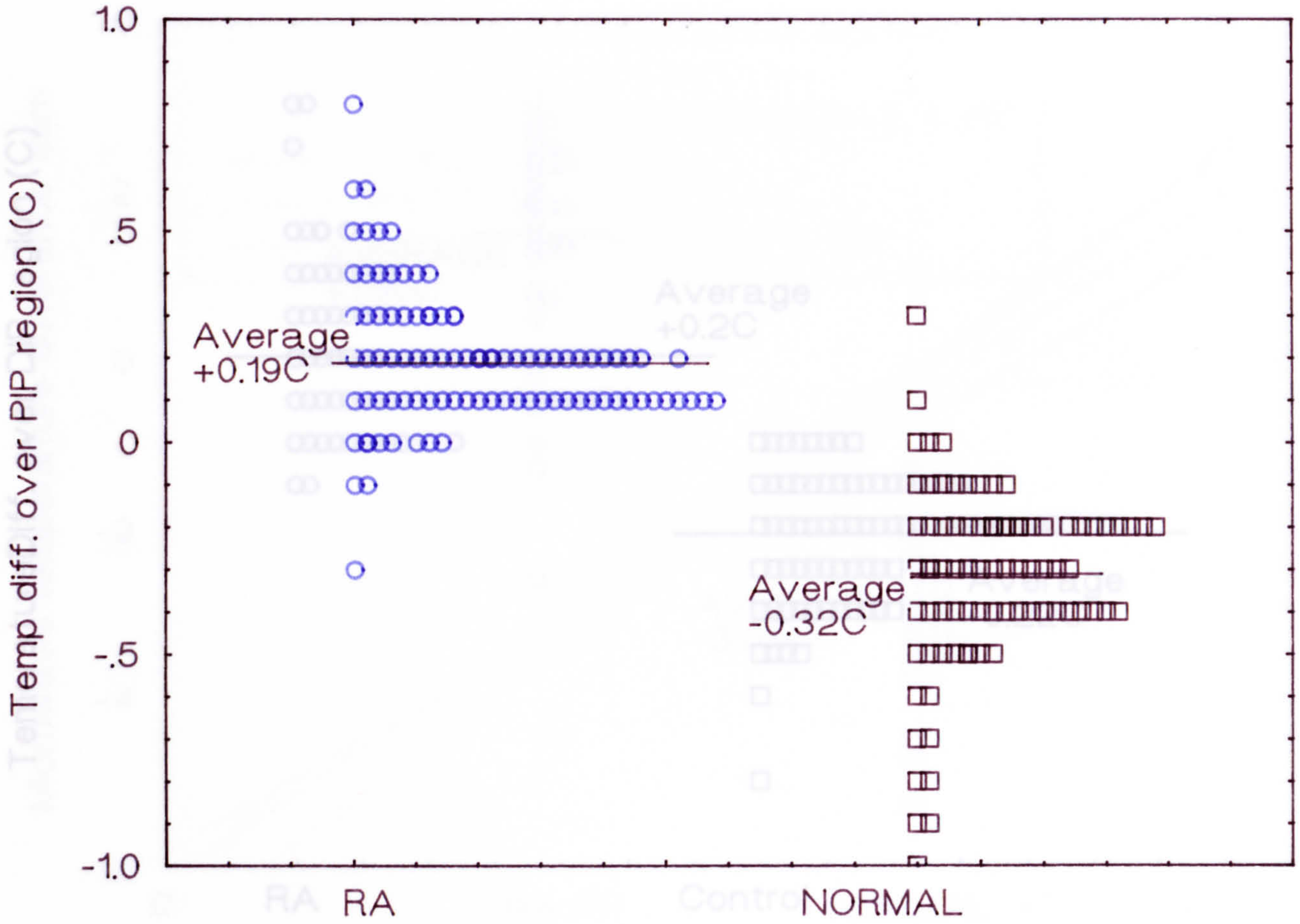

Fig. 6.14 Microwave temperature difference over the proximal inter-phalangeal joint in both normal and patient groups.

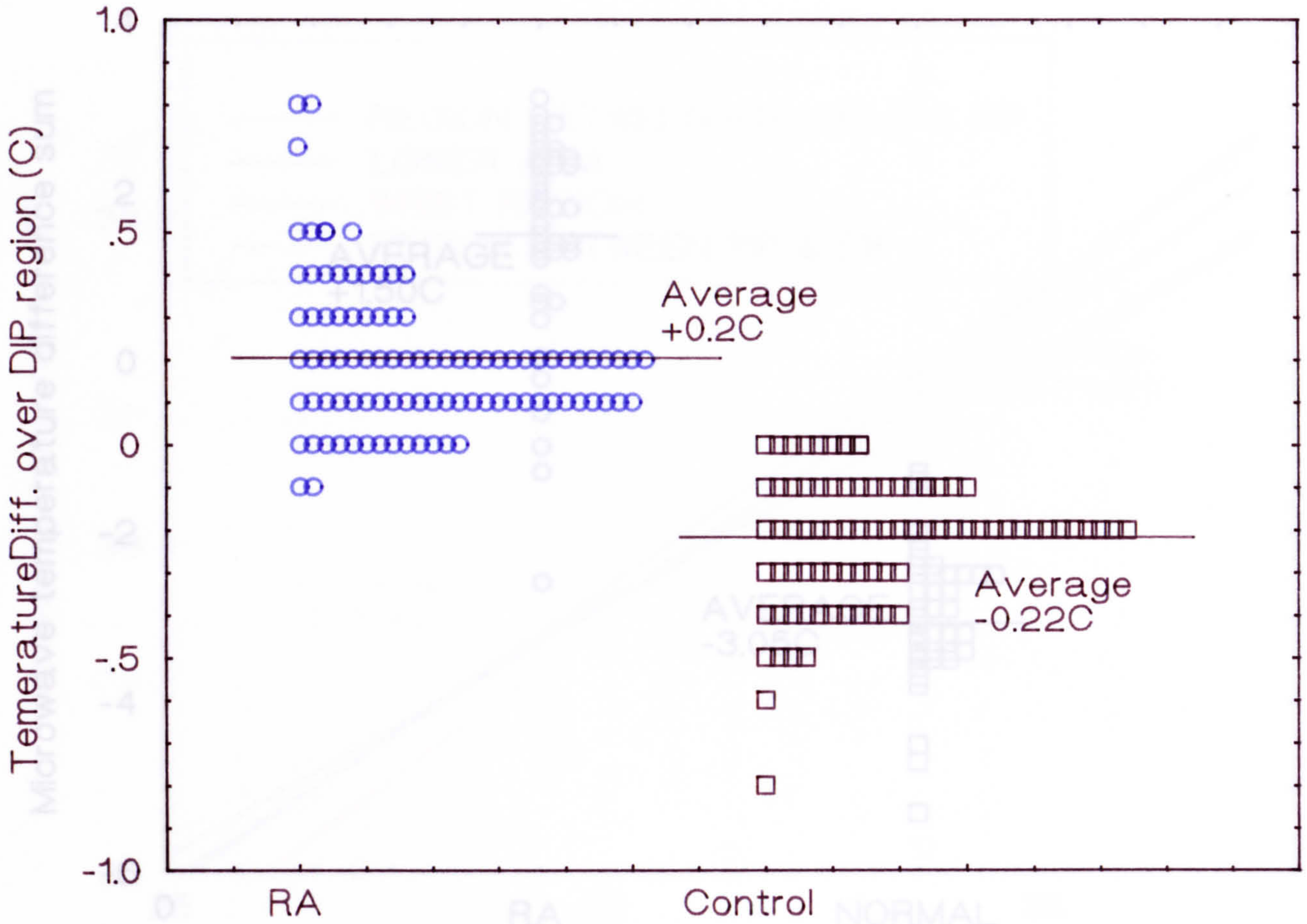

Fig. 6.15 Microwave temperature difference over the distal inter-phalangeal joint in both control and patient groups.

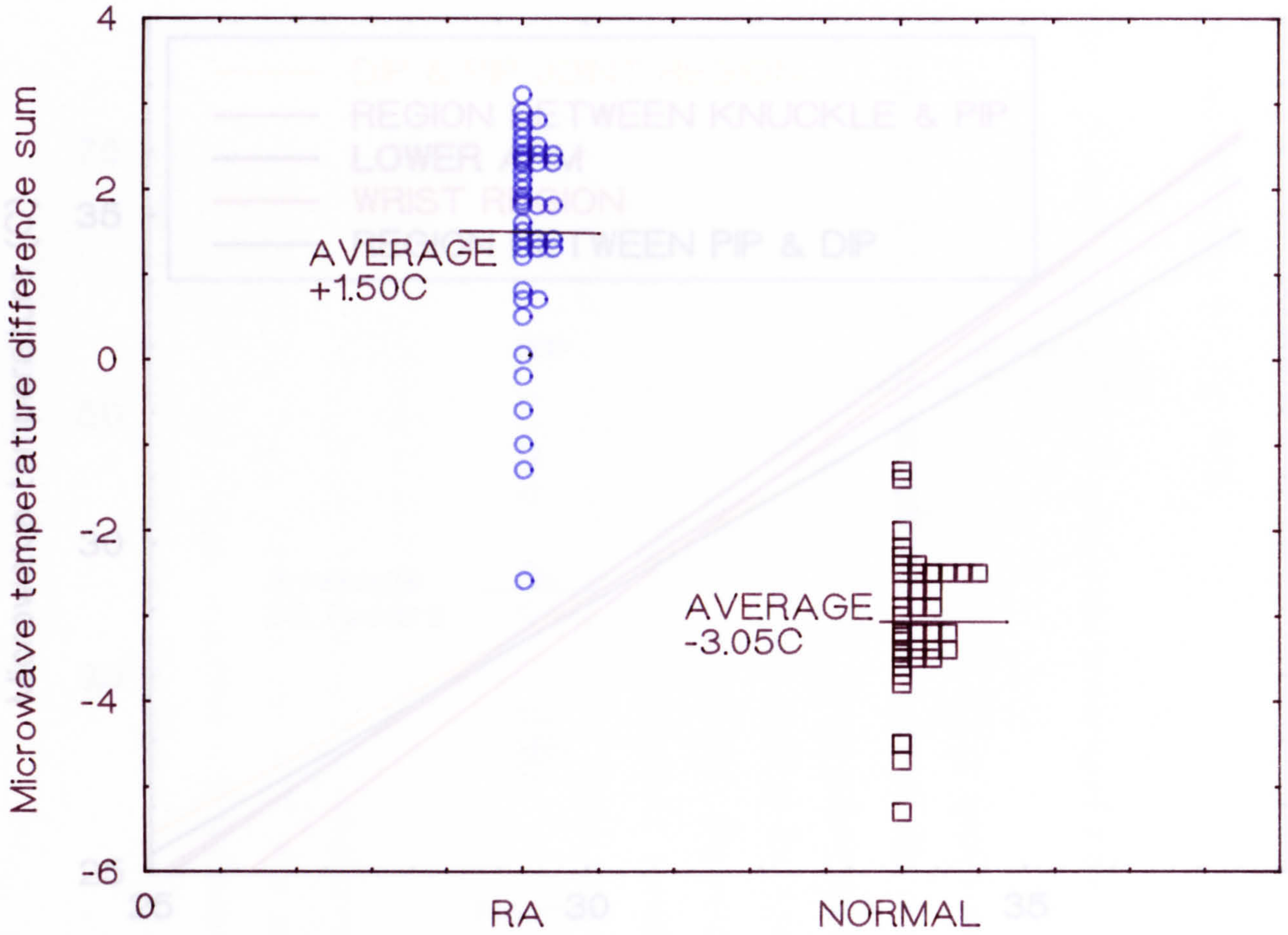

Fig. 6.16 Microwave temperature difference sum over both hands excluding wrist data for both normal and patient groups.

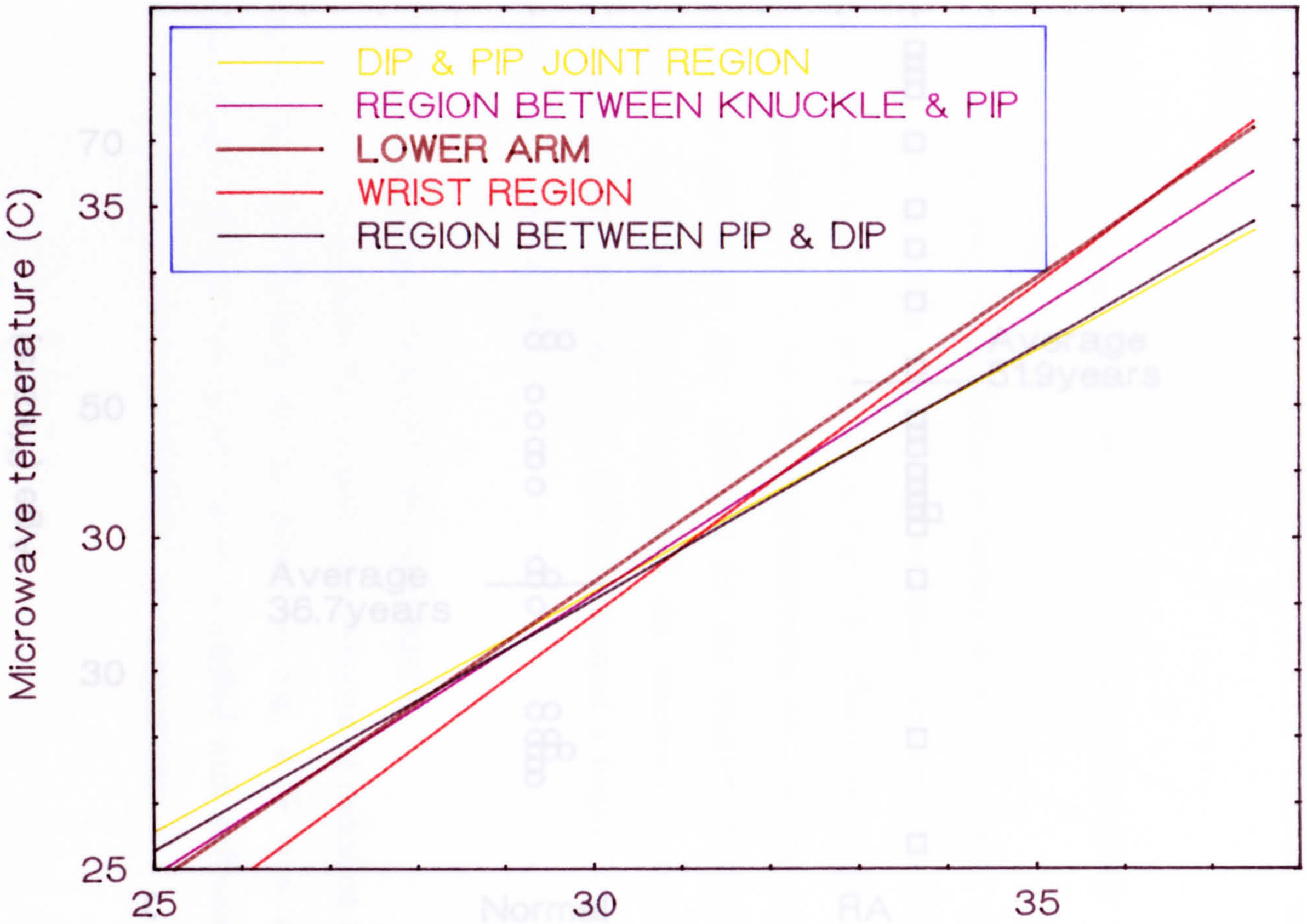

Fig. 6.17 Correlation of measured temperatures over all regions of interest.

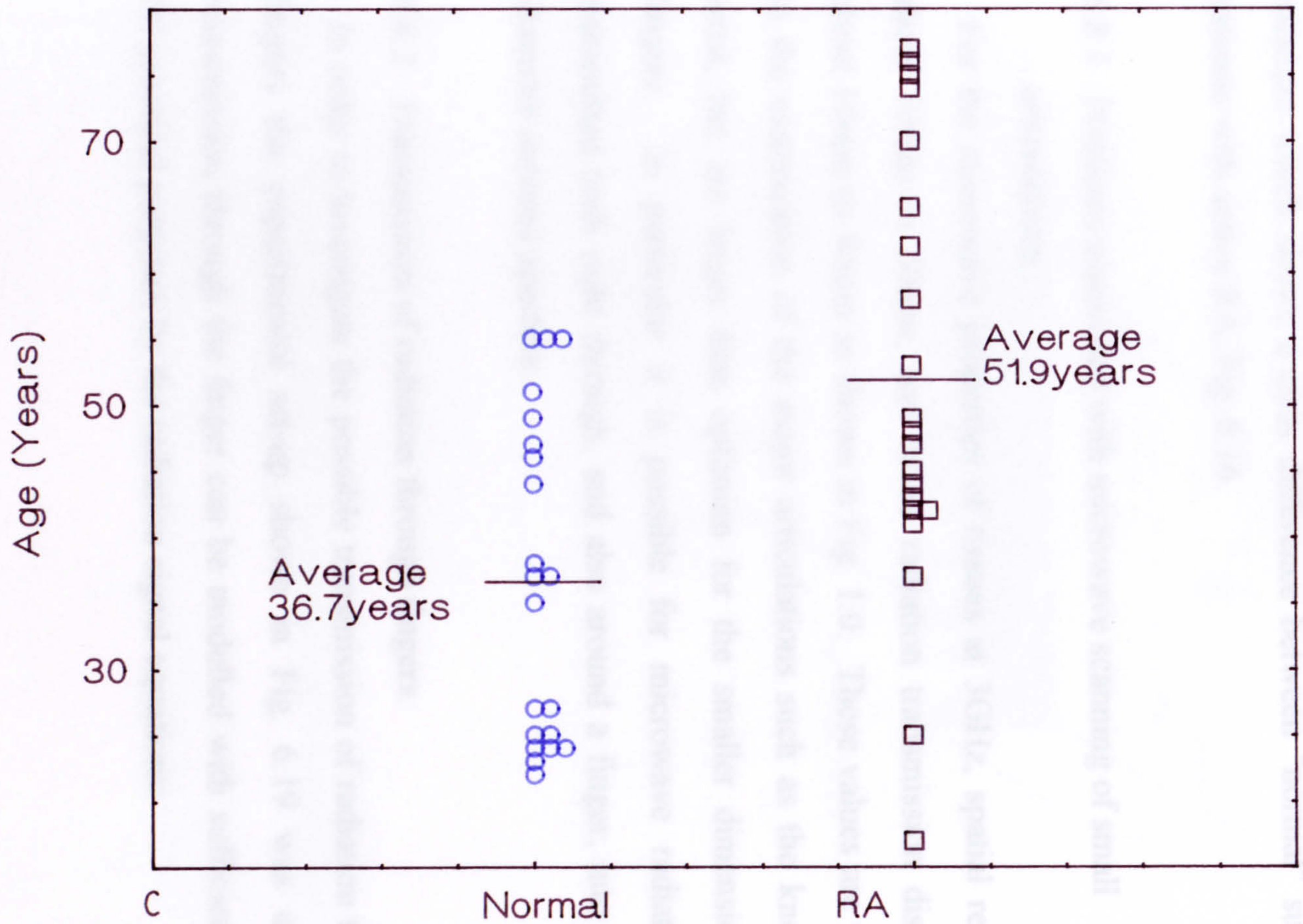

Fig. 6.18 Age range of subjects in both normal and RA groups.

The increase in temperature over the DIP joint was an interesting find as it appears to be generally accepted by clinicians that no such increase in temperature should occur.(Prof. R.D. Sturrock, personal communication) Further work in this region would therefore be worthwhile.

Combining all the finger joints together for a subject does seem to give a measure which shows a clear difference between "normal" subjects and patients with active RA, Fig. 6.16.

6.8.1 Problems associated with microwave scanning of small articulations.

For the microwave properties of tissues at 3GHz, spatial resolution is about 10mm to 20mm, and tissue radiation transmission distances are about 10mm to 40mm as shown in Fig. 1.0. These values are well suited to the examination of the major articulations such as the knee and the wrist, but are larger than optimum for the smaller dimensions of the fingers. In particular it is possible for microwave radiation to be transmitted both right through, and also around a finger, into the 25mm diameter antenna aperture.

6.8.2 Transmission of radiation through fingers.

In order to investigate the possible transmission of radiation through the fingers the experimental set-up shown in Fig. 6.19 was used. The transmission through the finger can be modelled with sufficient accuracy for practical purposes by the radiation signal equations:

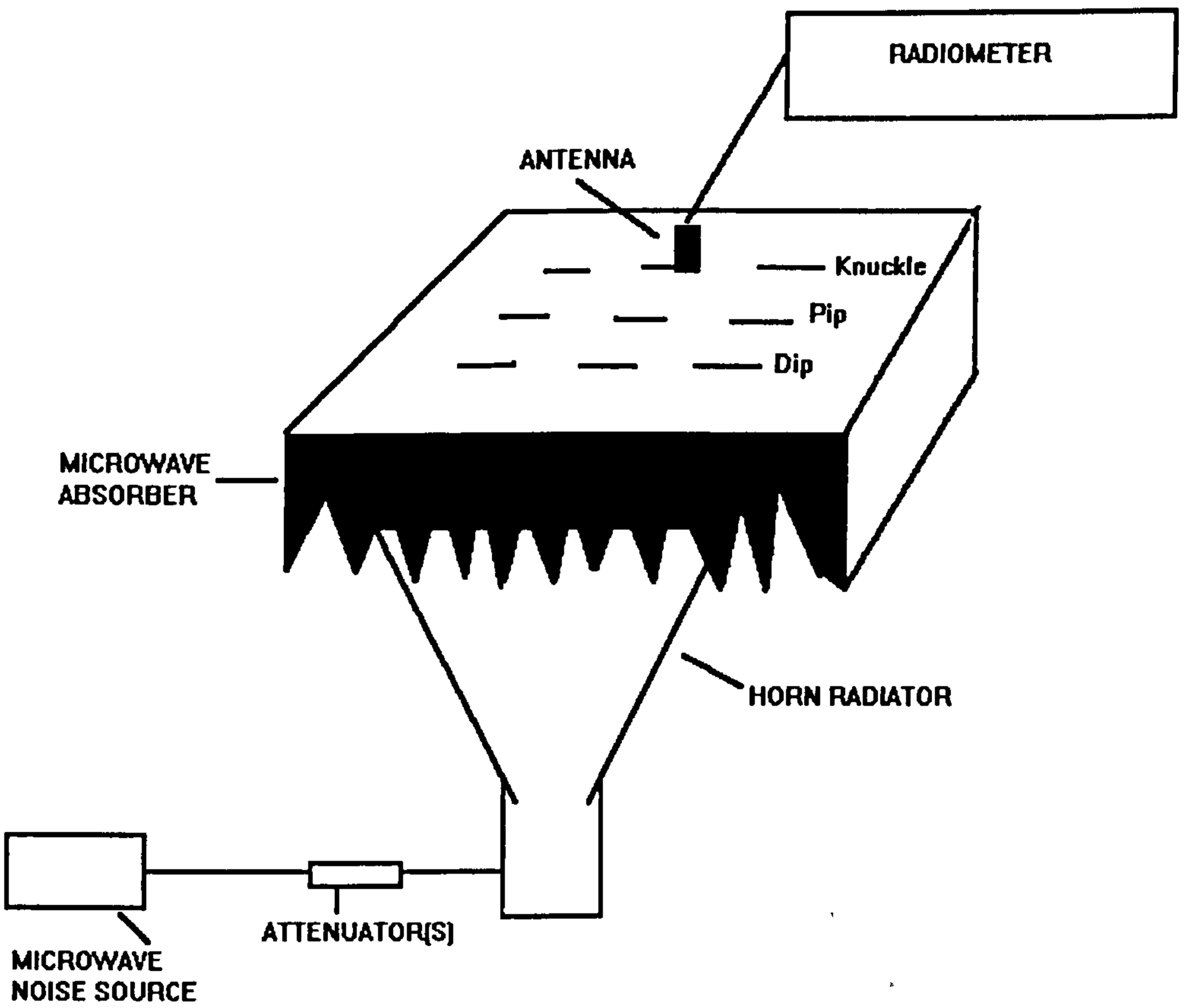

Fig. 6.19 Experimental set-up for transmission of microwave noise radiation through fingers.

$$S_1 = \alpha T_{off} + (1-\alpha) T_{finger}$$

$$S_2 = \alpha T_{on} + (1-\alpha) T_{finger} \qquad 6.8.2.1$$

where S_1, S_2 are the observed microwave temperatures when the noise radiation source is on and off, α is the absorption coefficient, T_{finger} is the true microwave temperature of the finger and T_{on}, T_{off} are the microwave temperatures seen through the material when the noise signal is on/off. Fig. 6.20 shows the distribution of the microwave temperature across the horn radiator when the radiation source is on/off. This was carried out for calibration purposes.

A 3×3 grid was marked on the absorption material and the microwave temperature was noted when the radiation source was both on/off. These temperatures are taken at specific points on the material corresponding to the metacarpal phalangeal joint (knuckle), proximal inter-phalangeal joint (pip) and the distal inter-phalangeal joint (dip) for the three central fingers (calibration points). This gives the value for T_{on} and T_{off}. A hand was then placed with the joints of interest corresponding to the calibration points on the absorption material and the microwave temperature noted as before with /without the radiation noise source.

Solving Eqns 6.8.2.1 simultaneously gives

$$\alpha = \frac{S_1 - S_2}{T_{off} - T_{on}} \qquad 6.8.2.2$$

where α is the fraction of the signal transmitted through the finger at T_{finger}.

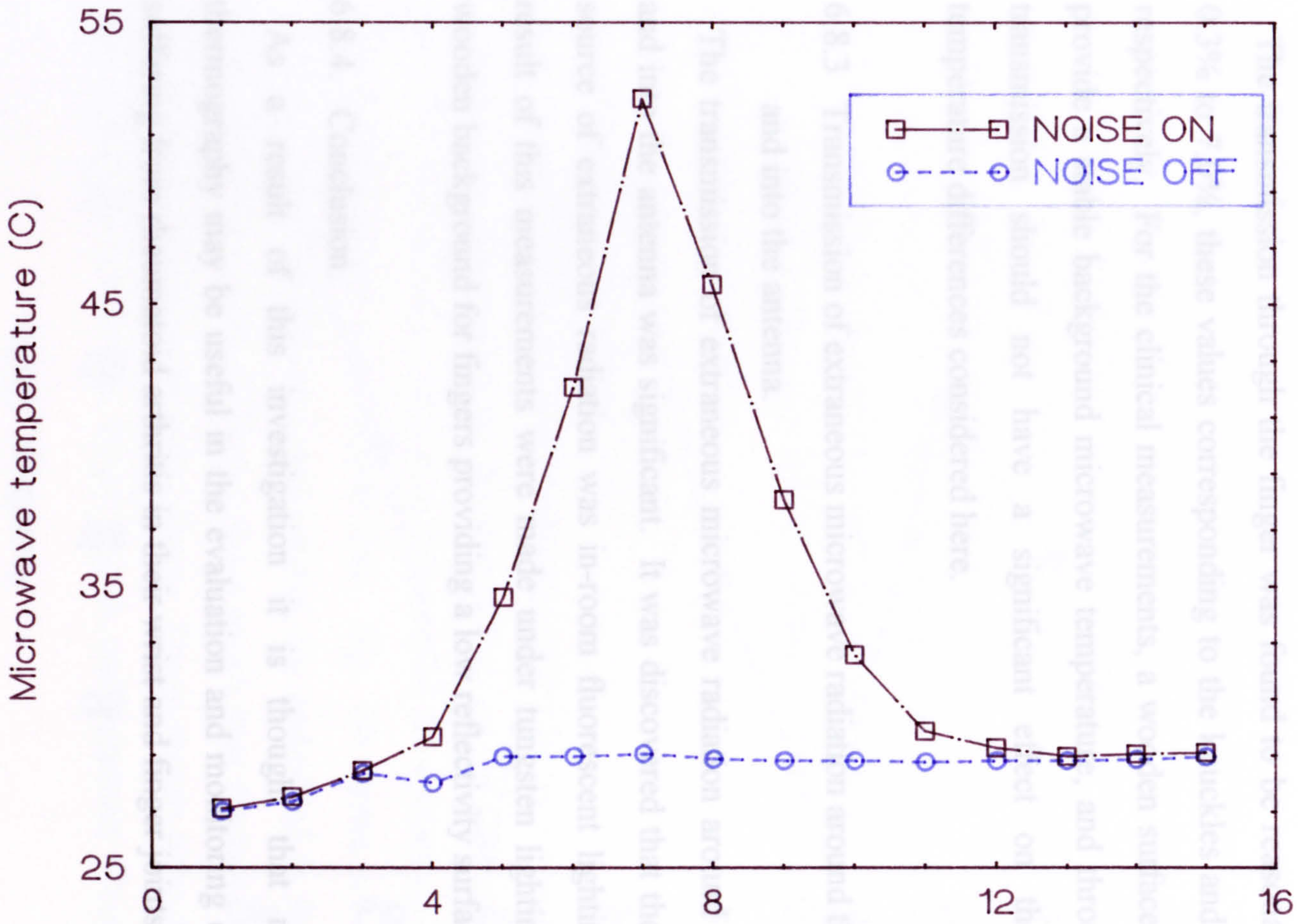

Fig. 6.20 Microwave temperature distribution across the horn radiator when the radiation source is on/off.

Fig. 6.21 shows how the average $\bar{\alpha}$ (average of the absorption coefficients calculated for subjects at specific joints) varies depending on the joint in question. It is clear from the graph that a minimum fraction of the signal is transmitted through the knuckle, the highest occurring at the dip joint.

The transmission through the finger was found to be reasonably small, 0.3% to 7.0%, these values corresponding to the knuckles and dip joints respectively. For the clinical measurements, a wooden surface was used to provide a stable background microwave temperature, and through finger transmission should not have a significant effect on the relative temperature differences considered here.

6.8.3 Transmission of extraneous microwave radiation around the finger and into the antenna.

The transmission of extraneous microwave radiation around the finger and into the antenna was significant. It was discovered that the principle source of extraneous radiation was in-room fluorescent lighting. As a result of this measurements were made under tungsten lighting, with a wooden background for fingers providing a low reflectivity surface.

6.8.4. Conclusion.

As a result of this investigation it is thought that microwave thermography may be useful in the evaluation and monitoring of patients suffering from rheumatoid arthritis in their wrist and finger joints.

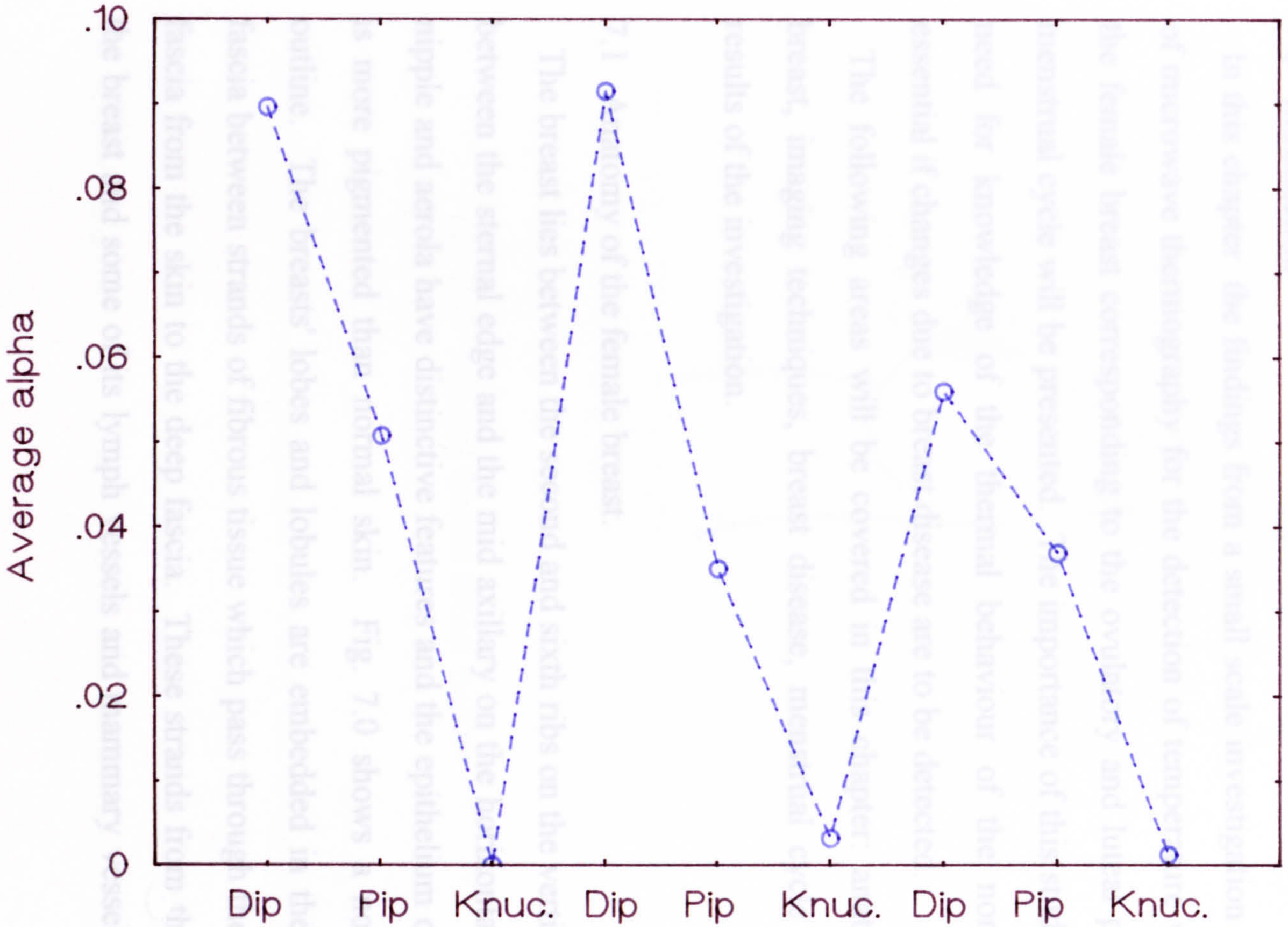

Fig. 6.21 Variation in the average absorption coefficient alpha over the Dip, Pip and Knuckle joints of the three central fingers.

CHAPTER 7.0 A MICROWAVE THERMOGRAPHIC STUDY INTO VARIATIONS IN NORMAL FEMALE BREASTS THROUGHOUT THE MENSTRUAL CYCLE

7.0 Introduction.

In this chapter the findings from a small scale investigation into the use of microwave thermography for the detection of temperature variations in the female breast corresponding to the ovulatory and luteal phase of the menstrual cycle will be presented. The importance of this study lies in the need for knowledge of the thermal behaviour of the normal breast, essential if changes due to breast disease are to be detected.

The following areas will be covered in this chapter: anatomy of the breast, imaging techniques, breast disease, menstrual cycle and finally results of the investigation.

7.1 Anatomy of the female breast.

The breast lies between the second and sixth ribs on the vertical axis and between the sternal edge and the mid axillary on the horizontal axis. The nipple and aerola have distinctive features and the epithelium of the aerola is more pigmented than normal skin. Fig. 7.0 shows a normal breast outline. The breasts' lobes and lobules are embedded in the superficial fascia between strands of fibrous tissue which pass through the superficial fascia from the skin to the deep fascia. These strands from the stroma of the breast and some of its lymph vessels and mammary vessels enter and

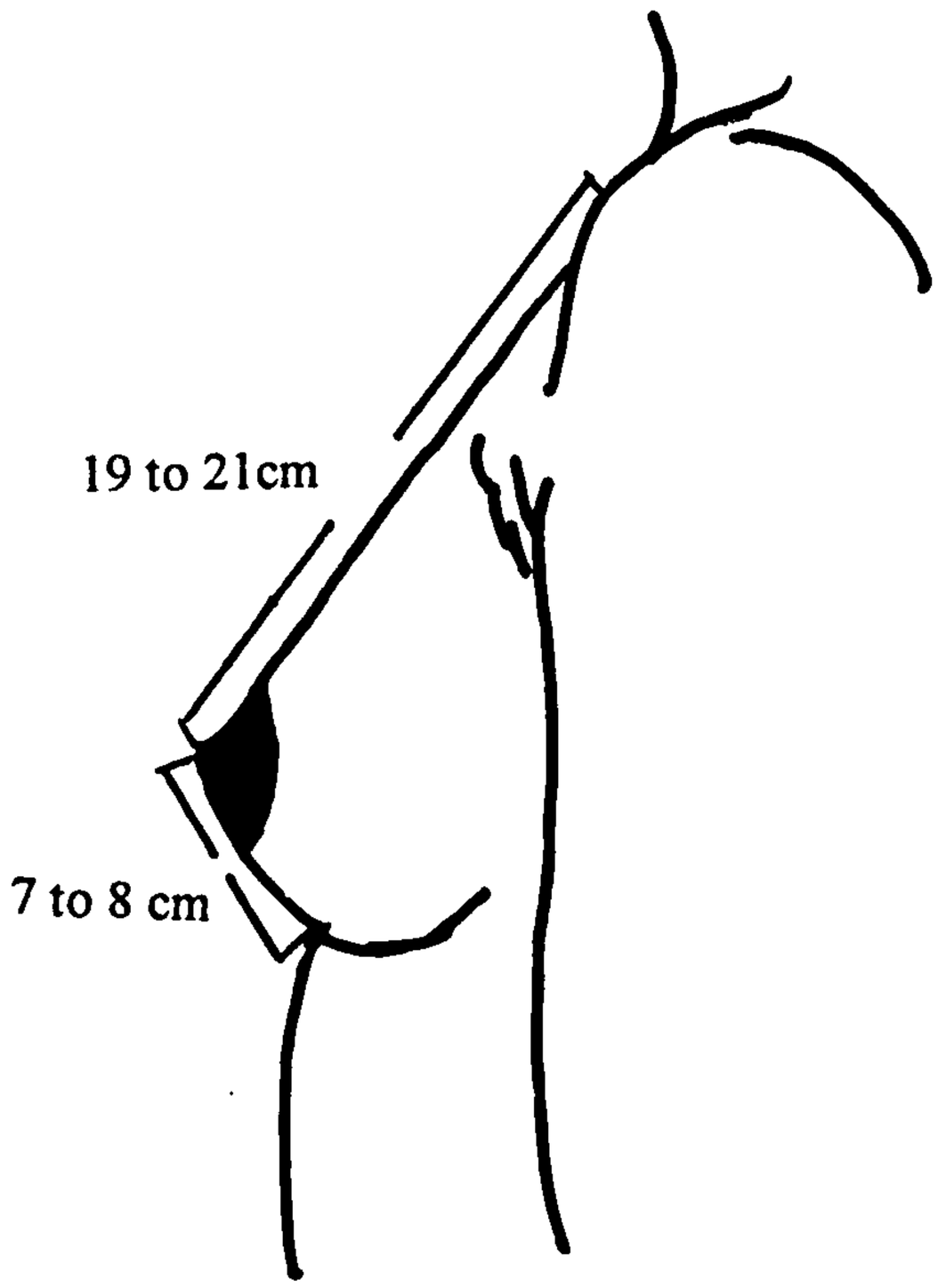

Fig. 7.0 Normal female breast outline.

leave the breast along these strands. Fig. 7.1 shows the internal structure of the female breast. The breast tubes which secrete the milk are grouped together into lobes, then subdivided into lobules and are all separated by the fibrous stroma. The lactiferous ducts, one from each lobe, converge upon the nipple. Under the aerola each duct expands to form a lactiferous sinus, and , narrowing again, opens on the summit of the nipple.(Romanes, G. J)

7.2 Breast disease.

Breast diseases can be split into two main groups, benign and malignant. Correct classification of benign conditions is just as important as for malignant disease, as they are more common than breast cancer, difficult to distinguish from it, and if an incorrect diagnosis is made at an examination the patient may well suffer severe emotional stress.

Any thermal disease detection technique is dependent on there being an inflammatory response in the breast to the development of disease. There are then two problems for unambiguous detection:

1. Seeing the inflammatory response within the natural temperature patterns and pattern variations of the breast.

2. distinguishing between responses to benign and malignant conditions.

Most benign diseases occur in the breast during three main periods of the reproductive life: development, mature reproductive life and involution

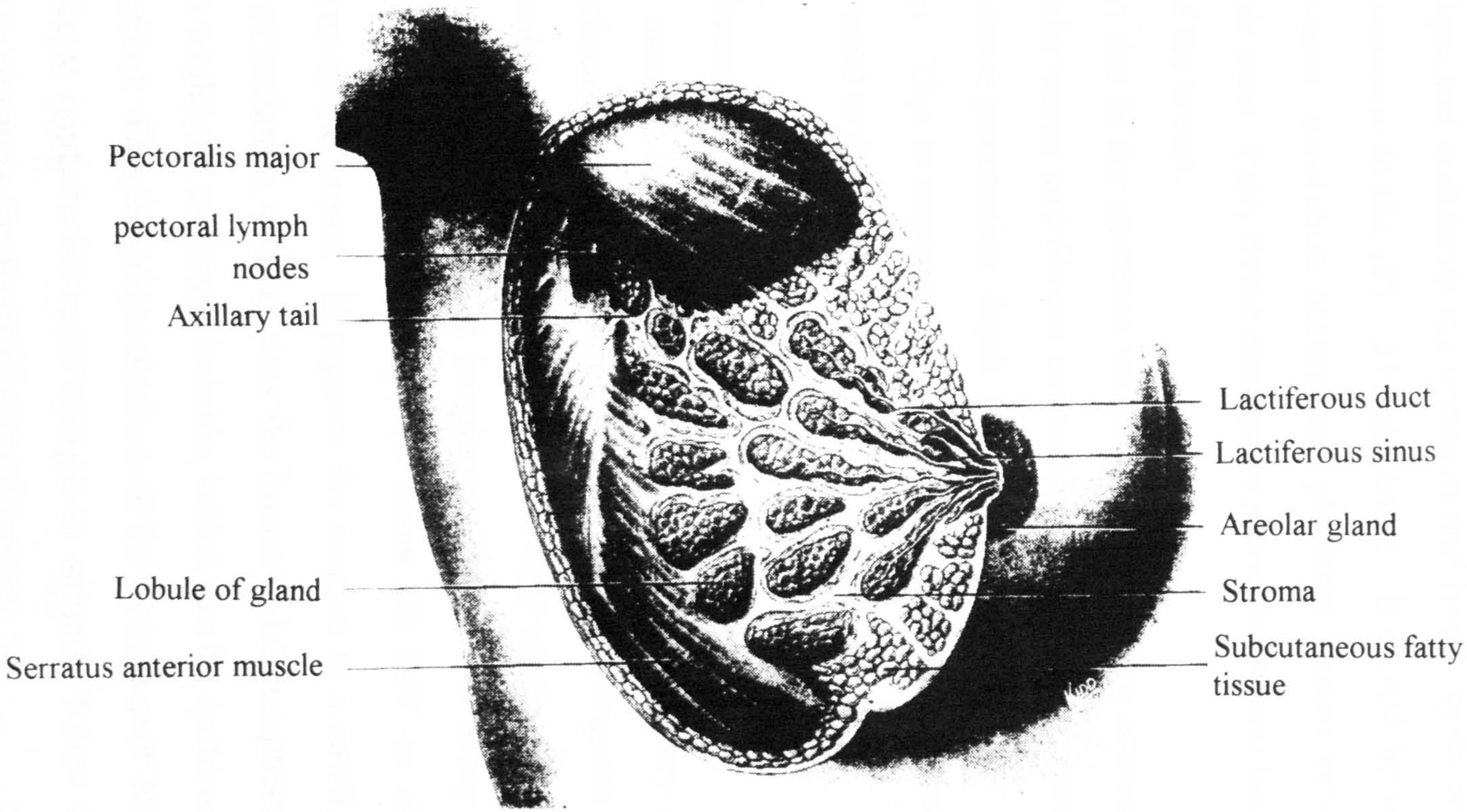

Fig. 7.1 Internal structure of the female breast.

(Dixon & Sainsbury). In women less than 25 years old the most common condition is fibroadenomas; in the age group (25 - 40) years cyclical mastalgia and nodularity are common and finally cysts are thought to be most common in the (35 - 55) age range. It should be noted that at the menopause, involution occurs and glandular tissues revert back to the infantile state. Fatty tissue disappears more slowly and becomes the major part of the breast.

Also due to the immense variation in the relative amounts of fat, water, glandular tissue and fibrous connective tissues which form the breast, the microwave penetration depth may be expected to vary from person to person. This is important in the use of microwave thermography and is considered in this study.

7.3 Breast imaging.

For imaging techniques to be of any clinical use they must be able to detect breast disease in the primary stages and distinguish between benign and malignant growths. The most commonly used, and probably the most effective method of breast imaging at present, is X-ray mammography. Mammography utilises X-rays of about 50 keV to obtain transverse pictures of the breast. It exposes the women to a small, but non-trivial, dose of radiation, and requires the breast to be compressed between two plates whilst the exposure is made, which can be quite uncomfortable for the patient. This technique works well for women over 35 years, however, the breast tends to be radio opaque in subjects below 35 years and so higher exposures are needed for good images.

Other imaging techniques include sonography, thermography and transillumination light scanning.

Breast Sonography is the ultrasound examination of the breast. It is a non-invasive technique which produces accurate cross-sectional images of the breast tissue. It can be performed with either an automated whole breast unit or a high frequency hand-held instrument. Automated breast units produce sequential thin-section whole breast images, allowing for the accurate detection of abnormalities. Thus, automated whole breast scanners are more appropriate for breast screening examinations than the hand-held units. The hand-held units are less expensive than the automated units and can be used for guided needle biopsy.(Basset, L. W., 1990). However, due to technical limitations such as inadequate resolution, inconsistent reproducibility and distortion of the breast architecture from compression, it is used mainly as a complement to mammography (Rubin et al, 1978). The most important clinical use of this technique is its ability to differentiate between cysts and solid masses.

Transillumination light scanning is also a non-invasive method. It relies on the differential transmission by breast tissues of non-ionising radiation in the red and near -infra-red range of the spectrum (Monsees, B, 1978).

Thermography is in the general sense a measure of temperature variations over the skin surface. There are many thermographic methods - liquid crystal, infra-red, and microwave thermography.

Liquid crystal thermography uses a system of cholesterol esters encapsulated in flexible mylar sheaths. When placed in direct contact with

the skin of the breast, a unique colour pattern appears which can be photographically recorded.(Monsees, B).

A number of groups have studied the use of infra-red imaging of female breasts for the detection of abnormalities. A discussion on the work carried out by Draper &Jones, Lloyd Williams and Verzini & Romani is given in section 7.8.3. A review of breast imaging was given by Jones, 1982.

The use of microwave thermography for the detection of breast disease is discussed in section 7.6.

Why is breast screening for cancer important ? Breast cancer is the commonest form of cancer among women in the U.K. Each year there are approximately 15,000 deaths from the disease, in comparison to ~75,000 deaths among women from all other forms of cancer. The U.K. mortality rate is the highest in the world. Neither the cause of breast cancer nor ways of preventing the disease are known, so the only way to substantially reduce the number of deaths from the disease is to detect it before the patient presents with the symptoms. Also, the effectiveness of treatment is related to the stage at which the disease is presented. In other words, a country wide screening programme must take place if the lives of thousands of women are to be saved.(Forrest, P).

7.4 Menstrual cycle.

The menstrual cycle is controlled by the brain. This cycle is caused by hormones and chemical messengers being released into the bloodstream at certain times by various glands. The sequence of hormonal changes

occurring in the menstrual cycle are shown in Fig. 7.2. At menstruation, plasma levels of the follicle stimulating hormone, FSH are rising, stimulating the growth of several Graafian follicles within the ovary. Only one follicle is chosen to house the developing ovum and as this follicle develops it produces increasing amounts of oestrogens (oestradiol). Now as the level of oestradiol rises in the early follicular phase, the production of FSH is suppressed, but oestradiol levels continue to increase until a critical level is reached. Approximately 24 hours after this level is reached there is a surge of lutenizing hormone, LH and to a smaller extent, FSH for one day only. Ovulation follows this surge within about 30 - 36 hours and the ruptured ovarian follicle develops into the corpus luteum which secretes both oestradiol and progesterone in the luteal phase of the cycle. Thus the levels of oestradiol and progesterone rise together after ovulation, reaching a maximum between days 18 and 22 of a 28 day cycle. In the last few days of the cycle, the corpus luteum degenerates, oestradiol and progesterone levels fall and menstruation begins a new cycle (Barlow, D & Mcpherson, A).

7.4.1 Effect of combined oral contraceptives on the menstrual cycle.

The combined oral contraceptive pill contains similar hormones to the oestrogen and progesterone produced by the ovary. As a result of this the pituitary gland reduces its output of the hormones FSH and LH. So the mid cycle surge of LH which is essential for egg release does not occur. Also with so little of the hormones from the pituitary reaching the ovaries

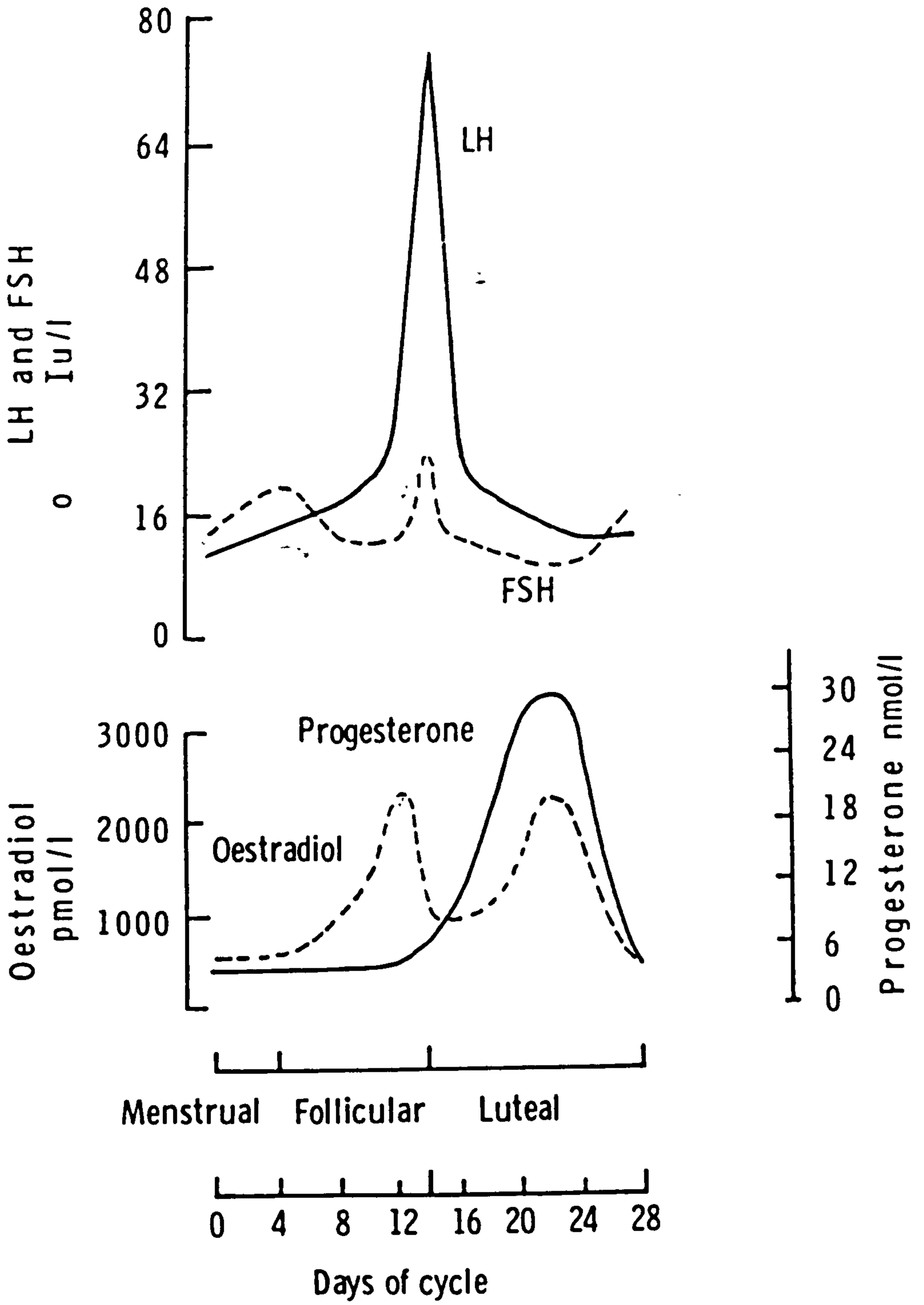

Fig. 7.2 Hormone changes throughout the menstrual cycle.

they go into a state of rest and produce minimal amounts of natural oestrogen and progesterone.

Thus while a women is taking the contraceptive pill the normal menstrual cycle stops. However, most systems of pill taking include a pill-free time, usually one week in every 28 days. The effect of cutting off the supply of pill hormones is to imitate the fall in the levels in the blood stream of their natural equivalents at the end of the normal cycle. This causes the shedding of the corpus luteum which the pills hormones have produced during the previous 21 days (Guillebaud). Two of the subjects in this study, subjects 3 and 4, were taking combined oral contraceptives (COC's) throughout the period of this research. The following COC's were used:

Subject	Name of COC	Name of oestrogen	Dose of oestrogen	Name of Progester-one	Dose of Progester-one
3	"Femodene"	ethinyl-oestradiol	30mcg	gestodene	75mcg
4	"Marvelon"	ethinyl-oestradiol	30mcg	desogest-rel	150mcg
	"Mercilon"	ethinyl-oestradiol	20mcg	desogest-rel	150mcg

Subject 4 changed pill type mid cycle and so an extended cycle length occurred. This will be considered again later in this chapter.

7.5 Monitoring of basal temperature

In a normal biphasic ovulatory cycle, following ovulation there is an increase in the morning basal body temperature. This increase in temperature is due to the raised levels of progesterone in the second half of the ovulatory cycle. The volunteers in this study were asked to monitor their basal temperatures throughout the period of research. Every morning when the volunteers awakened, prior to eating or drinking, they placed a thermometer under their tongue for approximately three minutes. They then recorded the temperature on a chart, an example of which is shown in Fig. 7.3. Ovulation shows its occurrence as a drop in temperature followed by a rise. The temperature should remain raised until the next menstrual cycle occurs. Figs 7.4 and 7.5 show the change in basal temperature throughout the cycles for subject 1, cycle 1 and subject 2, cycle 3. Ovulation took place between days 10 and 14 for subject 1 and occurred between days 11 and 15 for subject 2.

Now if ovulation is inhibited in any way, for example by taking a COC, it would be expected that the normal basal temperature curve would be monophasic. However, Fig 7.6 exhibits a decrease in temperature around days 10 - 12 followed by an elevation of temperature which remains during the cycle. This is a result of the synthetic progesterone's causing an increase in temperature. This effect is observed by some women taking COC's. Subject 4 however, shows no such temperature rise, her basal

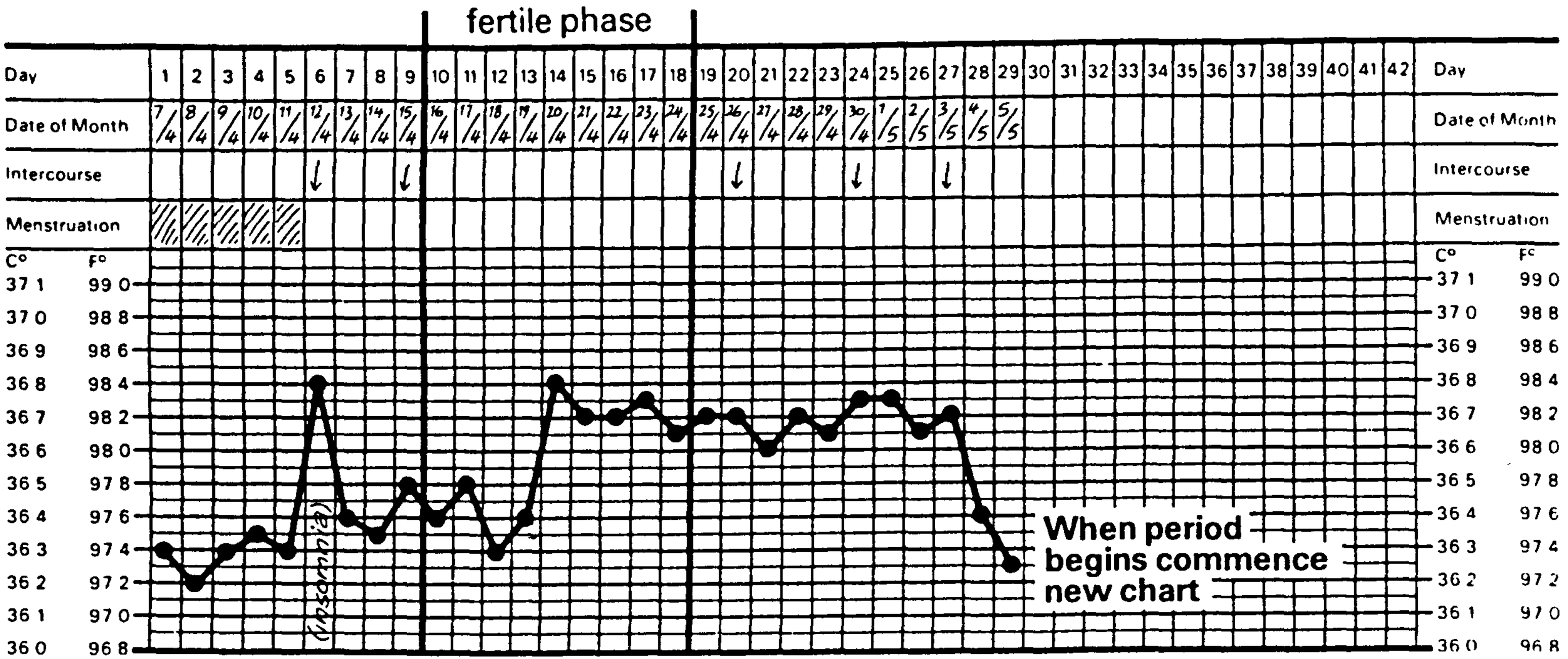

Fig. 7.3 Typical basal temperature chart.

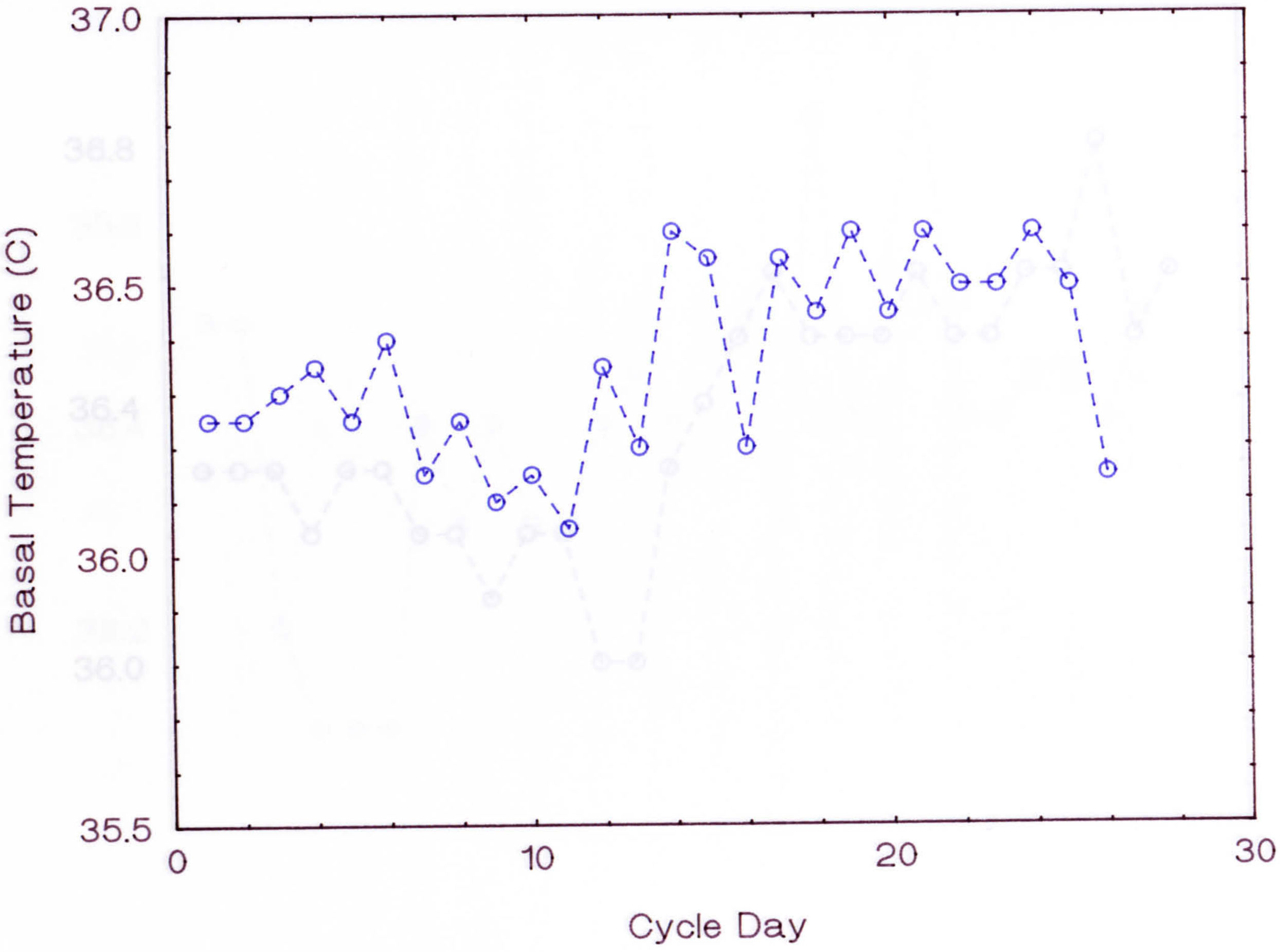

Fig. 7.4 Variation in basal temperature throughout the menstrual cycle, Subject 1, Cycle 1.

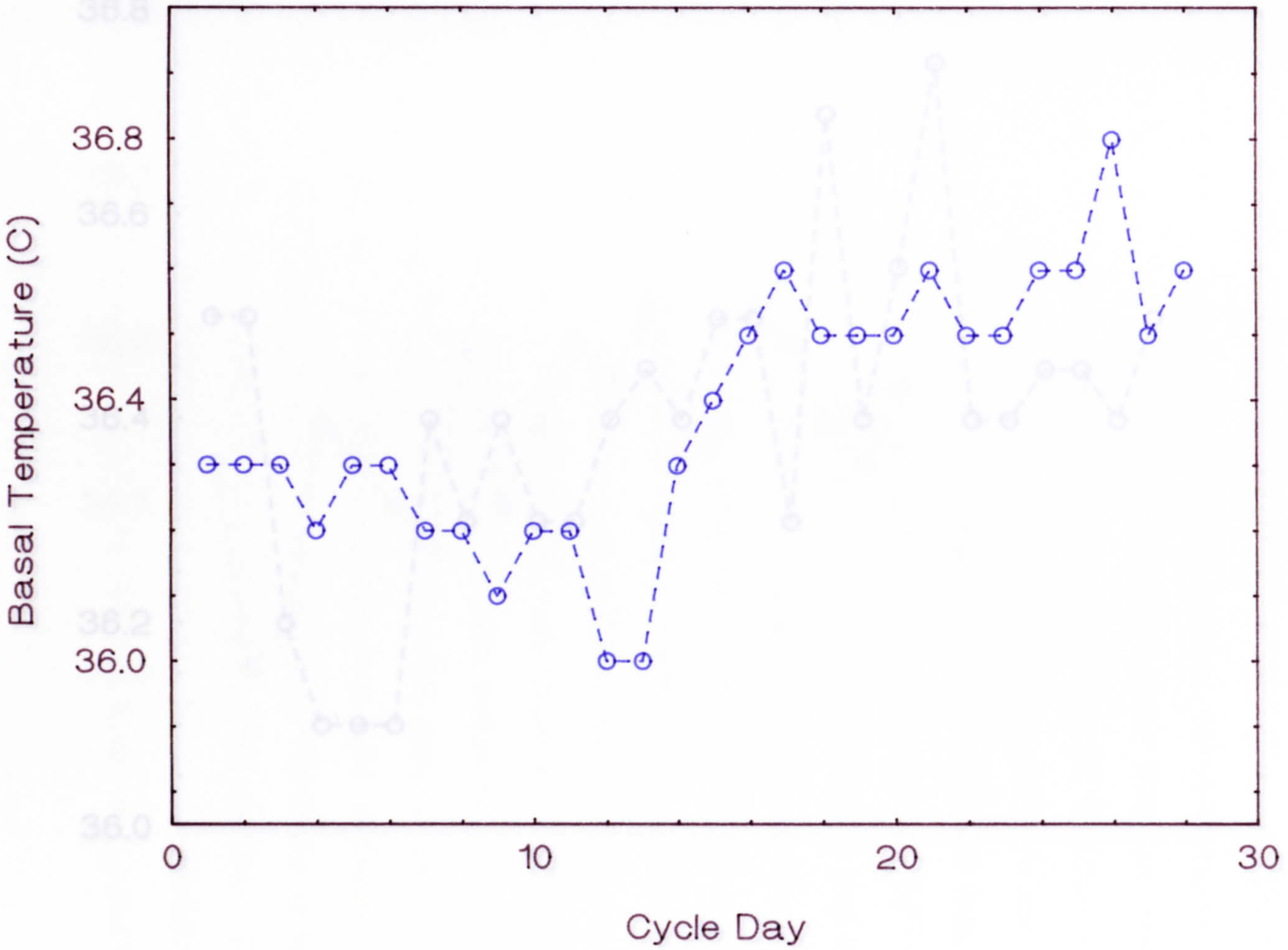

Fig. 7.5 Variation in basal temperature throughout the menstrual cycle, Subject 2, Cycle 3.

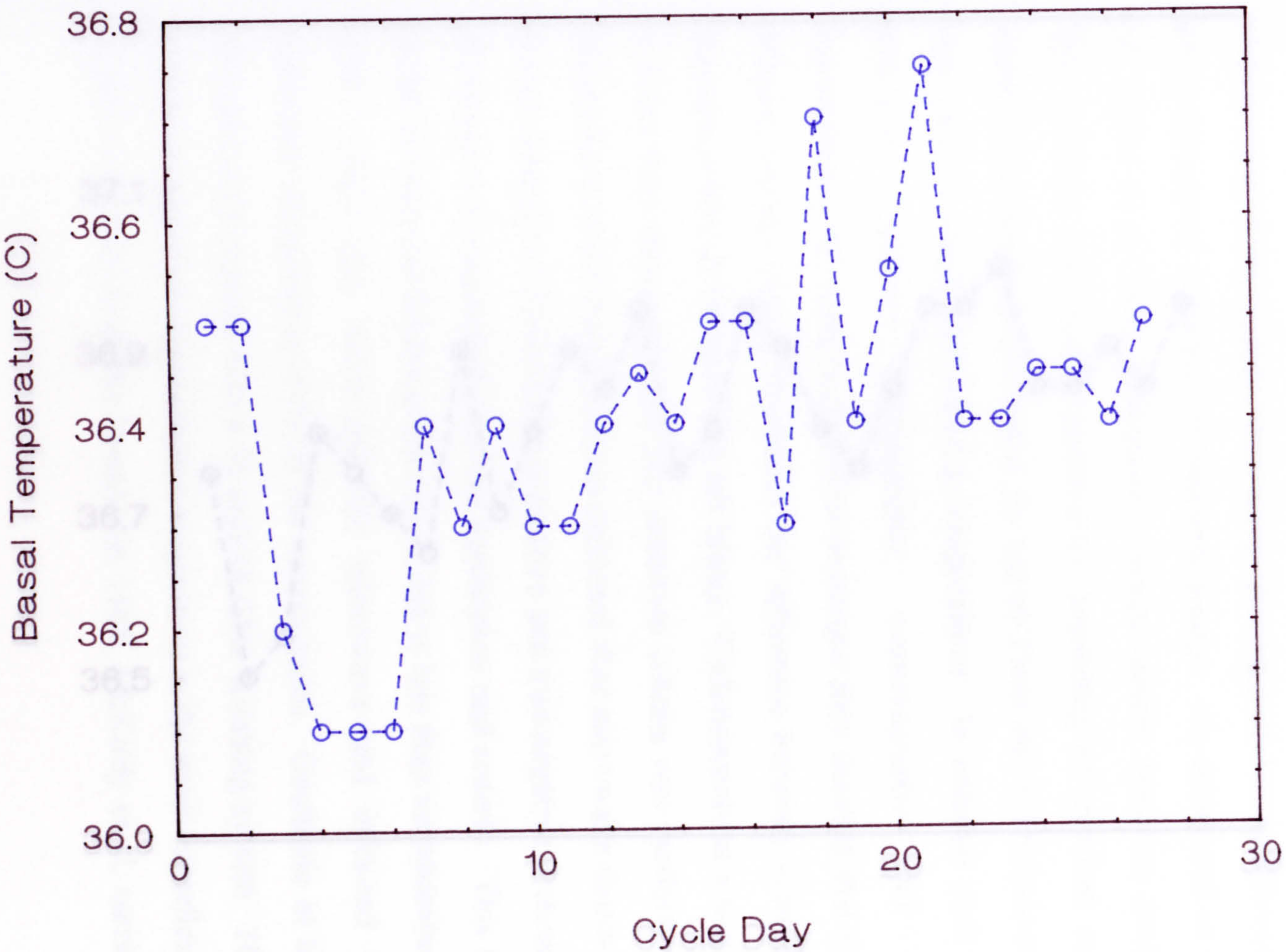

Fig. 7.6 Variation in basal temperature throughout the menstrual cycle, Subject 3, Cycle 2.

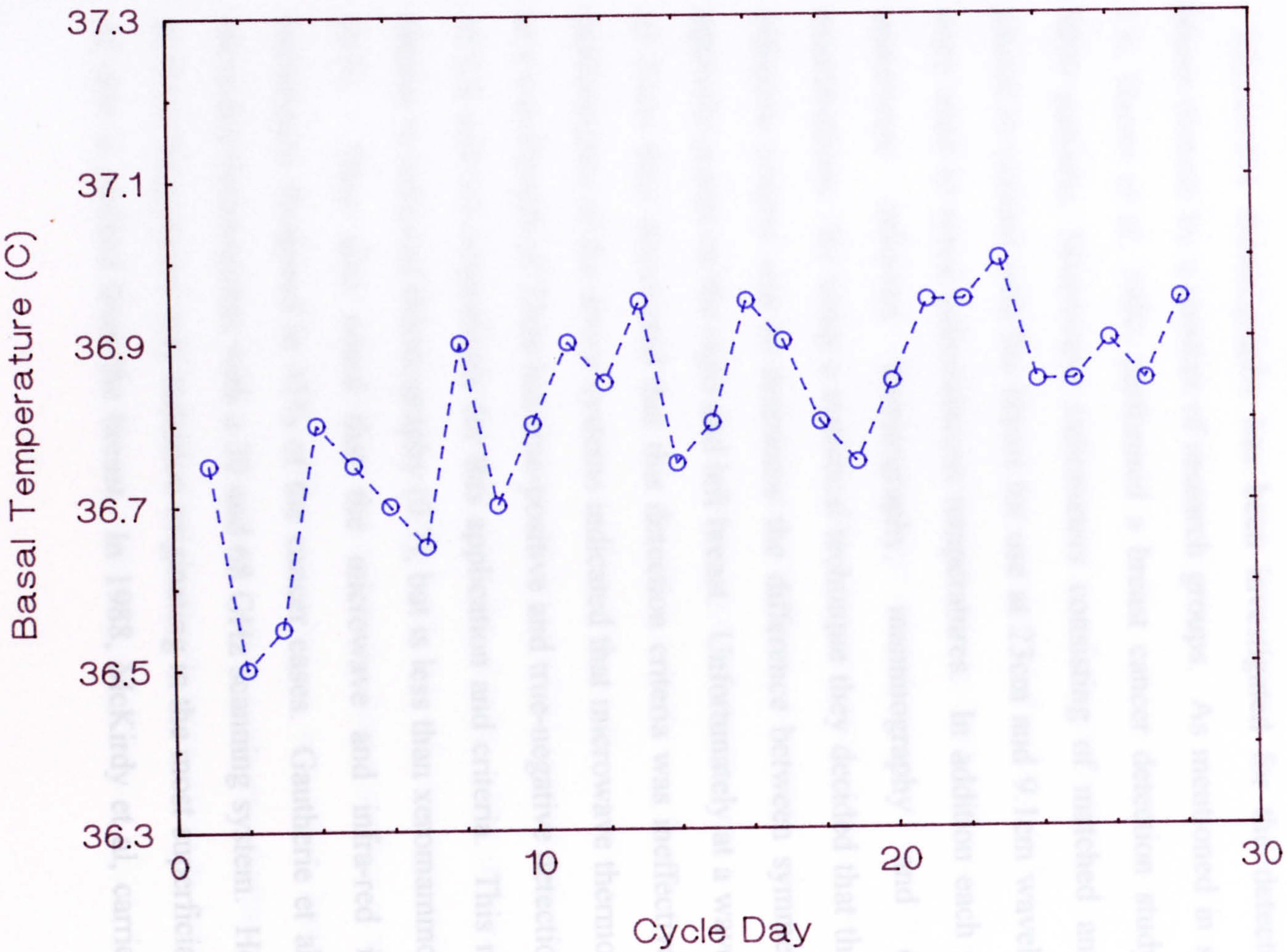

Fig. 7.7 Variation in basal temperature throughout the menstrual cycle, Subject 4, Cycle 2.

temperature chart is monophasic. This illustrates the difficulty of applying a general finding, here temperature - time variation, to a particular individual subject.

7.6 Microwave thermography of breasts.

Microwave thermography has been investigated for the detection of breast disease by a number of research groups. As mentioned in section 1.6, Barret et al, 1980, performed a breast cancer detection study of ~ 5000 patients. Microwave radiometers consisting of matched antennae placed in contact with the breast for use at 23cm and 9.1cm wavelengths were used to sense subcutaneous temperatures. In addition each patient underwent infra-red thermography, mammography and clinical examinations. By using a statistical technique they decided that the most effective criteria was to determine the difference between symmetrically opposite points on the right and left breast. Unfortunately at a wavelength of 23cm they discovered that this detection criteria was ineffective. The performance of the above systems indicated that microwave thermography at a wavelength of 23cm has true-positive and true-negative detection rates of 0.8 and 0.6 respectively for this application and criteria. This result is similar to infra-red thermography (0.7), but is less than xeromammography (0.9). They also noted that the microwave and infra-red imaging techniques disagreed in 41% of the cancer cases. Gautherie et al, 1979, recorded thermograms with a 30 and 68 GHz scanning system. However, at these frequencies only radiation originating in the most superficial layers of skin is emitted from the breast. In 1988, McKirdy et al, carried out a

study at the Western Infirmary , Glasgow. Two hundred and forty-three women with breast lumps were scanned using the Glasgow radiometer. Of these 243 women, 139 had breast cancer and 104 benign lesions. Positive results were obtained in 125 out of 139 cancers. All of the above results suggest that microwave thermography may have a role in the diagnosis of breast disease, particularly when it offers important advantages of inherent safety and ease of use.

7.7 Monitoring of breast temperatures throughout the menstrual cycle.

As mentioned in section 7.0, a knowledge of the thermal behaviour of the normal breast is essential if changes due to breast disease are to be detected. In order to determine the thermal behaviour of normal breasts the temperature variation over the breast was investigated using microwave and surface thermography with combined thermal and microwave modelling for analysis of the measurements.

7.7.1 Control group

Microwave and surface temperature scans of 21 normal subjects were measured with the Glasgow thermography system. The subjects were aged between 17 and 55, average age being 27. A grid was marked on both breasts and the antenna moved across the breast surface at a rate of 1cm/2.5secs. The infra-red surface temperature was taken immediately after the microwave scan using a hand held pyroelectric thermometer as described previously. The grid size was scaled according to breast size.

All of the measurements were taken in a limited room temperature range of 19 - 21 C.

From these 21 subjects, the scans could be placed into five categories. These being

Category	Description
1.	clear dipping pattern across the breast
2.	modest dipping across the breast
3.	flat trace across the breast
4.	patchy pattern
5.	asymmetric

Examples of the observed patterns are shown in Figs. 7.8 to 7.12. It was found that of the subjects scanned, 29% were in category 1, 24% in category 2, 33% were category 3, 9% category 4 and finally, 5% had asymmetric breast thermograms. Fig. 7.13 shows the frequency distribution of the breast scans obtained,

In 1969 Draper and Jones carried out the infra-red thermographic examination of normal breasts using a Pyroscan Mk 11b infra-red imaging scanner in an attempt to classify breast patterns in order to facilitate the identification of thermal abnormalities. On analysis of 442 clinically normal women they observed four different types of pattern which they grouped as follows: Group1 - cold breasts, Group 2 - some vascularity

CATEGORY 1 - 28.6% of subjects

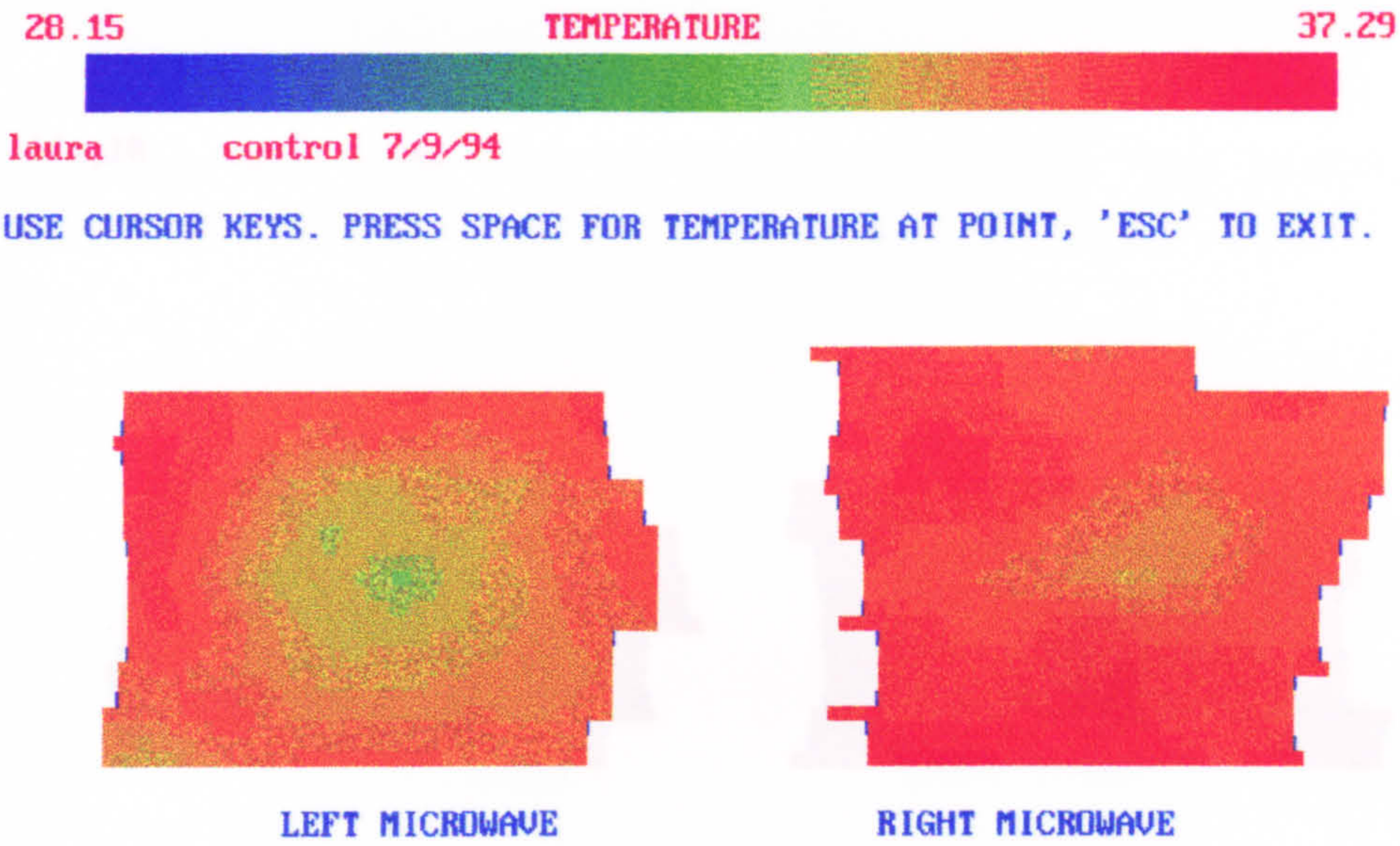

Fig. 7.8 Category 1 - clear dipping pattern across breasts

CATEGORY 1 - 28.6% of subjects

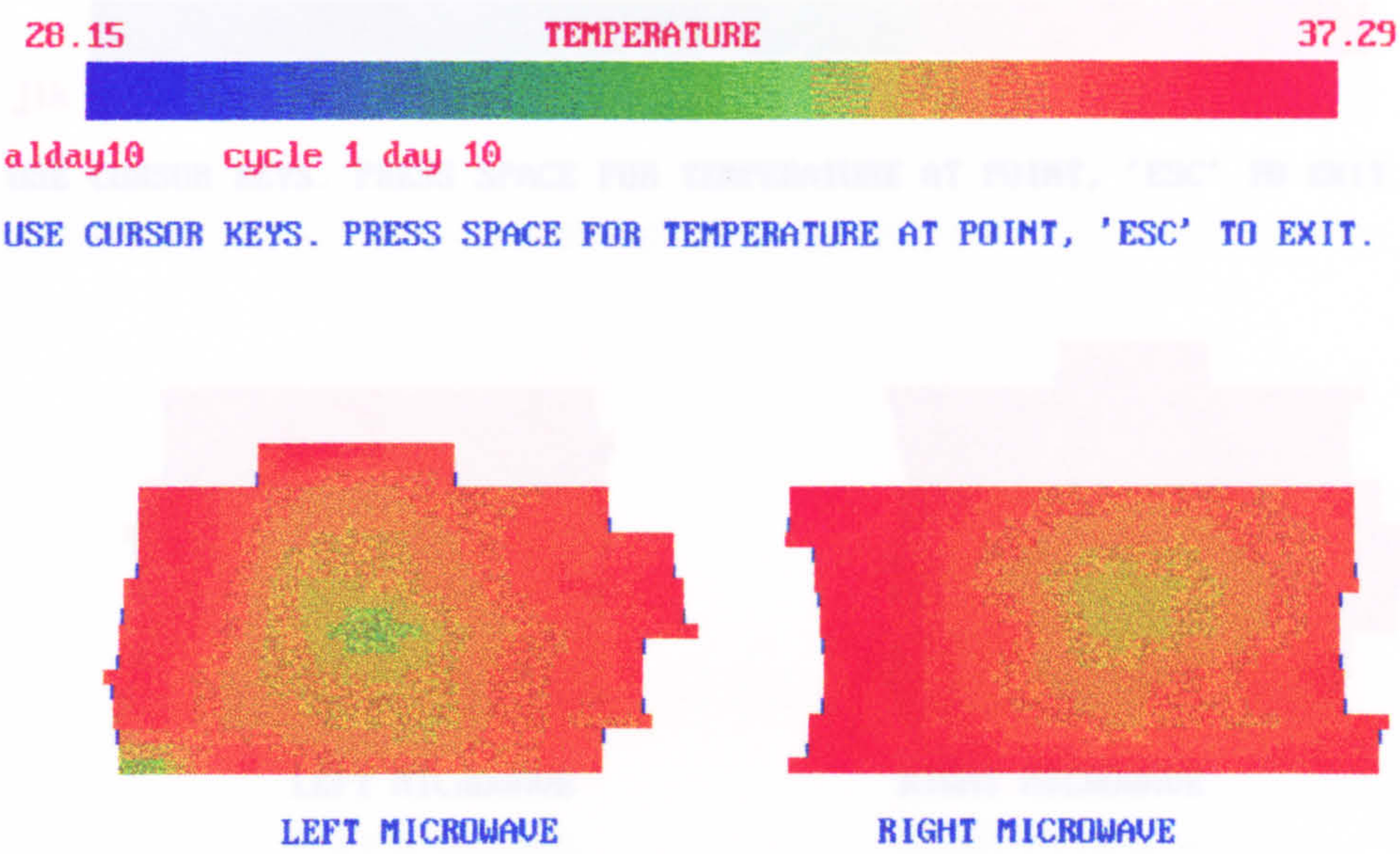

Fig. 7.8a Category 1 - clear dipping pattern across breasts

CATEGORY 2 - 23.8% of subjects

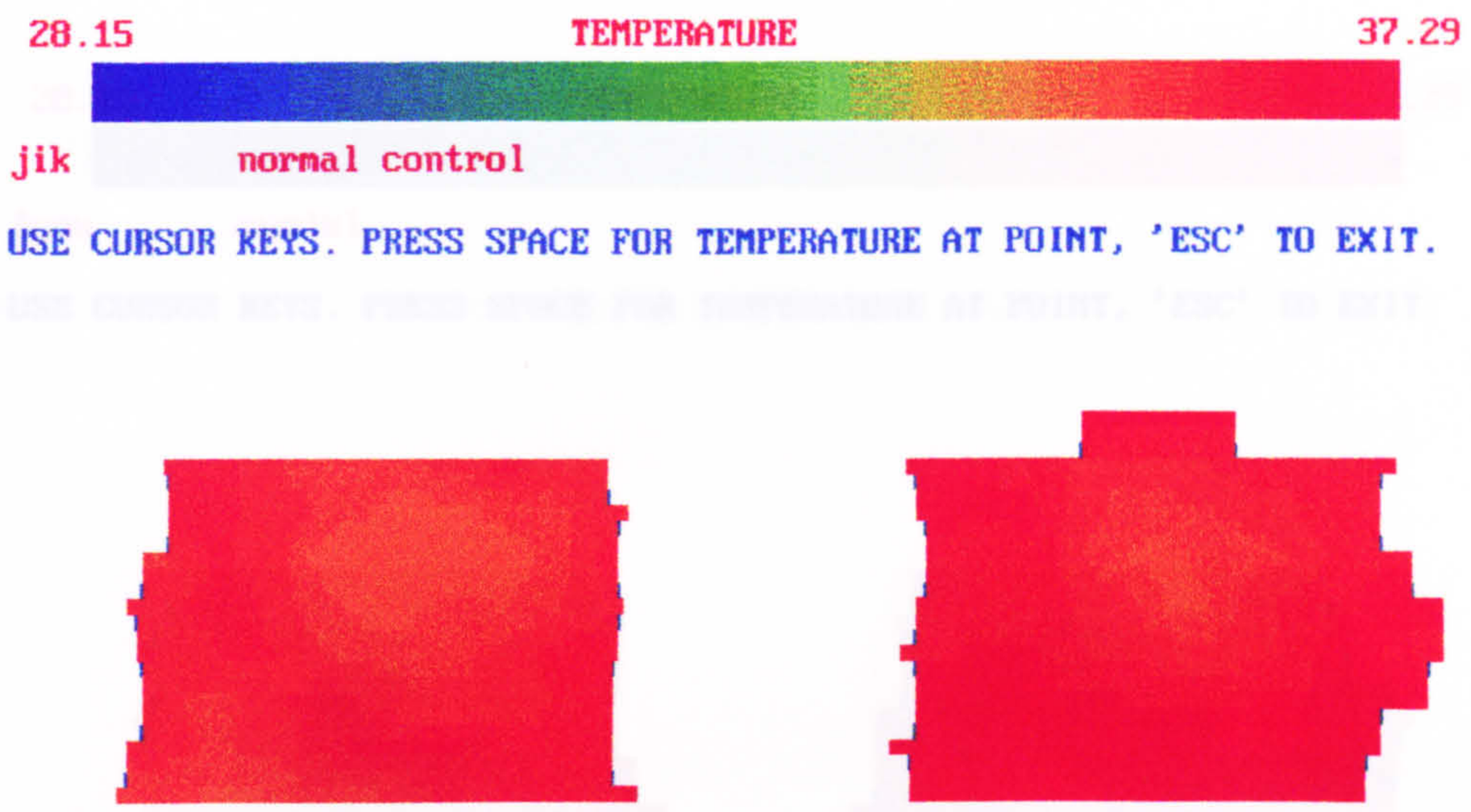

Fig. 7.9 Category 2 - modest dipping across breasts

CATEGORY 2 - 23.8% of subjects

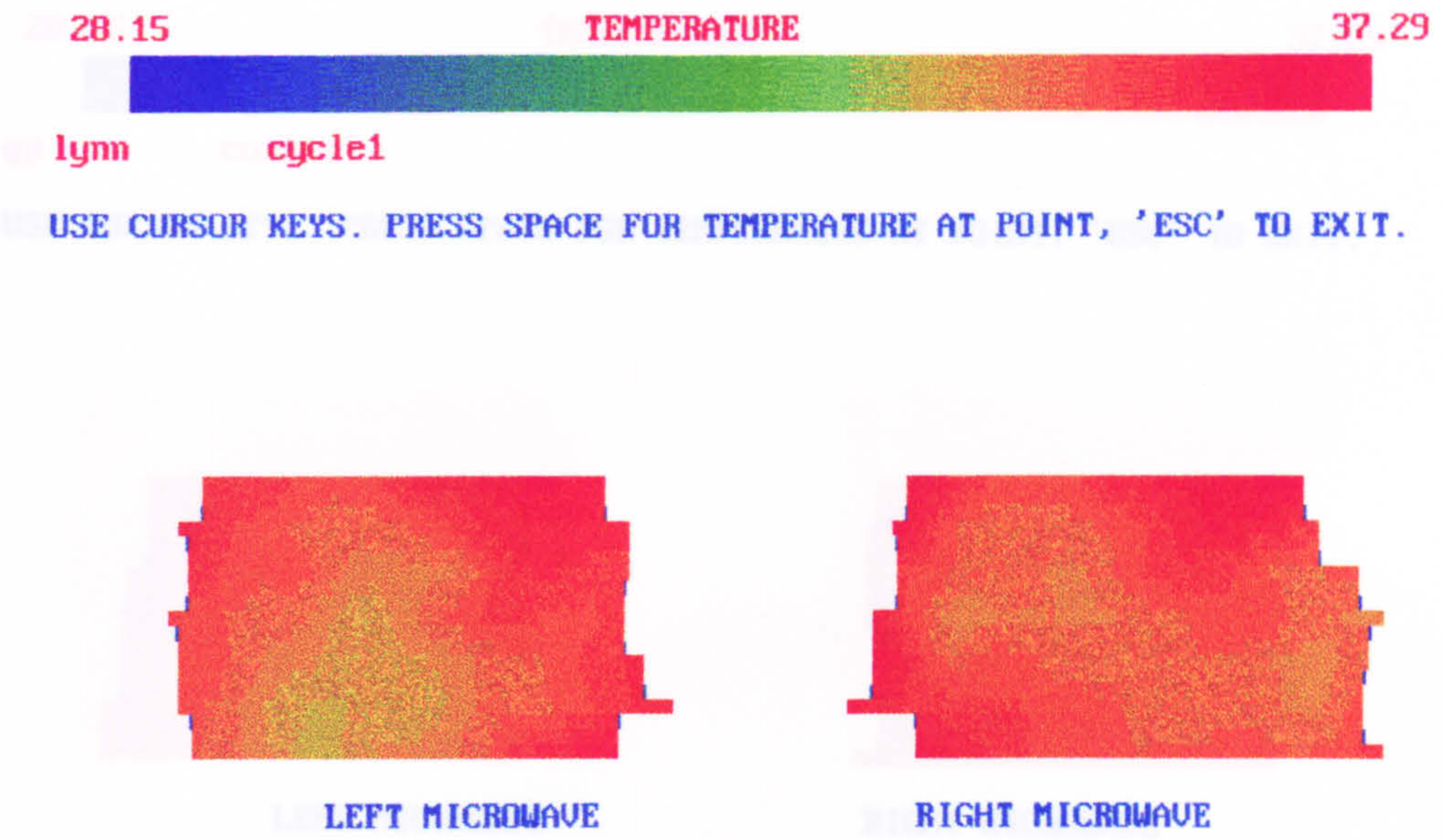

Fig. 7.9a Category 2 - modest dipping across breasts

CATEGORY 3 - 33.3% of subjects

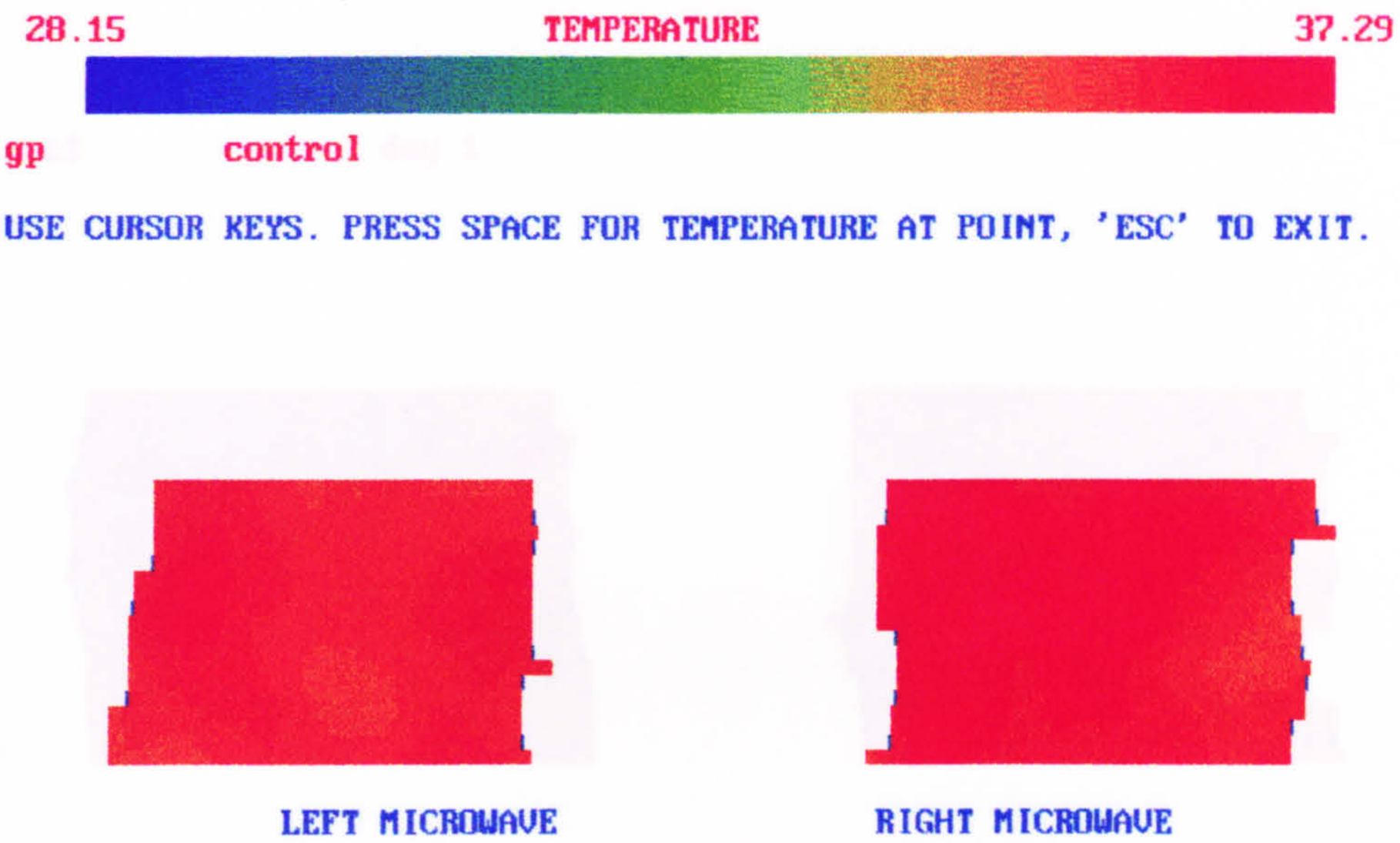

Fig. 7.10 Category 3 - warm breasts

CATEGORY 3 - 33.3% of subjects

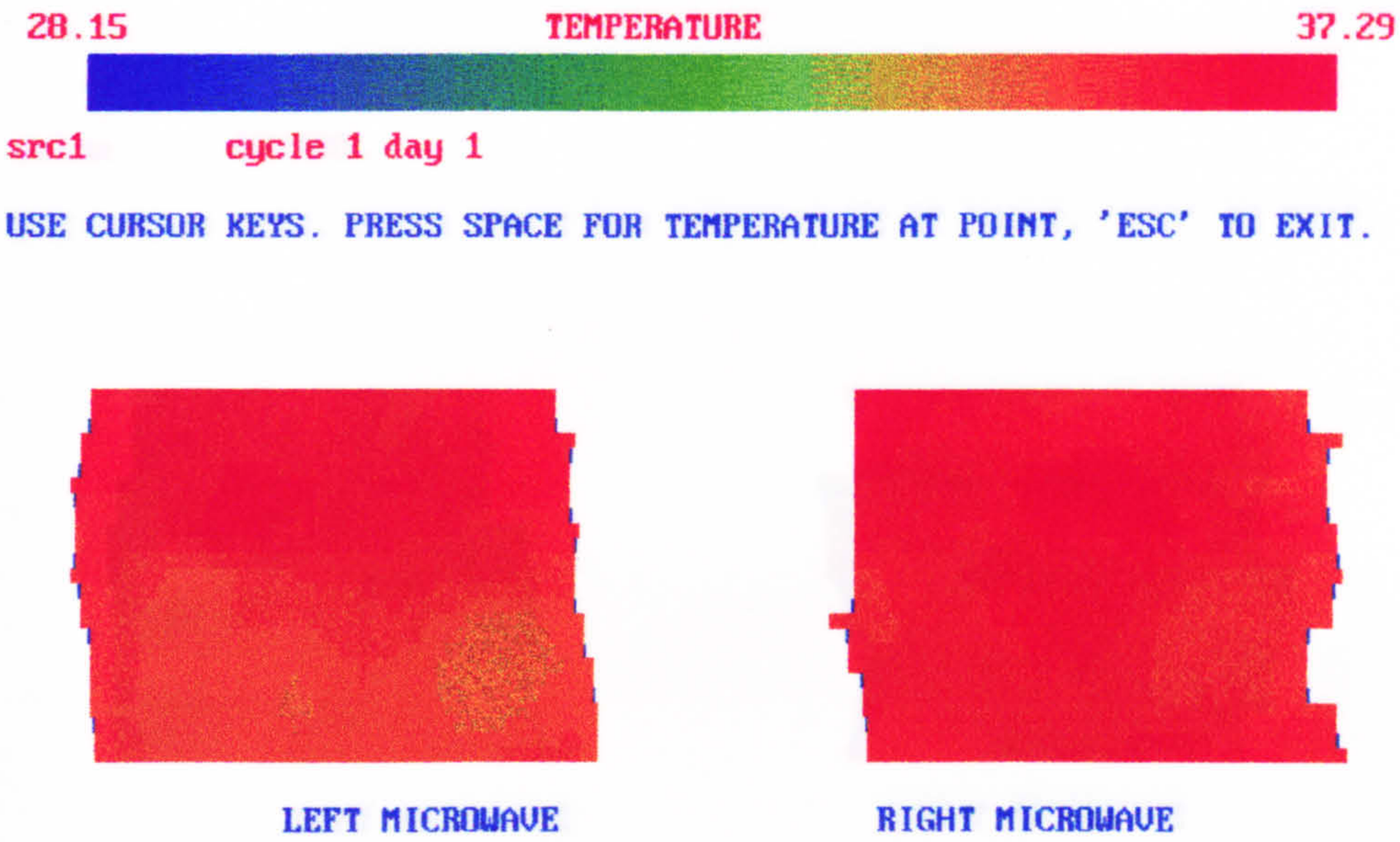

Fig. 7.10a Category 3 - warm breasts

CATEGORY 4 - 9.5% of subjects

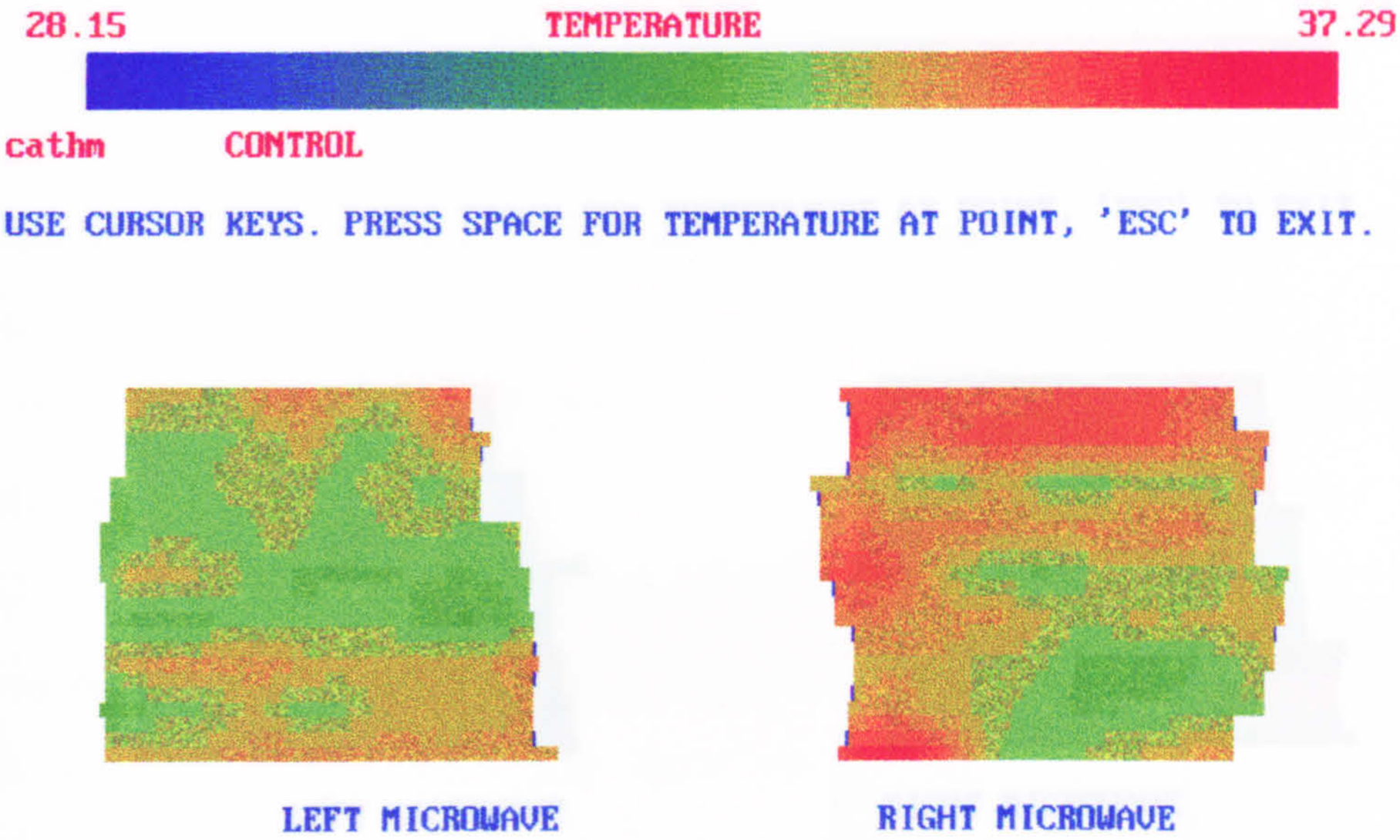

Fig. 7.11 Category 4 - patchy pattern

CATEGORY 5 - 4.8% of subjects

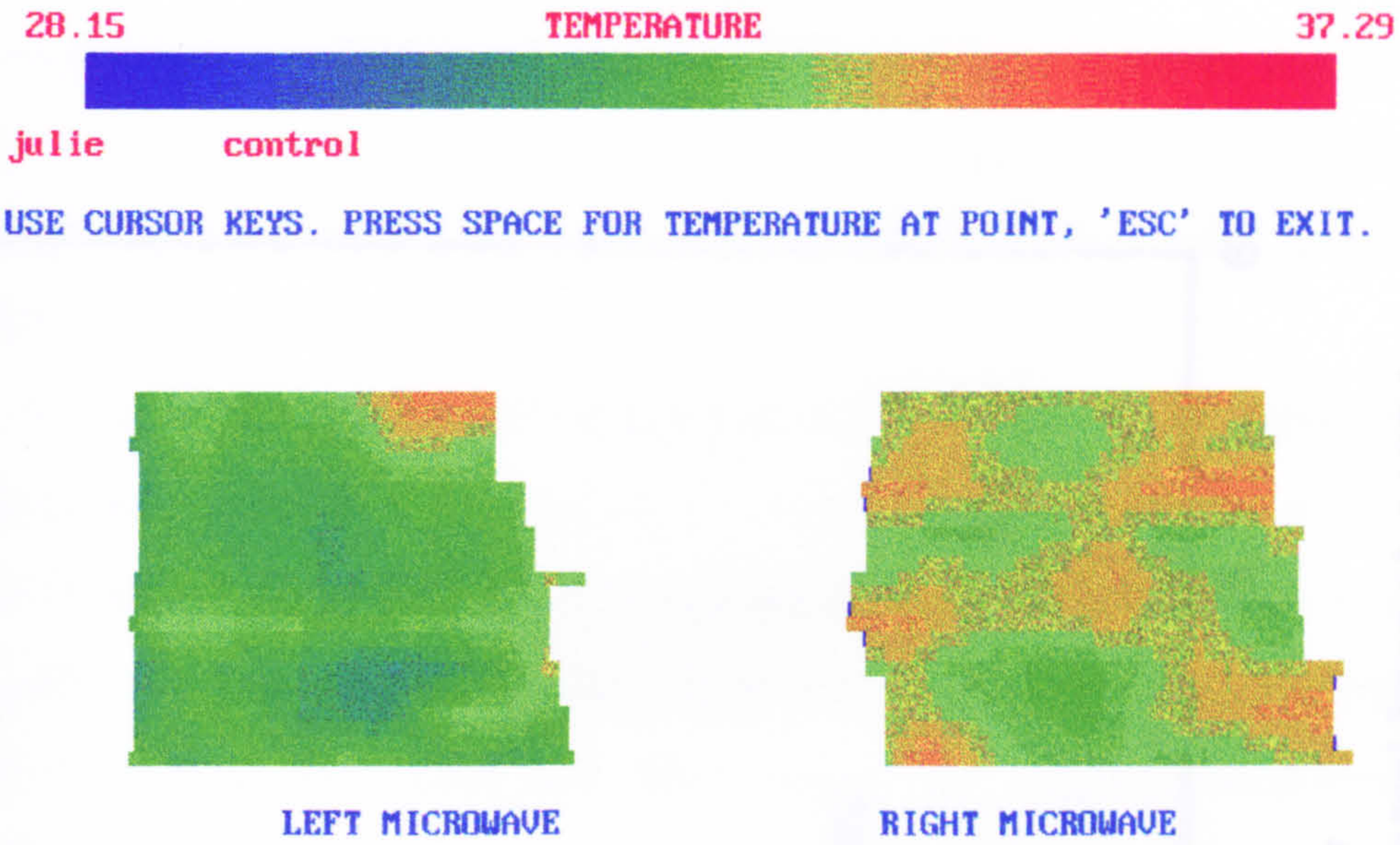

Fig. 7.12 Category 5 - asymmetrical breast pattern

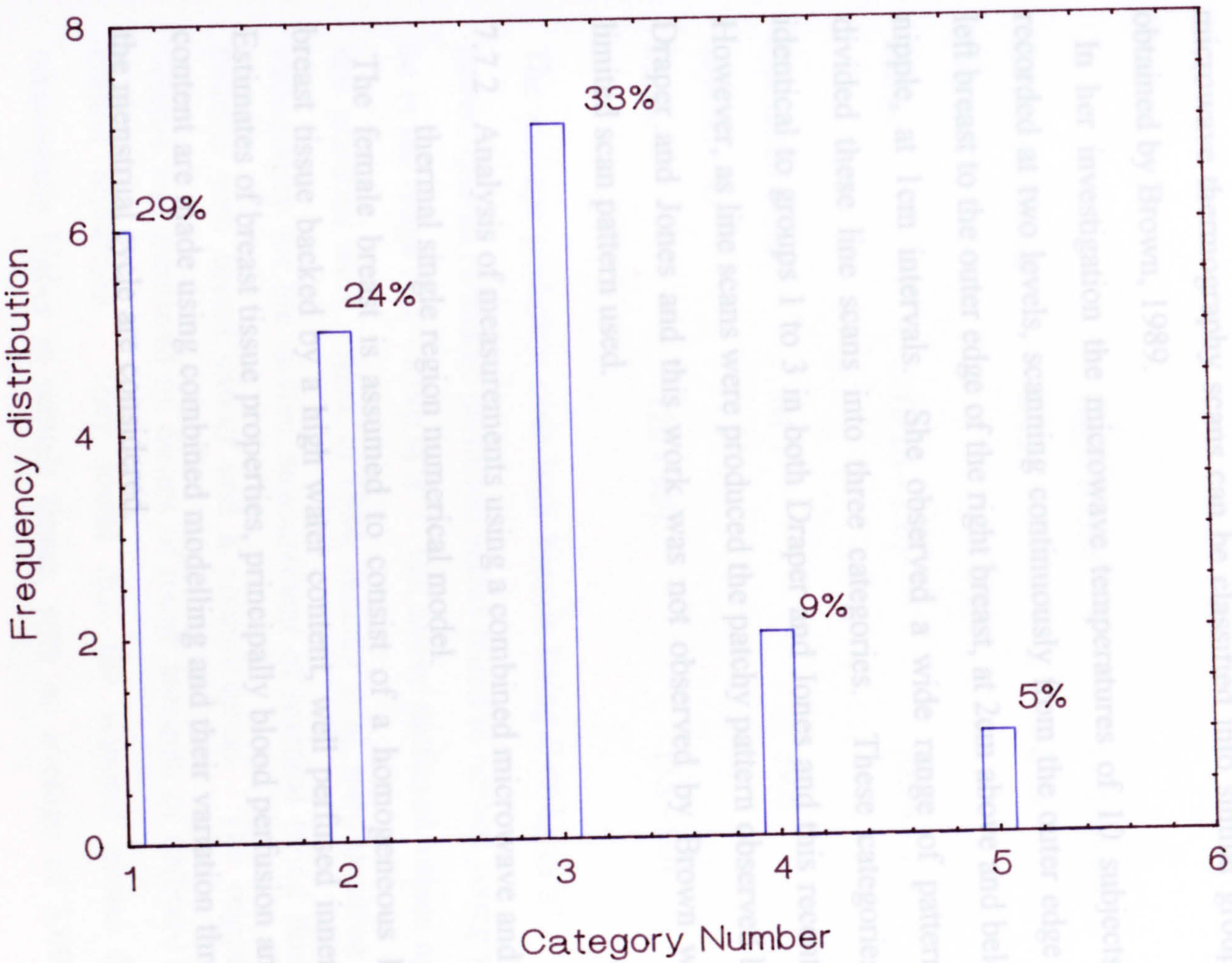

Fig. 7.13 Frequency distribution of control breast scans.

present, Group 3 - warm breasts and group 4 - patchy breasts. They also observed some patterns that could not be classified as the breast thermograms were asymmetric. So there are clear similarities between Draper and Jones infra-red classifications and the categories suggested for the microwave thermography technique findings. Further evidence that microwave thermography scans can be classified into similar groups was obtained by Brown, 1989.

In her investigation the microwave temperatures of 10 subjects were recorded at two levels, scanning continuously from the outer edge of the left breast to the outer edge of the right breast, at 2cm above and below the nipple, at 1cm intervals. She observed a wide range of patterns and divided these line scans into three categories. These categories were identical to groups 1 to 3 in both Draper and Jones and this recent work. However, as line scans were produced the patchy pattern observed by both Draper and Jones and this work was not observed by Brown with the limited scan pattern used.

7.7.2 Analysis of measurements using a combined microwave and thermal single region numerical model.

The female breast is assumed to consist of a homogeneous layer of breast tissue backed by a high water content, well perfused inner tissue. Estimates of breast tissue properties, principally blood perfusion and water content are made using combined modelling and their variation throughout the menstrual cycle are considered.

Superimposing Fig. 6.7 onto a graph of the average measured microwave and surface temperatures for an area of breast tissue shows that the single region numerical model fits the breast data reasonably well, Fig. 7.14. Using this modelling over the control subject data, the following estimates of effective perfusion ($kg\,m^{-3}s^{-1}$) and percentage water content were made:

	Right breast	Left breast
Effect. perfusion ($kg\,m^{-3}s^{-1}$)	0.73	0.59
Range	(0.26 - 2.0)	(0.19 - 1.3)
Estimated water content (%)	64.7	59.6
Range	(20 - 90)	(15 - 90)

The average perfusion over both breasts being $0.66\,kg\,m^{-3}s^{-1}$. In 1989, Brown quoted estimated perfusion values found in normal young women to be in the range $(0.2 - 2)\,kg\,m^{-3}s^{-1}$. The above perfusion values agree with this previous work. Also, in 1984, Beaney et al, used positron emission tomography for the in-vivo measurement of regional blood flow in both patients with breast cancer and a control group. The regional blood volume was measured by means of tracer amounts of carbon-11-labelled carbon monoxide. They found that the regional blood flow was consistently higher in tumour tissue, with an average of $3.09\,kg\,m^{-3}s^{-1}$,

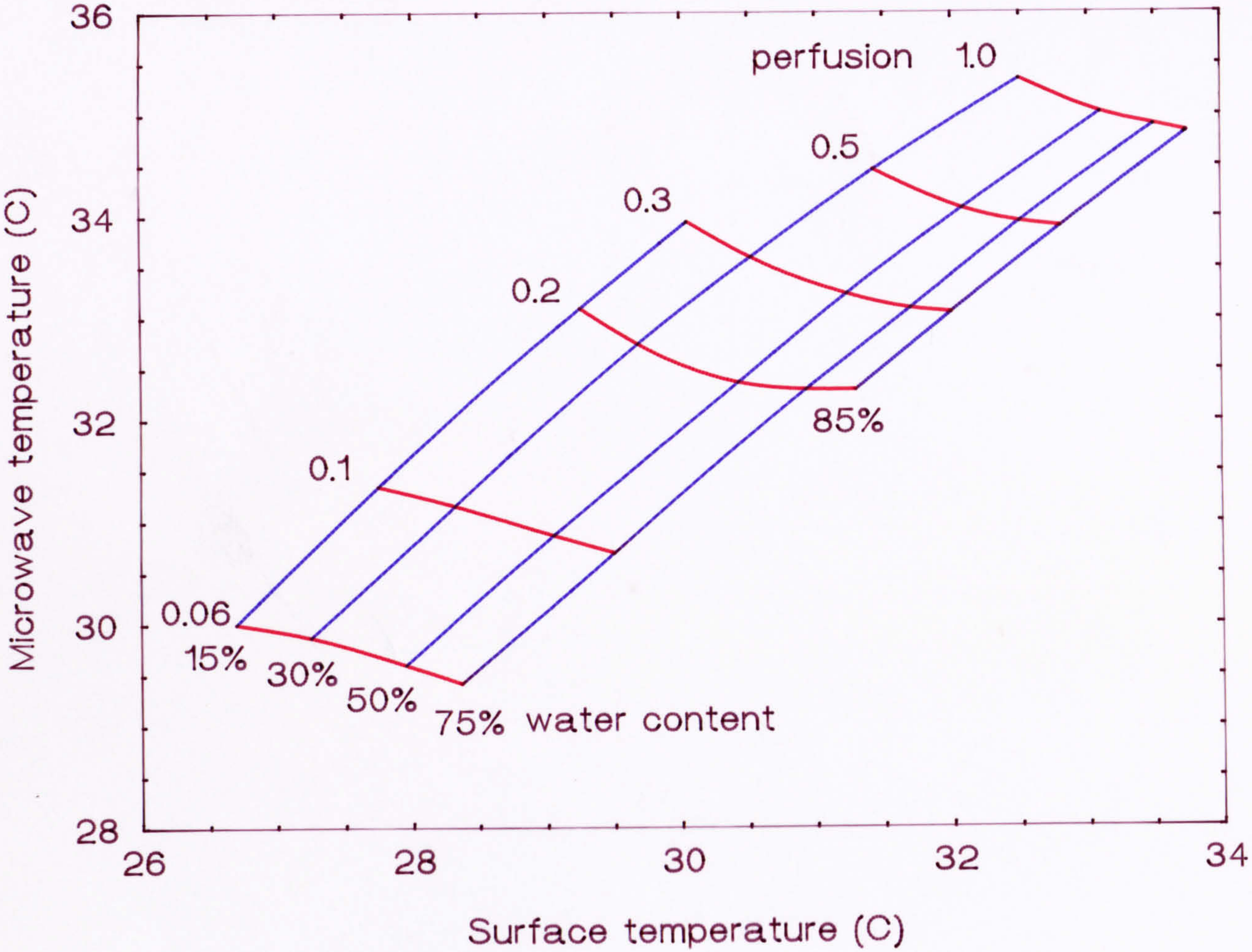
36
34
32
30
28
Microwave temperature (C)
perfusion 1.0
0.5
0.3
0.2
0.1
85%
0.06
15%
30%
50%
75% water content
26
28
30
32
34
Surface temperature (C)

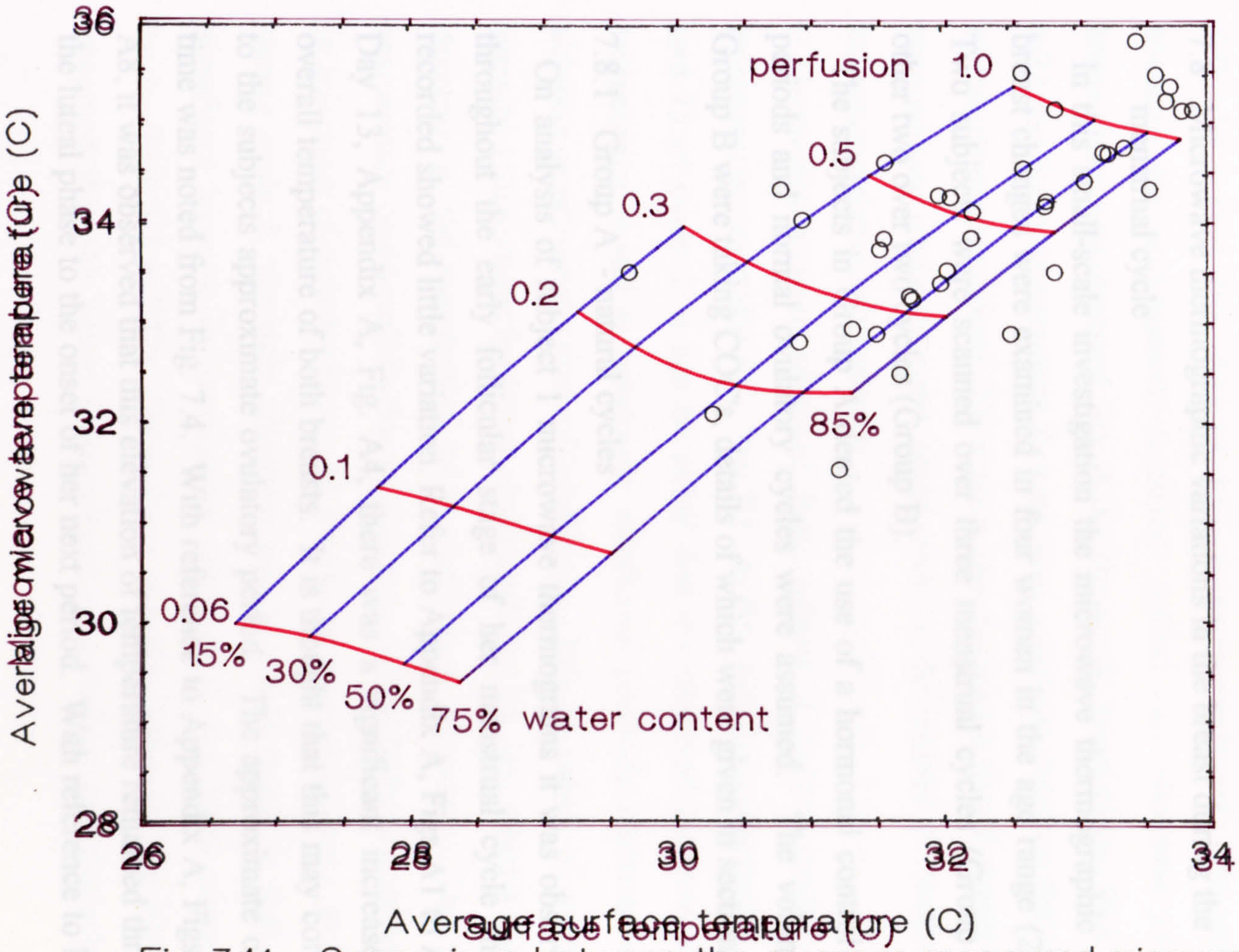

Fig. 7.14 Comparison between the average measured microwave and surface temperatures over an area of the female breast and the single region numerical model.

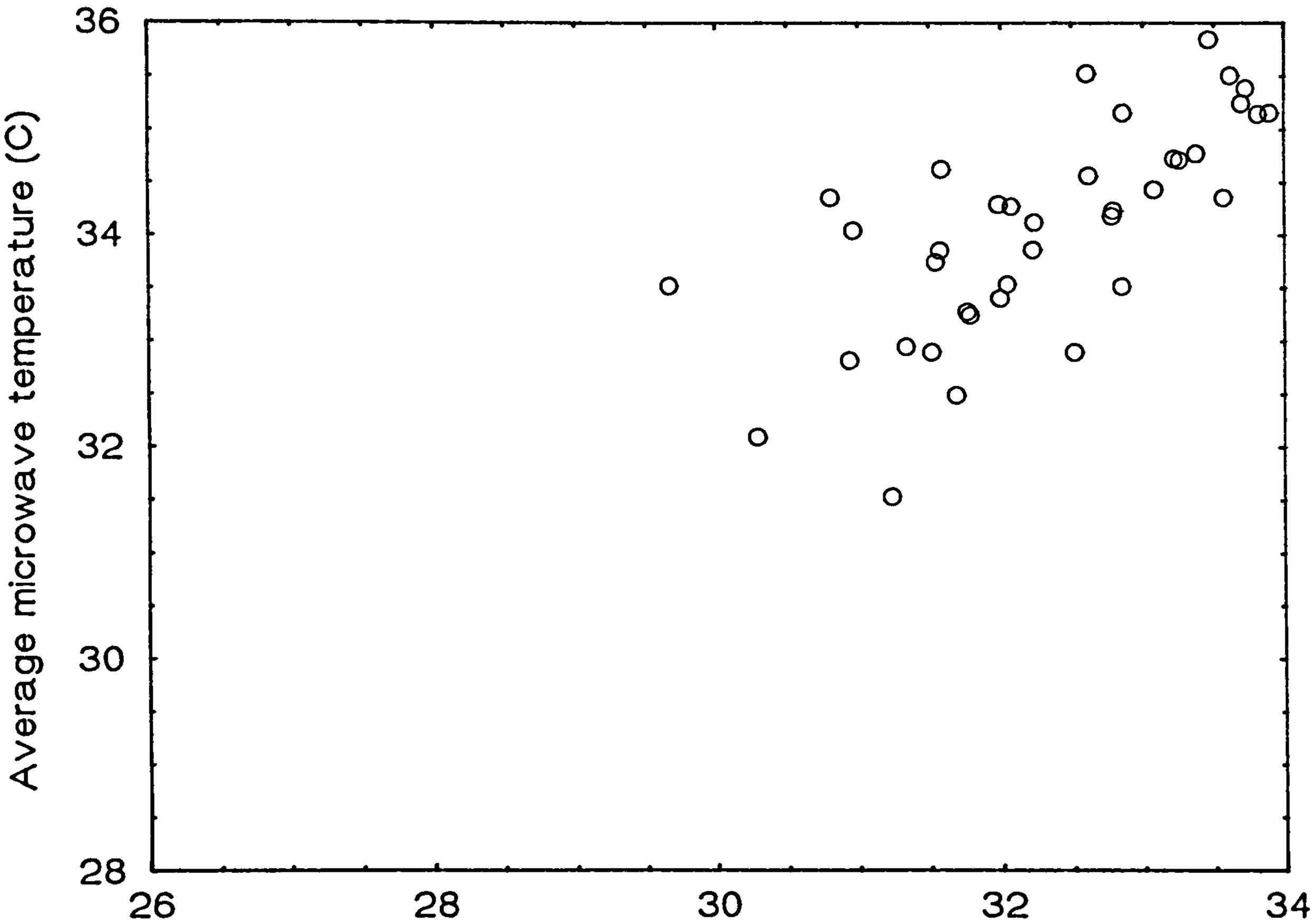

Fig. 7.14 Comparison between the average measured microwave and surface temperatures over an area of the female breast and the single region numerical model.

compared to an average blood flow of $0.65\,kg\,m^{-3}s^{-1}$ in normal breast tissue. This value agrees well with the estimated average blood perfusion given above. The changes in breast perfusion and water content throughout the menstrual cycle will be discussed later in this chapter.

7.8 Microwave thermographic variations in the breast during the menstrual cycle

In this small-scale investigation the microwave thermographic vascular breast changes were examined in four women in the age range (20 - 25). Two subjects were scanned over three menstrual cycles (Group A), the other two over two cycles (Group B).

The subjects in Group A denied the use of a hormonal control of their periods and normal ovulatory cycles were assumed. The volunteers in Group B were taking COC's, details of which were given in section 7.4.1.

7.8.1 Group A - natural cycles

On analysis of subject 1 microwave thermograms it was observed that throughout the early follicular stage of her menstrual cycle the scans recorded showed little variation. Refer to Appendix A, Figs A1 to A3. By Day 13, Appendix A, Fig. A4, there was a significant increase in the overall temperature of both breasts. It is thought that this may correspond to the subjects approximate ovulatory period. The approximate ovulation time was noted from Fig. 7.4. With reference to Appendix A, Figs. A5 to A8, it was observed that this elevation of temperature remained throughout the luteal phase to the onset of her next period. With reference to Figs. A9

to A12, the microwave thermograms appear to be asymmetric throughout cycle 2. However, the cycle length was only 12 days and this is likely to account for the irregular thermograms obtained. On interpreting the thermograms obtained during cycle 3, it was noted that the changes observed during cycle 1 were repeated. The breast scans throughout the follicular period, Fig. A13 to A17, were approximately the same, and towards the approximate ovulatory period, an elevation of breast temperature was observed, Fig. A18. During the luteal phase, Figs. A20 to A22, the breast temperature showed more variation, however the elevation of temperature remained. From these observations it would appear that the approximate ovulation point could well be determined by performing a microwave thermographic scan.

Thermograms were obtained from subject 2 over 3 cycles. With reference to Appendix A.1, Figs.B1 to B3, which correspond to days 7 and 15 of cycle 1, it can be noted that the observed increase in breast temperature, could as previously mentioned probably correlate with the subjects approximate time of ovulation. This elevation of temperature remained throughout the luteal phase until day 24, B6, when a significant decrease in the temperature of the left breast occurred. This drop in temperature could well be due to a drop in overall body temperature prior to the onset of menstruation. As a reduced number of scans were taken during cycle 2, the only comment which can be made is that again a significant increase in temperature occurred in the luteal phase of the cycle, (Figs. B8 to B12). On analysis of cycle 3, Figs B13 to B19, it was observed that the breast thermograms appeared to be relatively stable

throughout. No significant change in breast temperature was observed. This may be due to no ovulation occurring in this cycle due to stress or worry. However, overall, the same observations were noted for Subject 2 as seen for Subject 1.

7.8.2 Group B - Those using combined oral contraceptive

Subject 3 was scanned throughout 2 cycles. However, during cycle 1, the subject suffered from a nickel allergy. As a direct result her skin became inflamed. So only the thermograms obtained throughout cycle 2 will be discussed. With reference to Appendix A.2, Figs. C1 to C5, it is seen that the thermograms obtained remained similar throughout the follicular stage of her cycle. However, by day 16, Fig. C7, a definite elevation of temperature had occurred. It is thought that this elevation of breast temperature may correspond to the synthetic ovulatory period observed by some women whilst taking oral contraceptives. This possibility was noted in section 7.4.1. Also Fig. 7.6, shows that the subjects basal temperature decreased from day 11 to day 16, and so the increase in breast temperature coincides with the decrease in basal temperature. This is further evidence to suggest that breast microwave temperature patterns vary in a generally regular manner with what is probably the ovulatory cycle. This may be useful information for interpreting the microwave scans when looking for evidence of breast disease.

For medical reasons, subject 4 changed from "Marvelon" to "Mercilon" as mentioned in 7.4.1, in mid cycle, and so the subject had an extended

cycle length of 40 days. This made interpretation of the thermograms difficult. So for this reason only the thermograms obtained during cycle 2 will be considered. By referring to Appendix A.3, Figs. D1 to D8 it is shown that the breast temperatures remained similar throughout all the phases of the menstrual cycle. No elevation of temperature was noted in the ovulatory, luteal phases of the menstrual cycle. On analysis of the basal temperature chart associated with cycle 2, Fig. 7.7, it is observed that no synthetic ovulation had occurred. This could well be the reason for no significant changes occurring in the breast temperatures throughout the cycle.

In 1969, Draper and Jones carried out a study using an infra-red imaging scanner. They observed that the general temperature of the breasts seemed to remain steady until ovulation when an increase in breast temperature occurred. This increase remained throughout the luteal phase to the onset to the next period. They also performed similar scans on women taking oral contraception. Again they concluded that there appeared to be an increase in the breast temperature throughout the cycle. Llyod-Williams (1969) also stated that the vascular pattern of the breast will change in a normal menstrual period as a result of hormonal activity.

Finally, Verzini and Romani studied the infra-red thermographic vascular breast modification throughout the menstrual cycle and they too concluded that maximum vascularisation occurred during the ovulatory and luteal phases of the menstrual cycle.

It appears that infra-red thermograms indicate at least superficial vascular changes through the menstrual cycle. The microwave

thermographic findings of this study appear to be generally compatible with the surface thermographic findings.

7.9 Estimation of tissue properties using combined microwave and thermal modelling

The combined microwave and thermal single region numerical model, (Chapter 5.0), was used to estimate the effective perfusion and tissue water content of female breasts throughout the menstrual cycle for both groups.

7.9.1 Estimate of effective perfusion

Fig. 7.15, shows the estimated effective perfusion through the menstrual cycle for subject 1. From this graph a number of observations can be made. The first being that symmetry exists between left and right perfusion estimates. Also there appears to be an increase in the estimated perfusion throughout the approximate ovulatory period. It appeared that a pattern might exist, so an average of the perfusion estimates over 3 cycles for both breasts was obtained and plotted, Fig. 7.16. This graph appears to exhibit a distinct pattern. From Fig. 7.16, it appears that the lowest perfusion occurs during the follicular stage, followed by an increase in estimated perfusion throughout the possible ovulatory period. In the luteal phase of the cycle, the perfusion estimates appear to decrease, however they remain higher than the estimates made for the follicular phase. Estimates of perfusion and an average of the estimated perfusions for subject 2 are shown in Figs. 7.17 & 7.18 respectively. On studying these

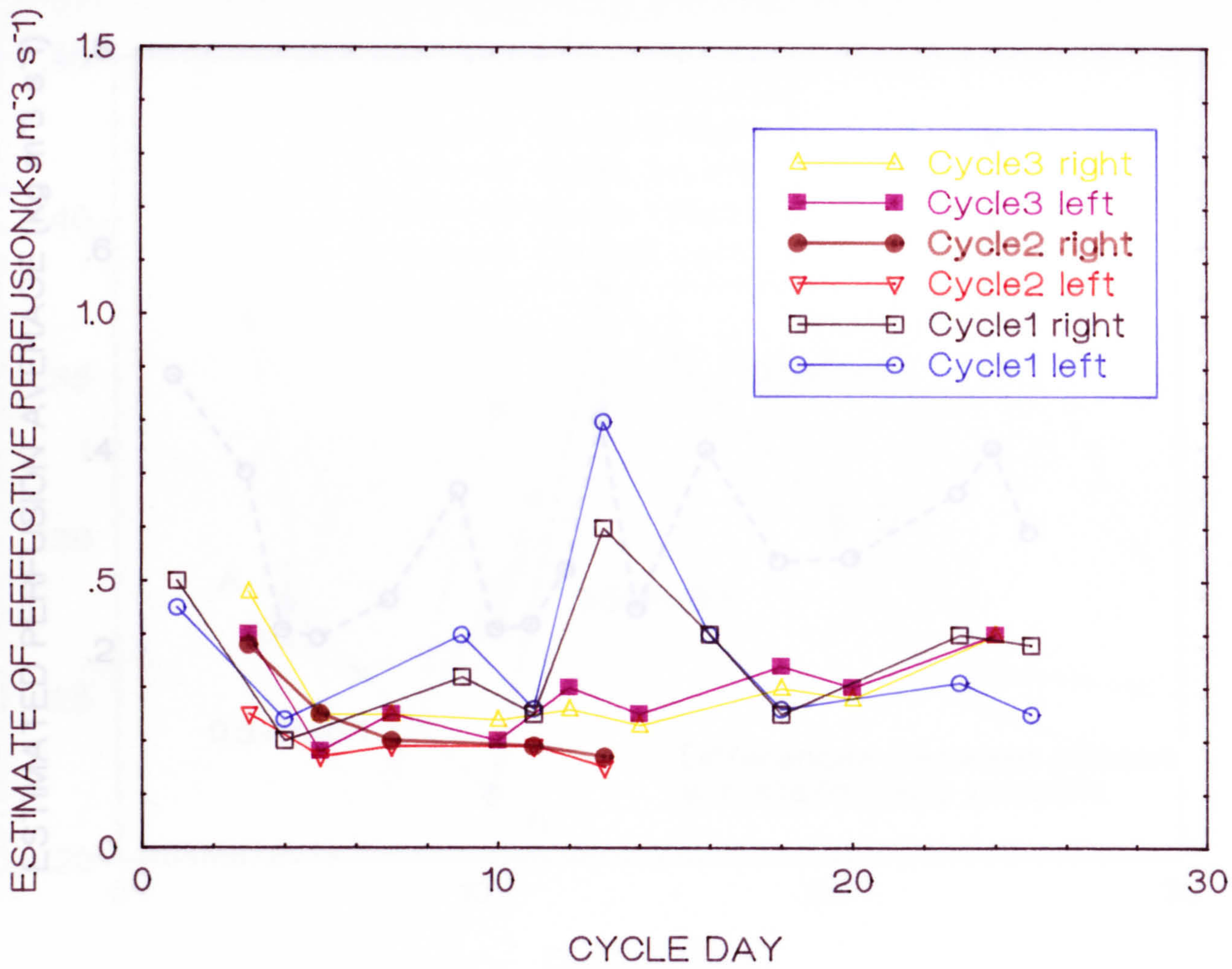

Fig. 7.15 Estimated effective perfusion throughout the menstrual cycle, Subject 1.

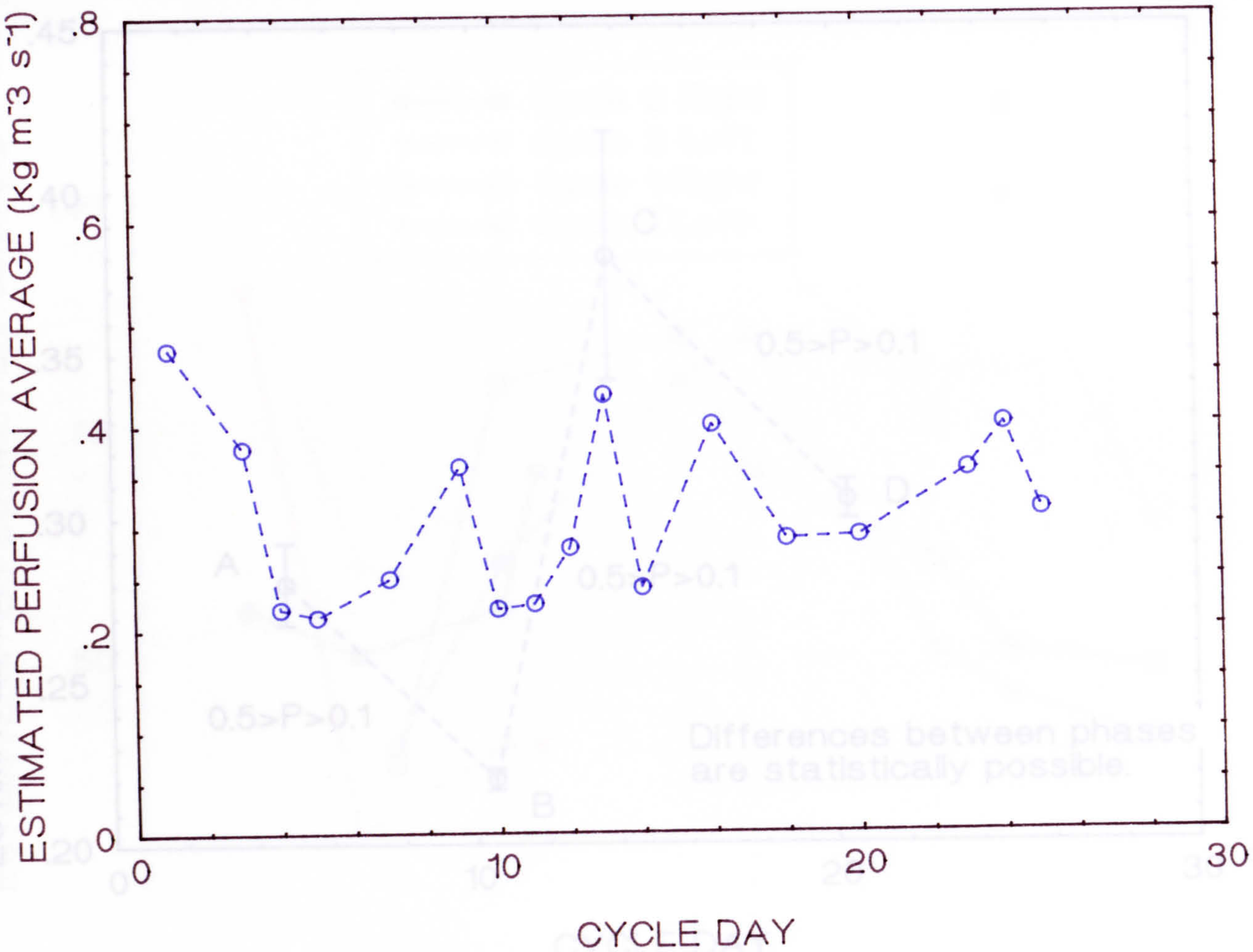

Fig. 7.16 Average of the estimated perfusion through 3 menstrual cycles, Subject 1.

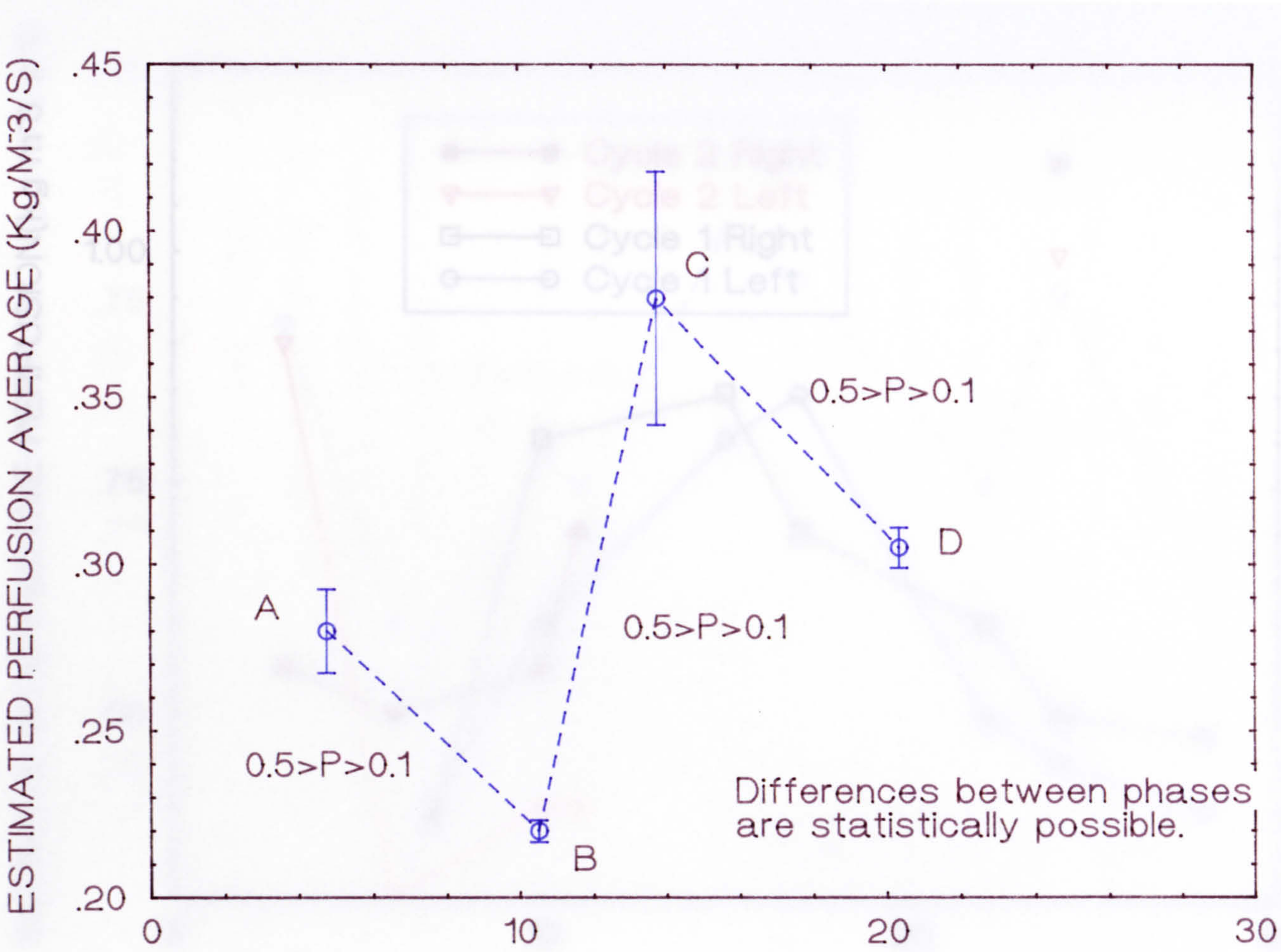

Fig. 7.16A Averaged perfusion over 3 cycles and comparison between different phases - Subject 1.

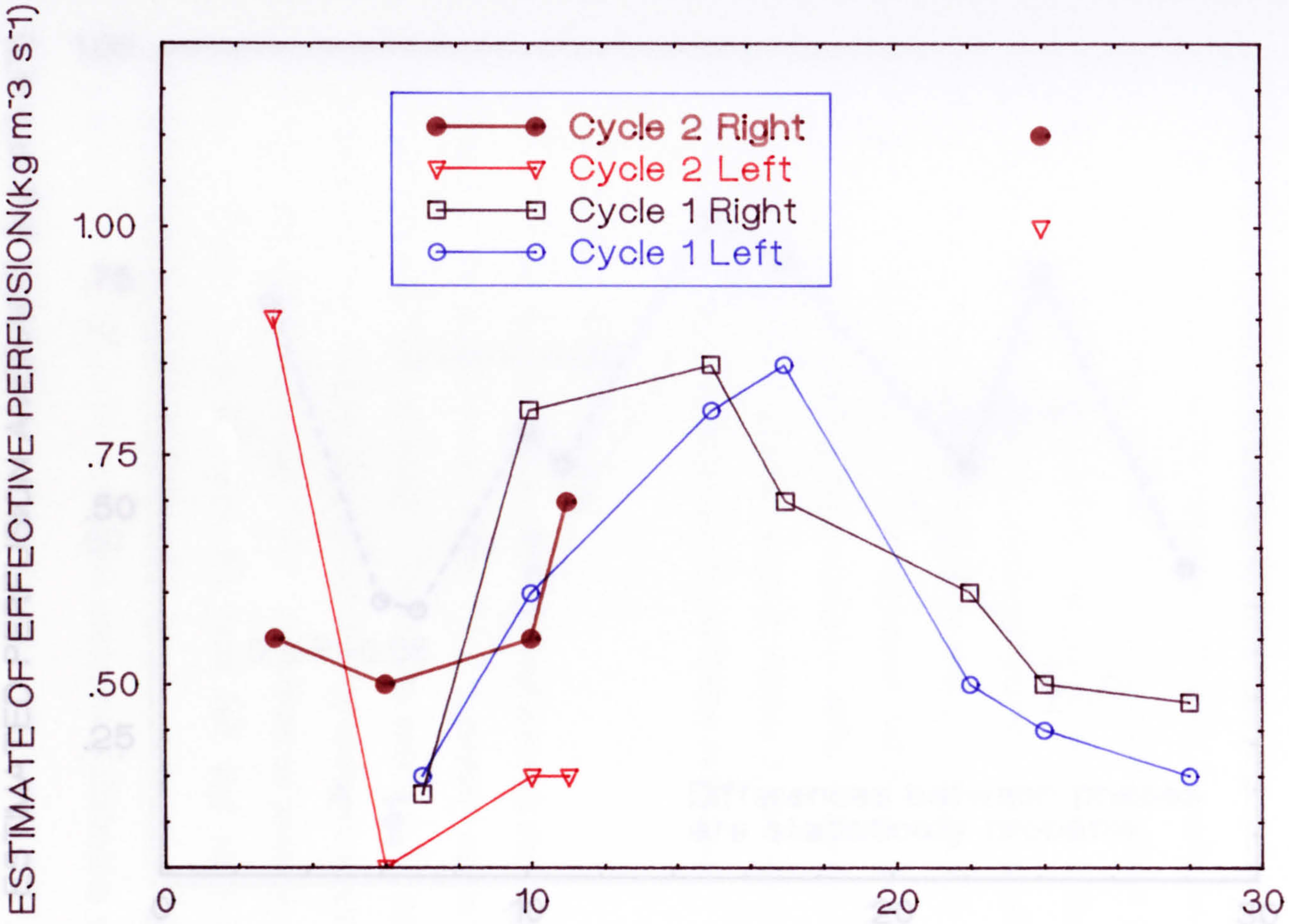

Fig. 7.17 Estimated effective perfusion throughout 2 menstrual cycles, Subject 2.

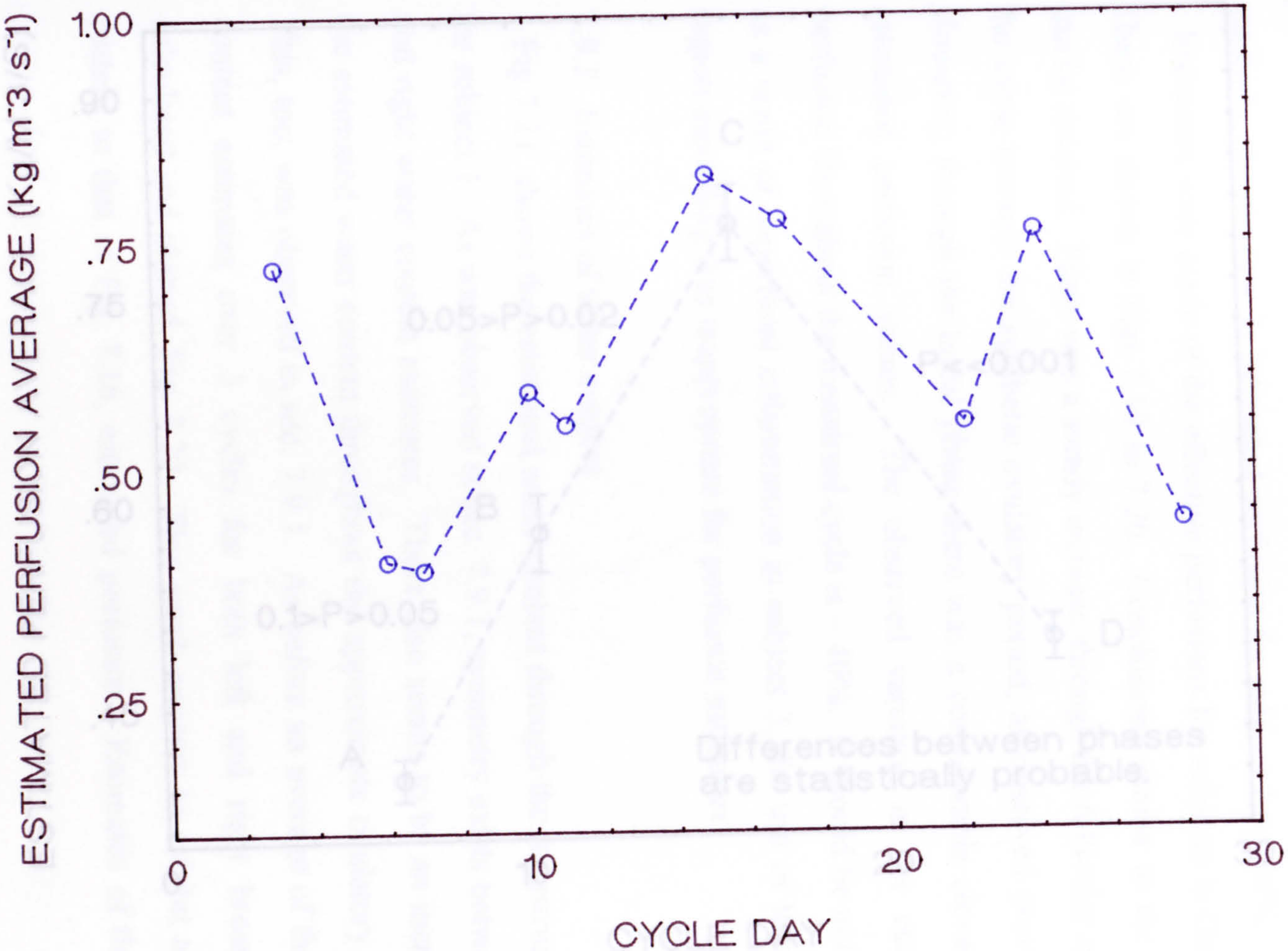

Fig. 7.18 Average of the estimated perfusion through 2 menstrual cycles, Subject 2.

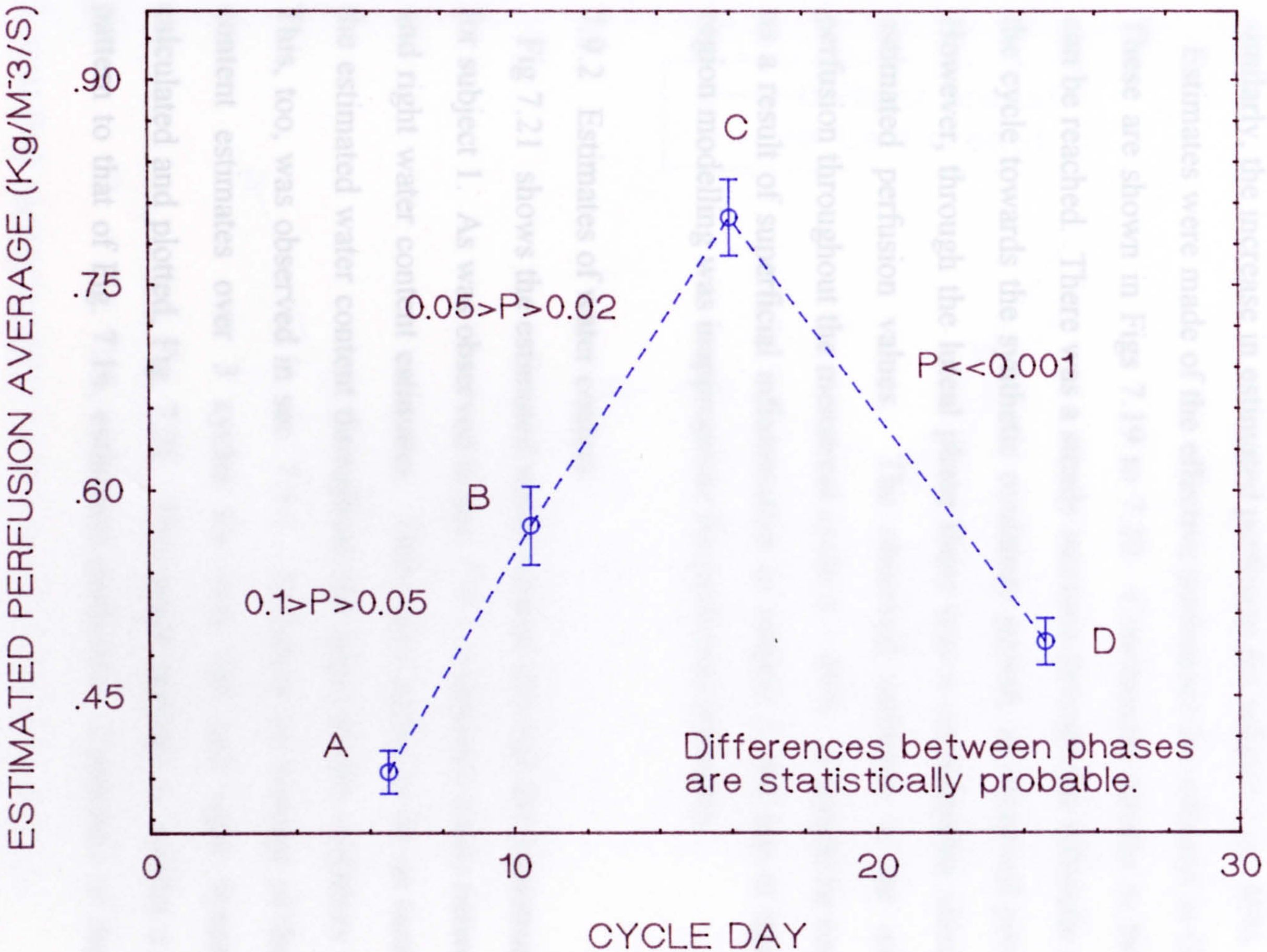

Fig. 7.18A Averaged pefusion over 2 cycles and comparison between different phases - Subject 2.

graphs the conclusions arrived at previously can be applied again. It would appear that the estimated perfusion in the breasts of women not taking a hormonal contraceptive varies significantly with a regular pattern throughout the natural menstrual cycle. The average of the estimated perfusion for subject 1 increases by ~42% throughout the menstrual cycle, similarly, the increase in estimated perfusion for subject 2 is ~46%.

Estimates were made of the effective perfusions for subjects in Group B. These are shown in Figs 7.19 to 7.20. Conclusions similar to the above can be reached. There was a steady increase through the follicular stage of the cycle towards the synthetic ovulatory period, as observed previously. However, through the luteal phase there was a considerable elevation of estimated perfusion values. The observed variation in the estimated perfusion throughout the menstrual cycle is ~ 40%. It should be noted that as a result of superficial inflammation in subject 3, the use of this single region modelling was inappropriate for perfusion estimates.

7.9.2 Estimates of water content

Fig 7.21 shows the estimated water content through the menstrual cycle for subject 1. As was observed in sec. 7.9.1, symmetry exists between left and right water content estimates. There also seems to be an increase in the estimated water content throughout the approximate ovulatory period. This, too, was observed in sec. 7.9.1. As before an average of the water content estimates over 3 cycles for both left and right breasts was calculated and plotted, Fig. 7.22. This graph appears to exhibit a similar pattern to that of Fig. 7.16, estimated perfusion. Estimates of the water

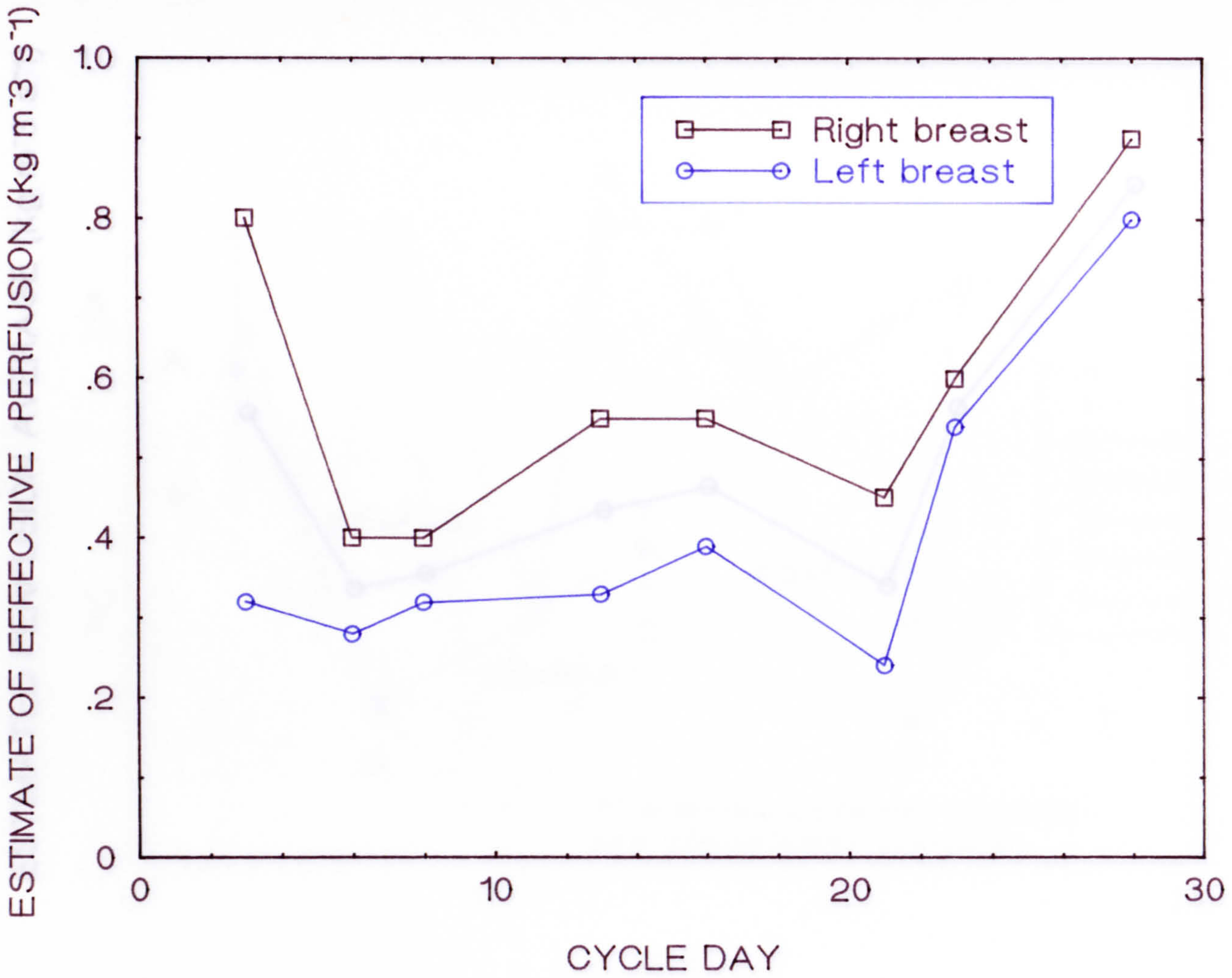

Fig. 7.19 Estimated effective perfusion throughout the menstrual cycle, Subject 4.

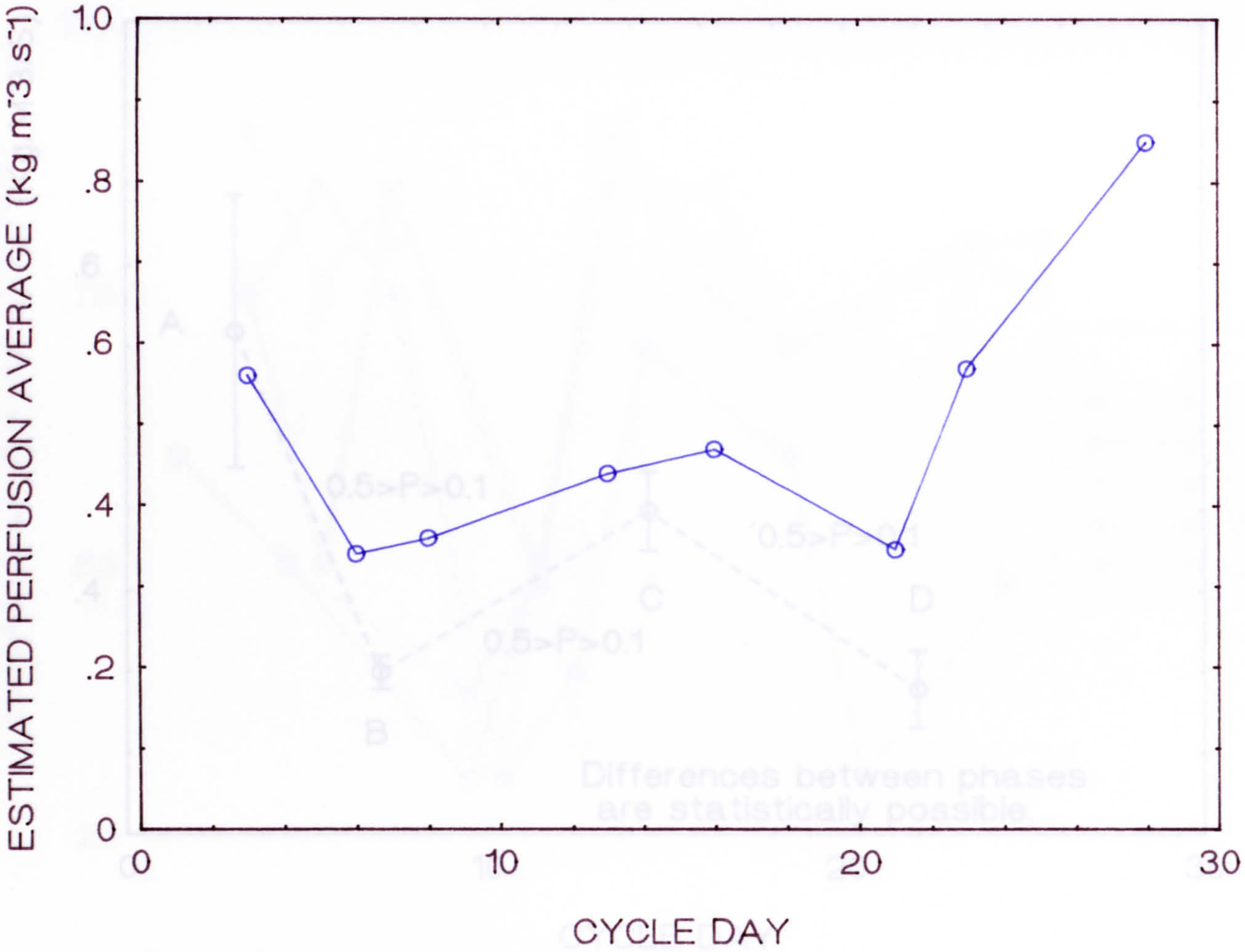

Fig. 7.20 Average of the estimated perfusion through the menstrual cycle, Subject 4.

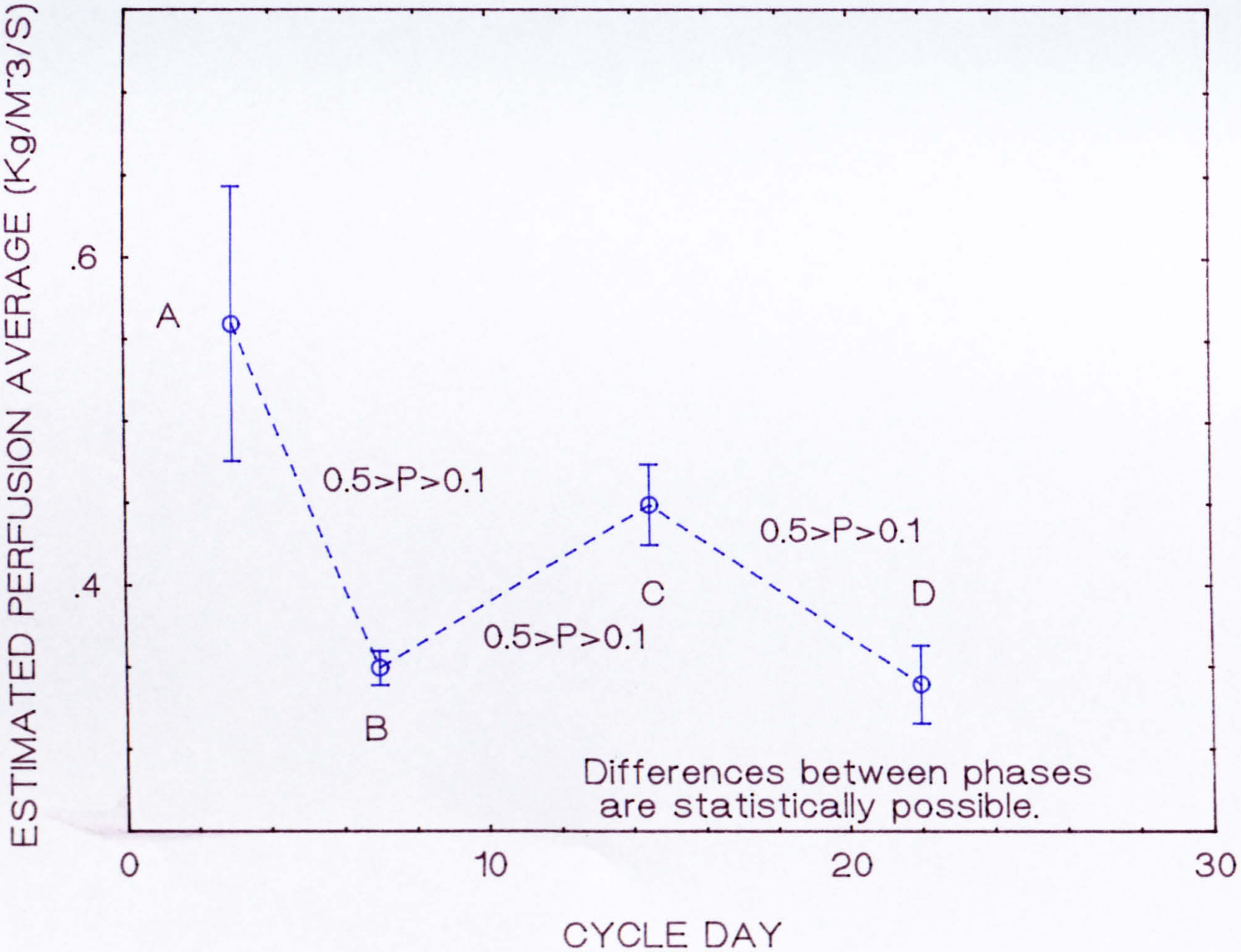

Fig. 7.20A Averaged perfusion over 1 cycle and comparison between different phases - Subject 4.

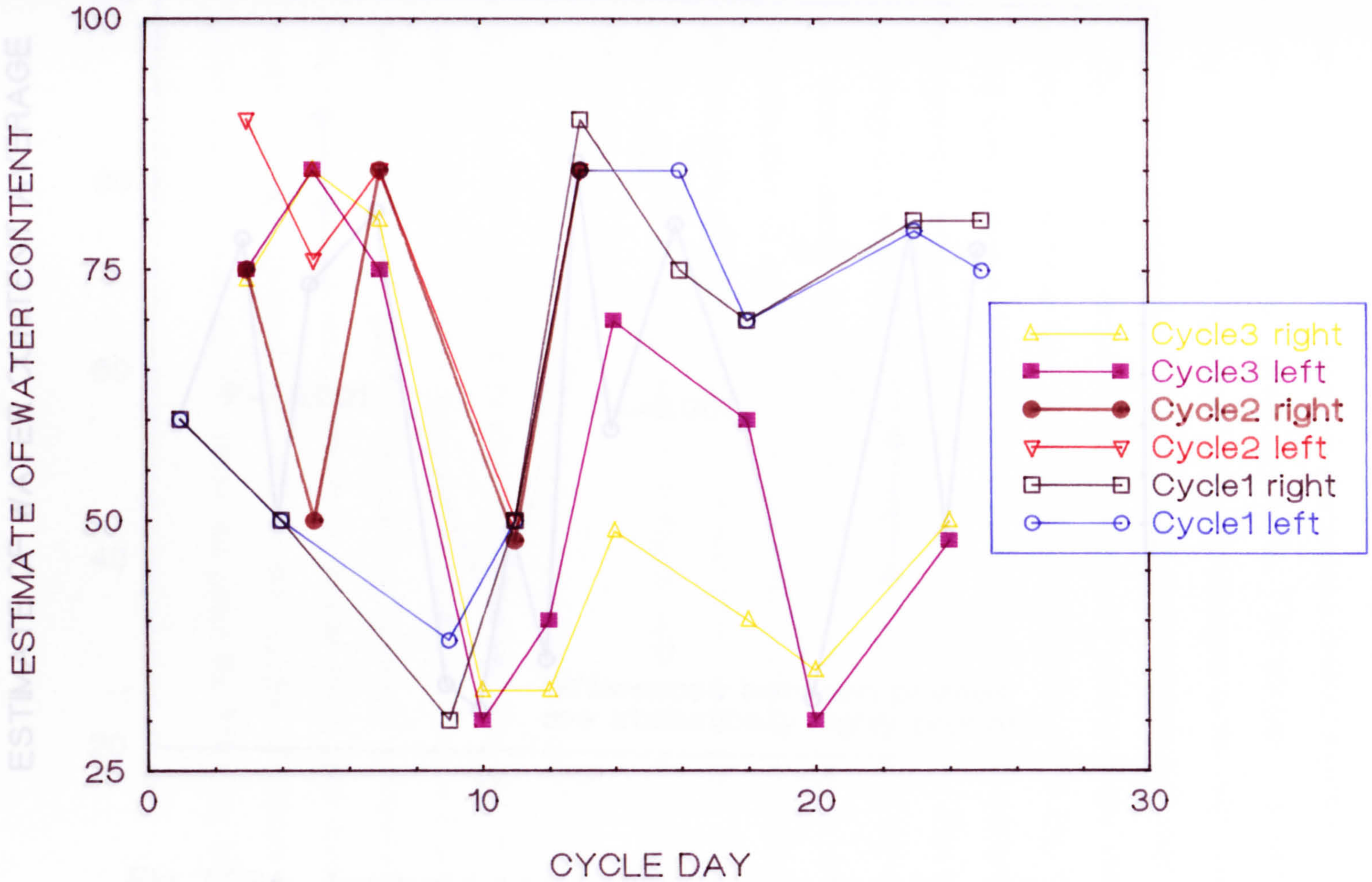

Fig. 7.21 Estimated water content throughout the menstrual cycle, Subject 1.

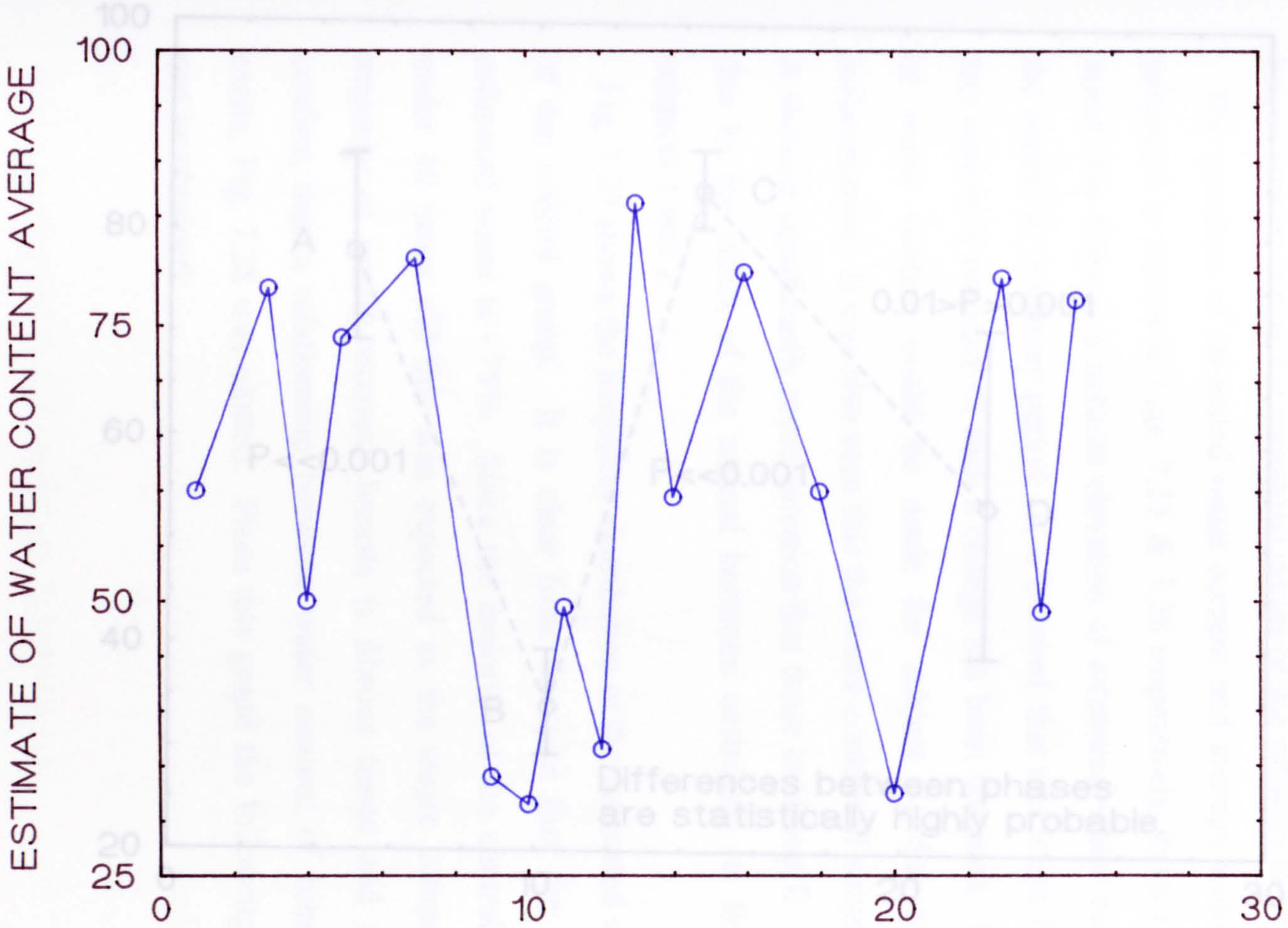

Fig. 7.22 Average of estimated water content through 3 menstrual cycles, Subject 1.

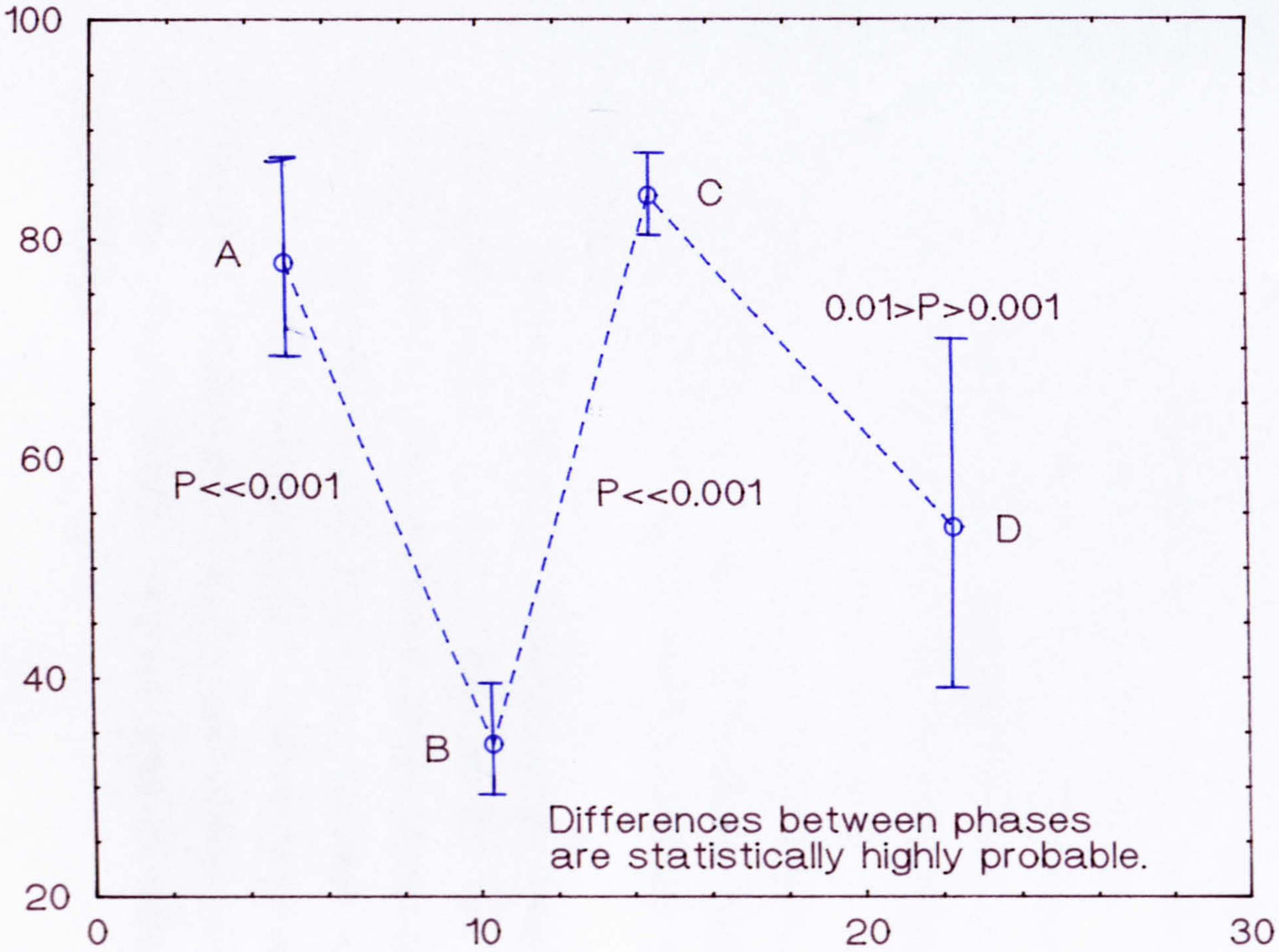

Fig. 7.22A Averaged water content over 3 cycles and comparison between different phases - Subject 1.

content and the average water content over 2 cycles for subject 2 are given in Figs. 7.23 & 7.24. On studying these graphs, it is clear that the water content decreases throughout the approximate ovulatory period rather than increasing. No distinct similarities to Fig. 7.18 are seen. In summary, it was observed that a significant variation occurred in the water content of breast tissues during the menstrual cycles of the subjects in Group A.

The variation of estimated water content and average water content for subject 4 is shown in Figs. 7.25 & 7.26 respectively, from Fig. 7.26 it is noted that there is a definite elevation of estimated water content around the synthetic ovulatory period. It is believed that this is the first time that any objective measure of such a change has been obtained. No estimates of water content could be made for subject 3, due to superficial inflammation. It was also seen that the water content of subjects in Group A showed significantly more variation that those in Group B. This may be due to the effect of the natural hormone oestrogen on the breasts of subjects 1 and 2.

Fig. 7.27 shows the frequency distribution of the estimated water content of the control group. It is clear from this plot that the predominant estimated water is ~75%. Since the majority of the control group were under 40 years old this was expected as the major component of the majority of young womens breasts is fibrous tissue and muscle. To confirm that a relationship between water content of breasts and age exists, Fig. 7.28 was plotted. From this graph the following information can be obtained:

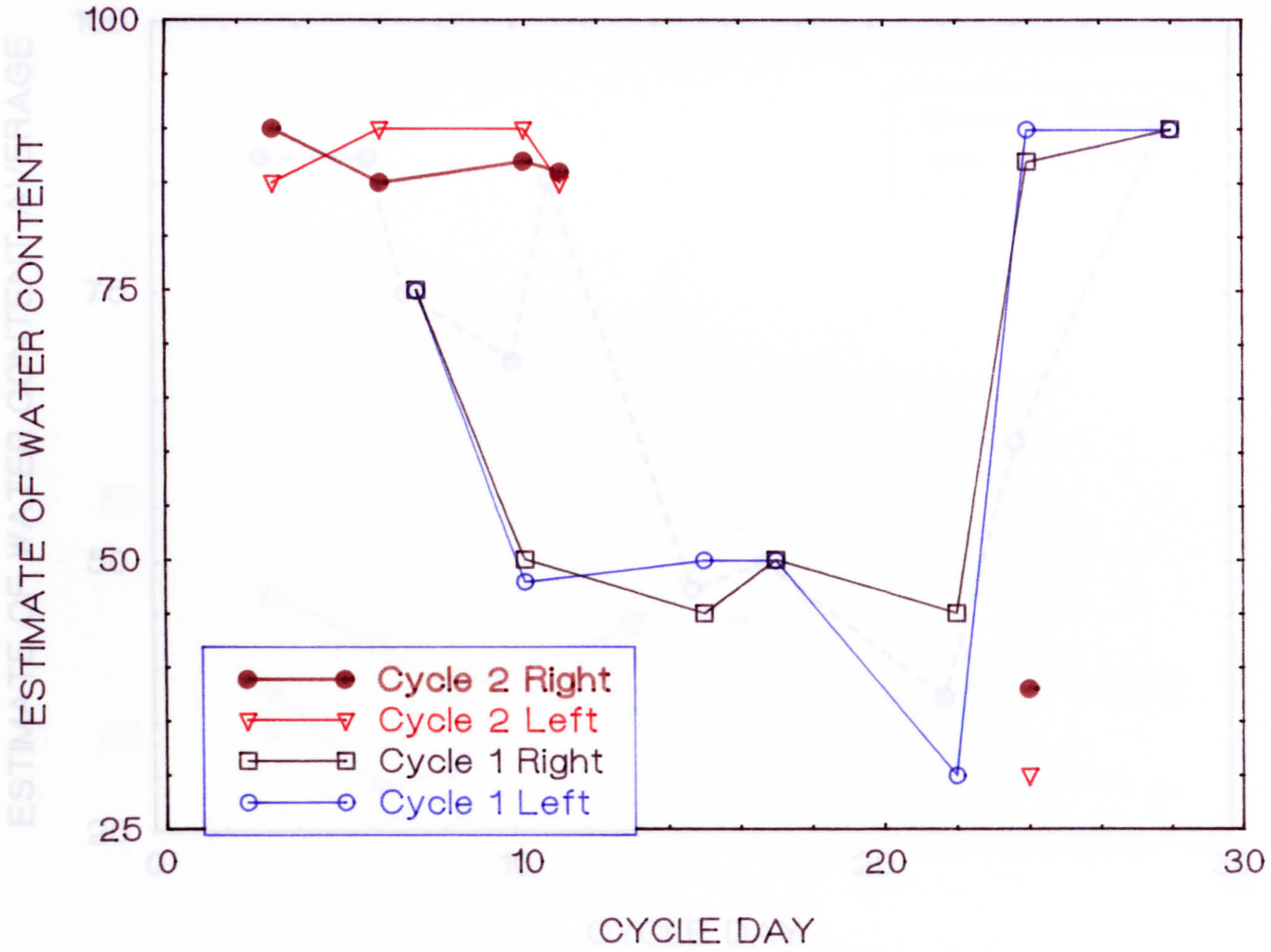

Fig. 7.23 Estimated water content throughout 2 menstrual cycles, Subject 2.

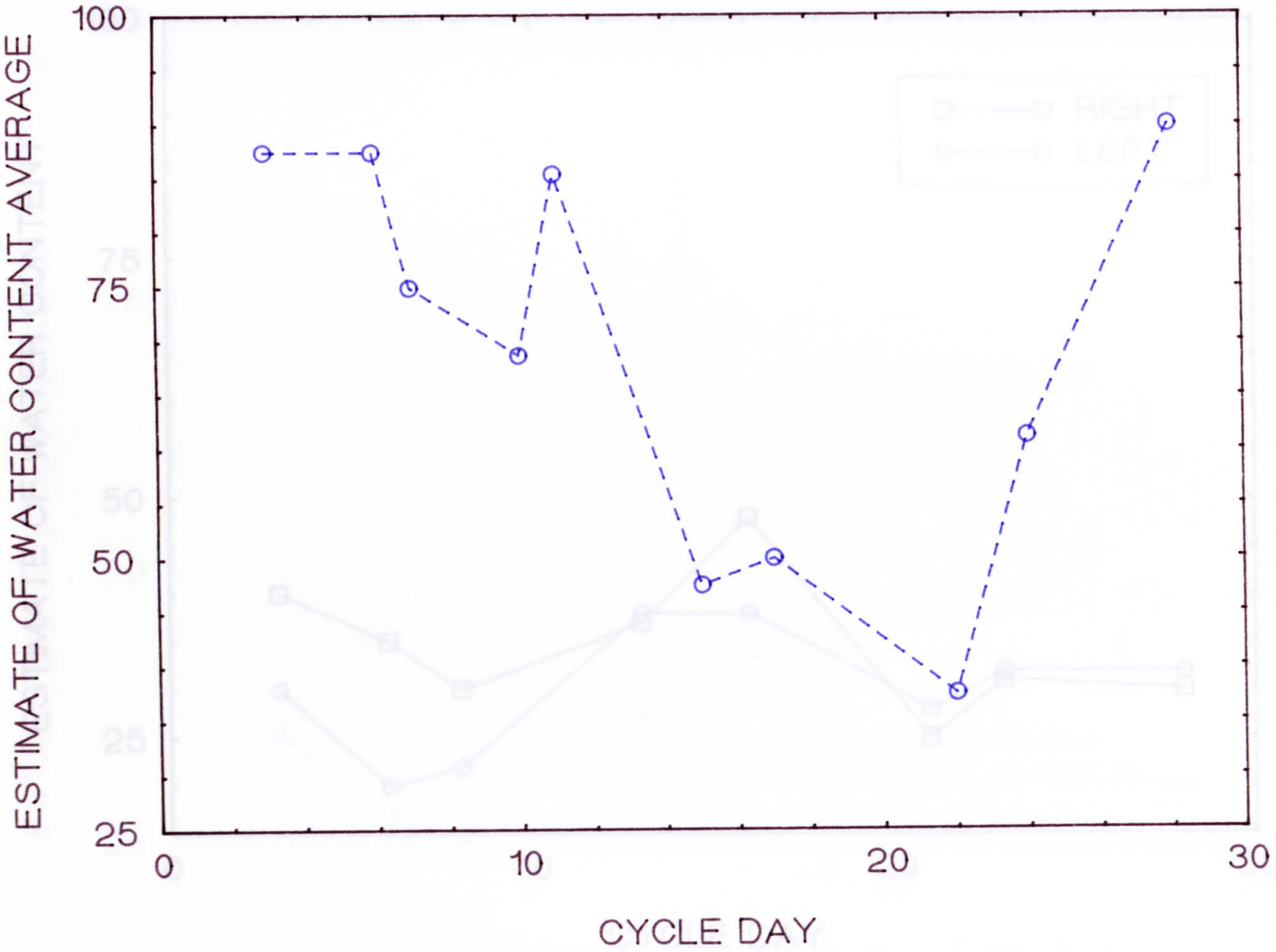

Fig. 7.24 Average of estimated water content through 2 menstrual cycles, Subject 2.

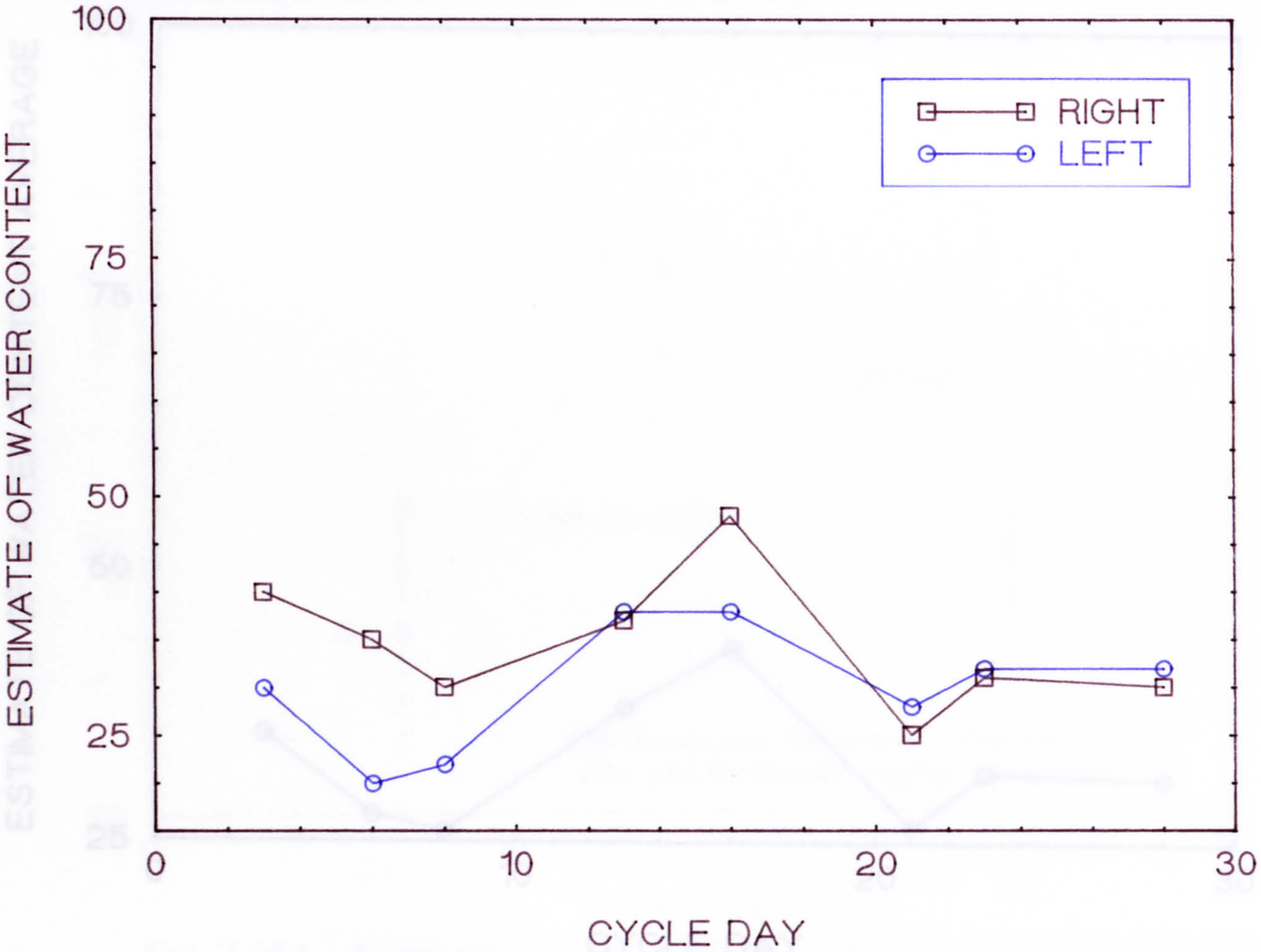

Fig. 7.25 Estimated water content through the menstrual cycle, Subject 4.

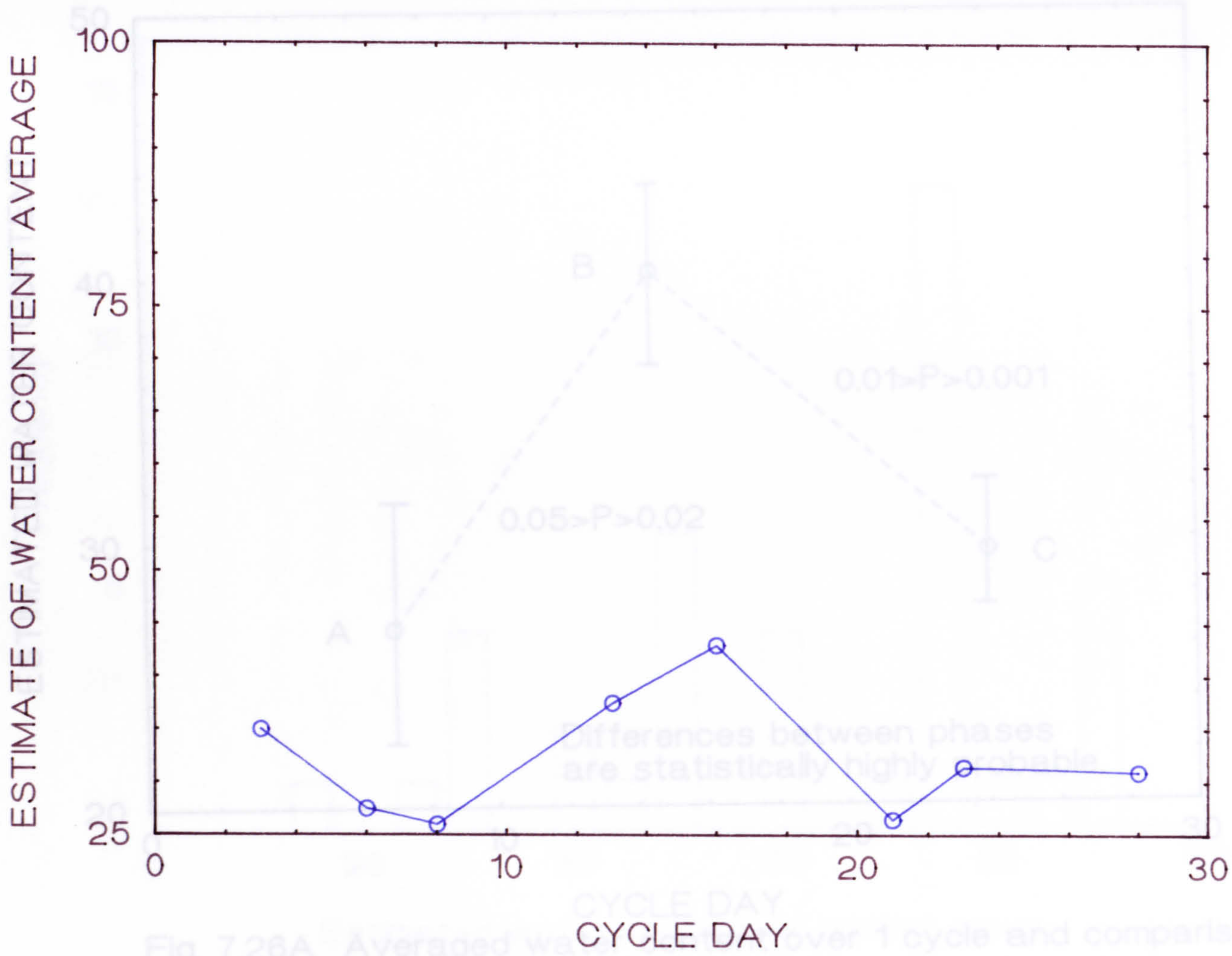

Fig. 7.26 Average of estimated water content through the menstrual cycle, Subject 4.

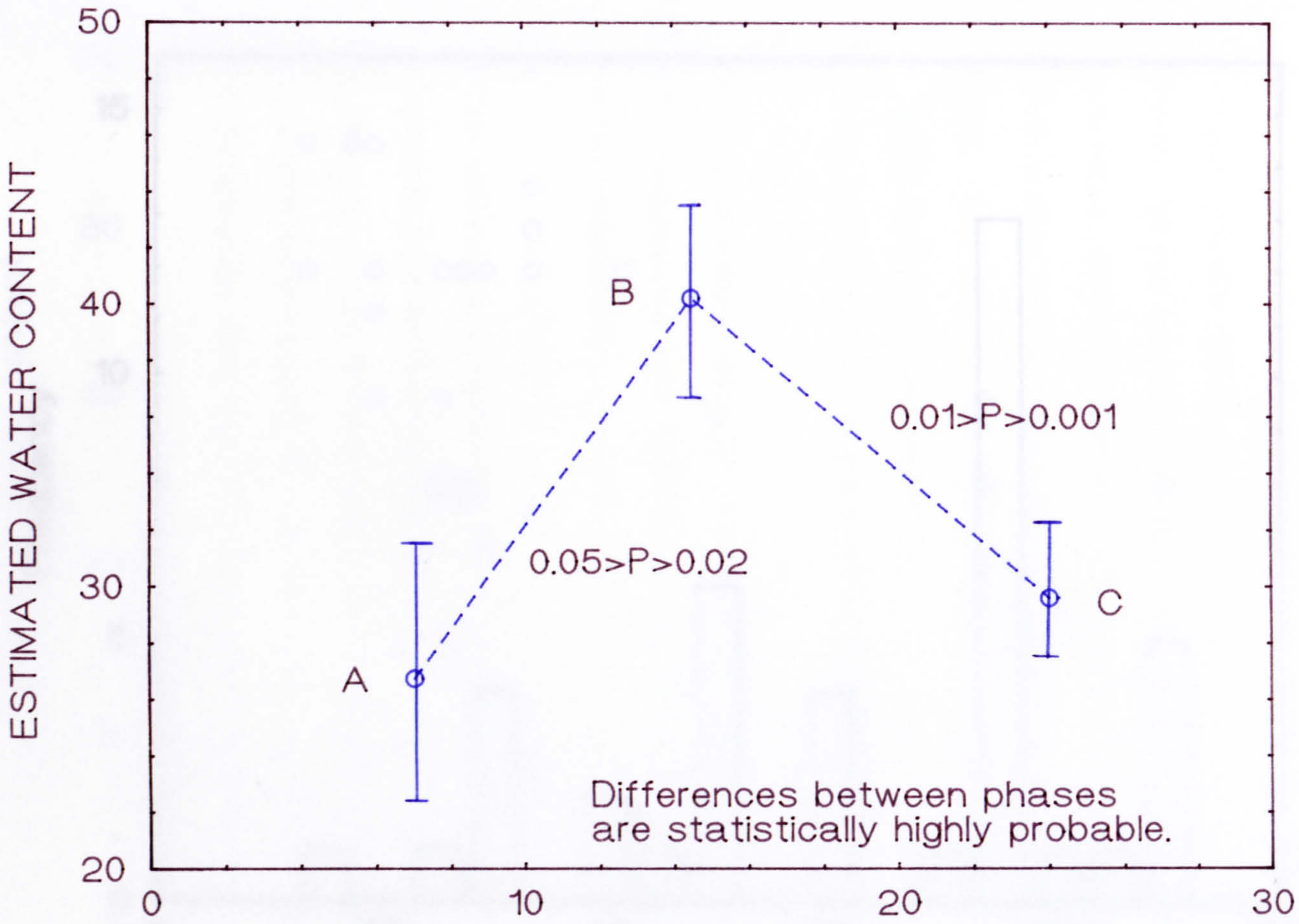

Fig. 7.26A Averaged water content over 1 cycle and comparison between different phases - Subject 4.

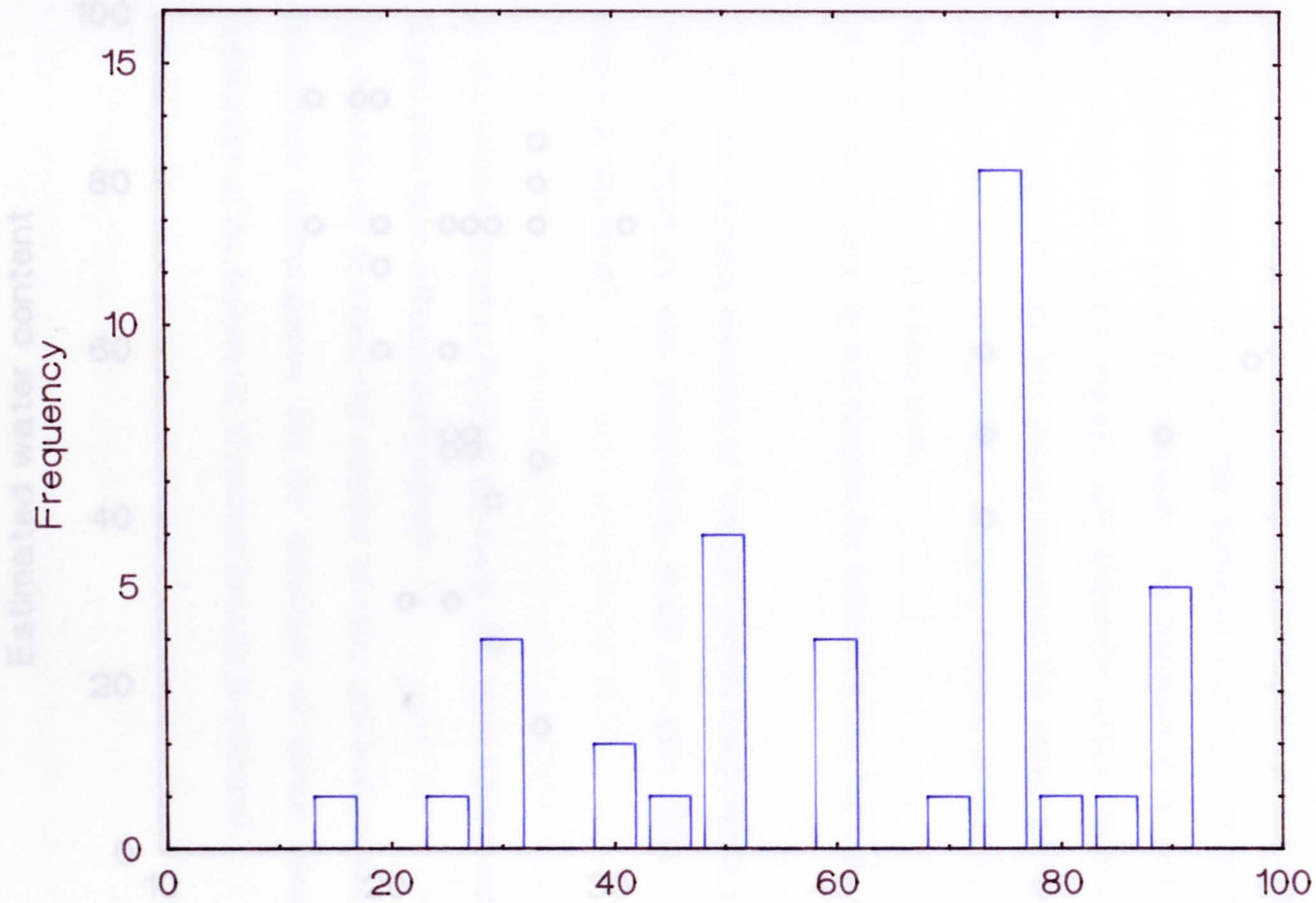

Fig. 7.27 Frequency distribution of the estimated water content of the control group.

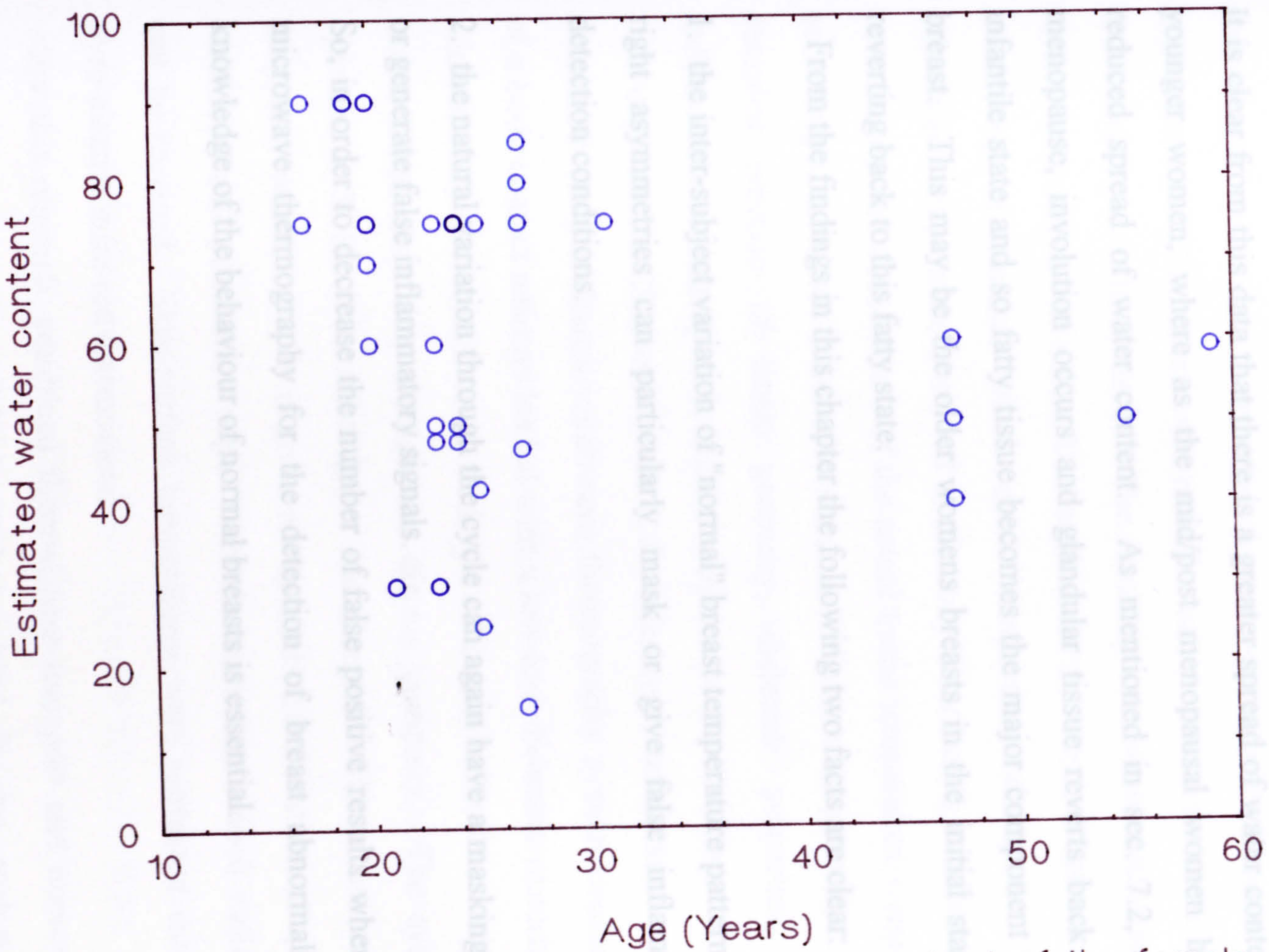

Fig. 7.28 Relationship between water content of the female breast and age (Years).

Age (Years)	Average water content	Range of water content
Under 40 years	63.5%	(15 - 90)%
Over 40 years	51.8%	(40 - 60)%

It is clear from this data that there is a greater spread of water contents in younger women, where as the mid/post menopausal women have a reduced spread of water content. As mentioned in sec. 7.2, at the menopause, involution occurs and glandular tissue reverts back to its infantile state and so fatty tissue becomes the major component of the breast. This may be the older womens breasts in the initial stages of reverting back to this fatty state.

From the findings in this chapter the following two facts are clear:

1. the inter-subject variation of "normal" breast temperature patterns, left-right asymmetries can particularly mask or give false inflammation detection conditions.

2. the natural variation through the cycle can again have a masking effect, or generate false inflammatory signals.

So, in order to decrease the number of false positive results when using microwave thermography for the detection of breast abnormalities, a knowledge of the behaviour of normal breasts is essential.

CHAPTER 8. CONCLUSIONS.

All bodies with a temperature above absolute zero emit electromagnetic energy. Microwave thermography is the technique of measuring this thermal radiation emitted from body tissues at centimetric wavelengths to obtain information about internal body temperature patterns. At the lower microwave frequencies, approximately 3GHz, microwave radiation can penetrate the order of a few centimetres in body tissue. The resulting microwave temperature pattern information can aid medical staff in the detection, diagnosis and monitoring of diseases which cause temperature changes. The microwave temperature observed at the body's surface is a summation over the viewed tissue layers of the actual tissue temperature weighted according to the tissue microwave attenuation factors. In general, it is a complex function of tissue geometry, dielectric properties, the radiometer antenna response, and the temperature distribution.

As explained in Chapters 4, 6 & 7, the microwave temperatures were measured using a clinical microwave thermography system consisting of a body contact antenna loaded with a low-loss dielectric material to minimise impedance mismatch, feeding a calibrated radiometer receiver and a temperature data storage and display computer. The system operates at 3GHz (10cm free-space wavelength). The measurement frequency was chosen as it gives an optimum combination of spatial resolution and penetration depth within tissues from which radiation can be received. Skin surface temperatures were measured using a pyro-electric infra-red thermometer.

For this research, combined thermal heat transport and microwave radiation analytical models have been used in the analysis of

temperature measurement data over three body regions; the quadriceps muscle, the patella, and the female breasts. 1 - dimensional analytical and 1 - & 2 - dimensional numerical models were used for the quadriceps region. For the patella and breasts the 1 - dimensional numerical and analytical models were used. The main factors considered in these models are the water content of the tissue and the blood perfusion through the tissue. This is because the tissue water content determines both the microwave penetration depth and thermal conductivity and the blood perfusion rate is the dominant factor in the heat supply to tissue.

In the rheumatology investigations, Chapter 6, microwave thermography has been used for the objective assessment of inflammation in the patella and wrist and finger joints of patients with rheumatoid arthritis by comparison with similar information obtained from a control group of subjects.

It was found that the measured surface and microwave temperatures agree well in both absolute values and relative variation with modelled temperatures over the quadriceps region for both "normal" and RA patients. Tissue thermal and microwave properties vary from those of muscle to those of fat as expected. The range of estimated perfusion values found for "normal" subjects quadriceps were from 0.01 - 0.72 $kg\,m^{-3}s^{-1}$ and for patients with RA the estimated values were from 0.08 - $1.42\,kg\,m^{-3}s^{-1}$. The ranges of estimated patella perfusion found were from 0.003 - $0.11\,kg\,m^{-3}s^{-1}$ for "normal" subjects and from 0.02 - $4.24\,kg\,m^{-3}s^{-1}$ for patients with RA. These values were found to be similar to but slightly lower than those reported in literature as measured by radioisotope clearance methods. Changes in this heat

supply by arterial blood are considered to be a good measure of disease activity. The rheumatoid arthritis group showed on average a slightly higher tissue attenuation factor, $118m^{-1}$ compared with $95m^{-1}$ for normal subjects. This is consistent with a tendency for there to be higher water content in the soft tissue of the diseased joints.

Temperature profiles along the three central fingers showed a wide range of patterns even in young normal subjects. The elevation of temperature over the affected joints was found to be lower than over the larger joints, but this is to be expected because of the larger surface area to tissue volume ratio. Combining all the finger joints together appears to give a measure which shows a clear difference between young, normal subjects and patients with RA. From the results it is thought that microwave thermography may be useful in the evaluation and disease monitoring of patients suffering from RA in their wrist and finger joints.

With measured environmental, oral, microwave and infra-red surface temperatures, combined thermal heat transport and microwave radiation analytical modelling has been used to estimate the effective perfusion and water content of the female breast. In a group of 21 control subjects, aged between 17 and 55, the estimated blood perfusion was found to be in the range (0.19 - ~2.0) $kg\,m^{-3}s^{-1}$. This range agrees well with the findings of other investigations. The water content was estimated to be from (15 - 90)%, ranging from fatty breast tissue to mainly muscle. The breast thermograms obtained could be split into five categories; 29 % of women showing a dipping pattern across the breasts, 24 % showing less decrease in temperature across the breast, 33 % of women had a flat trace, patchy thermograms were obtained

for 9 % of the control group and finally 5% of the women had asymmetric thermograms. These findings are in agreement with Draper & Jones (1969) infra-red classifications.

Microwave thermography has been used in the past for detection of breast abnormalities, in particular breast cancer. However, a problem arose due to the high false-positive detection rate. For this study this area of work involved using the microwave thermography system for the detection of temperature variation in the female breasts throughout the menstrual cycle.. This study was essential as knowledge of the thermal behaviour of normal breasts is needed if changes due to breast disease are to be detected. The natural changes in the female breasts were monitored throughout six natural menstrual cycles and four cycles of women taking oral contraceptives. None of the women reported breast pain at any time through out the period of research. Overall, it was found that the general temperature of the female breasts monitored remains steady until ovulation when an increase in temperature occurred. This increase in temperature remained throughout the luteal phase to the onset of the next period. These temperature changes also occurred in the breasts of women taking oral contraceptives. This is evidence to suggest that breast microwave temperature patterns vary in a regular manner with what is probably the ovulatory cycle. This may provide useful information when looking for evidence of breast disease.

In general the effective perfusion was lowest during the menstrual/early follicular stage of the menstrual cycle, followed by an increase during the ovulatory period. Through the luteal phase the estimated effective perfusion decreases but remains higher than the perfusion in the early stages of the menstrual cycle.

Estimates of the water content were made and it was found that the water content varied significantly during the menstrual cycle. It was also observed that more variance occurred during the cycles of women not taking oral contraceptives. This may be due to the effect of the natural hormones oestrogen and progesterone on the breasts.

The combined microwave and thermal modelling has been very successfully applied to the analysis of the temperature data information obtained in the rheumatology and breast studies presented in Chapters 6 and 7. For the body regions considered relatively simple 1-D modelling gives useful measures of effective perfusion and tissue water content. The values obtained for tissue perfusion and water content are in agreement with values found by other techniques.

Future work at Glasgow research group includes using microwave thermography as a method of investigating inflammatory causes of renal failure. This would be advantageous as fewer people would need to undergo a biopsy. The menstrual cycle investigation could be extended to include women with breast abnormalities. This would verify whether the technique could distinguish between natural changes in the thermal properties of the breast and breast disease.

Presently microwave thermography has no secure niche in the medical world, hopefully its potential will soon be recognised and accepted. The results of this research highlight that the microwave thermography technique is inherently safe, simple to perform and can most importantly provide medically useful information.

APPENDIX A

Menstrual thermograms, Subject 1.

SUBJECT 1 - CYCLE 1

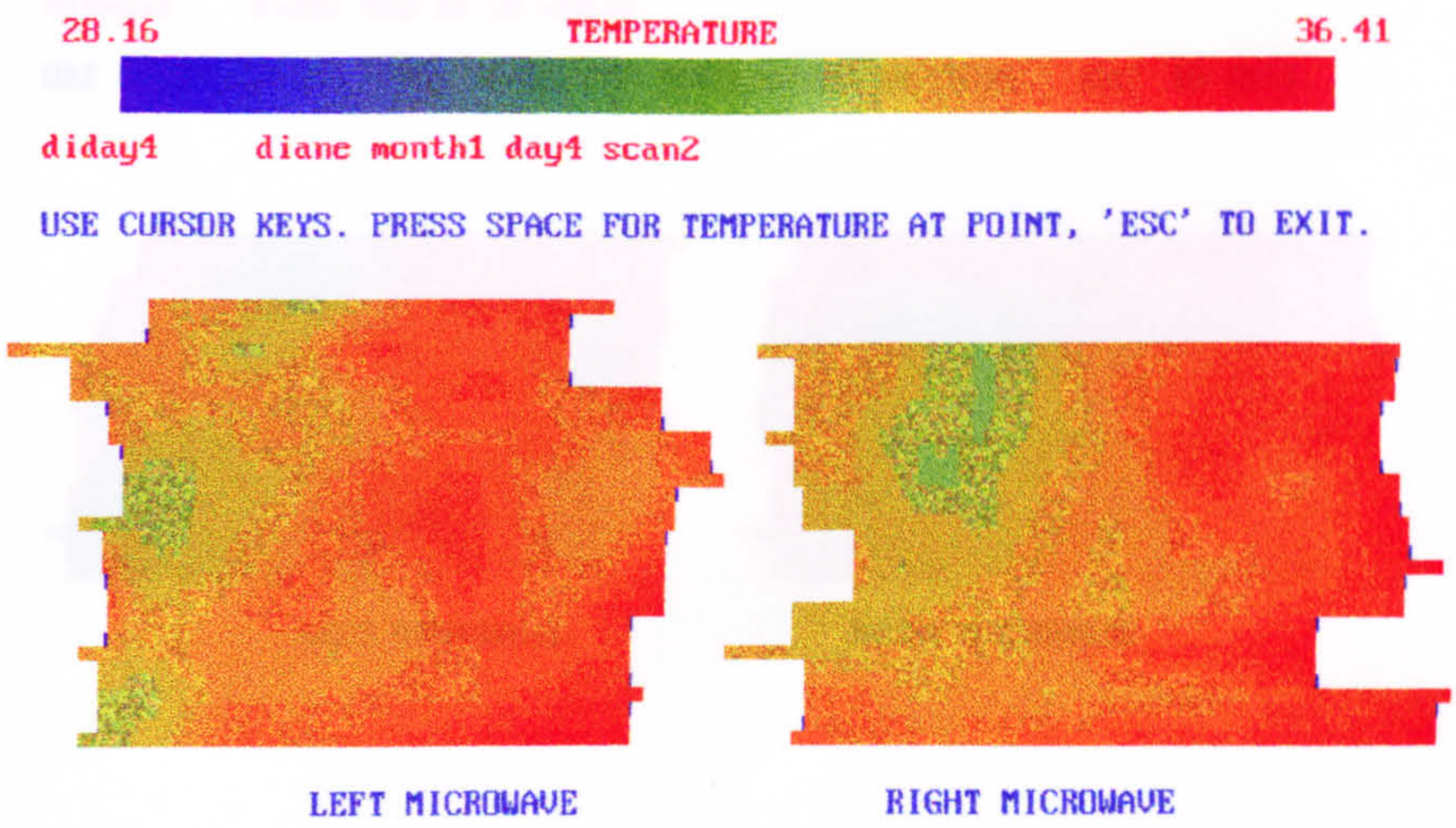

Fig. A1 Microwave breast thermogram, Subject 1, Cycle 1, Day 4

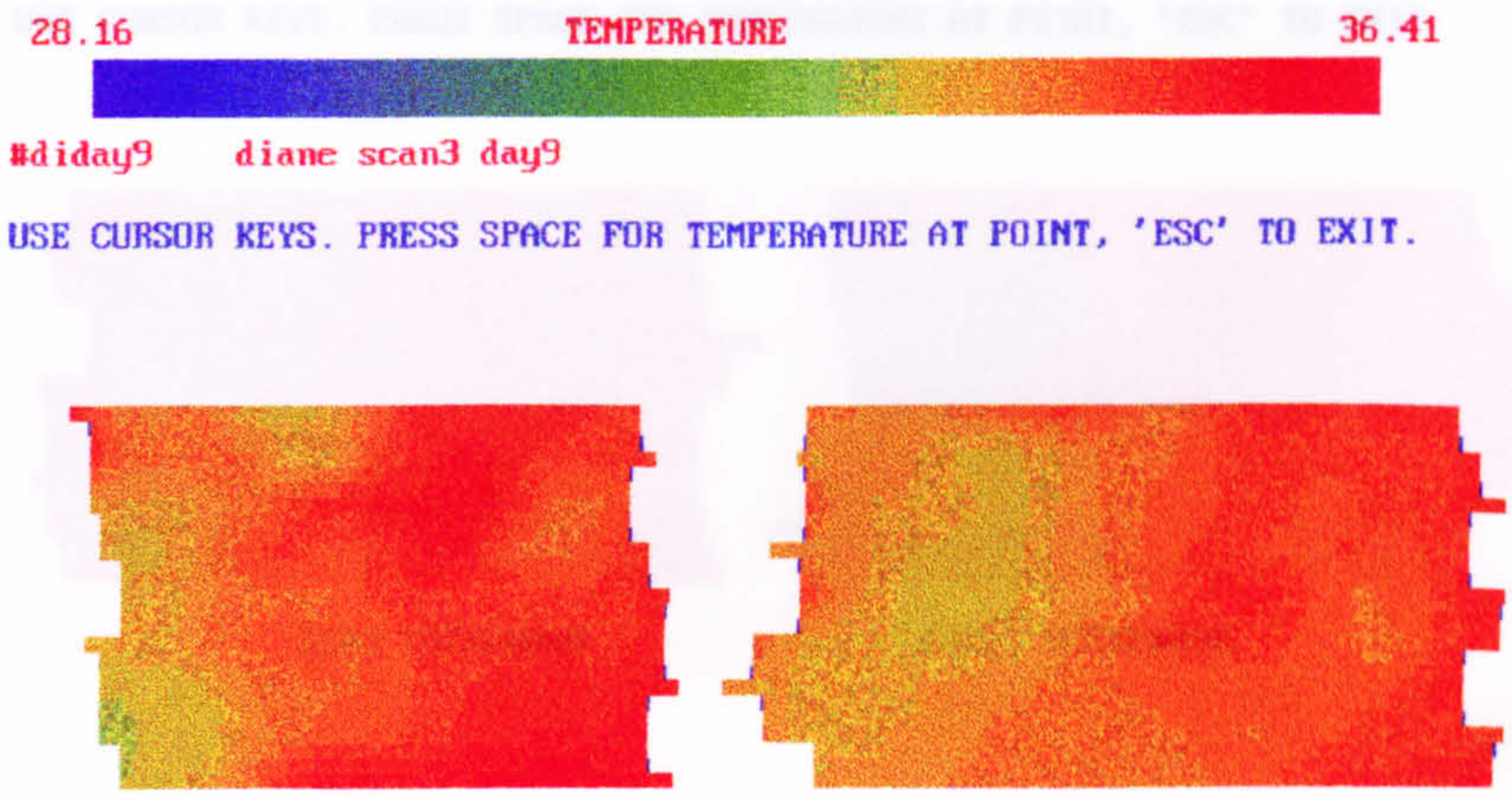

Fig. A2 Microwave breast thermogram, Subject 1, Cycle 1, Day 9

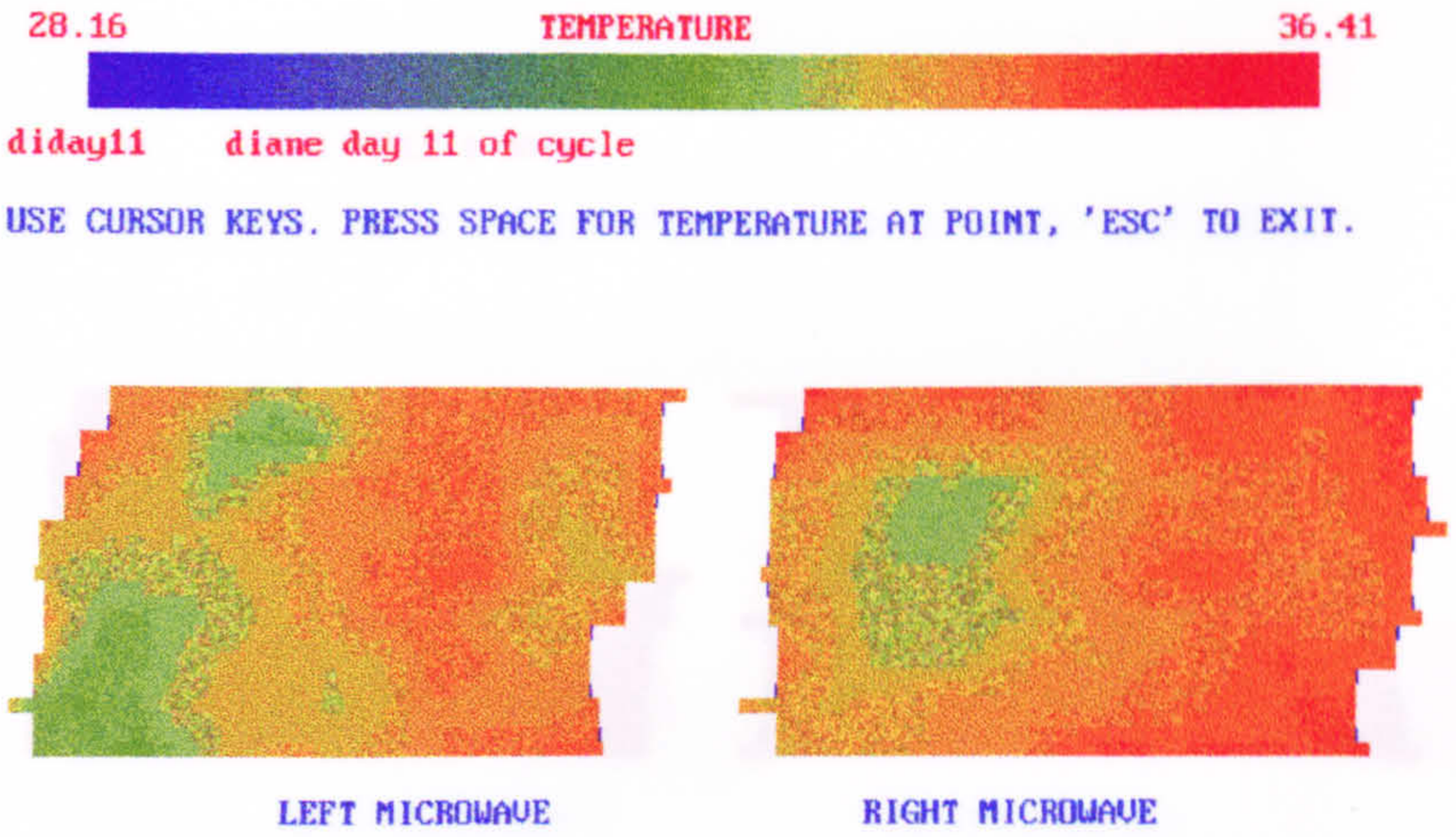

Fig. A3 Microwave breast thermogram, Subject 1, Cycle 1, Day11

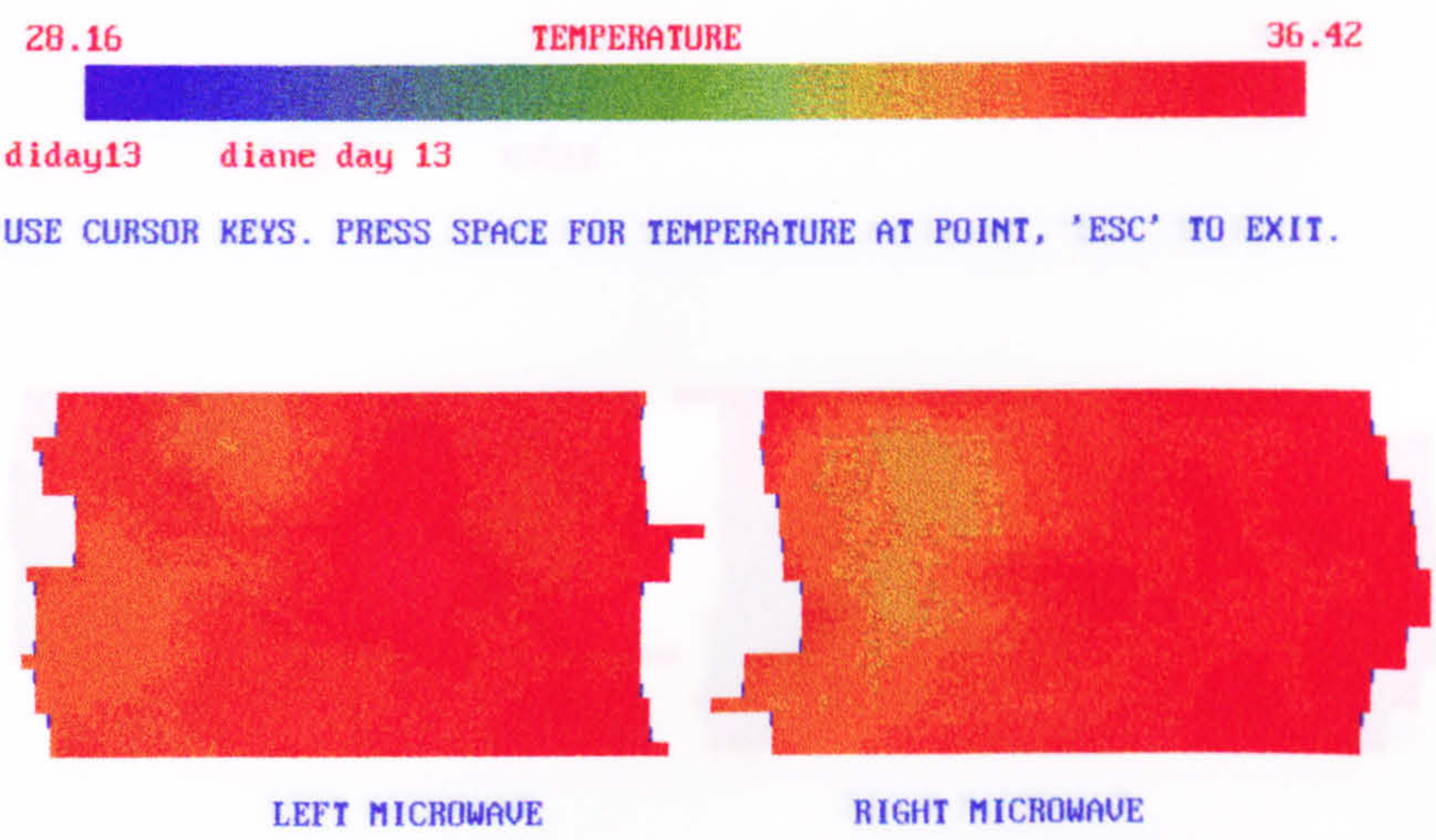

Fig. A4 Microwave breast thermogram, Subject 1, Cycle 1, Day 13

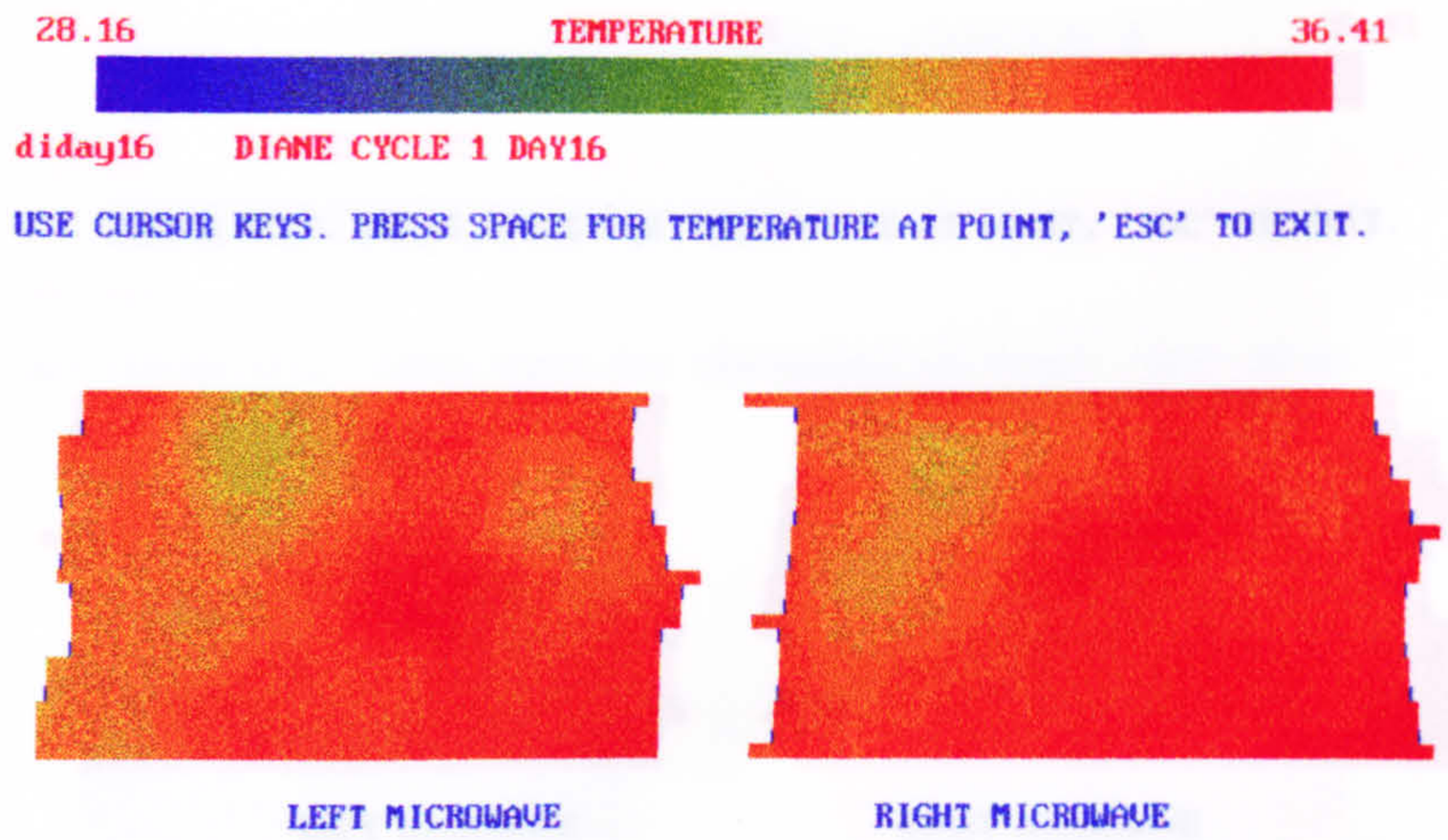

Fig. A5 Microwave breast thermogram, Subject 1, Cycle 1, Day16

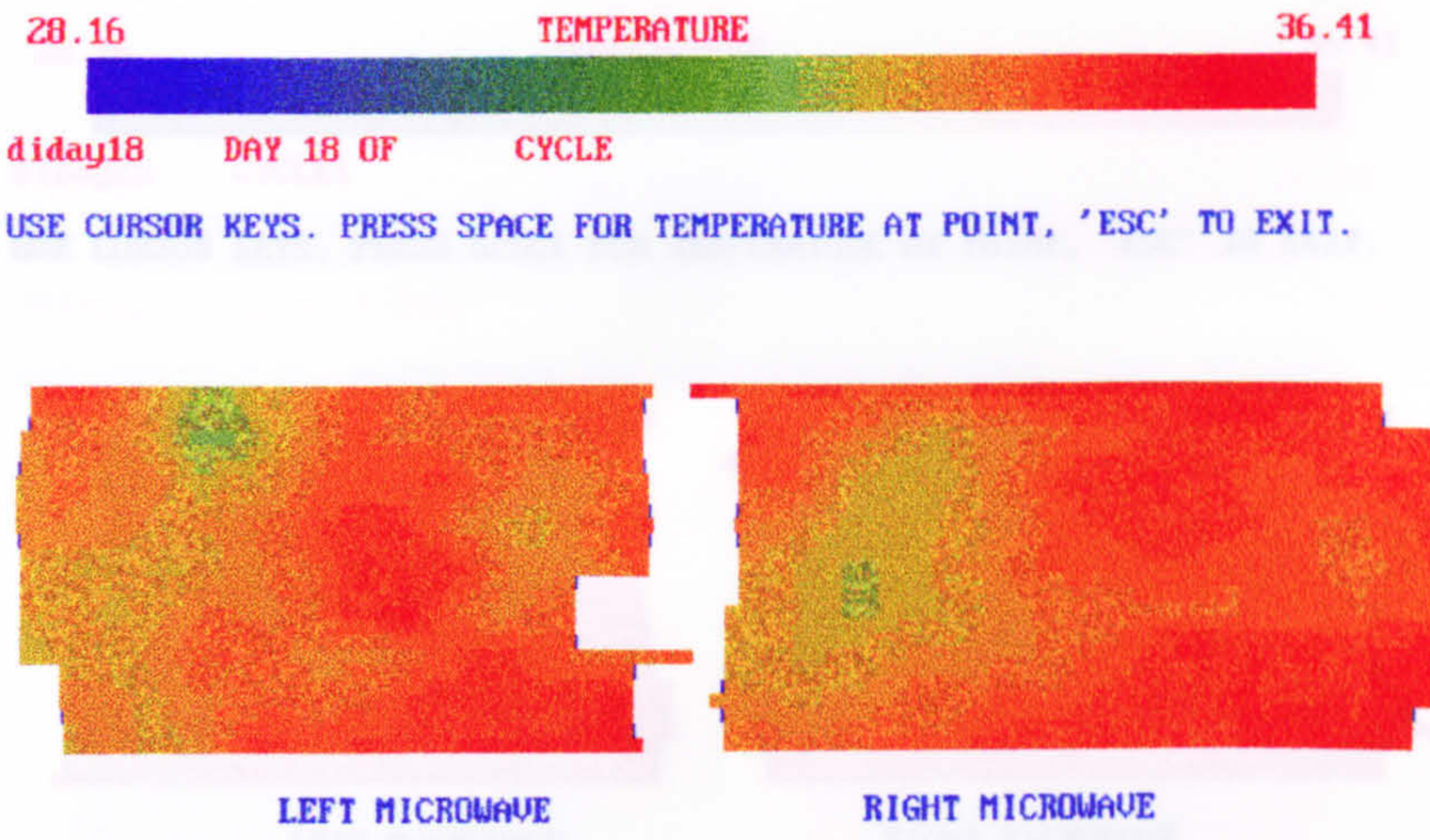

Fig. A6 Microwave breast thermogram, Subject1, Cycle 1, Day 18

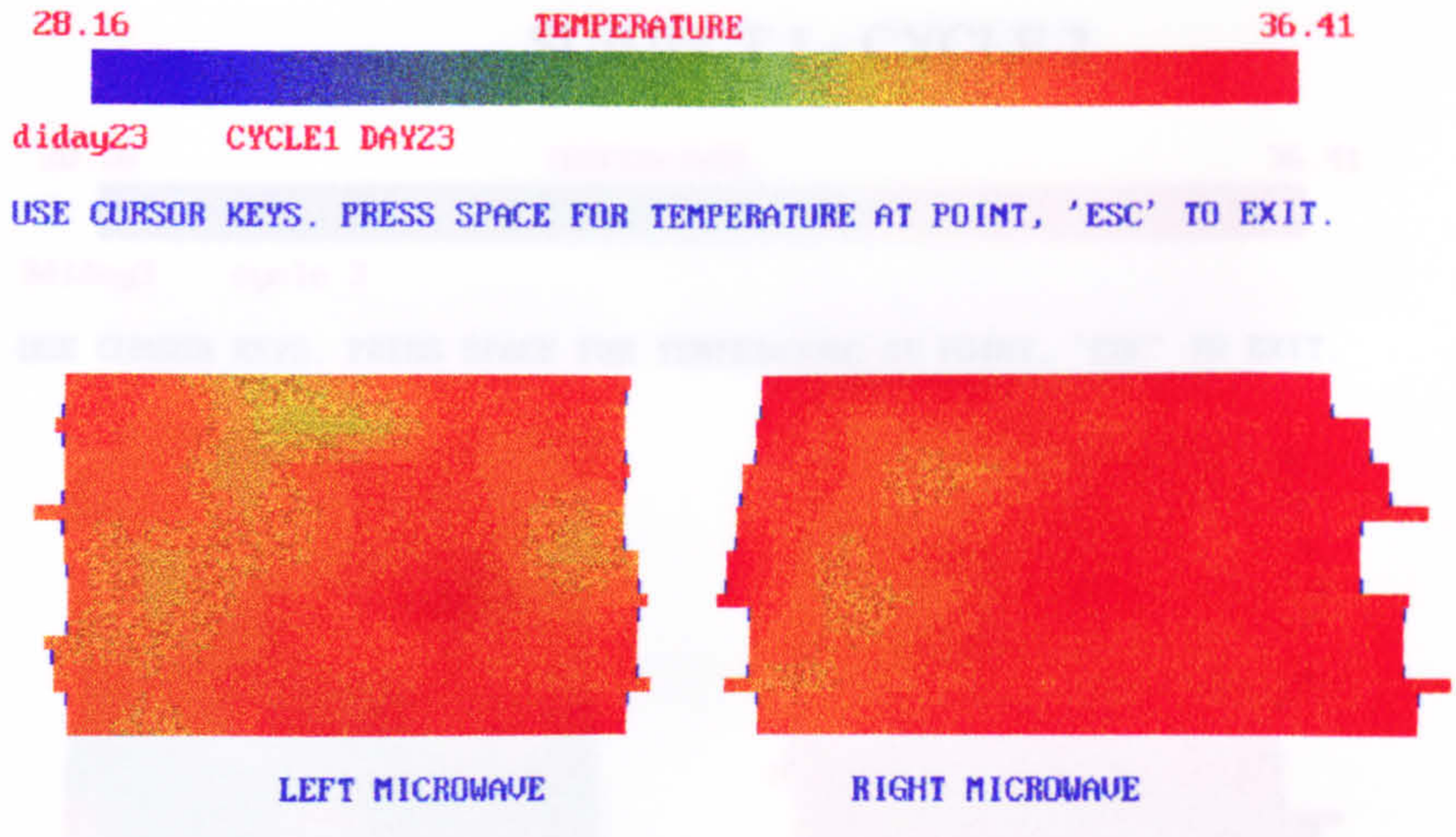

Fig. A7 Microwave breast thermogram, Subject 1, Cycle 1, Day 23

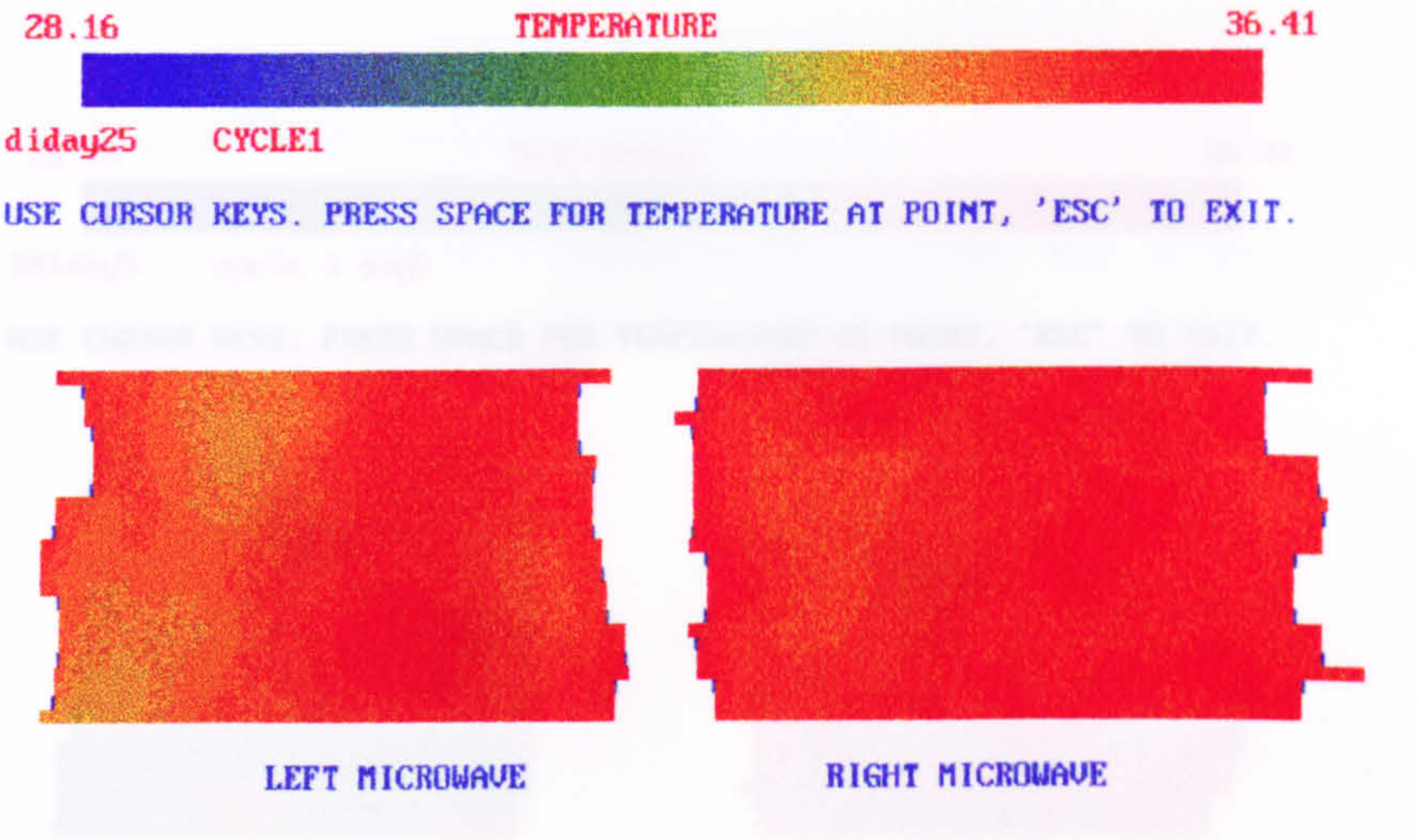

Fig. A8 Microwave breast thermogram, Subject 1, Cycle 1, Day 25

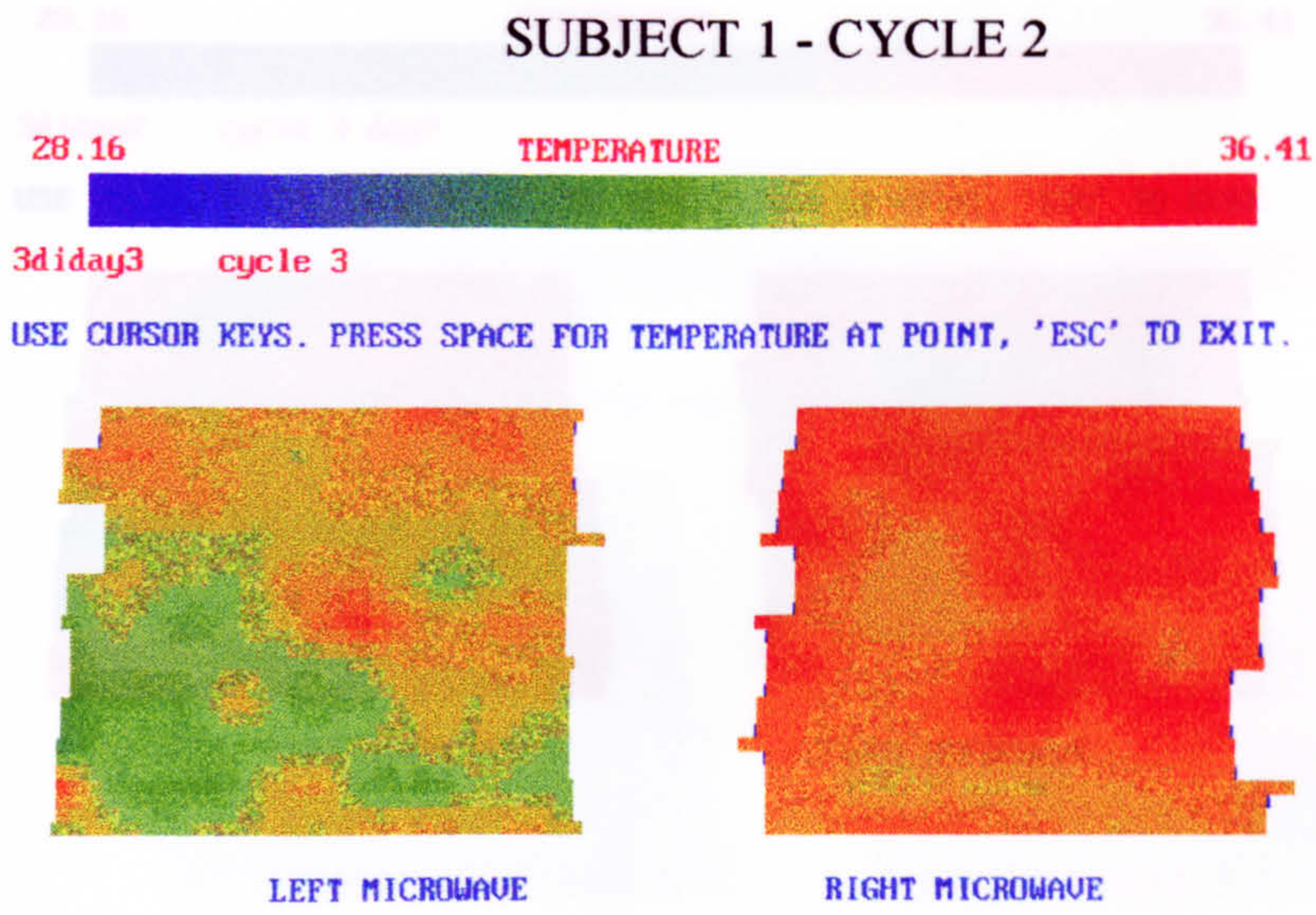

Fig. A9 Microwave breast thermogram, Subject 1, Cycle 2, Day 3

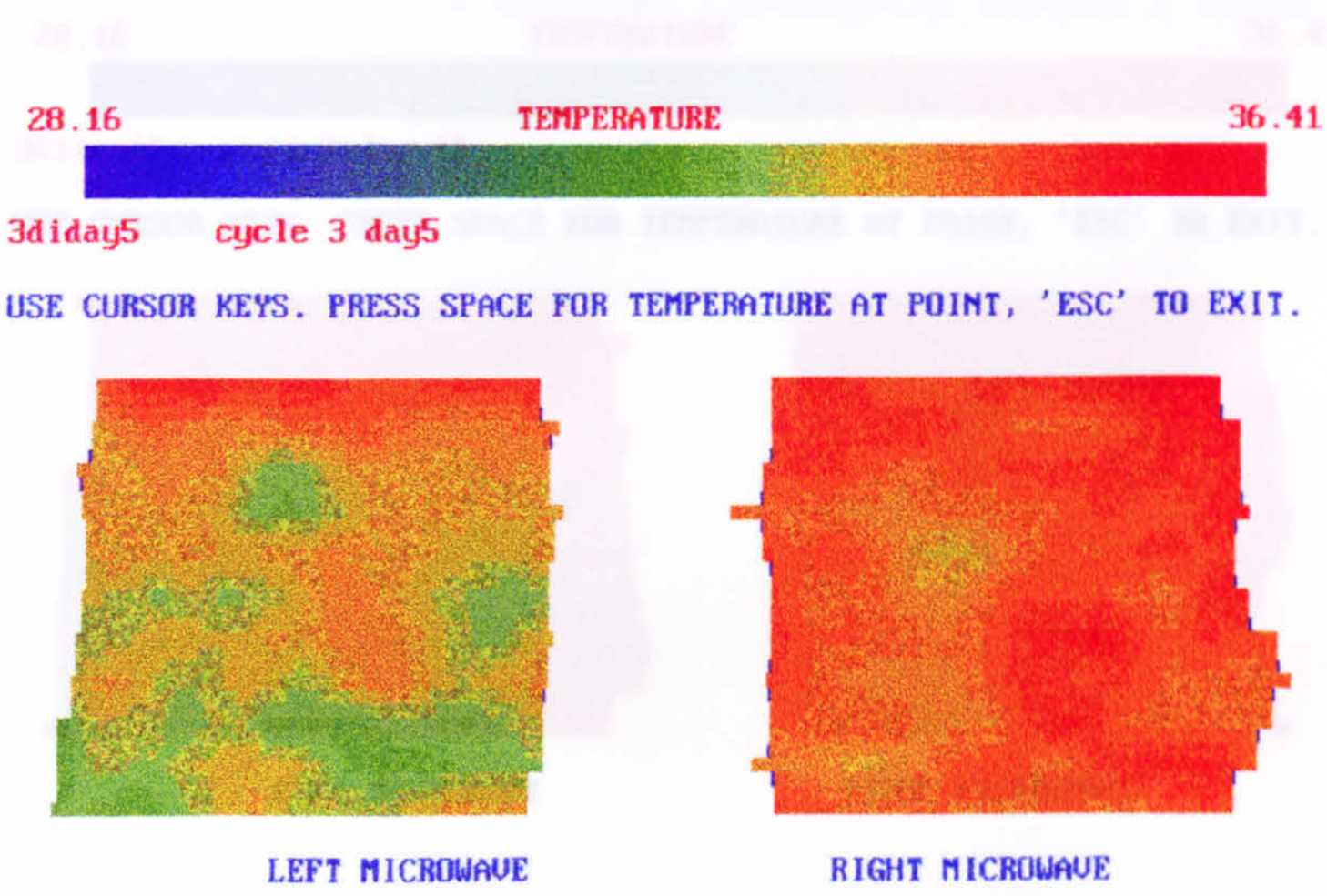

Fig. A10 Microwave breast thermogram, Subject 1, Cycle 2, Day 5

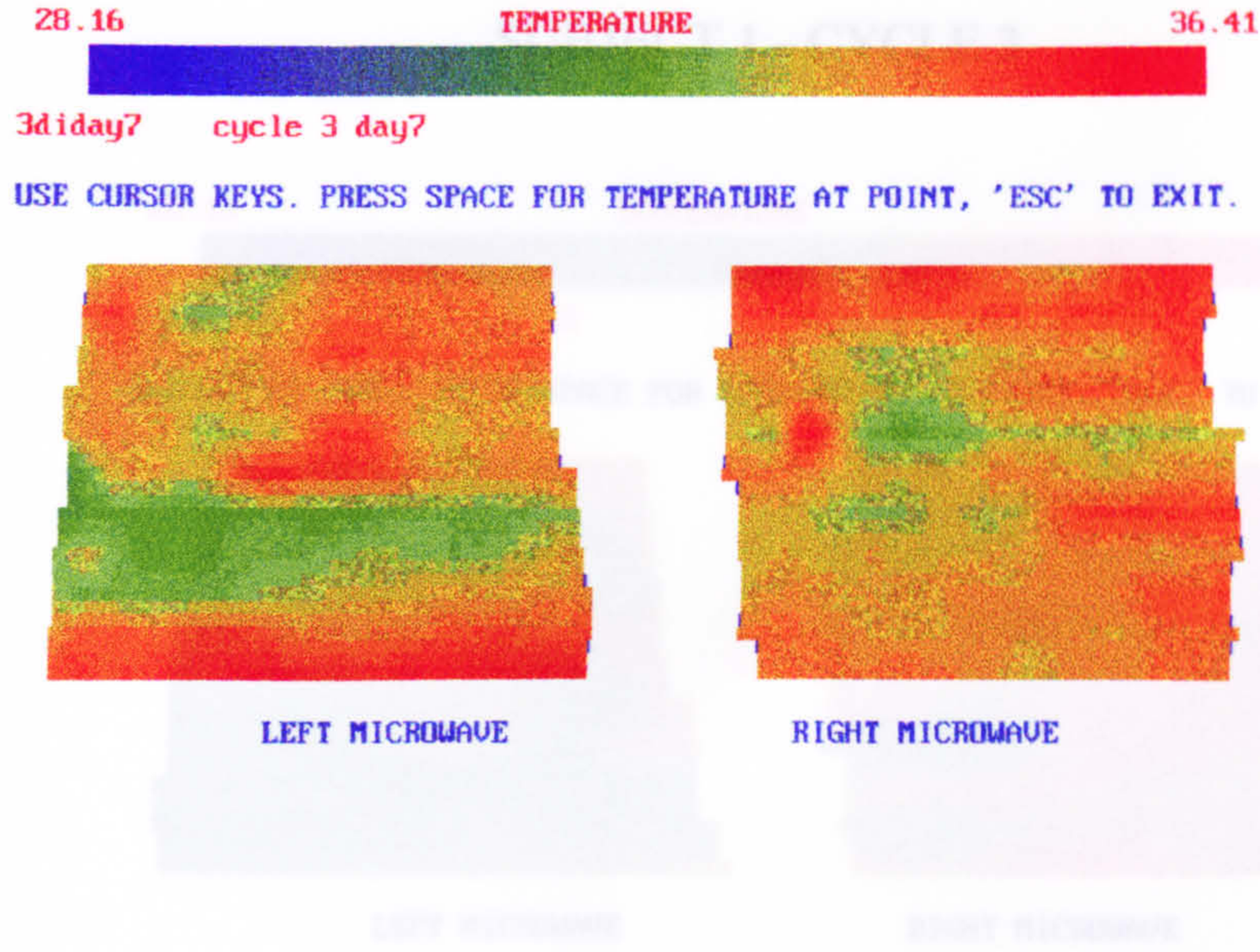

Fig. A11 Microwave breast thermogram, Subject 1, Cycle 2, Day 7

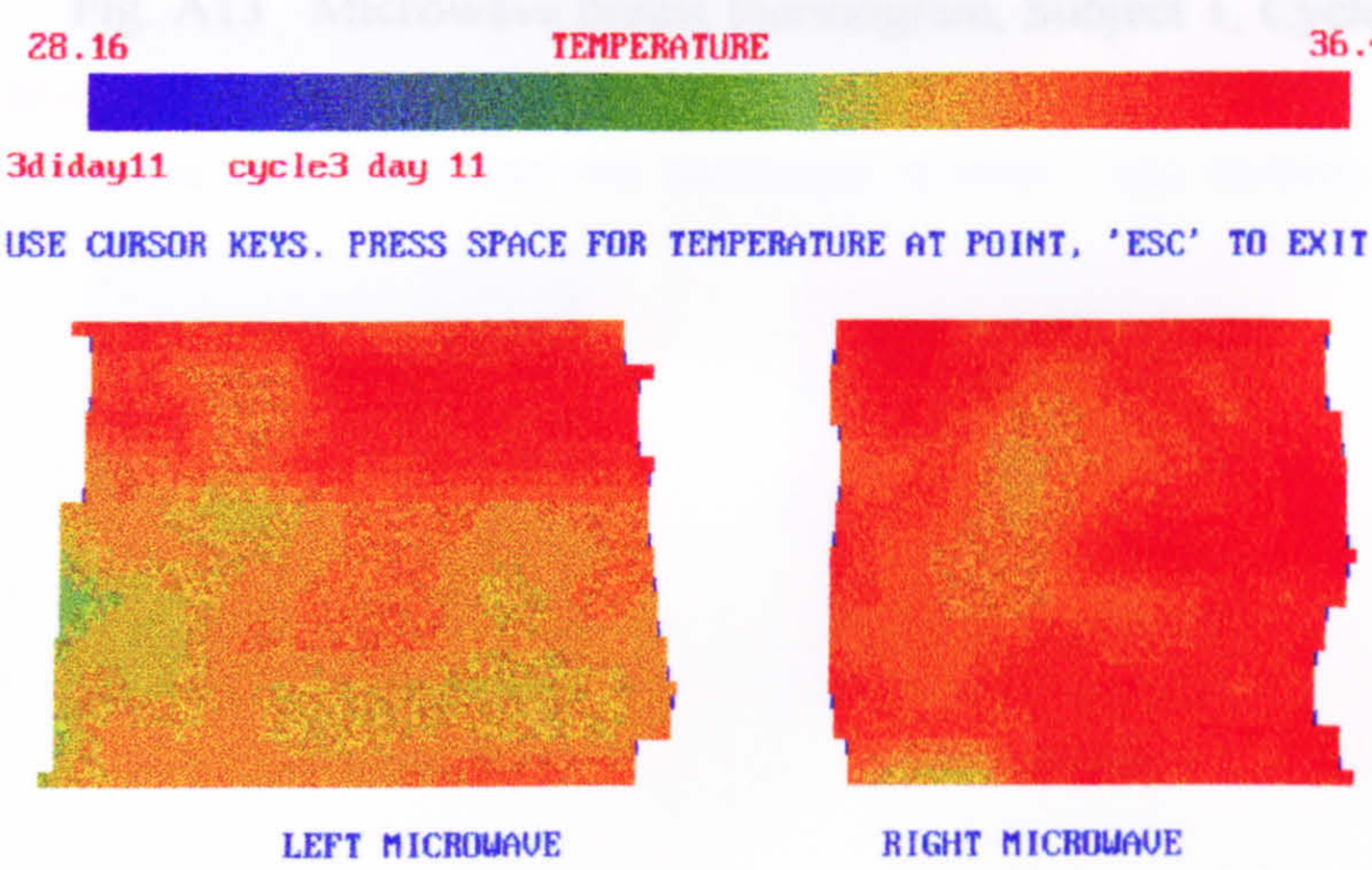

Fig. A12 Microwave breast thermogram, Subject 1, Cycle 2, Day 11

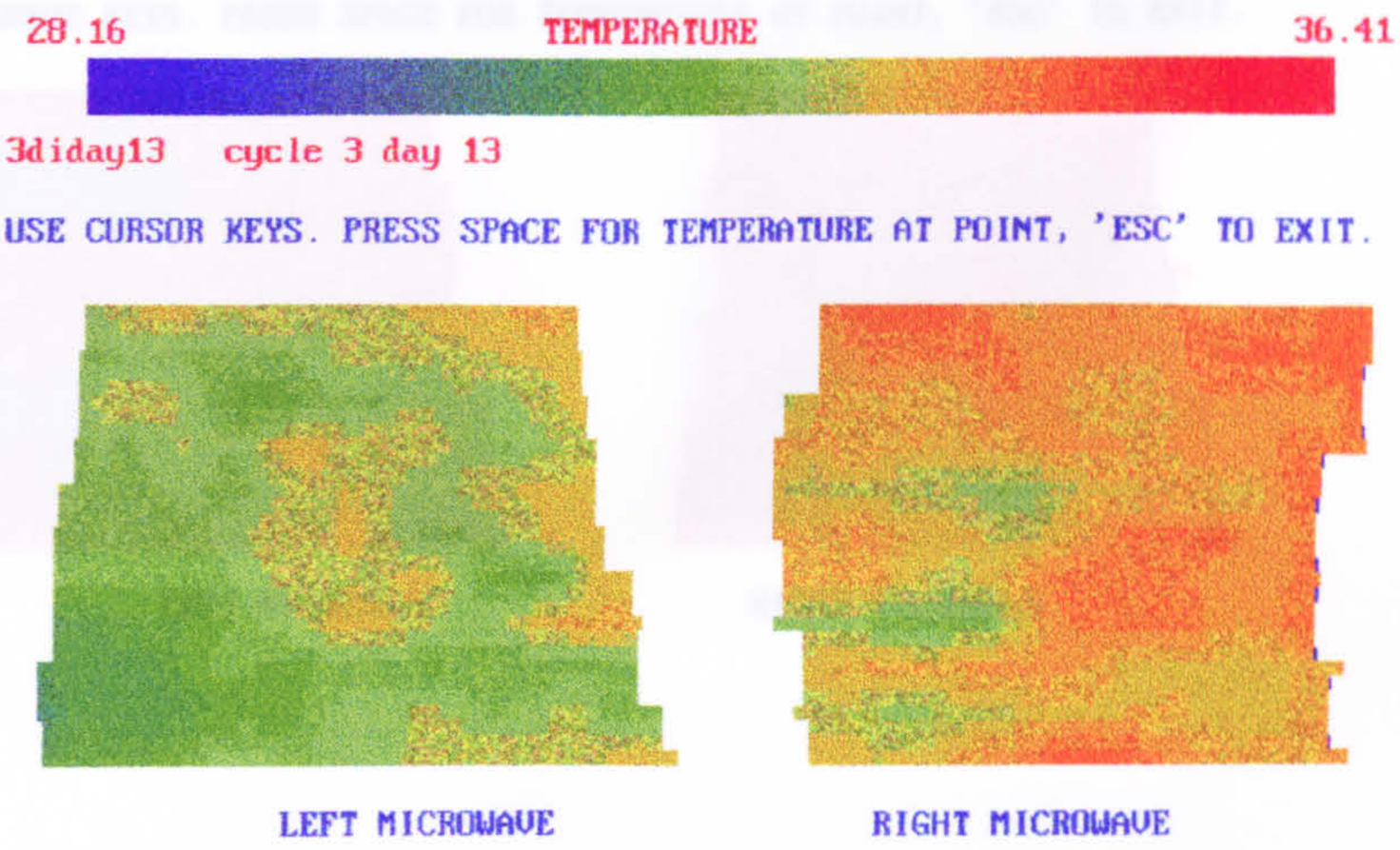

Fig. A13 Microwave breast thermogram, Subject 1, Cycle 3, Day 1

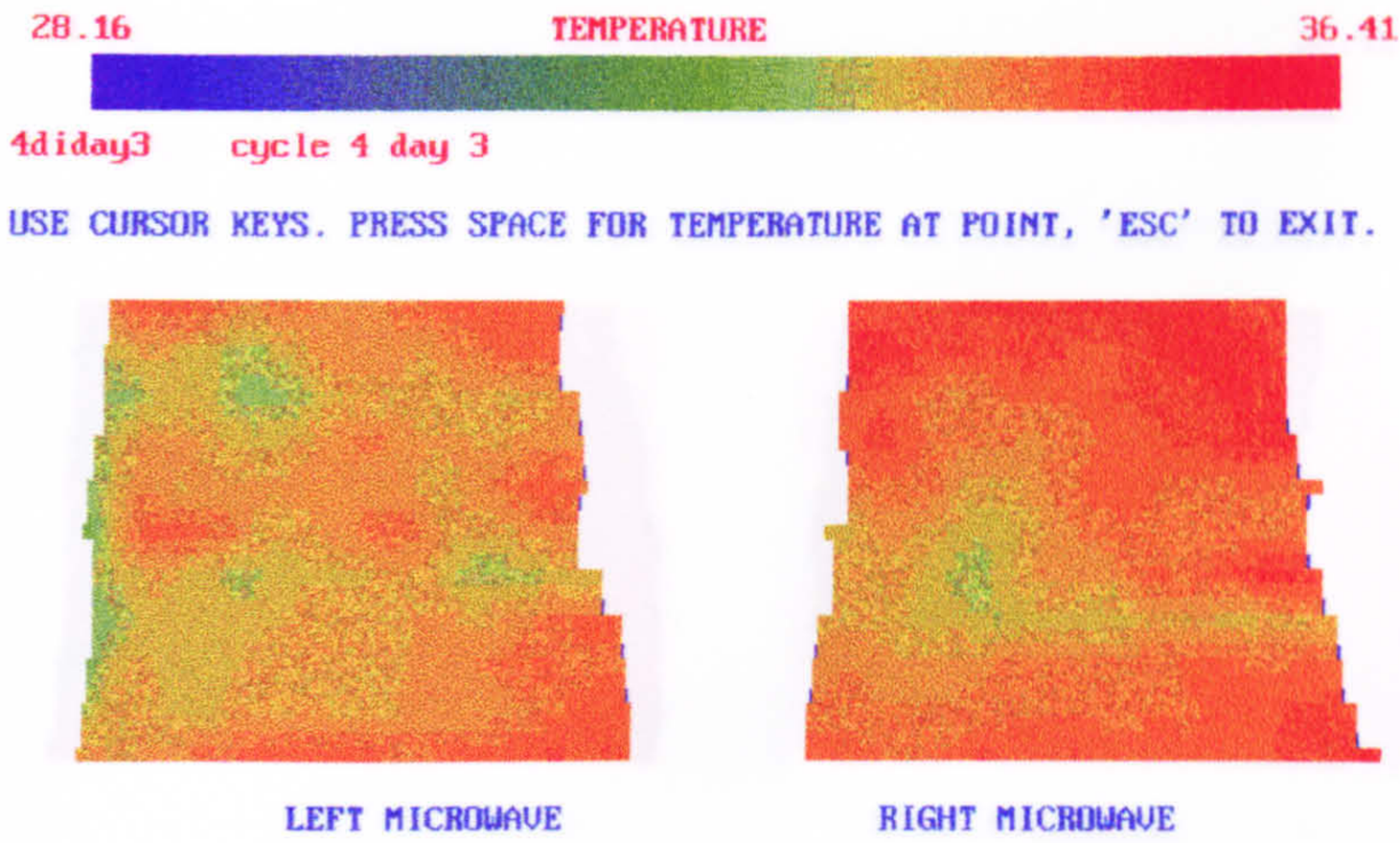

Fig. A14 Microwave breast thermogram, Subject 1, Cycle 3, Day 3

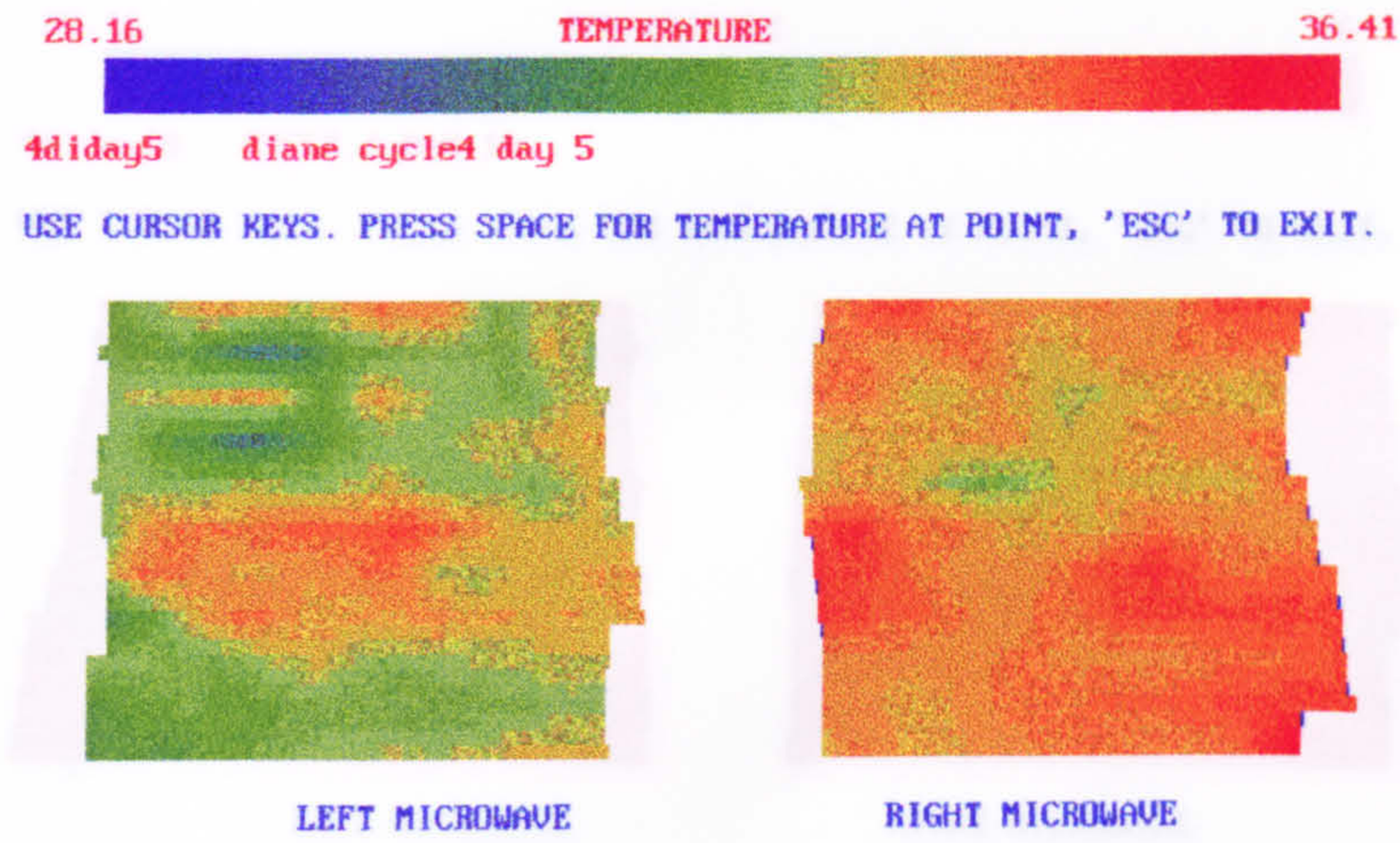

Fig. A15 Microwave breast thermogram, Subject 1, Cycle 3, Day 5

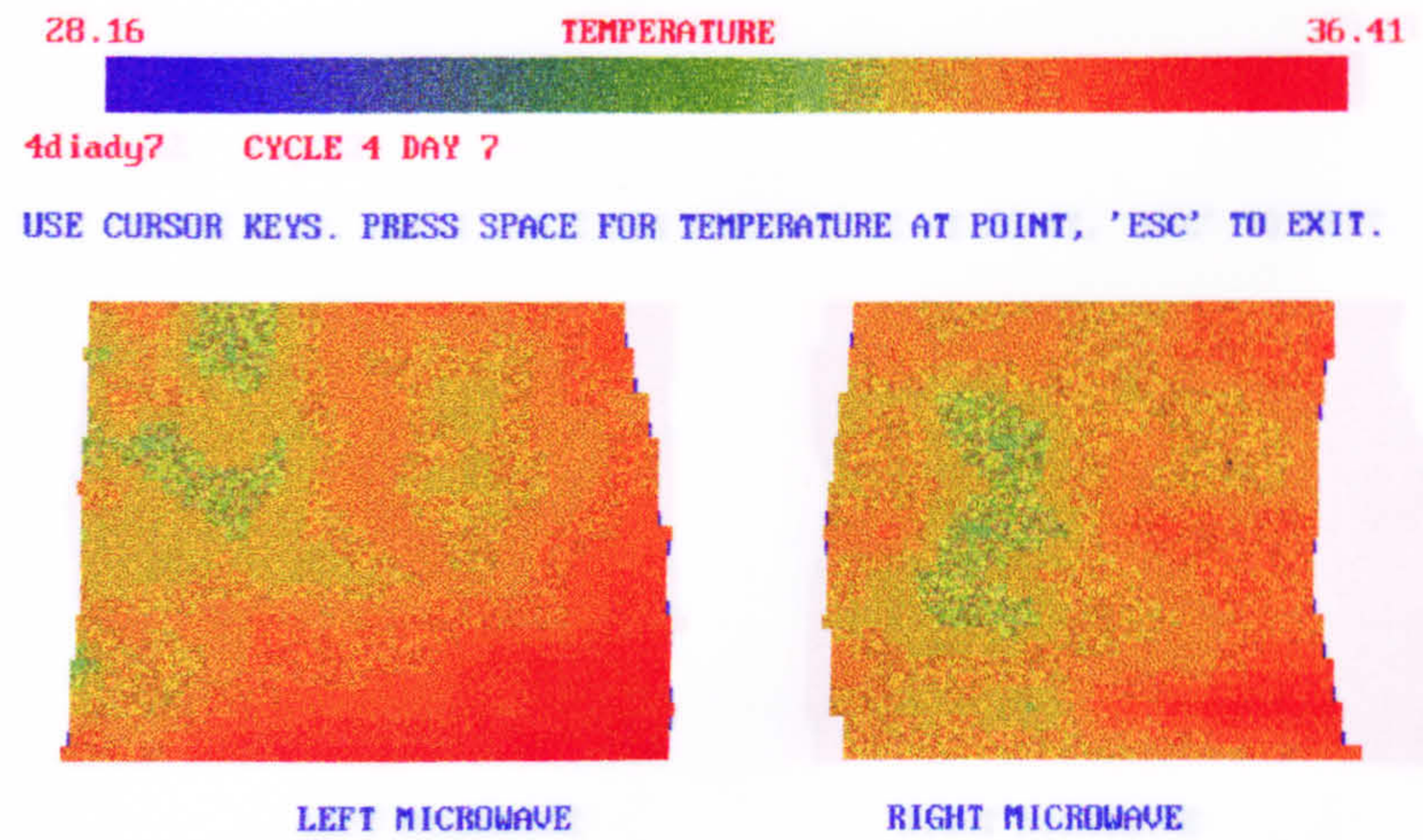

Fig. A16 Microwave breast thermogram, Subject 1, Cycle 3, Day 7

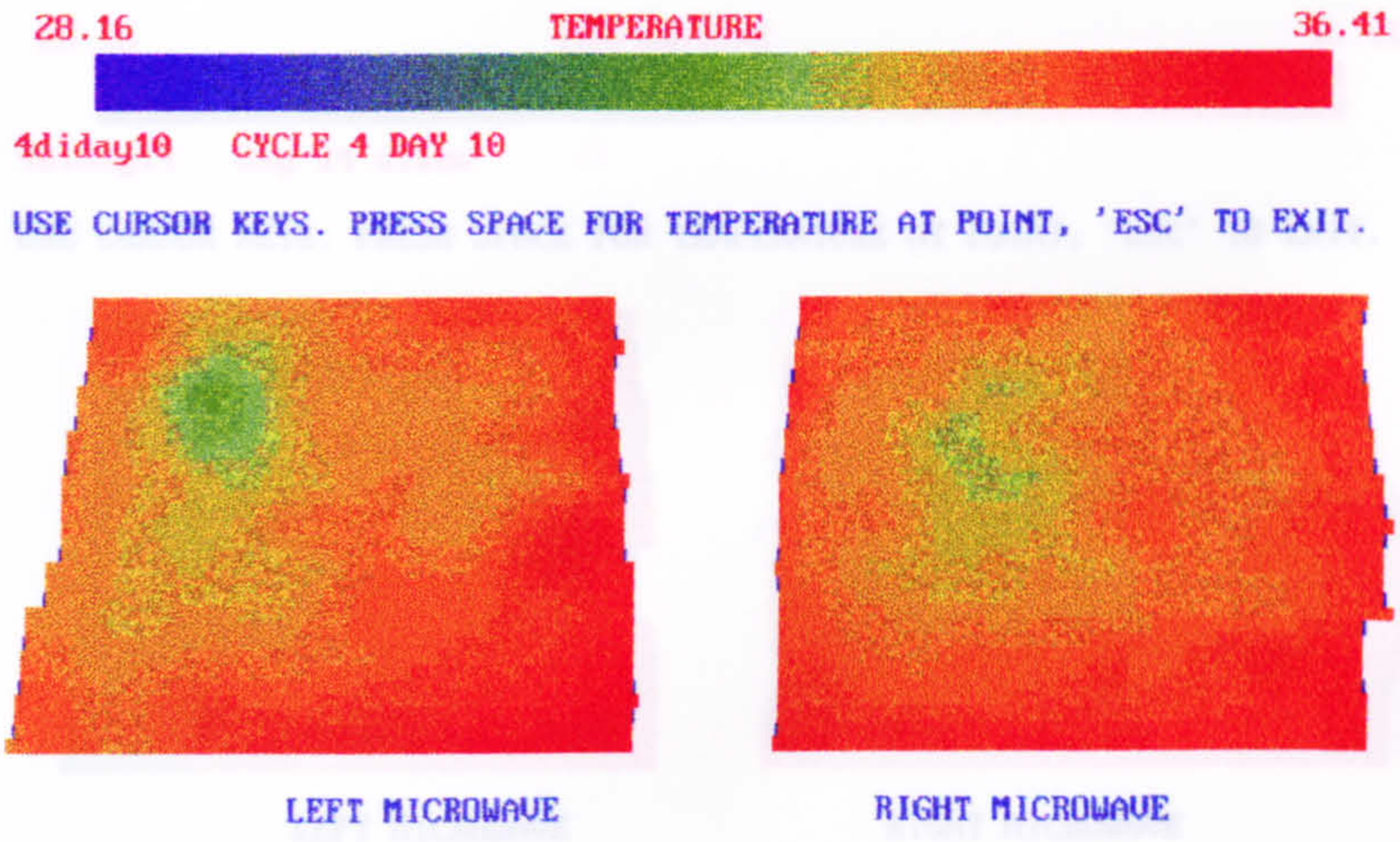

Fig. A17 Microwave breast thermogram, Subject 1, Cycle 3, Day 10

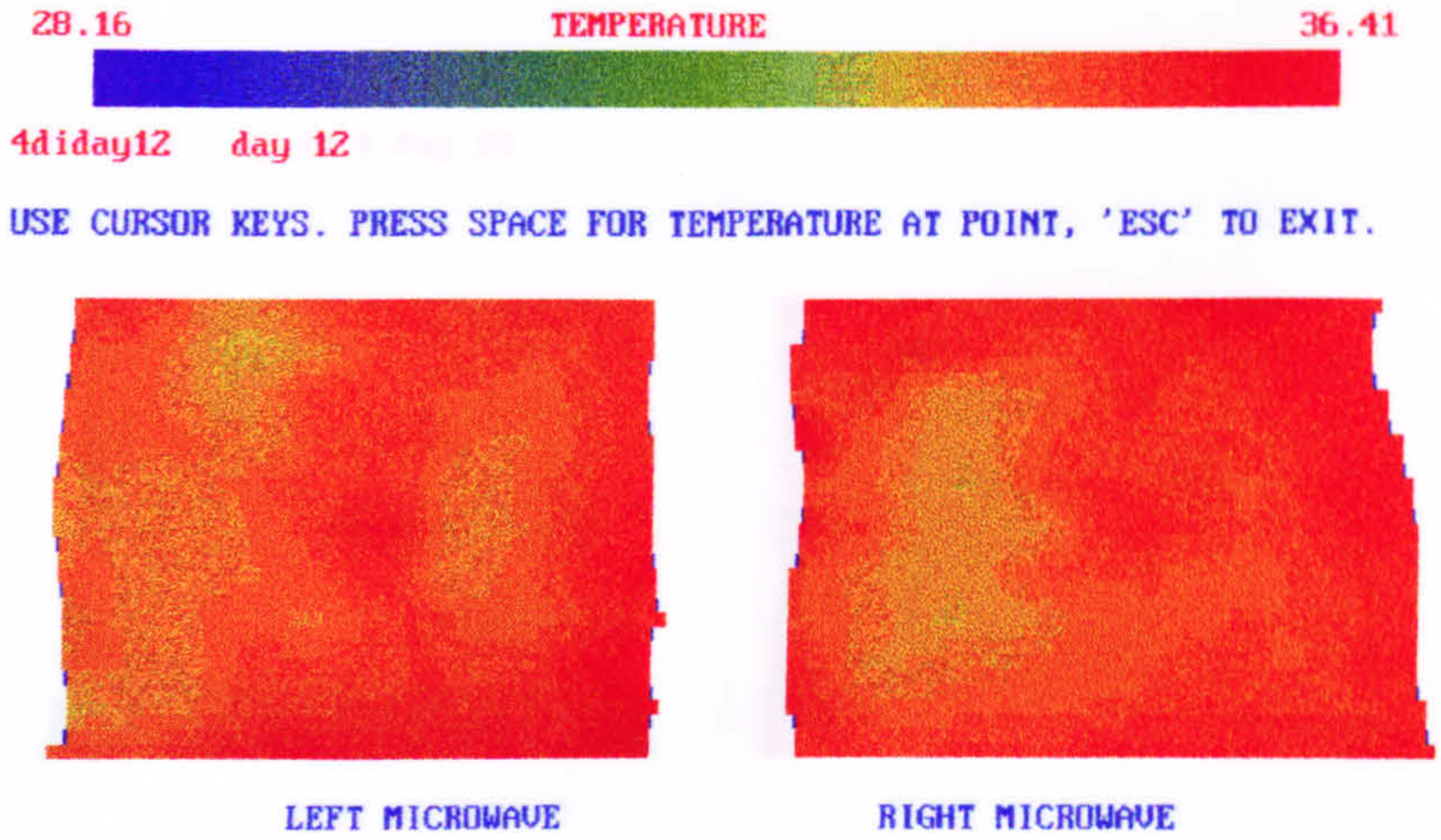

Fig. A18 Microwave breast thermogram, Subject 1, Cycle 3, Day 12

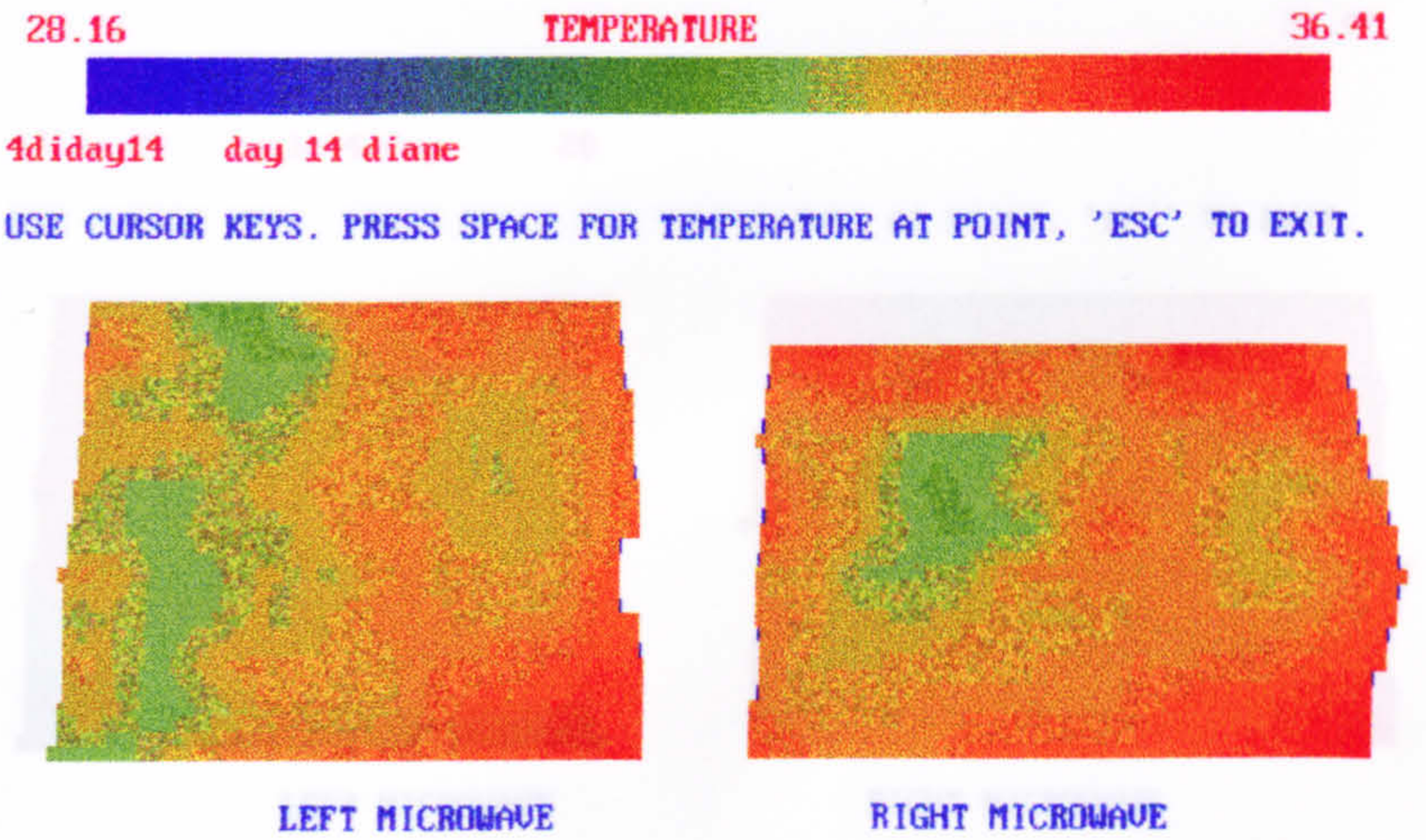

Fig. A19 Microwave breast thermogram, Subject 1, Cycle 3, Day 14

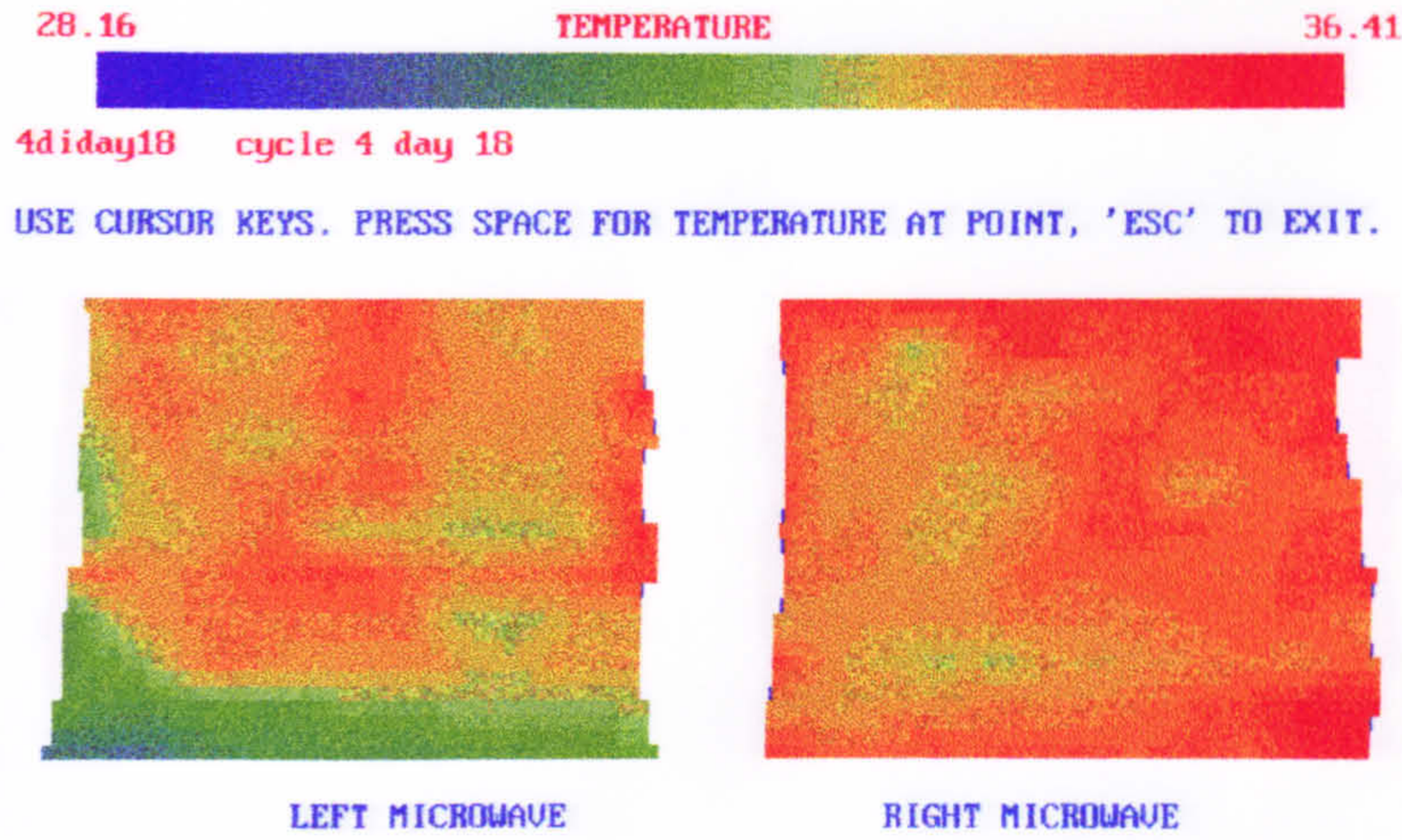

Fig. A20 Microwave breast thermogram, Subject 1, Cycle 3, Day 18

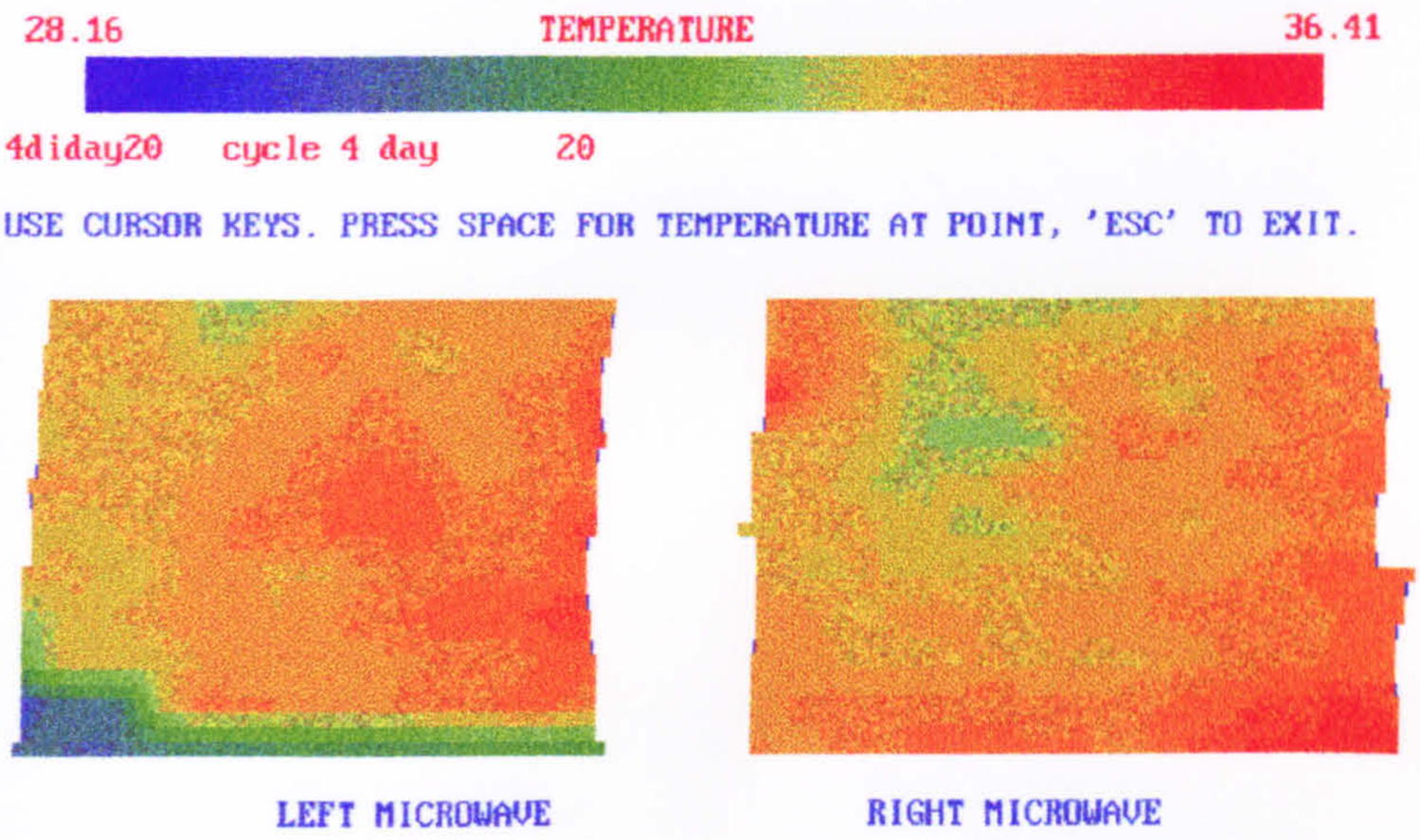

Fig. A21 Microwave breast thermogram, Subject 1, Cycle 3, Day 20

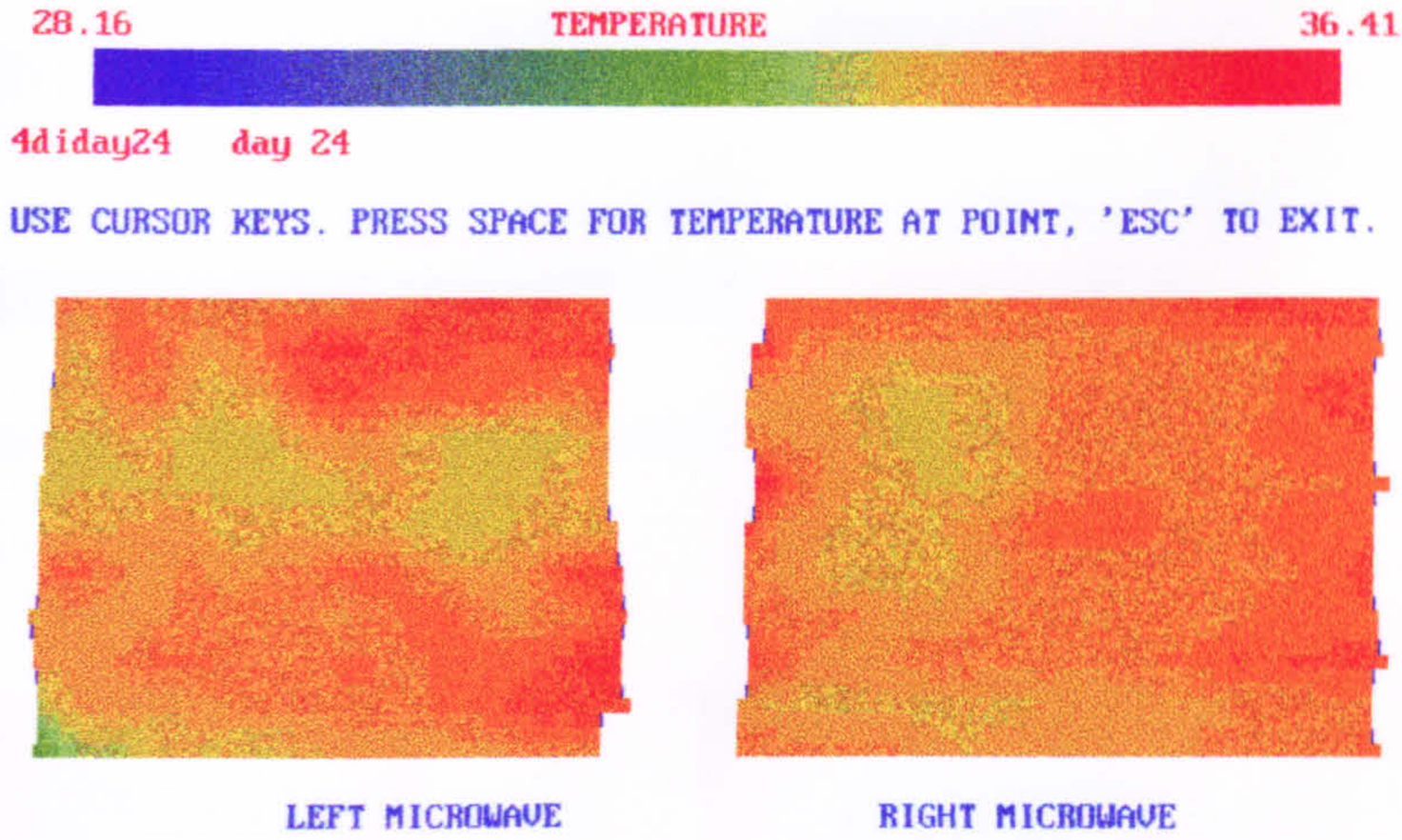

Fig. A22 Microwave breast thermogram, Subject 1, Cycle 3, Day 24

APPENDIX A.1

Menstrual thermograms, Subject 2.

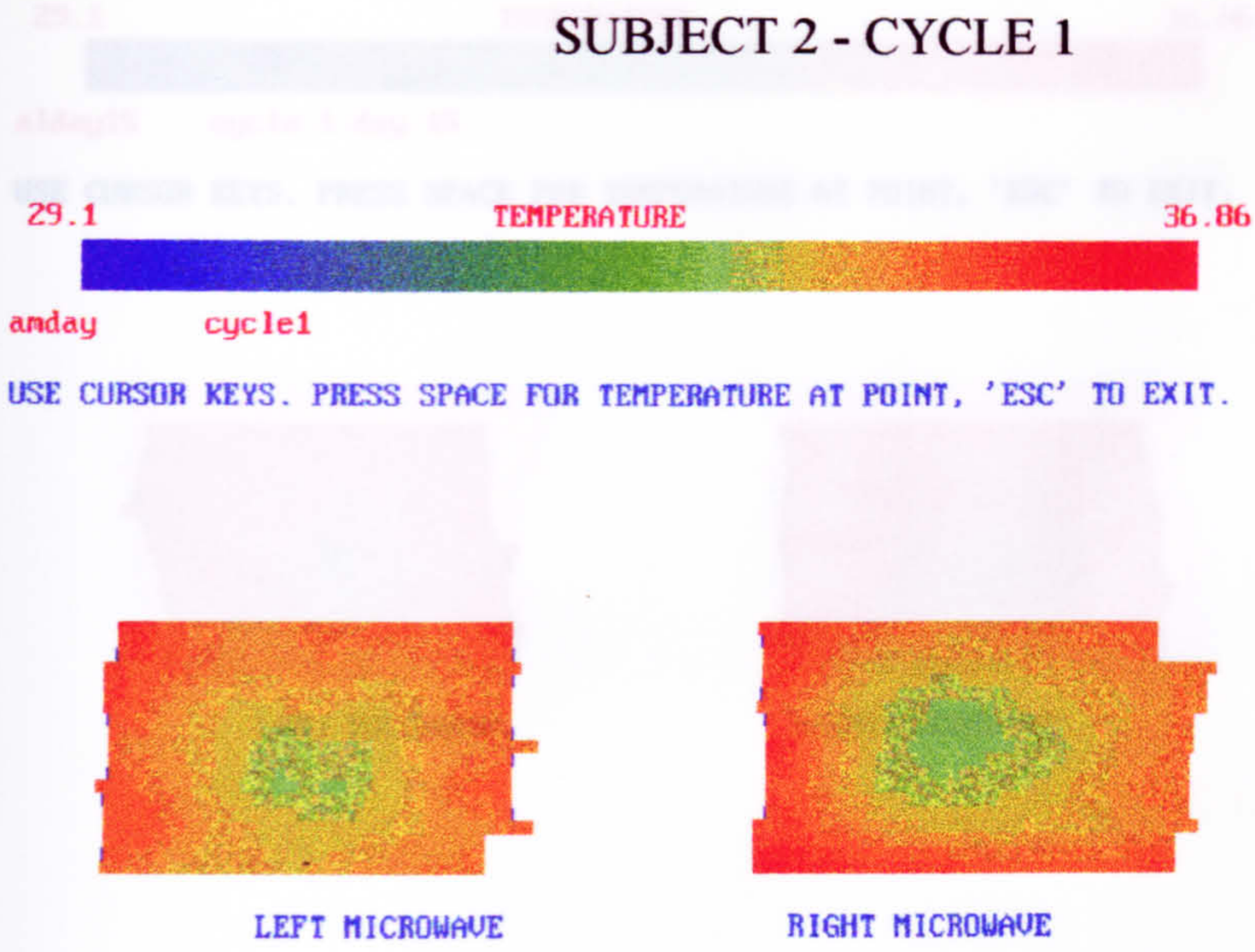

Fig. B1 Microwave breast thermogram, Subject 2, Cycle 1, Day 7

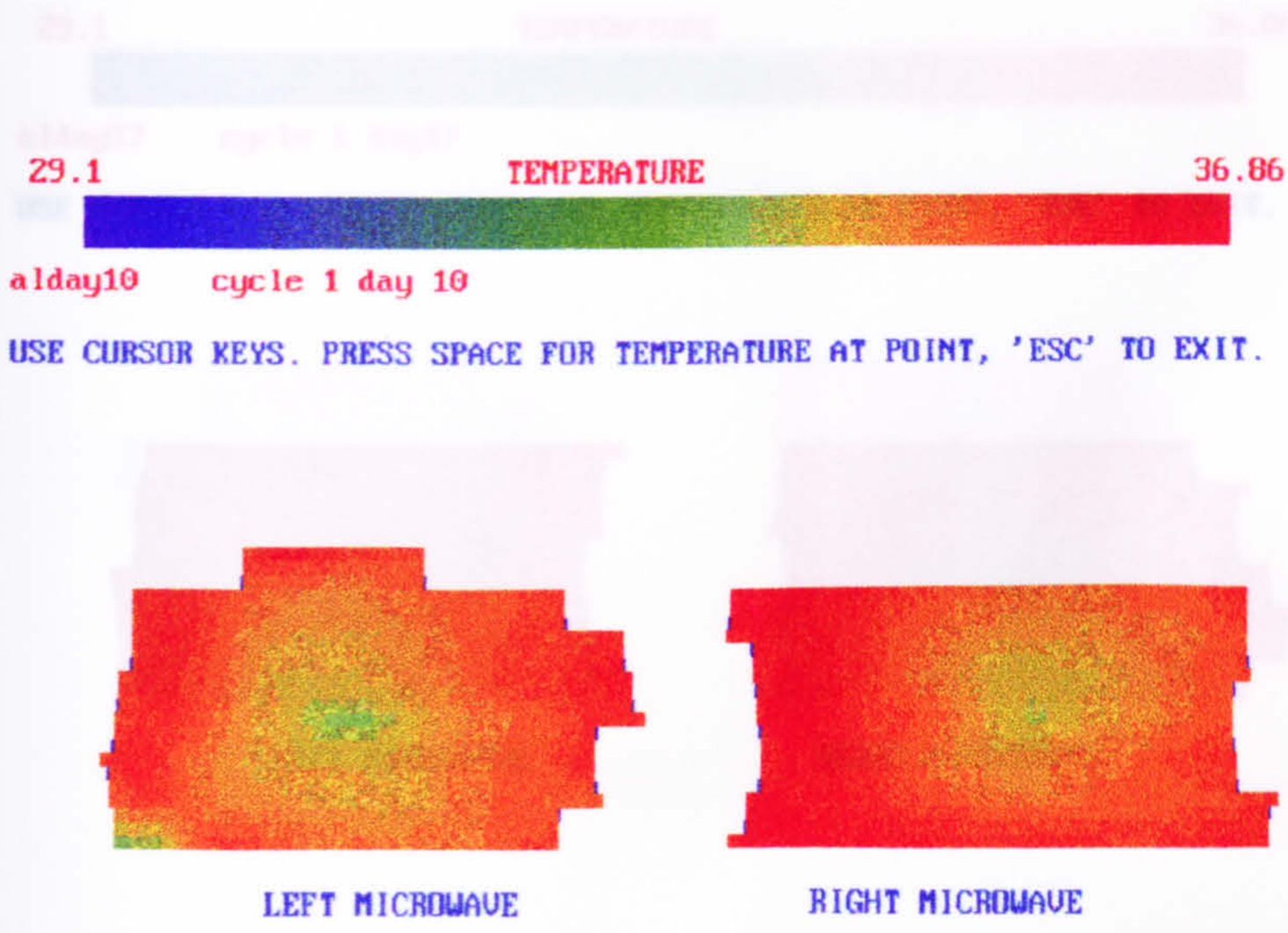

Fig. B2 Microwave breast thermogram, Subject 2, Cycle 1, Day 10

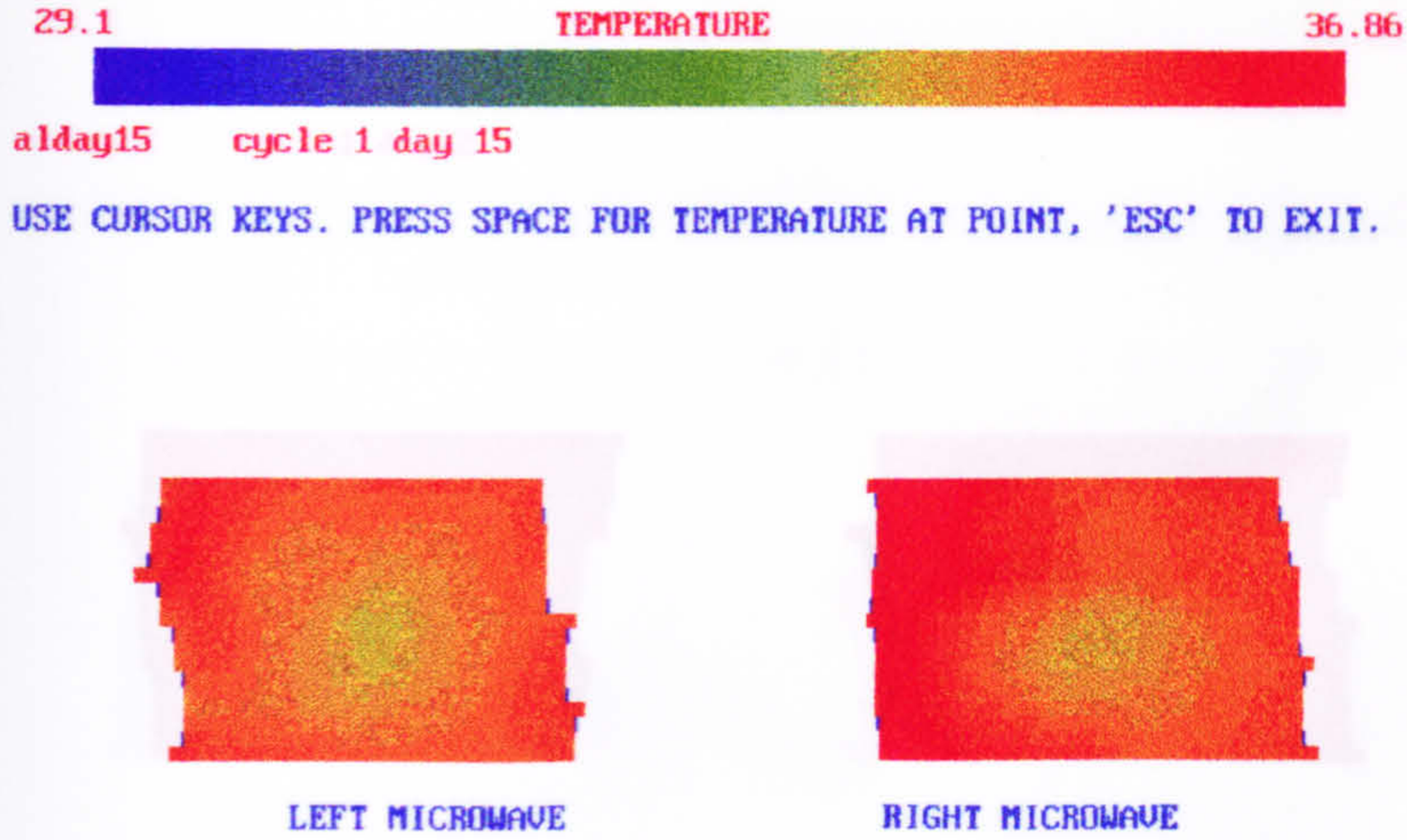

Fig. B3 Microwave breast thermogram, Subject 2, Cycle 1, Day 15

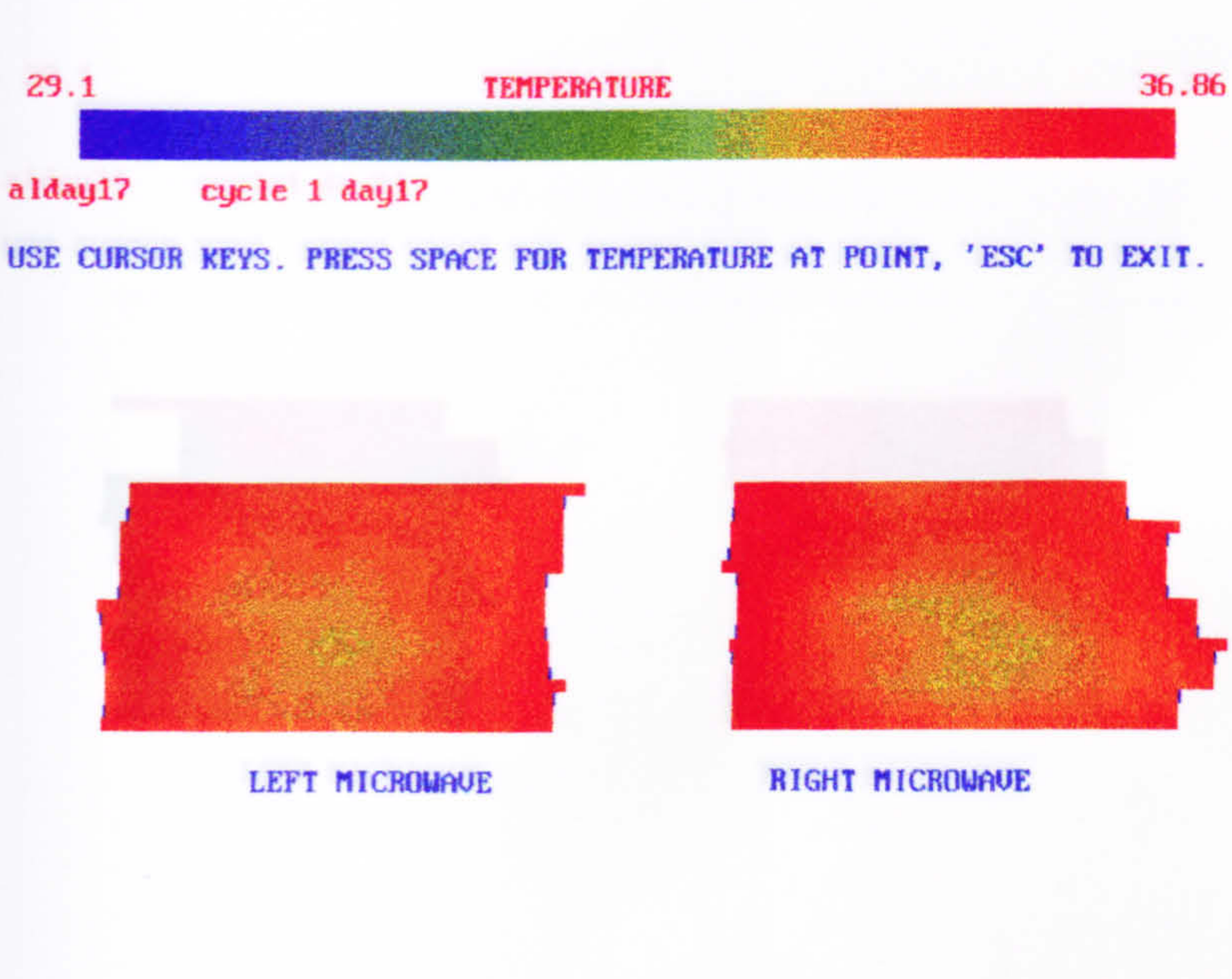

Fig. B4 Microwave breast thermogram, Subject 2, Cycle 1, Day 17

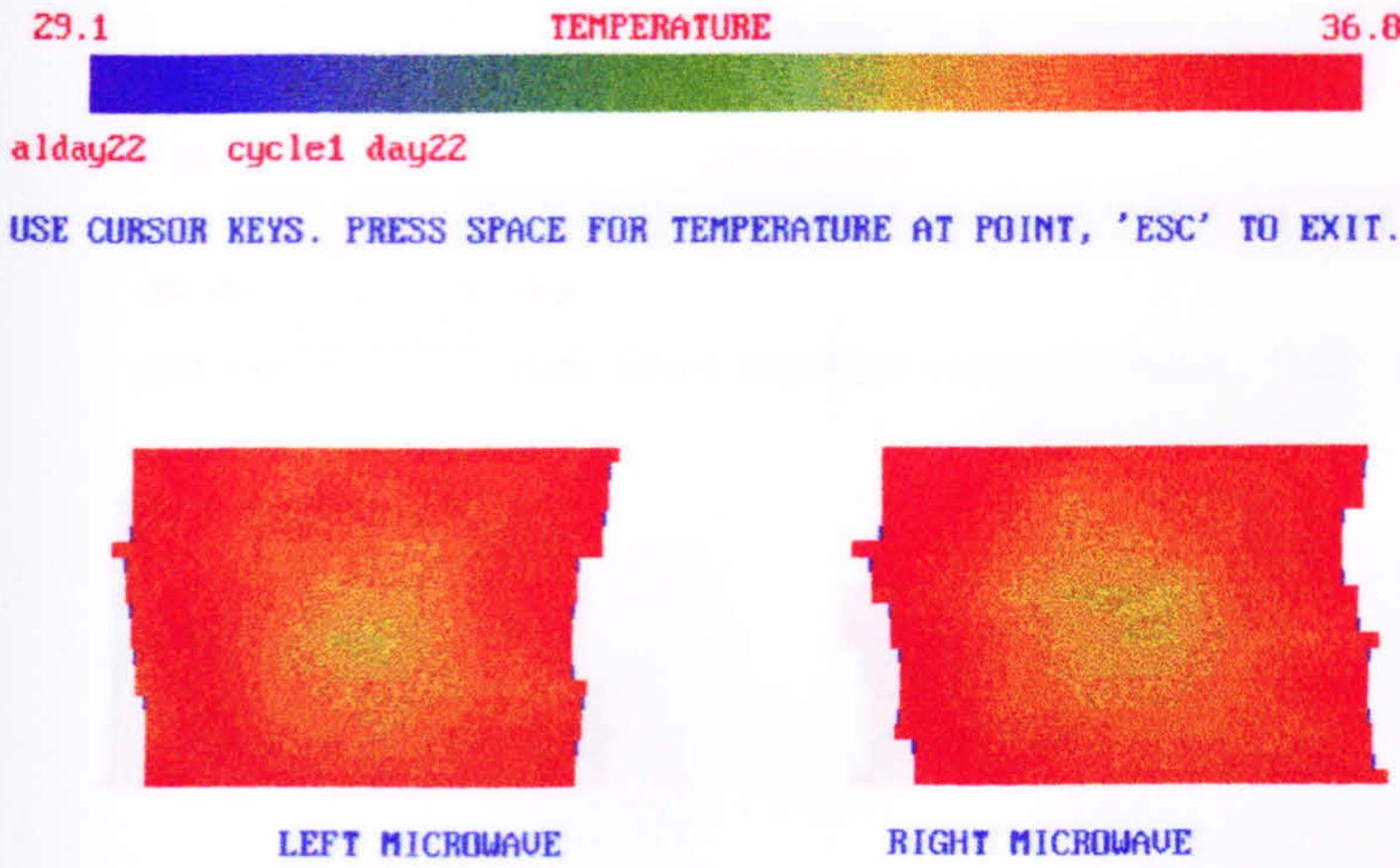

Fig. B5 Microwave breast thermogram, Subject 2, Cycle 1, Day 22

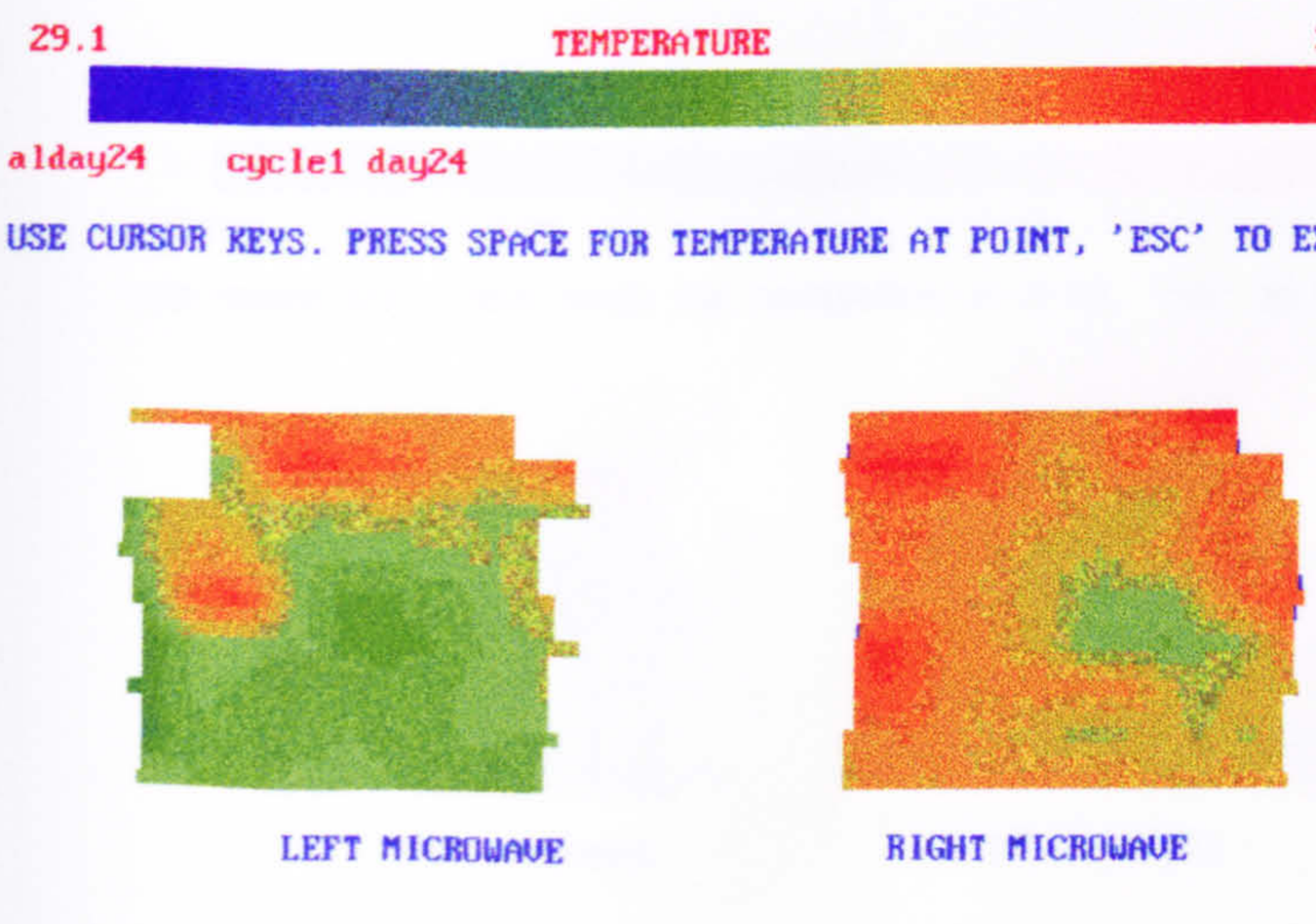

Fig. B6 Microwave breast thermogram, Subject 2, Cycle 1, Day 24

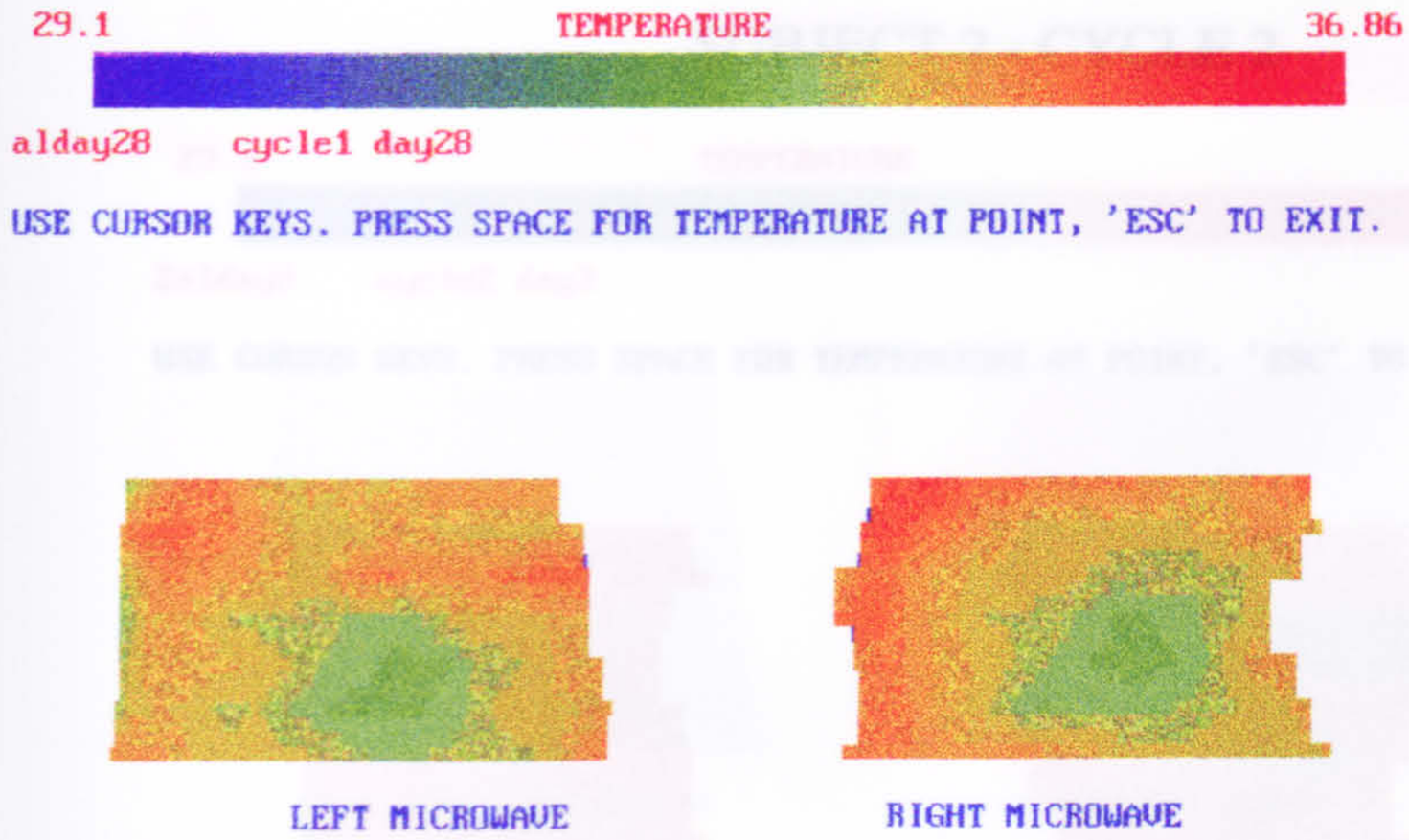

Fig. B7 Microwave breast thermogram, Subject 2, Cycle 1, Day 28

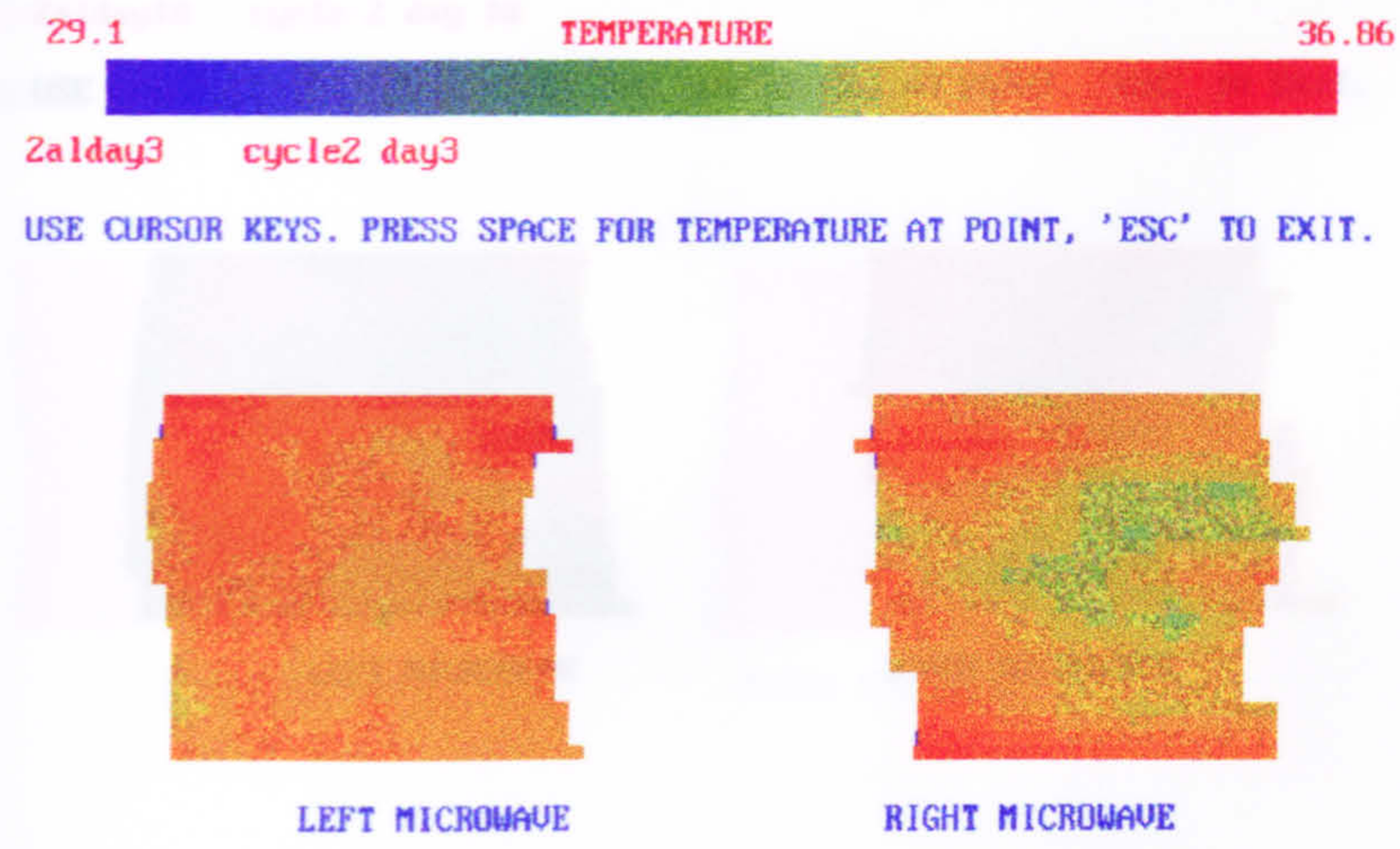

Fig. B8 Microwave breast thermogram, Subject 2, Cycle 2, Day 3

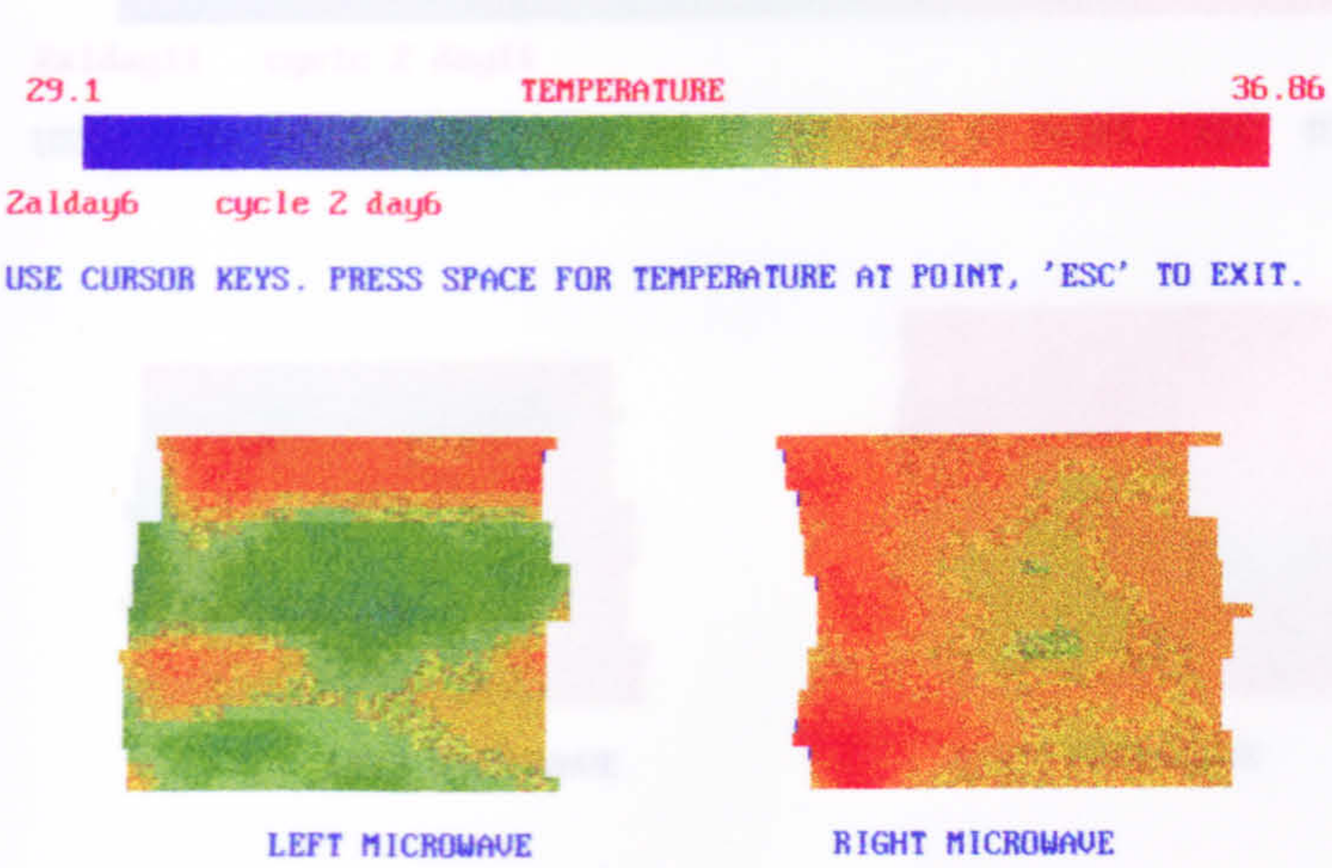

Fig. B9 Microwave breast thermogram, Subject2, Cycle 2, Day 6

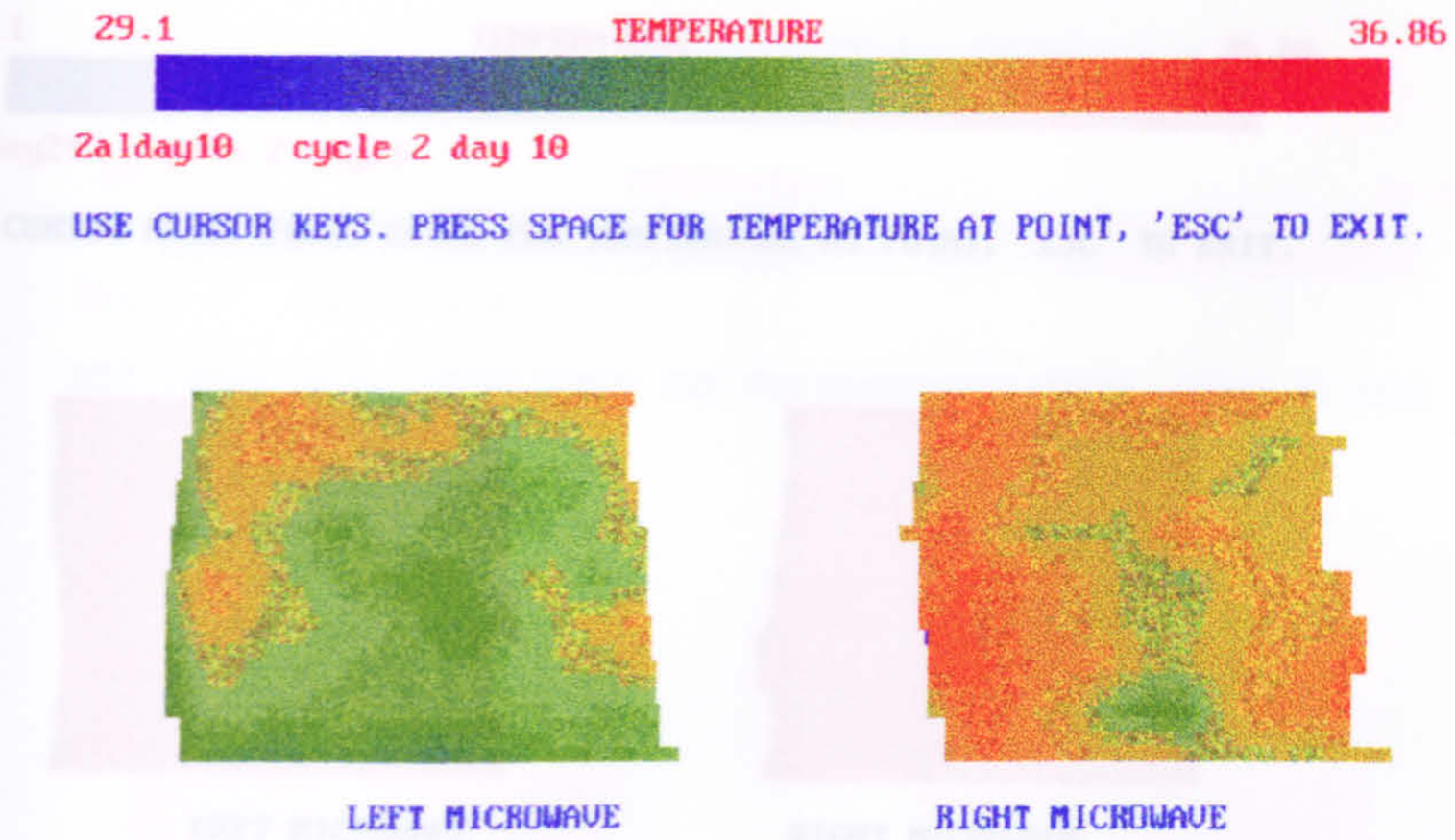

Fig. B10 Microwave breast thermogram, Subject 2, Cycle 2, Day 10

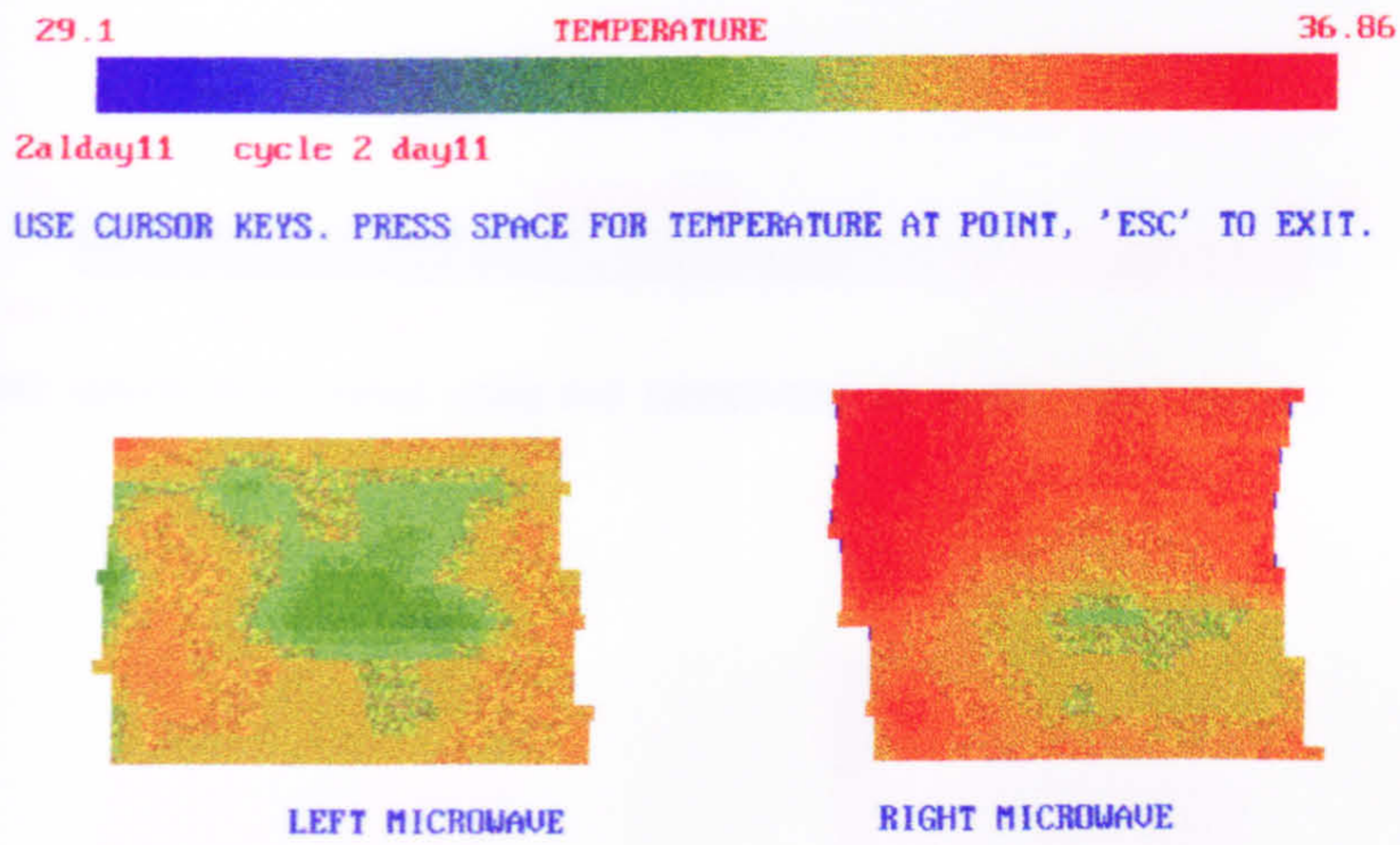

Fig. B11 Microwave breast thermogram, Subject 2, Cycle 2, Day 11

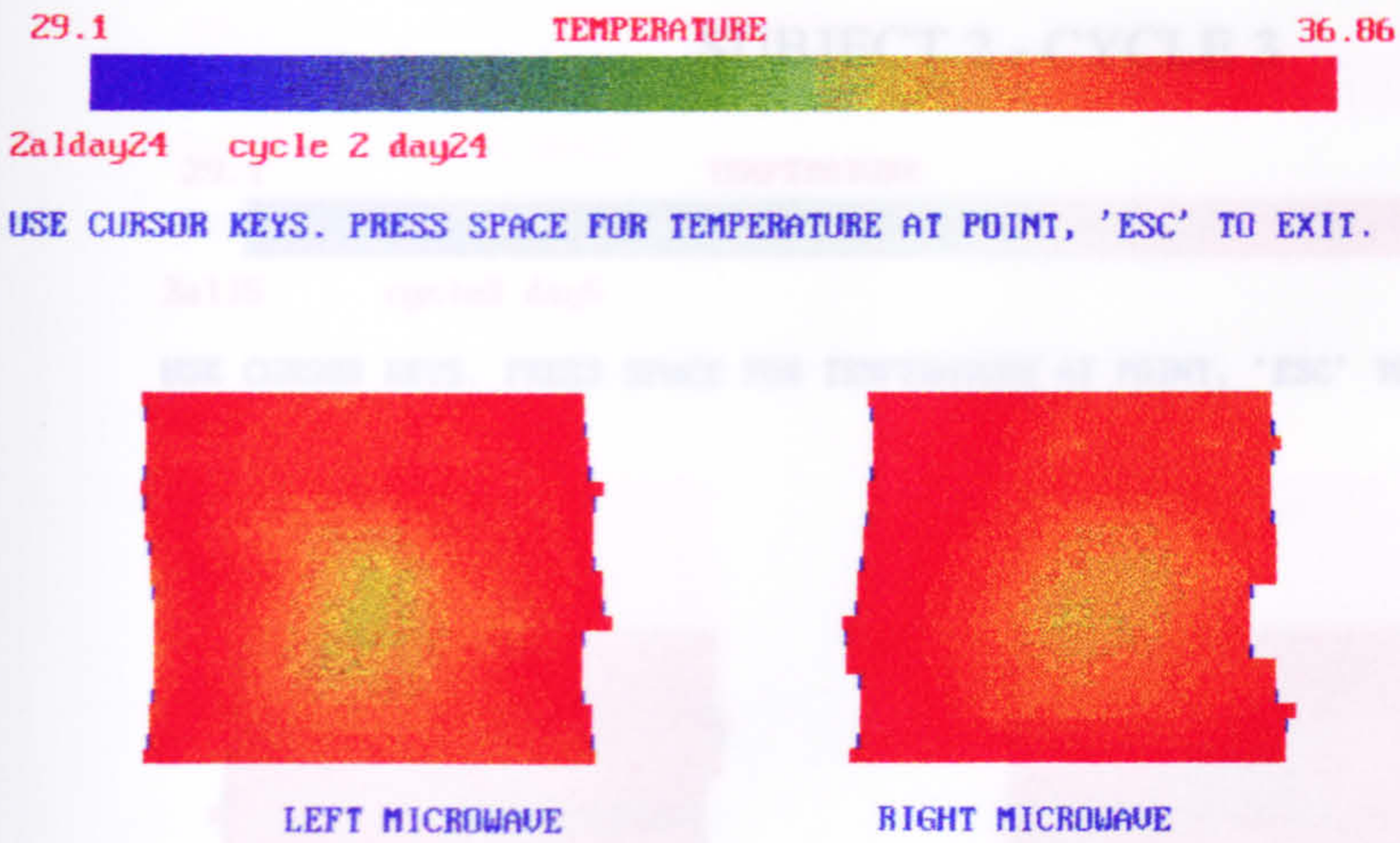

Fig. B12 Microwave breast thermogram, Subject 2, Cycle 2, Day 24

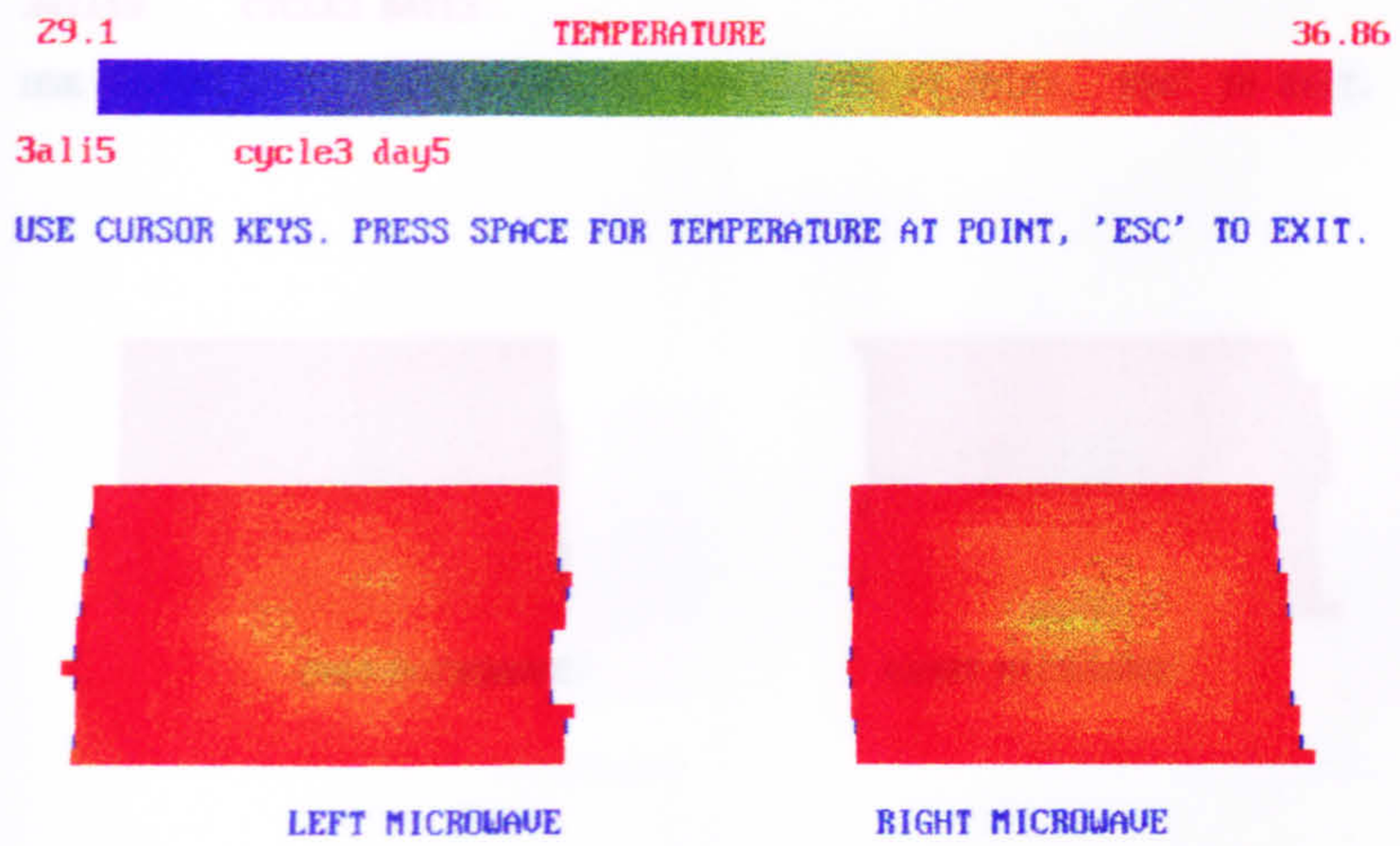

Fig. B13 Microwave breast thermogram, Subject 2, Cycle 3, Day 5

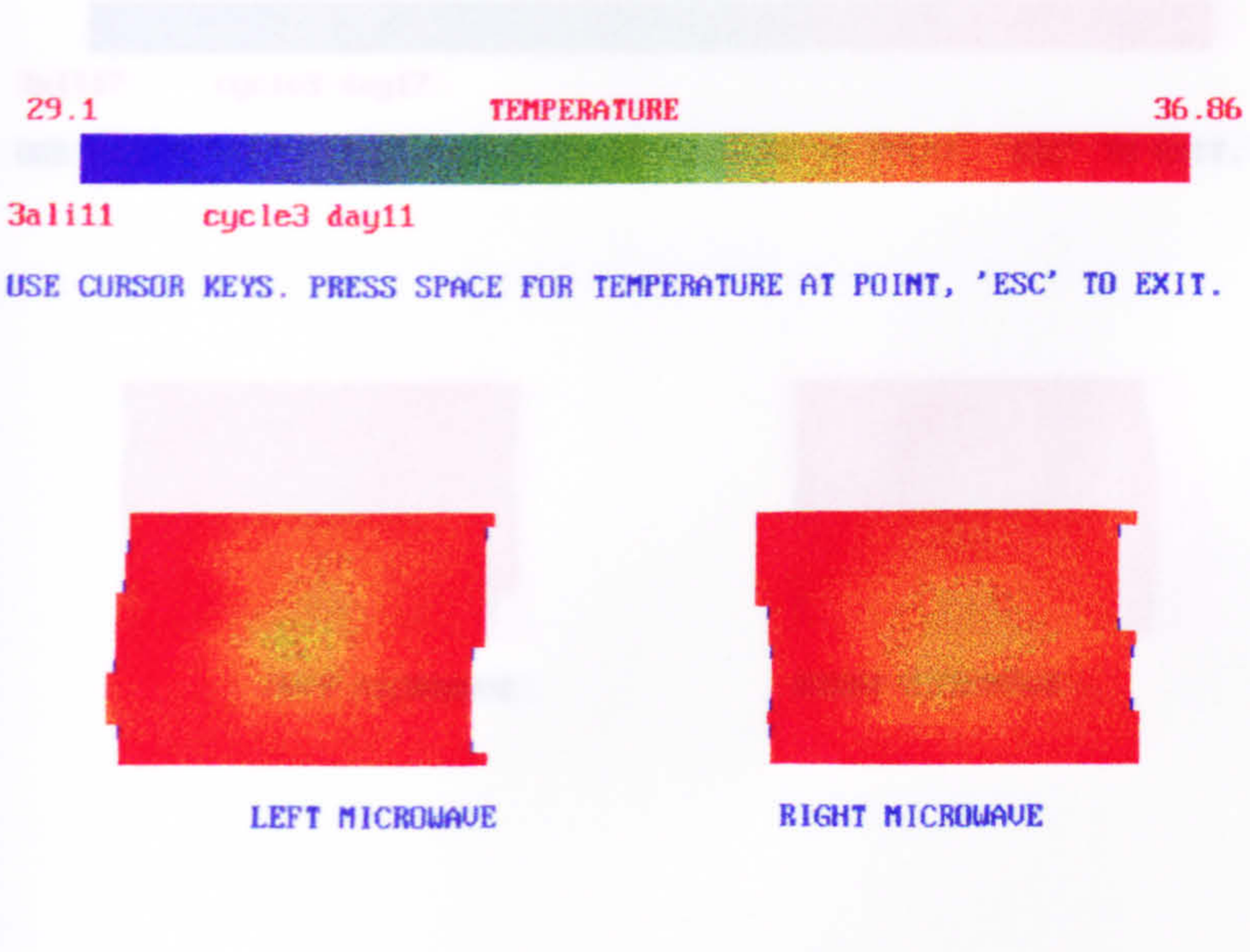

Fig. B14 Microwave breast thermogram, Subject 2, Cycle 3, Day 11

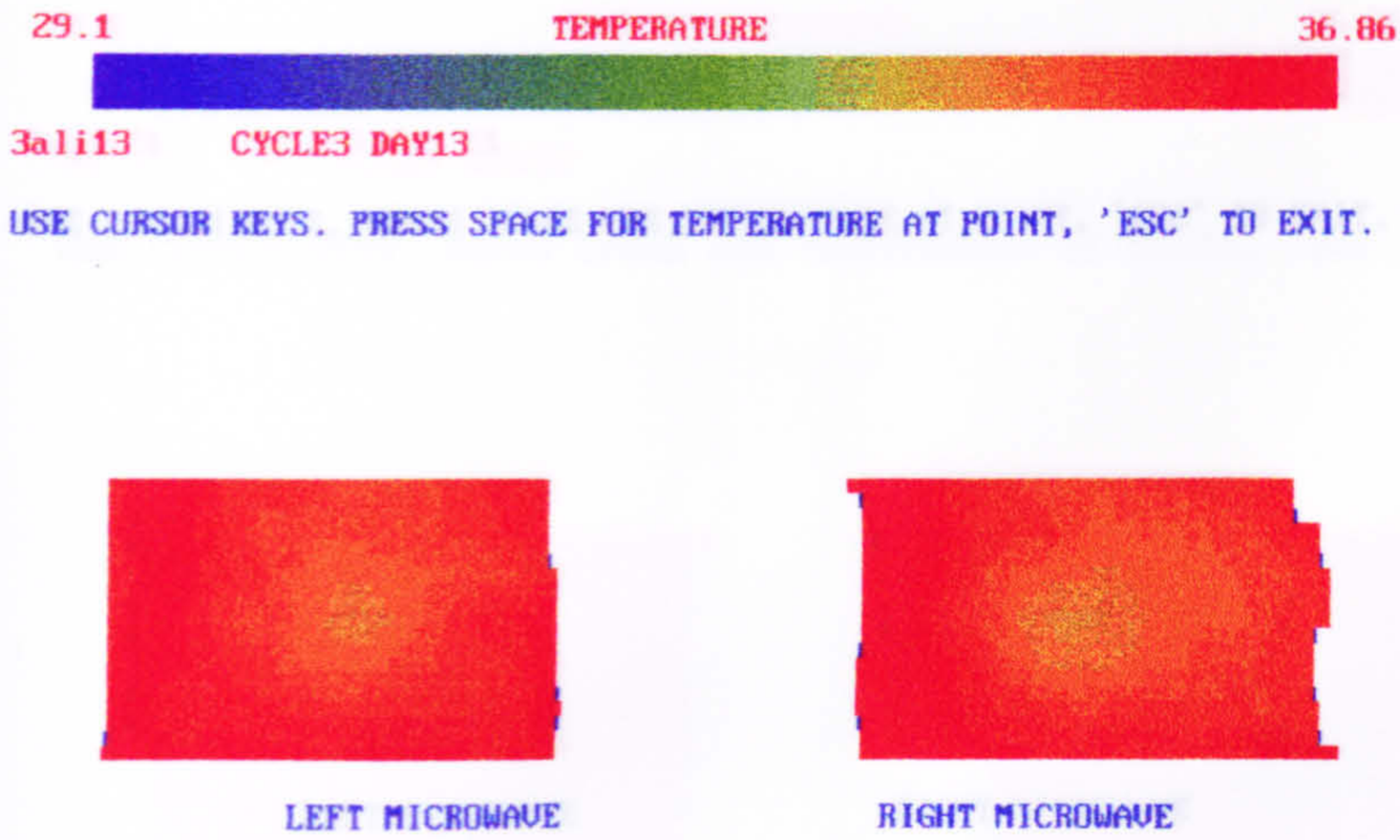

Fig. B15 Microwave breast thermogram, Subject 2, Cycle 3, Day 13

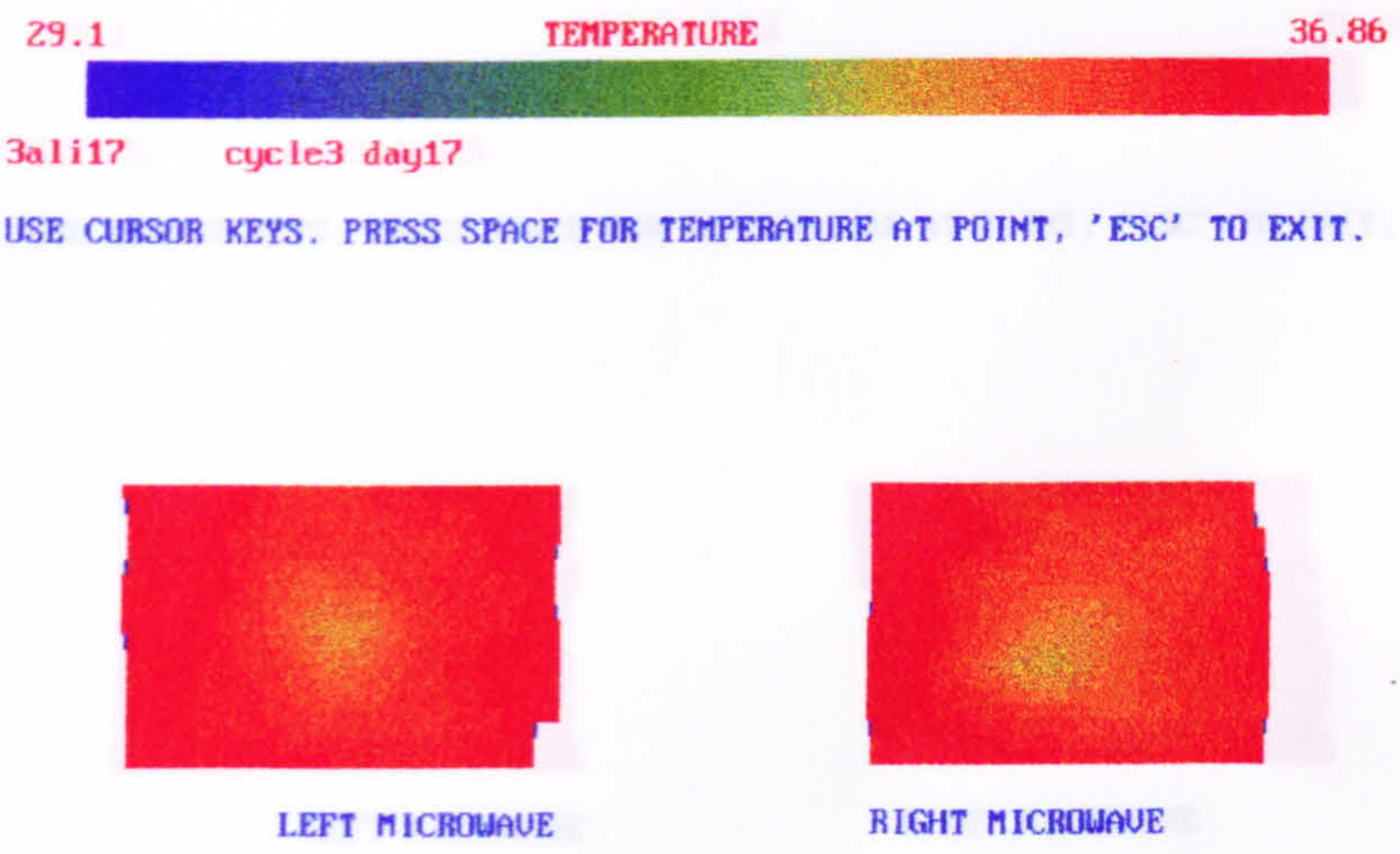

Fig. B16 Microwave breast thermogram, Subject 2, Cycle 3, Day 17

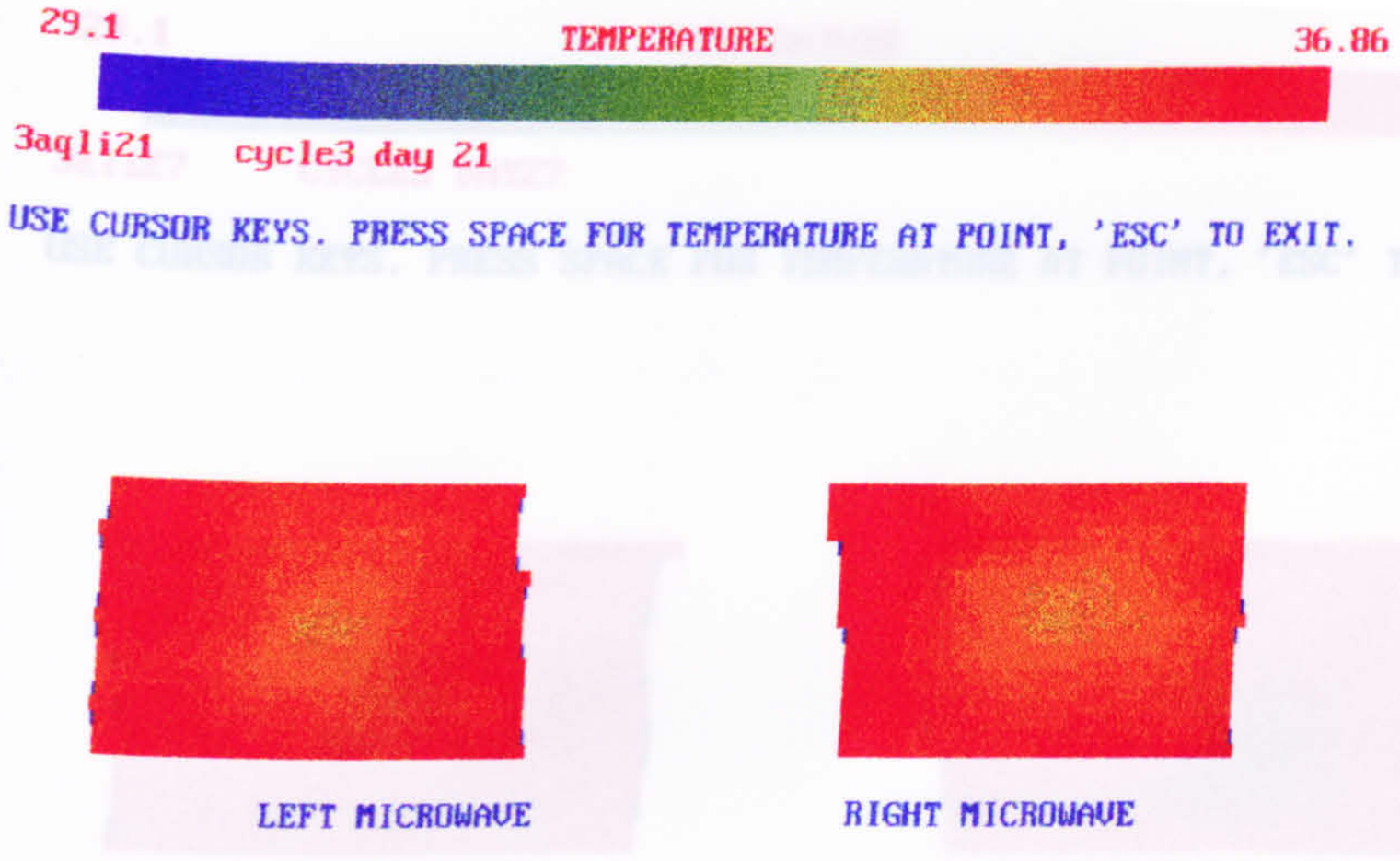

Fig. B17 Microwave breast thermogram, Subject 2, Cycle 3, Day 21

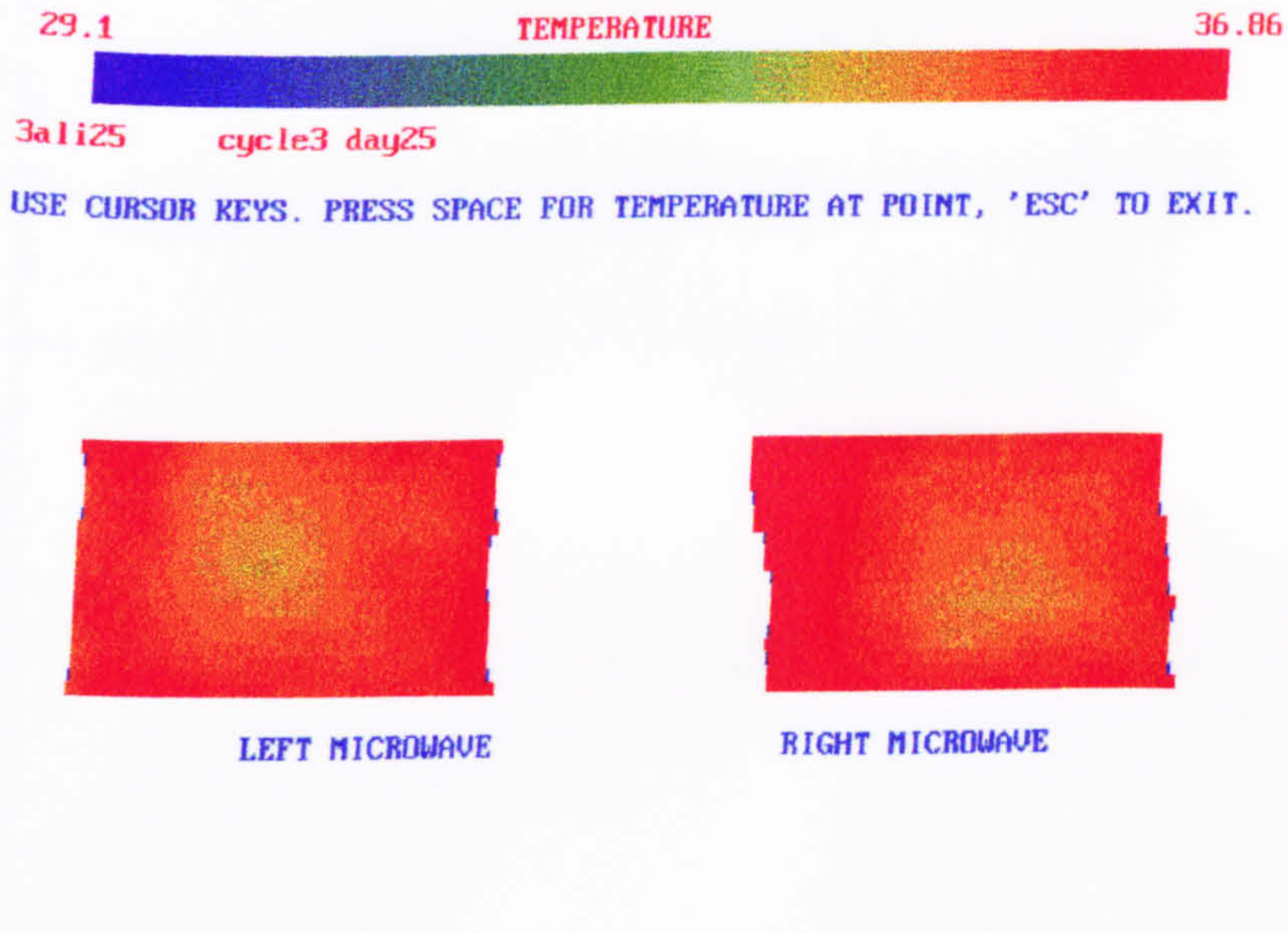

Fig. B18 Microwave breast thermogram, Subject 2, Cycle 3, Day 25

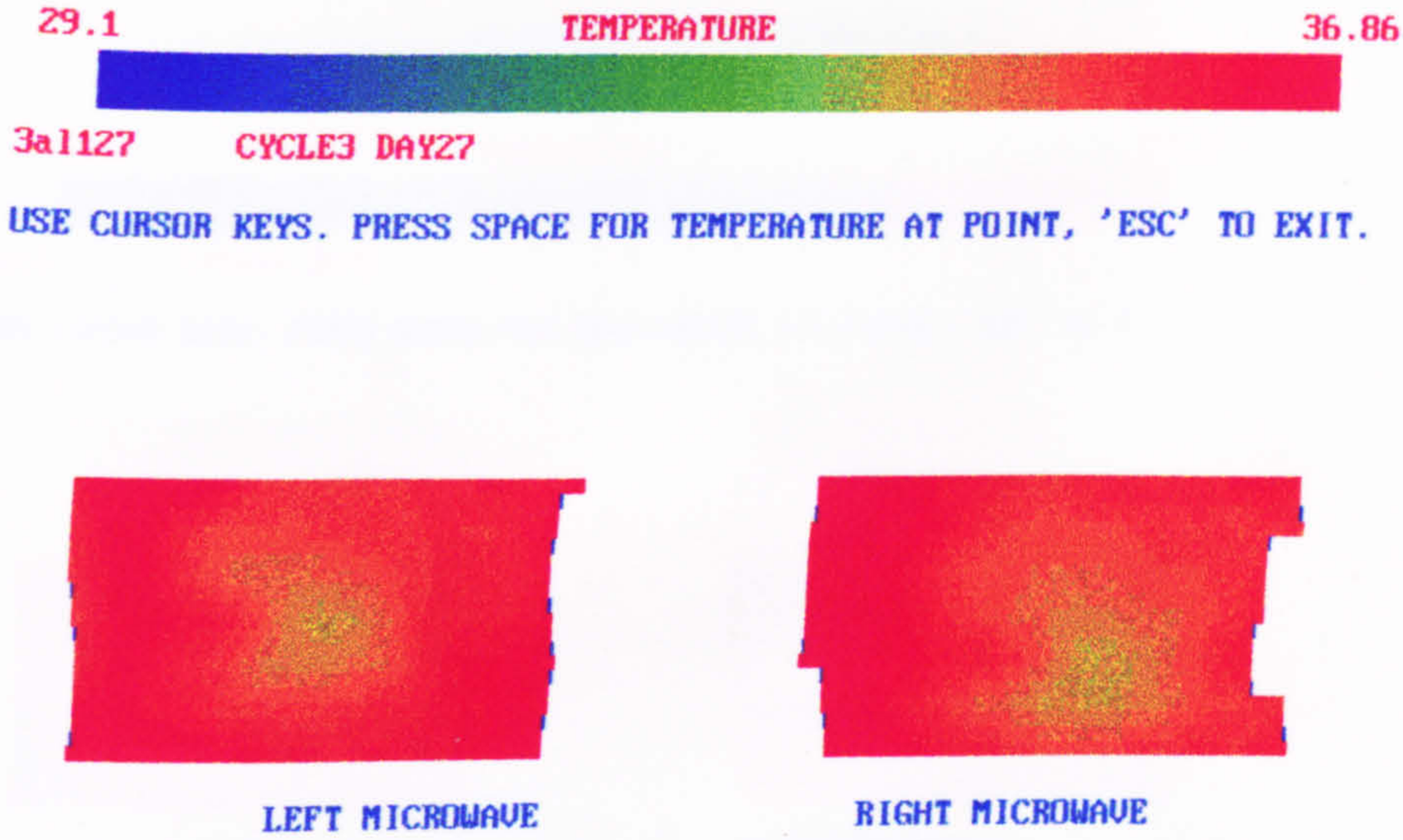

Fig. B19 Microwave breast thermogram, Subject 2, Cycle 3, Day 27

APPENDIX A.2

Menstrual thermograms, Subject 3.

SUBJECT 3 - CYCLE 2

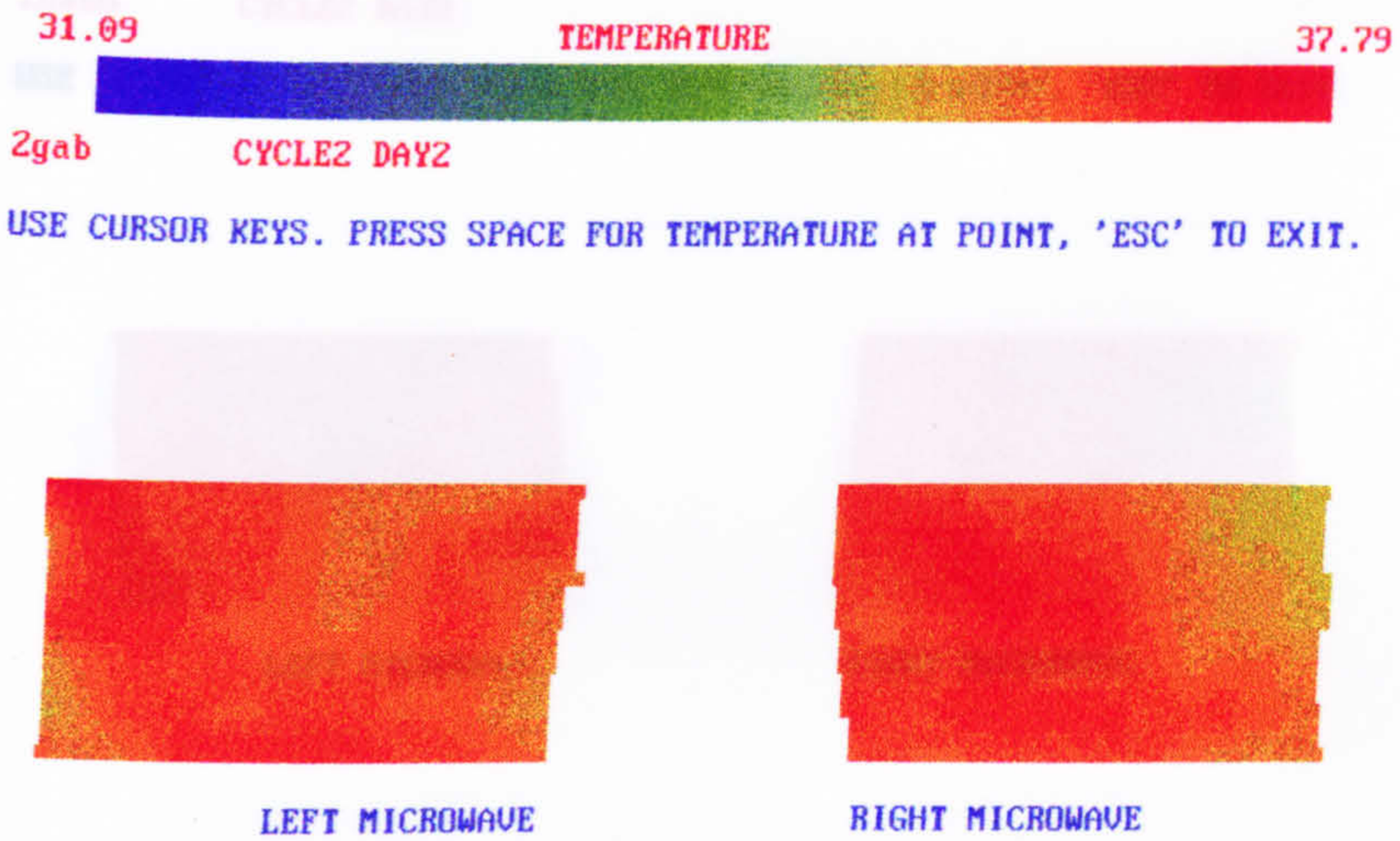

Fig. C1 Microwave breast thermogram, Subject 3, Cycle 2, Day 2

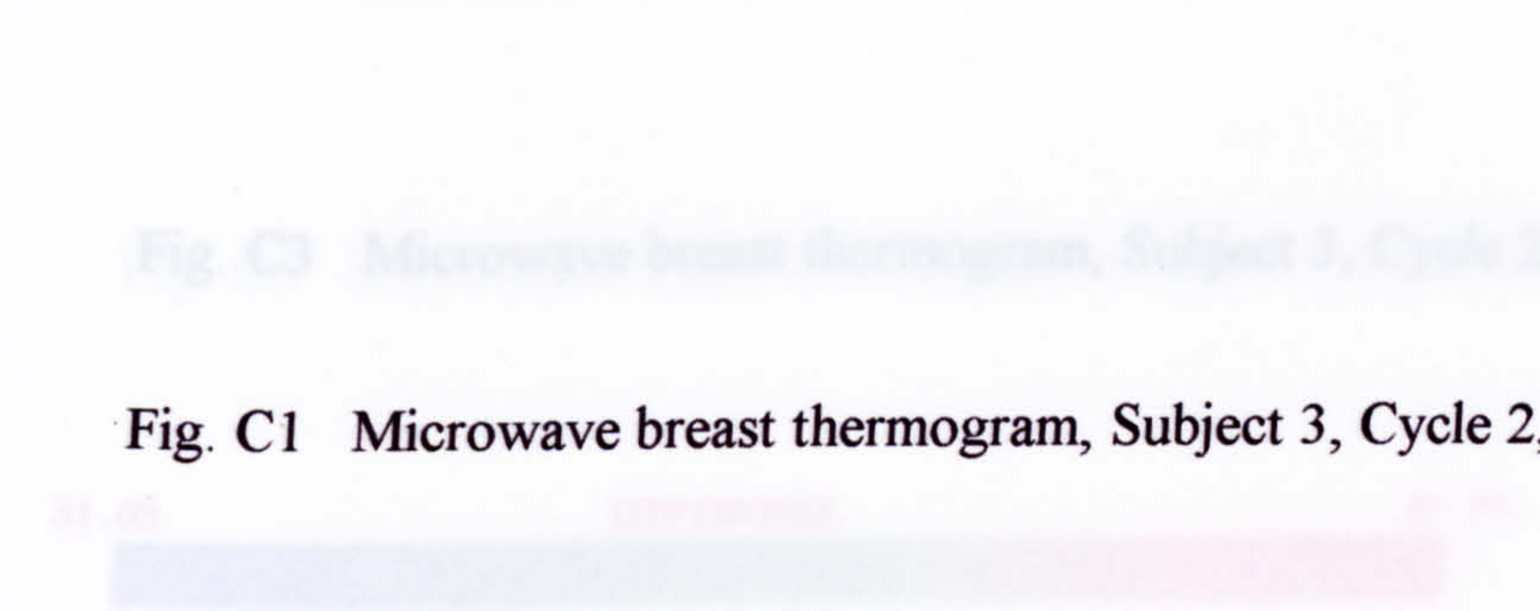

Fig. C2 Microwave breast thermogram, Subject 3, Cycle 2, Day 4

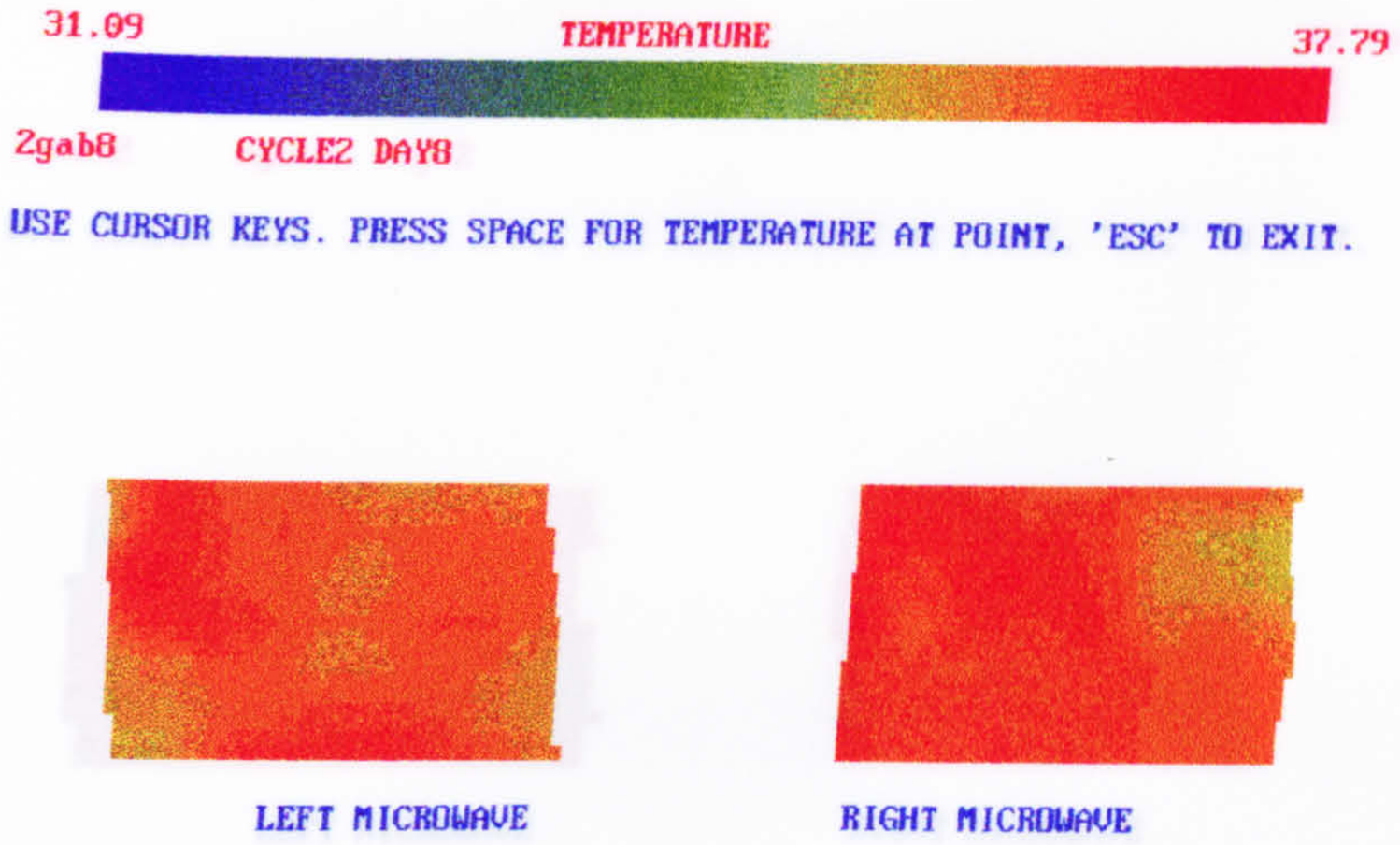

Fig. C3 Microwave breast thermogram, Subject 3, Cycle 2, Day 8

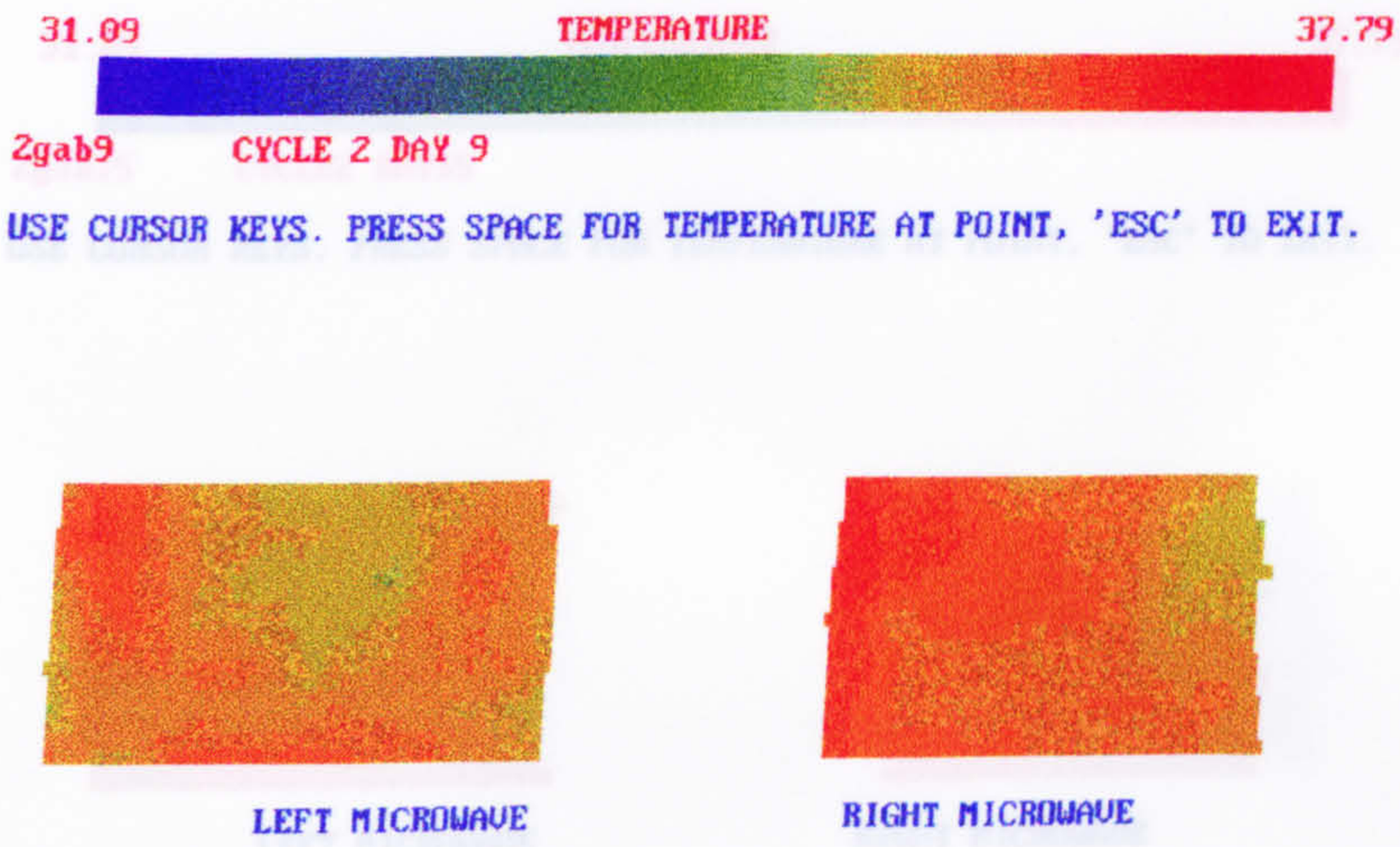

Fig. C4 Microwave breast thermogram, Subject 3, Cycle 2, Day 9

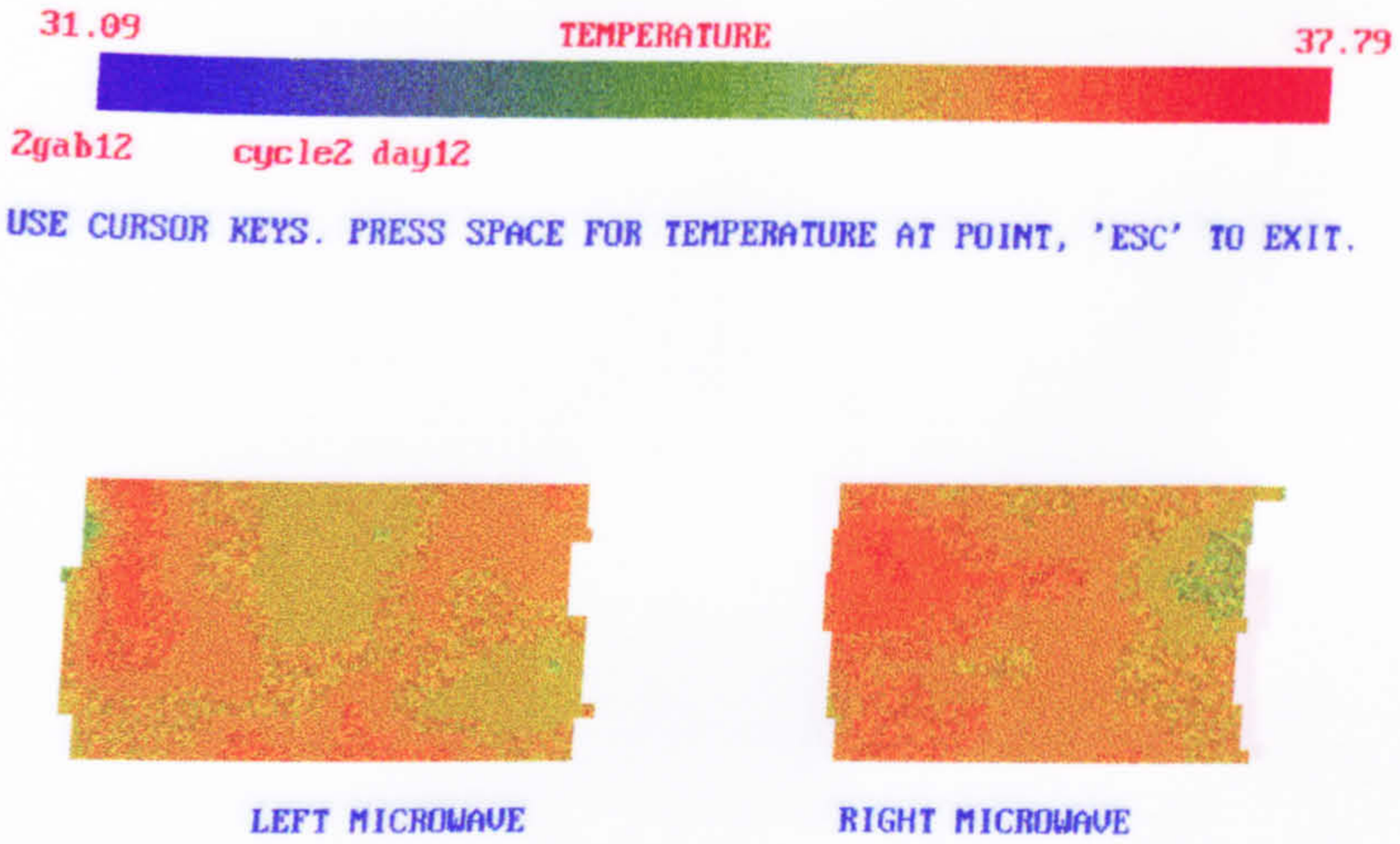

Fig. C5 Microwave breast thermogram, Subject 3, Cycle 2, Day 12

Fig. C6 Microwave breast thermogram, Subject 3, Cycle 2, Day 15

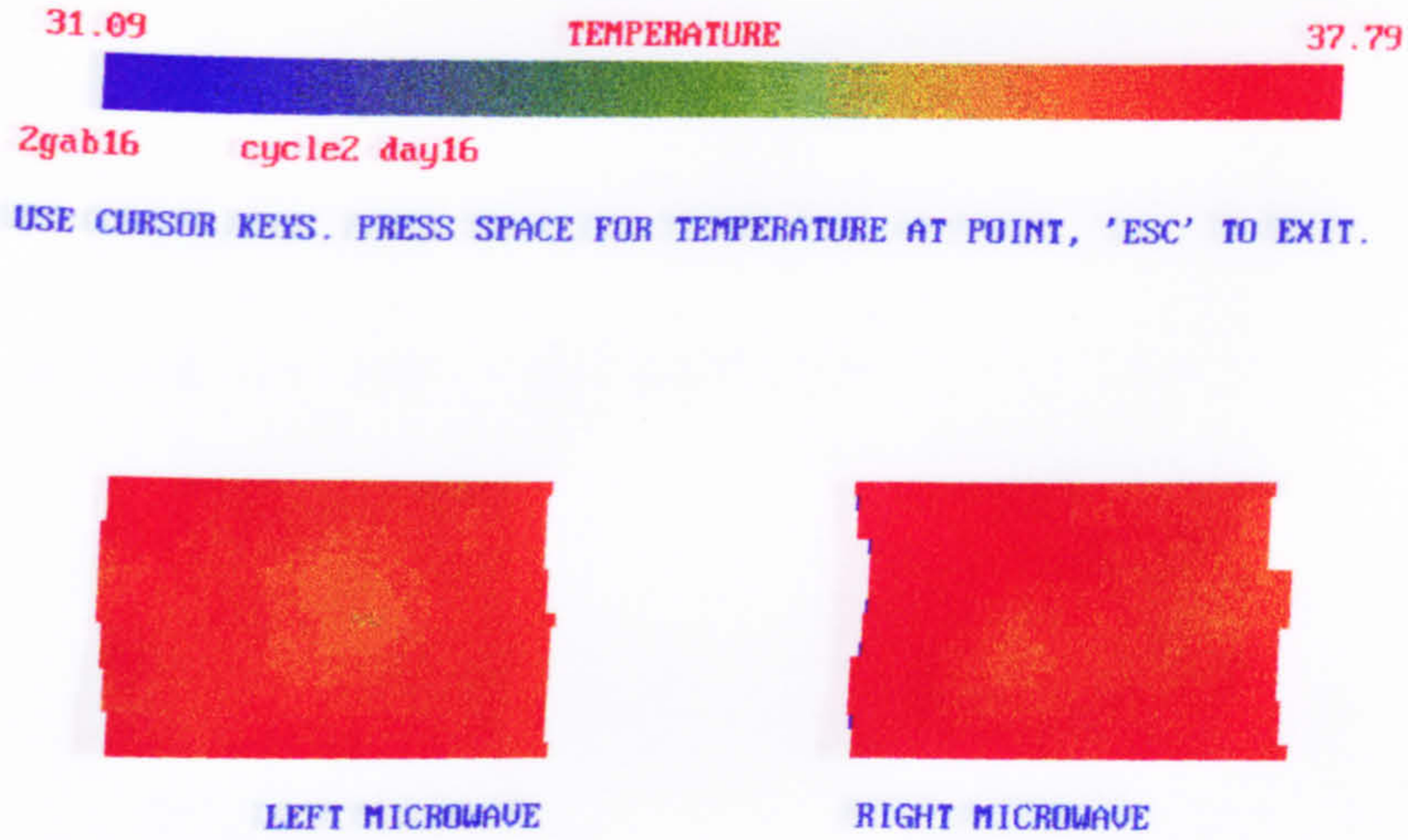

Fig. C7 Microwave breast thermogram, Subject 3, Cycle 2, Day 16

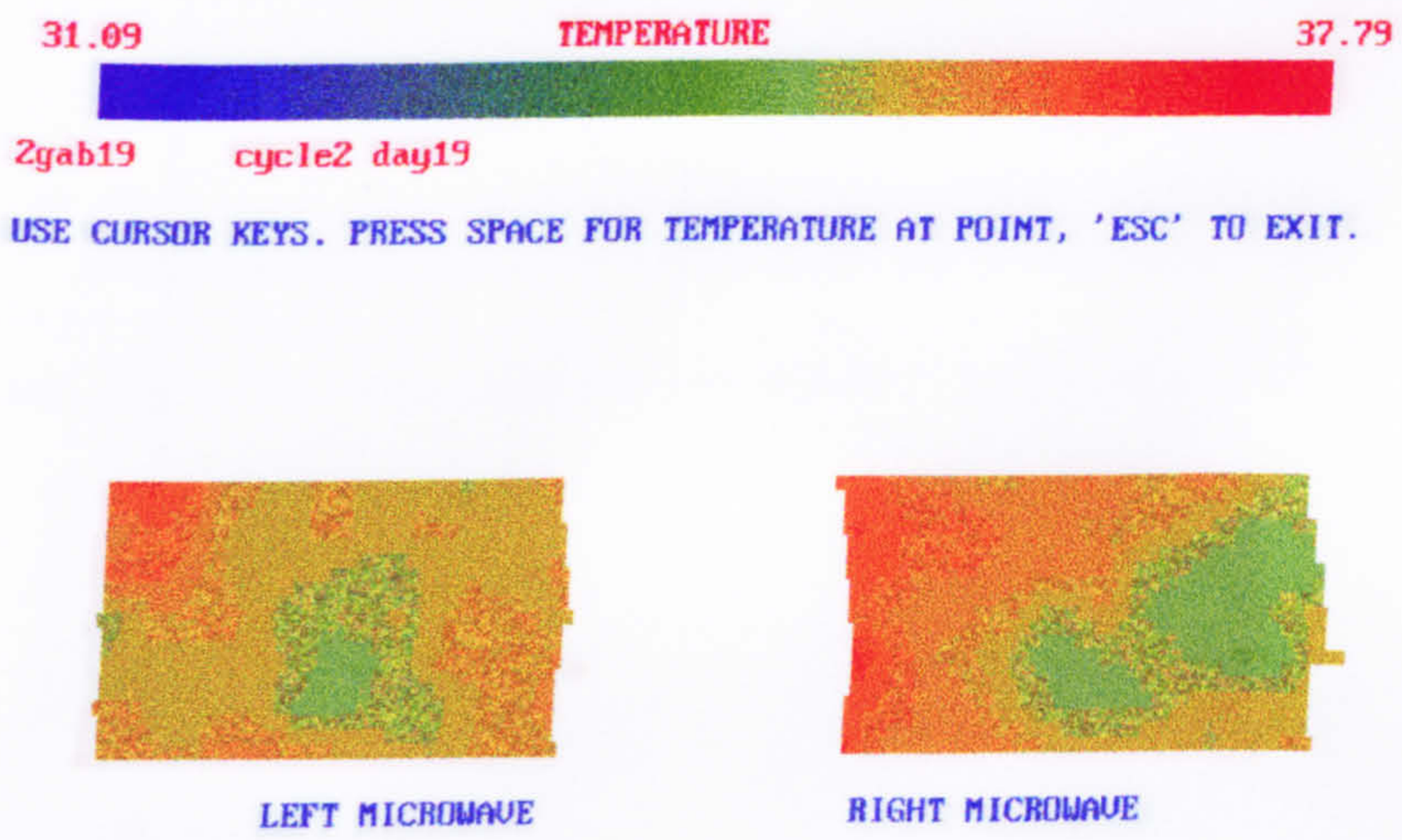

Fig. C8 Microwave breast thermogram, Subject 3, Cycle 2, Day 19

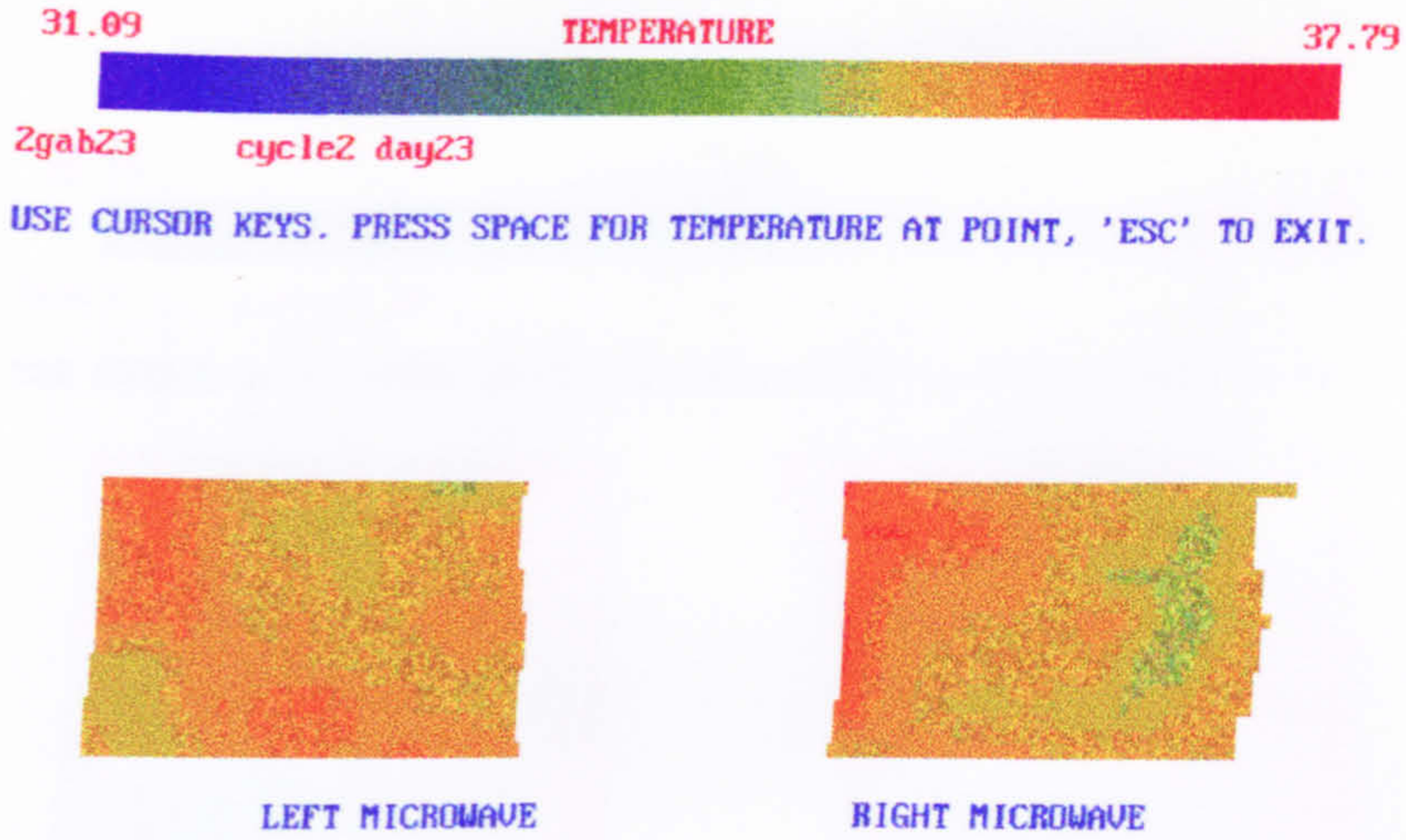

Fig. C9 Microwave breast thermogram, Subject 3, Cycle 2, Day 23

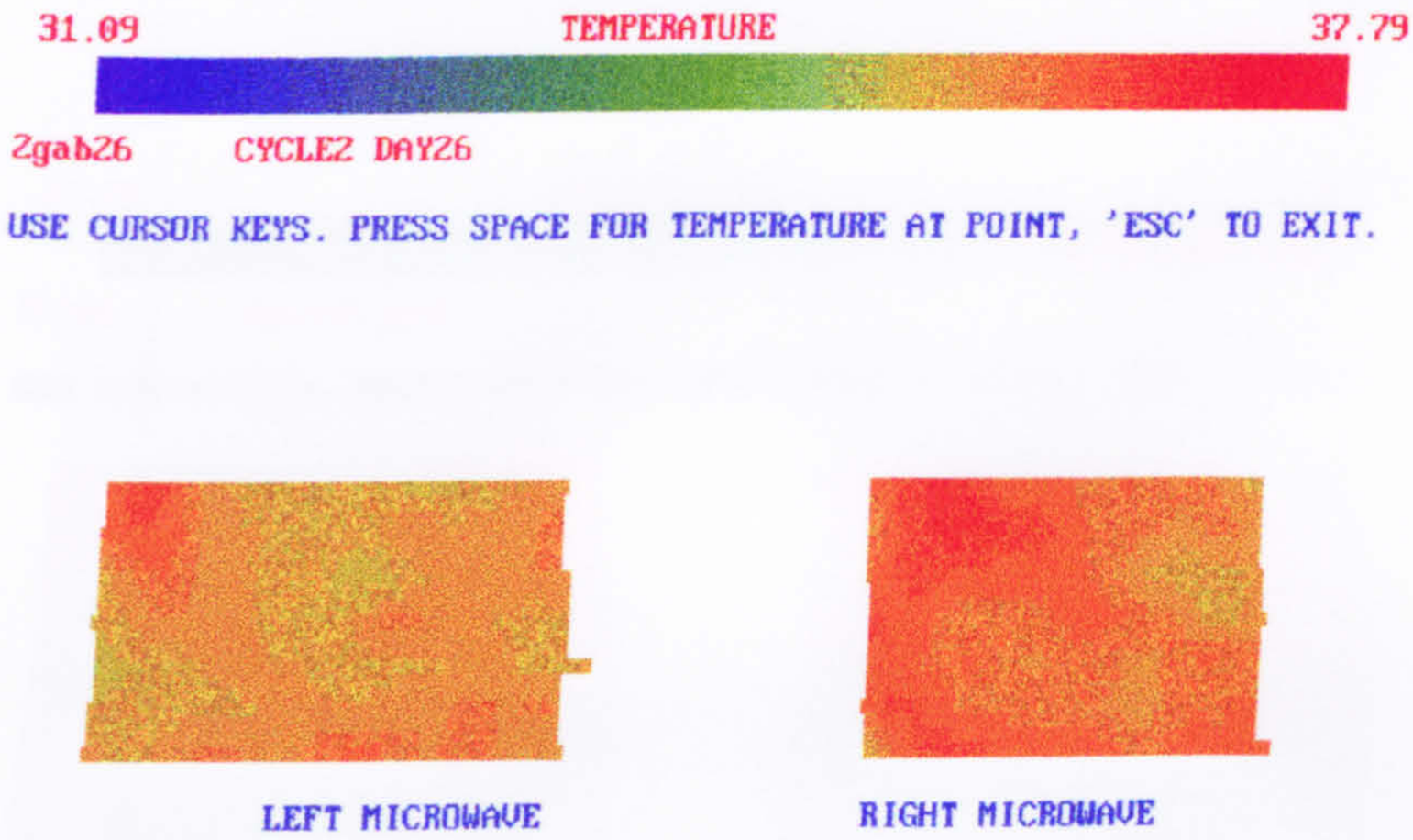

Fig. C10 Microwave breast thermogram, Subject 3, Cycle 2, Day 26

APPENDIX A.3

Menstrual thermograms, Subject 4.

SUBJECT 4 - CYCLE 2

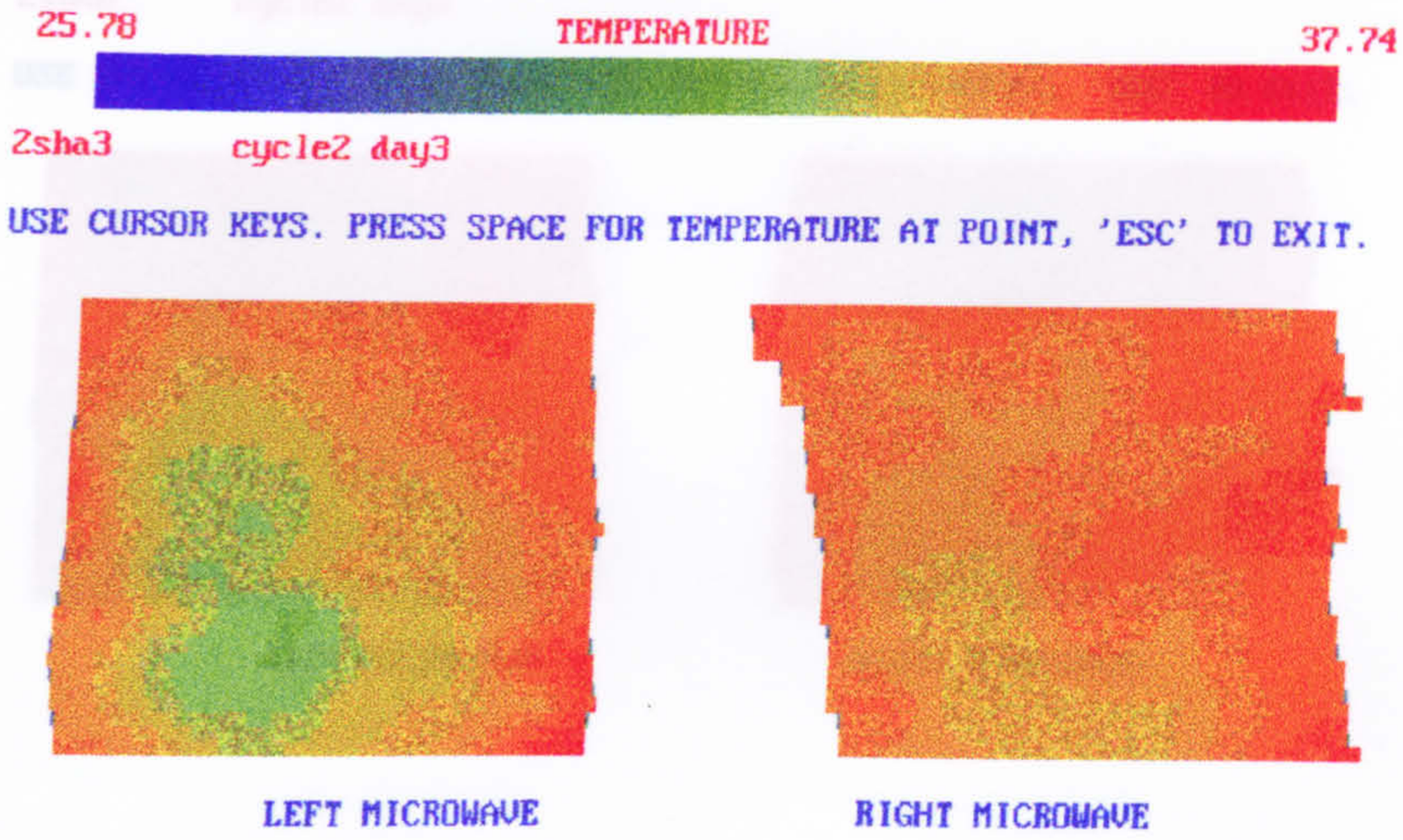

Fig. D1 Microwave breast thermogram, Subject 4, Cycle 2, Day 3

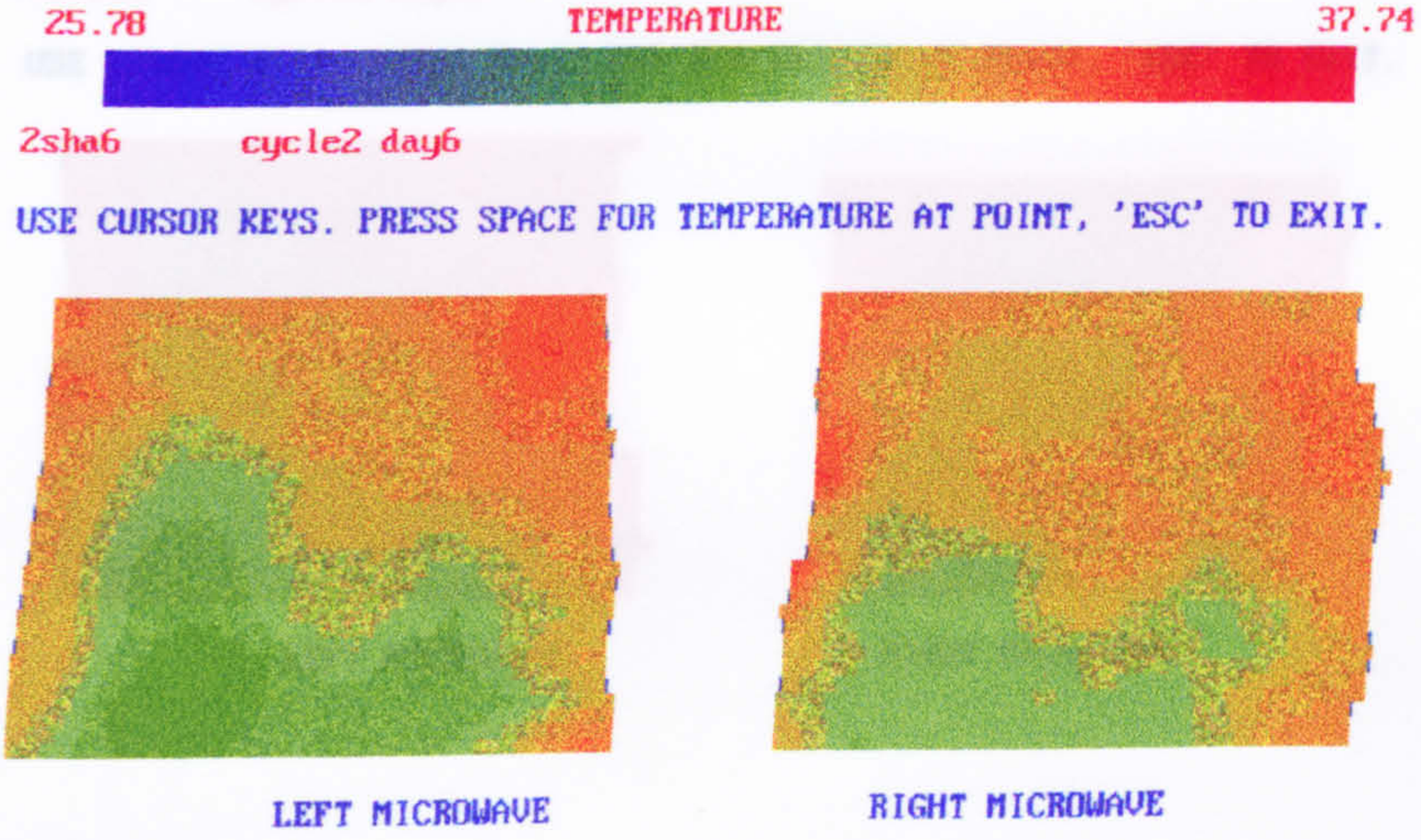

Fig. D2 Microwave breast thermogram, Subject 4, Cycle 2, Day 6

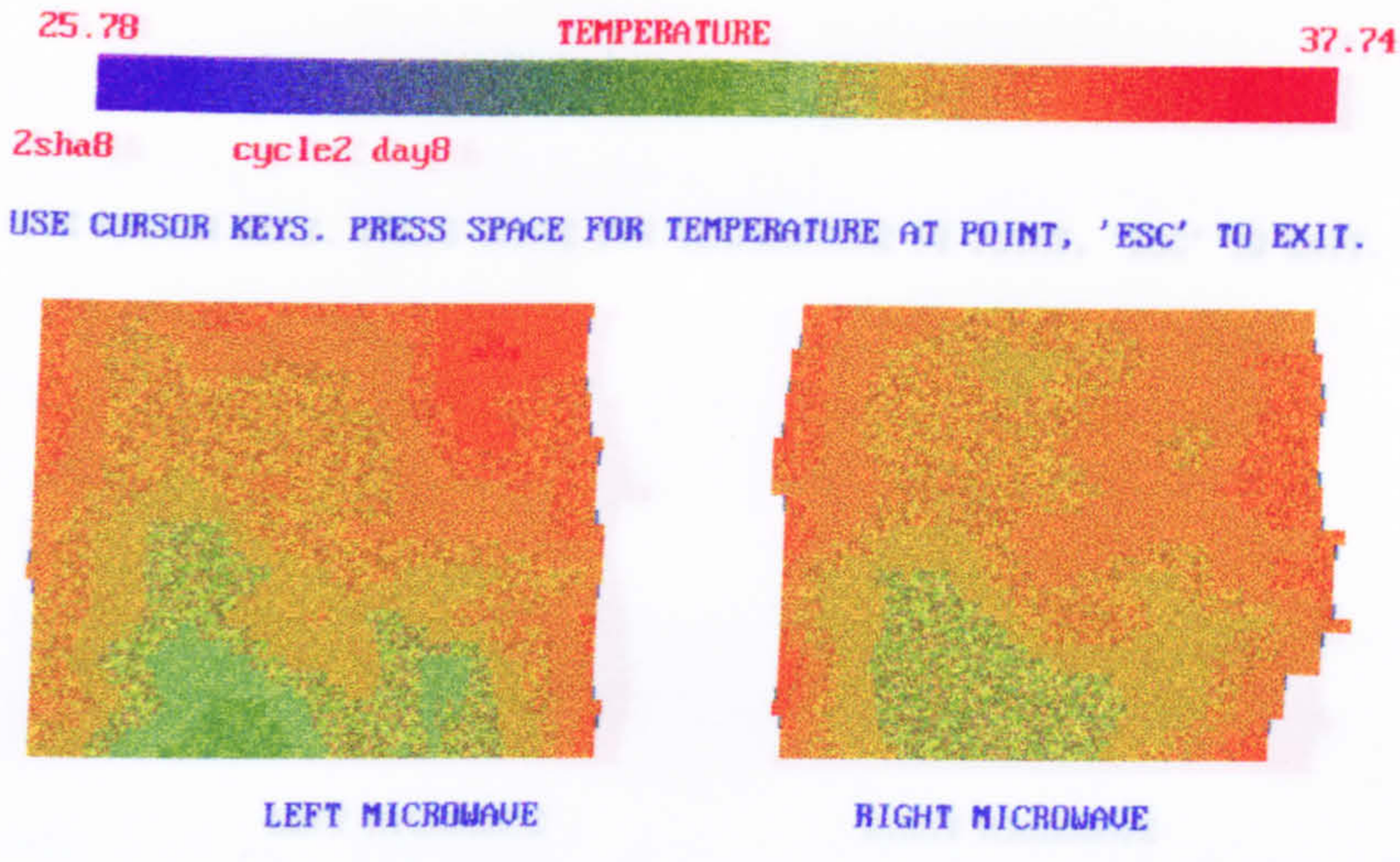

Fig. D3 Microwave breast thermogram, Subject 4, Cycle 2, Day 8

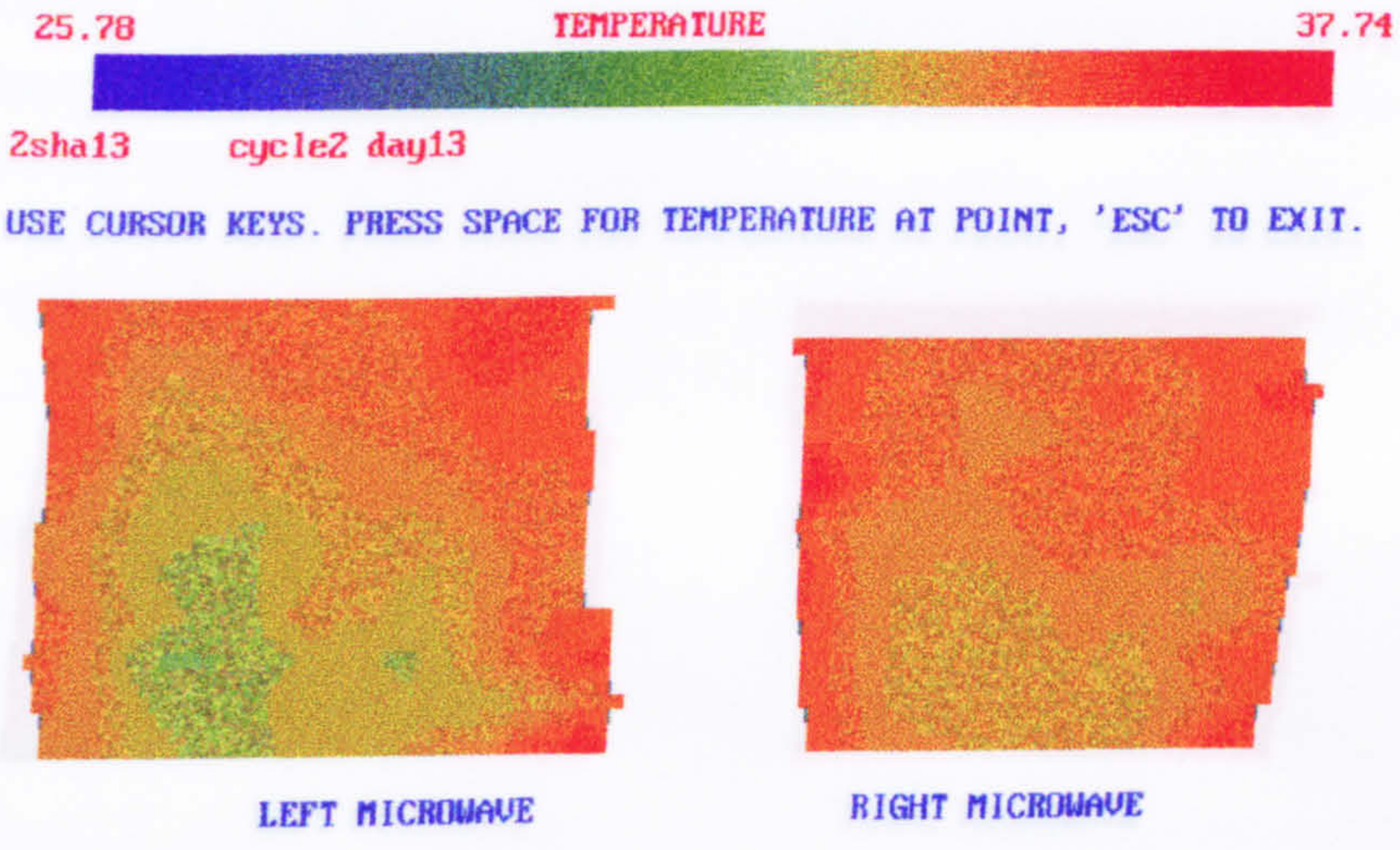

Fig. D4 Microwave breast thermogram, Subject 4, Cycle 2, Day 13

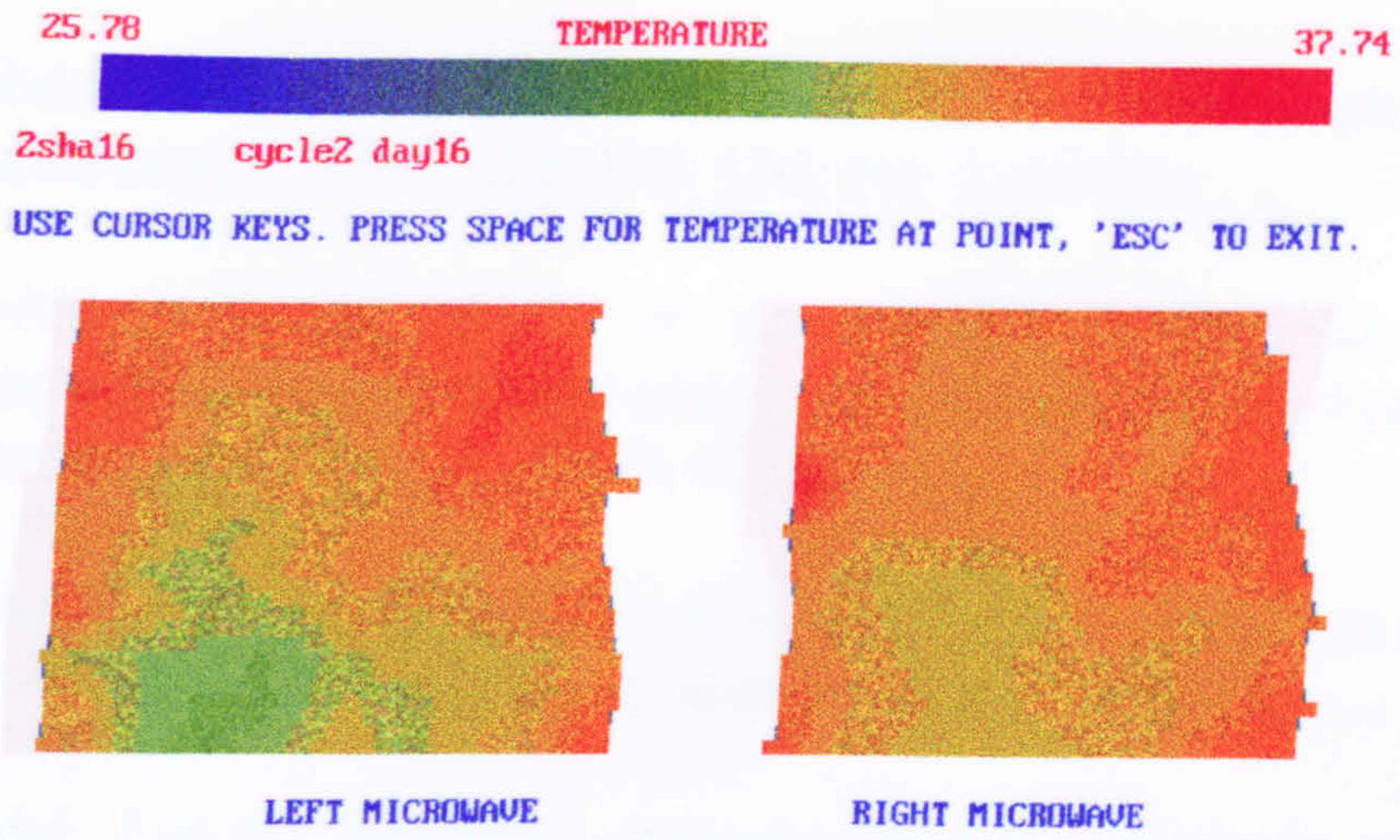

Fig. D5 Microwave breast thermogram, Subject 4, Cycle 2, Day 16

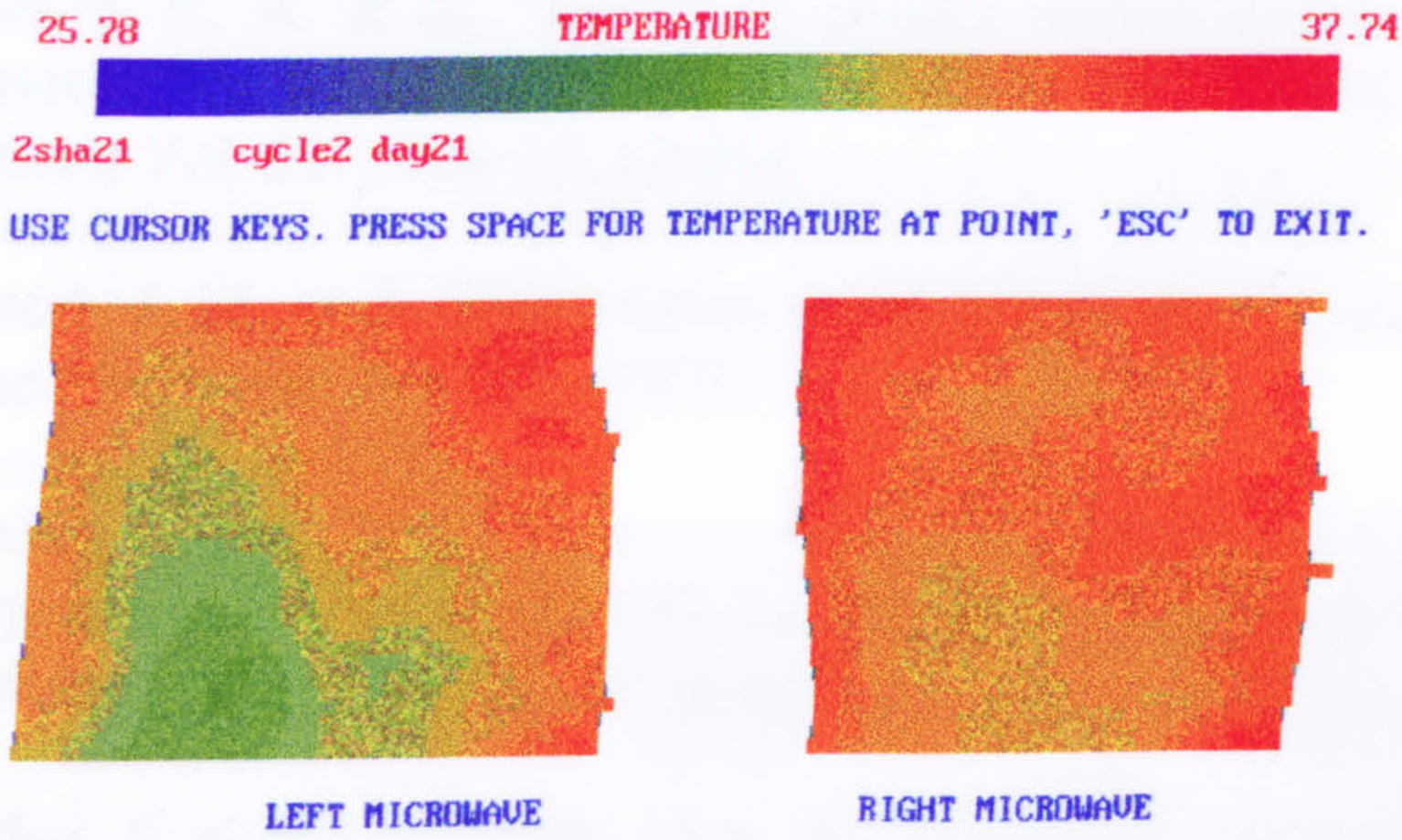

Fig. D6 Microwave breast thermogram, Subject 4, Cycle 2, Day 21

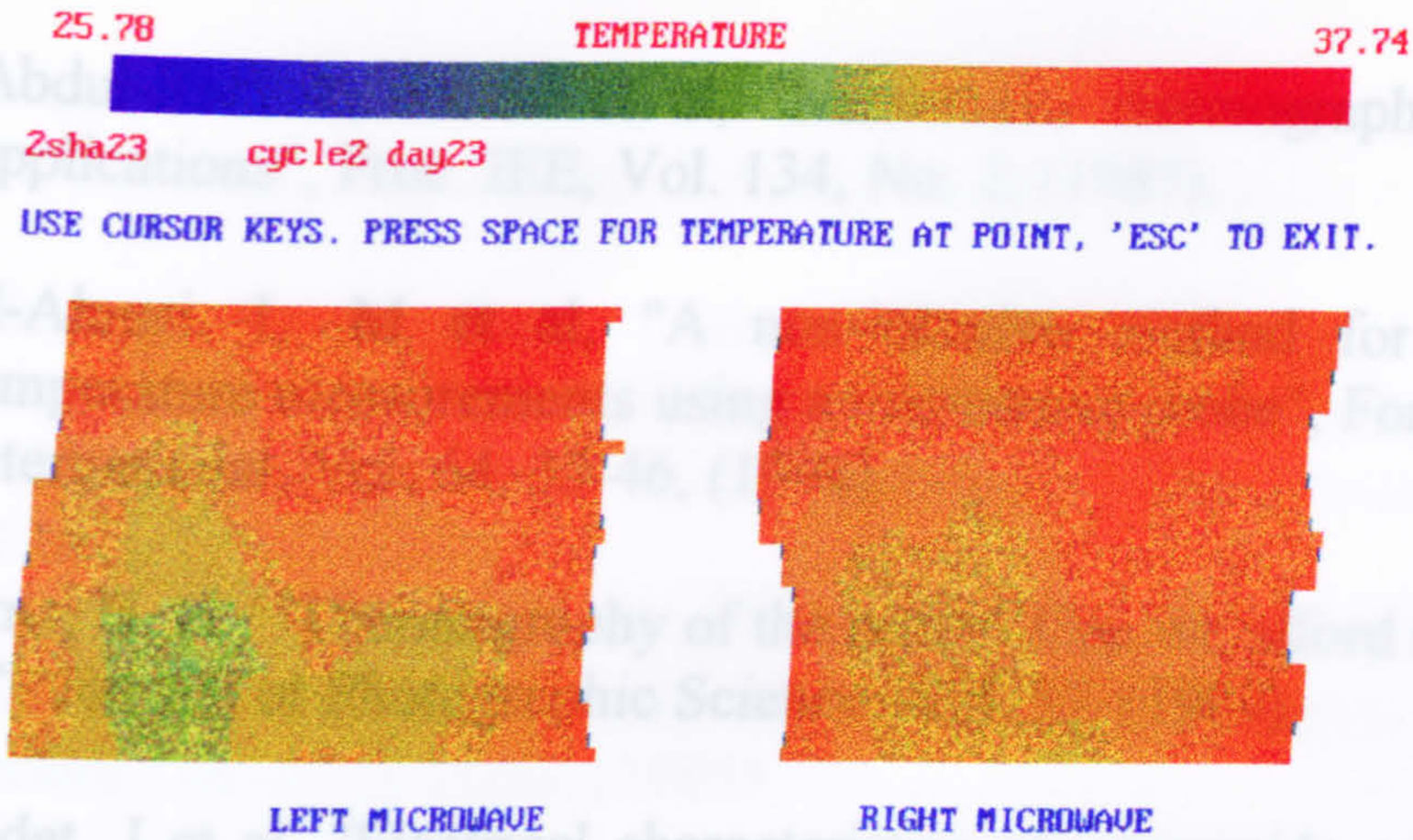

Fig. D7 Microwave breast thermogram, Subject 4, Cycle 2, Day 23

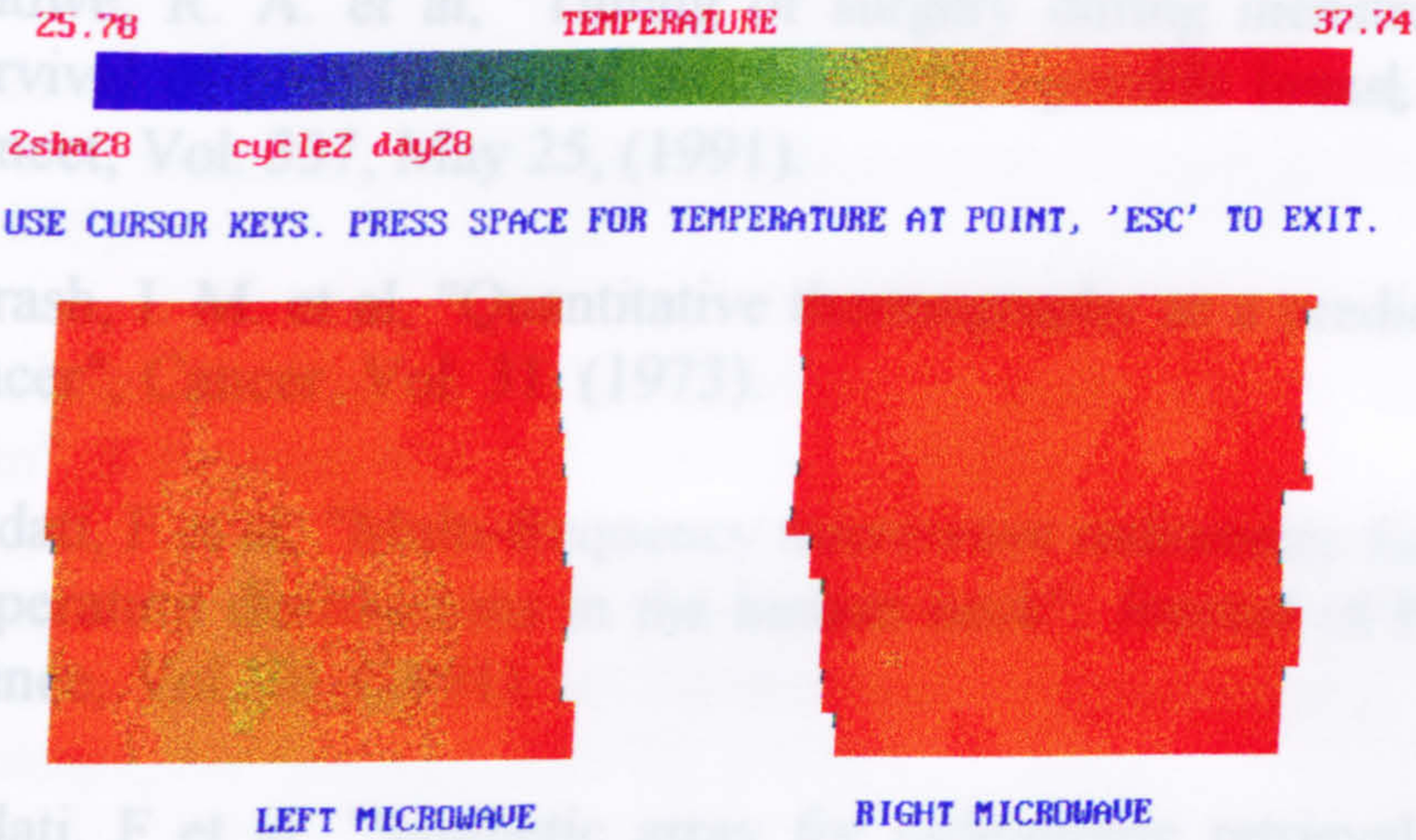

Fig. D8 Microwave breast thermogram, Subject 4, Cycle 2, Day 28

Abdul-Razzak, M. M et al, "Microwave thermography for medical applications", Proc. IEE, Vol. 134, No. 2, (1987).

al-Alousi, L. M et al, "A non-invasive method for post-mortem temperature measurements using a microwave probe", Forensic Science International, Vol. 64, 35-46, (1994).

Arns, H. H., "Thermography of the breast- Can we afford to do without it?", Journal of Photographic Science, Vol. 37, (1989).

Audet, J et al, "Electrical characteristics of waveguide applicators for medical applications", Journal of Microwave Power, Vol. 15, No. 3, (1980).

Backstrom, T & Cartensen, H., "Estrogen and progesterone in plasma in relation to premenstrual tension", Journal of Steroid Biochemistry, Vol. 5, (1974).

Badwe, R. A. et al, "Timing of surgery during menstrual cycle and survival of premenopausal womem with operable breast cancer", The Lancet, Vol. 337, May 25, (1991).

Barash, I. M. et al, "Quantitative thermography as a predictor of breast cancer", Cancer, Vol. 31, (1973).

Bardati, F et al, "Multi-frequency microwave radiometry for retrieval of temperature distributions in the human neck", Journal of Photographic Science, Vol. 39, (1991).

Bardati, F et al, "Synthetic array for radiometric retrieval of thermal fields in tissues", IEEE Trans. Microwave Theory & Techniques, Vol. 34, No. 5, (1986).

Bardati, F. & Domenico, S., "On the emissivity of layered materials", IEE Trans, Geoscience and Remote Sensing, Vol. 22, No. 4, (1984).

Barret, A. H et al, "Microwave thermography in the detection of breast cancer", Amer. J. Roent., Vol. 134, 365-368, (1980).

Basset, L. W & Gambhir, S., "Breast imaging for the 1990's", Seminars in Oncology, Vol. 18, No. 2(April), 80-86, (1991).

Beaney, R. P et al, "Positron emission tomography for in-vivo measurement of regional blood flow, oxygen utilization, and blood volume in patients with breast carcinoma", The Lancet, 1, 131-134, (1984).

Bleaney, B. I & Bleaney, B, "*Electricity and magnetism*", 3rd edition, Oxford University Press, (1985).

Bocquet, B et al, "Visibility of local thermal structures and temperature retrieval by microwave radiometry", Electronics Letters, Vol. 22, No. 3, (1986).

Bowman, H. F. et al, "Theory, measurement, and application of thermal properties of biomaterials", Annual Review of Biophysics & Bioengineering, Vol. 4, (1975).

Bowman, R. R, "A probe for measuring temperature in radio-frequency heated material", IEEE Trans. Microwave Theory & Techniques, Jan. (1976).

Brebner, D. F et al, "The diffusion of water vapour through human skin", J. Physiol. Vol.132, 225-231, (1956).

Broquetas, A et al, "Active microwave computed tomography cylindrical scanner for biomedical applications", Journal of Photographic Science, Vol. 37, (1989).

Brown, V. J., "Development of combined modelling techniques for microwave thermography", PhD thesis, (1989).

Buettner, K. "Diffusion of water through human skin", J. Appl. Physiol., Vol. 6, 299-241, (1953).

Burn, I., "The diagnosis and treatment of early breast cancer", The Practioner, Vol. 228, (1984).

Campbell, A., "Measurements and analysis of the microwave dielectric properties of tissue", PhD Thesis, Universtity of Glasgow, (1990).

Campbell, A & Land, D. V, "Dielectric properties of female human breast tissue measured in vitro at 3.2 GHz", Phys. Med. Biol., Vol. 37, No.1, (1992).

Carr, K. L, "Thermography", 2746-2759, (1982).

Chandrasekhar, S, "*An introduction to the study of stellar structure*", Dover Publications, Inc., (1939).

Cheever, E et al, "Depth of penetration of fields from rectangular apertures into lossy materials", Trans. Microwave Theory & Techniques, Vol. 35, No. 9, (1987).

Cole, K. S & Cole, R. H, "Dispersion and absorption in dielectrics: Alternating current characteristics", Journal of Chemical Physics, Vol. 9, (1941).

Cole, K. S et al, "Electrical analogues for tissues", Experimental Neurology, 24, 459-473, (1969).

Collins, A. J & Cosh, J. A, "Temperature and biochemical studies of joint inflammation - A preliminary investigation" Ann. Rheum. Dis., Vol. 29, (1970).

Collins et al, "Quantitation of thermography in arthritis using multi-isothermal analysis I. The thermographic index.", Ann. Rheum. Dis., 113-115, (1974).

Cook, H. F, "The dielectric behaviour of some types of human tissues at microwave frequencies.", Brit. J. Appl. Phys., 2, 295-300, (1951).

Cooke, R & Kuntz, I. D., "The properties of water in biological systems", Annu. Rev. Biophys. Bioeng., 3, 95-126, (1974).

Cooper, R ,"The electrical properties of salt water solutions over the frequency range 1-4000 Mc/s", Journal of Institution of Electrical Engineers, Vol. 93, Part 3, No. 22, (1946).

Corson, D & Lorrain, P, "*Introduction to electromagnetic fields and waves*", W. H. Freeman & Company, (1962).

Cosh, J. A. & Ring, F. J., "Techniques of heat detection used in the assessment of rheumatic diseases", J. Radiol., Electrol., Vol. 48, 84-89, (1967).

Cosh, T. A & Ring, E. F. J, "Thermography and rheumatology", Phys. Med., Vol. 10, 342-348, (1970).

De Silva, M et al, "Assessment of inflammation in the rheumatoid knee joint: correlation between clinical, radioisotopic, and thermographic methods.", Ann. Rheum. Dis., Vol. 45, 277-280, (1986).

Deighton, C., "Rheumatoid arthritis", Med. International, Vol. 22, No. 3, 136-144, (1992).

Devereaux M. D. et al , "Disease activity indexes in rheumatoid arthritis; a prospective, comparative study with thermography", Ann. Rheum. Dis., Vol. 44, 434-437, (1985).

Dick, C. W et al, "Clinical studies on inflammation in human knee joints: Xenon clearances correlated with clinical assessment in various arthritides and studies on the effect of intra-articularly administered hydrocortisone in rheumatoid arthritis", Clinical Science, Vol. 38, (1970).

Dick, W. C & Grennan, D. M., "Radioisotopes in the study of normal and inflammed joints", Clinics in Rheumatic Diseases, Vol. 2, No. 1, April, (1976).

Dick, W. C et al, "Derivation of knee joint synovial perfusion- Using Xenon clearance technique", Ann. Rheum. Dis., Vol. 29, (1970).

Dick, W. C et al, "Indices of inflammatory activity", Ann. Rheum. Dis., Vol. 29, (1970).

Dick, W. C et al, "Isotope studies in normal and diseased knee joints.", Clinical Science, Vol. 40, 327-336, (1971).

Dick, W. C et al, "Measurement of joint inflammation: A radioisotopic method", Ann. Rheum. Dis., Vol. 29, (1970).

Dixon, M & Sainsbury, R, "*Diseases of the breast*", Churchill Livingstone, (1993).

Draper, J. W & Boag, J. W, "Skin temperature distributions over veins and tumours", Phys. Med. Biol., Vol. 16, No. 4, 645-654, (1971).

Draper, J. W & Boag, J. W, "The calculation of skin temperature distributions in thermography", Phys. Med. Biol., Vol. 16, No. 2, 201-211, (1971).

Draper, J. W & Jones, C. H., "Thermal patterns of the female breast", Br. Journal of Radiology, Vol. 42, 401-410, June, (1969).

Duck, F. A., "Ultrasound colour-coded doppler imaging", Journal. of Photographic Science, Vol. 37, 82-83, (1989).

Edeiken, S., "Mammography and palpable cancer of the breast", Cancer, Vol. 61, 263-265, (1988).

Edenhofer, P et al, "Near field characteristics of antenna sensors for microwave thermography: preliminary results of multi-spectral radiometric experiments." in Biomedical Thermology, M. Gautherie & E. Albert (eds), Alan R. Liss, Inc., 523-537, (1982).

Edrich, J & Smyth, C. J., "Arthritis inflammation monitored by subcutaneous millimetre wave thermography", Journal of Rheumatology, Vol. 5, No. 1, (1978).

Edrich, J et al, "Imaging thermograms at centimetre and millimetre wavelengths", Annals of New York Academy of Science, Vol. 335, 456-471, (1980).

Edrich, J., "Centimetre and millimetre wave thermography- A survey on tumour detection", Journal. of Microwave Power, Vol. 14, No. 2, (1979).

Enander, B & Larsen, G., "Microwave radiometric measurements of the temperature inside a body", Electronics Letters, Vol. 22, No. 3, (1986).

Enander, B. & Larsen, G. "Microwave radiometric measurements of the temperature inside a body", Electronics Letters, Vol.10, No. 15, (1974).

Encinar, J. A. & Rebollar, J. M, "Convergence of numerical solutions of open-ended waveguide by modal analysis and hybrid modal-spectral techniques", IEEE Trans. Microwave Theory & Techniques, Vol. 34, No.7, (1986).

Enel, L et al, "Improved recognition of thermal structures by microwave radiometry", Electronics Letters, Vol. 20, No. 7, (1984).

England, T. S., "Dielectric properties of the human body for wavelengths in the 1-10cm range.", Nature, Vol. 166, 480, (1950).

Erb, H. & Kallenberger, A., "The action of an oral high-dosed oestrogen -progestagen combination on the human breast", Acta Endocrinologica, Vol. 70, 143-155, (1972).

Estin, A. J et al, "Absolute measurement of temperatures of microwave noise sources", Miscellaneous Temperature Measurement Methods, 997-1003.

Fallone, B. G et al, "Non-invasive thermometry with a clinical X-ray CT scanner", Med. Phys., 9, 715 -721, (1982).

Feldman, F., "Thermography of the hand and wrist: Practical applications", Hand Clinics, Vol.7, No. 1, (1991).

Forrest, P et al, "Breast cancer screening", Dept. of Health and Social security, (1986).

Foster, K. R & Cheever, E. A, "Microwave radiometry in biomedicine", Bioelectromagnetics, Vol. 13, 567-579, (1992).

Foster, K. R & Schepps, J. L., "Microwave dielectric studies on proteins", Bioelectromagnetics, Vol. 3., 29-43, (1982).

Foster, K. R et al, "Effect of surface cooling and blood flow on the microwave heating of tissue", IEEE Trans Biomedical Eng., Vol. 25, No. 3, (1978).

Fraser, S et al, "Microwave thermography- an index of inflammatory joint disease", British Journal of Rheumatology, Vol. 26, 37-39, (1987).

Fraser, S. M et al, "Microwave thermography in rheumatic disease", Engineering in Medicine, Vol. 16, No. 4, (1987).

Fricke, H, "A mathematical treatment of the electric conductivity and capacity of disperse systems", Phys. Rev., 24, 575, (1924).

Fricke, H., "A mathematical treatment of the electric conductivity and capacity of disperse systems", Phys. Rev., 26, 678, (1925).

Fricke, H., "The complex conductivity of a suspension of stratified particles of spherical or cylindrical form", Journal of Phys. Chem., Vol. 59, 168-170, (1954).

Gautherie, M. et al, "Millimeter-wave thermograpghy - Application to breast cancer", Journal of Microwave Power, Vol. 14, No. 2, (1979).

Gedded, L. A & Baker, L. E, "The specific resistance of biological material- A compendium of data for the biomedical engineer and physiologist", Med. & Biol., Vol. 5, 271-293, (1967).

Ghandi, O. P. et al,."Millimeter wave absorption spectra of biological samples", Bioelectromagnetics, Vol. 1, 285-298, (1980).

Giaux. G et al, "Imagerie thermique micro-onde a 3GHz pour l' exploration des tumeurs du sein", Bulletin Du Cancer, Vol. 75, No. 7, 661, (1988).

Goodman, A. B., "Insensible water loss from human skin as a function of ambient vapor concentration", J. Appl. Physiol., Vol. 26, No. 2, (1969).

Grant, E. H., *"Dielectric properties of biological tissue"*, Biomedical Thermology, 475-484, (1982).

Guillebaud, J, *"The pill"*, 4th edition, Oxford University Press, (1991).

Gustafsson, S. E et al, "Analytical calculation of the skin temperature distribution due to subcutaneous heat production in a spherical heat source", Phys. Med. Biol., Vol. 20, No. 2, 219-224, (1975).

Guy, A. W, "Electromagnetic fields and relative heating patterns due to a rectangular aperture source in direct contact with bilayered biological tissue", IEEE Trans. Microwave Theory & Techniques, Vol. 19, No. 2, (1971).

Haataja, M., "Evaluation of the activity of rheumatoid arthritis.", Scan. J. Rheumatol., 4(suppl), 1-54, (1975).

Haimovici, N, "Three years experience in direct intra-articular temperature measurement" in *Biomedical Thermology*. Gautherie, M & Albert, E (eds.), Allan R Liss, Inc., (1982).

Haller, J, "*Hormonal contraception*", Los Altos, California, (1969).

Hardy, J. D & Du Bois, E. F, "The technic of measuring radiation and convection", J. Nutrition, Vol. 15, No. 5, (1937).

Hasted, J. B, "*Water: A comprehensive treatise Vol. 1*", Francks, F (eds.), Plenum, New York, (1972).

Herrick, J. F. et al, "Dielectric properties of tissues important in microwave diathermy", Fed. Proc., Vol. 9, 60, (1950).

Hill, R. M. & Jonscher, A. K ,"The dielectric behaviour of condensed matter and its many body interpretation", Contemp. Phys., Vol. 24, No. 1,.75-100, (1983).

Hrushesky, W. J. M, "Breast cancer and the menstrual cycle", Journal of Surgical Oncology, Vol. 53, No. 1-3, (1993).

Huskisson, E. C et al, "Measurement of inflammation: comparison of technetium clearance and thermography with standard methods in a clinical trial", Ann. Rheum. Dis., Vol. 32, (1973).

Ilowite, N. T. et al, "Assessment of pain in patients with juvenile rheumatoid arthritis: relation between pain intensity and degree of joint inflammation", Ann. Rheum. Dis., Vol. 51, 343-346, (1992).

Iskander, M. F & Durney, C. H, "Microwave methods of measuring changes in lung water", Journal of Microwave Power, Vol. 18, No. 3, (1983).

Joachimowicz, N et al, "Quantitative microwave tomography for non-invasive control of hyperthermia. Preliminary numerical results", Journal of Photographic Science, Vol. 39, (1991).

Jones, C. H & Dodhia, P., "Microwave radiometry: Heterogeneous phantom studies", Journal of Photographic Science, Vol. 37, (1989).

Jones, C. H., "Interpretation problems in thermography of the female breast", Bibl. Radiol., Vol. 5, 96-108, (1969).

Jones, C. H., "Methods of breast imaging", Phys. Med. Biol., 27, 463-499, (1982).

Kelso , M. B et al, "Recent investigations of combined thermal and microwave modelling of body regions for the interpretation of microwave thermographic images", IEE Colloquium on Application of microwaves in medicine, 8/1-8/6, 28 Feb., (1995).

Khatkhatay, I. et al, "Excretory profile of inhibin-like peptide (ILP) during human menstrual cycle...", Euro. Journal of Obs. Gyn. and Repro. Biology, Vol. 55, 117-121, (1994).

Kraszewski, A et al., "In vivo and In vitro dielectric properties of animal tissues at radio frequencies", Bioelectromagnetics, 3, 421-432, (1982).

Kraus, J. D, "*Radio astronomy*", McGraw-Hill Book Company, (1966).

Land, D. V & Campbell, A. M, "A quick accurate method for measuring the microwave dielectric properties of small tissue samples", Phys. Med. Biol., Vol. 37, No. 1, (1992).

Land, D. V, "A clinical microwave thermography system", Proc. IEE, Vol. 134, No. 2, (1987).

Land, D. V. et al, "Clinical testing of combined thermal and microwave radiometric tissue modelling", The Journal of Photographic Science, Vol. 39, (1991).

Land, D. V., "Microwave thermography- A new medical technique?", Proc. R.P.S, No. 6, (1987).

Land, D. V., "Radiometer receivers for microwave thermography", Microwave Journal, Tech. Feature, 196-201, May, (1983).

Land, D. V., "The generation of the microwave thermographic image", Journal of Photographic Science, Vol. 37, (1989).

Land, D.V., "Application of the non-resonant perturbation technique to the measurement of high frequency fields in biological phantom materials", Electronics Letters, 70-71, (1988).

Lapayowker, M. S et al, "Criteria for obtaining and interpreting breast thermograms", Cancer, Vol. 38, 1931-1935, (1976).

Larsen, L. E. & Jacobi, J. H., "Medical applications of microwave imaging", IEEE Press, Inc. New York, (1986).

Levine, H. & Papas, C. H, "Theory of circular diffraction antenna", Journal of Applied Physics, Vol. 22, No. 1, (1951).

Linnander, B., "When it's toohot to use infra-red thermography", IEEE Circuits and Devices Mag., Vol. 9, No. 4, (1993).

Love, T. J., "Thermography as an indicator of blood perfusion", Annals New York Acad. Science, 429-433, (1980).

Ludeke, L. M et al, "Radiation balance microwave thermograph for industrial and medical applications", Electronics Letters,, Vol. 14, No. 6, (1978).

MacDonald, A. G et al, "Microwave thermography as a non-invasive assessment of disease activity in inflammatory arthritis", Clinical Rheumatology, Vol. 13, No. 4, 589-592, (1994).

Macphie, R. H & Zaghloul, A. I , "Radiation from a rectangular waveguide with infinite flange- Exact solution by the correlation matrix method", IEEE Trans. on Antennas and Propogation, Vol. AP-28, No. 4, (1980).

Mahmoud, S. F & Beal, J. C, "Scattering of surface waves at a dielectric discontinuity on a planar waveguide", IEEE Trans. Microwave Theory & Techniques, Vol. 23, No. 2, (1975).

Makiniac, J. W., "Arterial blood supply of the breast", Arch. Surg., Vol. 47, 329-343, (1943).

Mamouni, A., "Radiometrie microonde en champ proche:Applications medicales (Thermographie Microonde)", These pour le titre de Docteur es-sciences physiques, (1988).

Mamouni, A et al, "Computation of near-field microwave radiometric signals: Definition and experimental verification", IEEE Trans. Microwave Theory & Techniques, Vol. 39, No. 1, (1991).

Mamouni, A et al, "Computation of three-dimensional radiometric signals detected in microwave imaging", Journal of Photographic Science, Vol. 39, (1991).

Mamouni, A et al, "Introduction to correlation microwave thermography", Journal of Microwave Power, Vol. 18, No. 3, (1983).

Marchant, D. J & Nyrirjesy, I (editors), "*Breast disease*", Grune & Stratton, (1978).

Marcuse, D , "Radiation losses of tapered dielectric slab waveguides", Bell System, Technical Journal, 273-290, (1970).

Marino, A. A et al, "Dielectric determination of bound water of bone", Phys. Med. Biol., Vol. 12, No. 3, 367-378, (1967).

Marr, C. M., "Microwave thermography: A non-invasive technique for investigation of injury of the superficial digital flexor tendon in the horse", Equine Veterinary Journal, Vol. 24, No. 4, 269-273, (1992).

McAdams, W. H., "*Heat transmission*", McGraw-Hill Book Company, Inc., (1933).

McKirdy, M. J et al, "Microwave thermography in the diagnosis of breast disease", Proc. of The British Institute of Radiology, 726, (Aug., 1988).

McPherson, A (editor), "*Women's problems in general practice*", Oxford University Press, (1988).

Mimi, M & Land, D. V., "Nonresonant perturbation measurement of antenna electromagnetic field configurations for biomedical applications", Journal of Photographic Science, Vol. 39, 161-163, (1991).

Mimi, M., "An investigation of radiometer and antenna properties for microwave thermograpgy", PhD thesis, (1990).

Mitchell, D. et al, "Radiant and convective heat transfer of nude men in dry air", J. Appl. Physiol., Vol. 26, No. 1, (1969).

Mitchell, D. et al, "Measurement of the total normal emissivity of skin without the need for measuring skin temperature", Phys. Med. Biol., 12, 359-366, (1967).

Mitchell, G. W & Basset, L. W (editors), "*The female breast and its disorders*", Williams & Wilkins, (1990).

Monsees, B., "Thermography, Transmulliation Light Scanning, and Magnetic Resonance Imaging", The Female Breast and Its Disorders, Mitchell, G.W. & Basset, L. W, (eds), (1990).

Nguyen, D. D et al, "Microwave thermography-the modelling of probes and approach towards thermal pattern recognition..", Proc. 10th European Microwave Conference, Warsaw, (1980).

Onsager, L., "Electric moments in liquids", J. Am. Chem. Soc., 58, (1936).

Osman, M. M & Afify, E. M., "Thermal modelling of the normal woman's breast", Journal of Biochemical Engineering, Vol. 106, (1984).

Parry, C. E et al, "Breast thermograms in ovulatory and anovulatory menstrual cycles", British Journal of Radiology, Vol. 45, 507-509, (1972).

Paterson, J et al, "Assessment of rheumatoid inflammation in the knee joint", Ann. Rheum. Dis., Vol. 37, 48-52, (1978).

Pawsey, J. L & Bracewell, R. N, "*Radio astronomy*", Oxford, Clarendon Press, (1955).

Pennes, H. H, "Analysis of tissue and arterial blood temperatures in the resting human forearm", J. Appl. Physiol., Vol. 1, No. 2, (1948).

Pethig, R & Kell, D. B., "The passive electrical properties of biological systems: their significance in physiology, biophysics and biotechnology", Phys. Med. Biol., Vol. 32, No. 8, 933-970, (1987).

Pethig, R , "Dielectric properties of biomedical materials: Biophysical and medical applications", IEEE Trans. Electrical Insulation, Vol. E1-19, No. 5, (1984).

Pethig, R., "Dielectric properties of body tissues", Clin. Phys. Physiol. Meas., Vol. 8, Suppl. A., 5-12, (1987)

Pichot, C et al, "Active microwave imaging of inhomogeneous bodies", IEEE Trans on Antennas and Propogation, Vol. 33, No. 4, (1985).

Pinals, R. S., "Miscellaneous methods for assessment of articular disease", Clinics Rheum. Dis., 9, 559-570, (1983).

Porter, B. B et al, "Synovial perfusion of clinically normal knee joints in patients with rheumatoid arthritis: An isotope study", Ann. Rheum. Dis., Vol. 29, (1970).

Porter, D. R & Sturrock, R. D, "Medical management of rheumatoid arthritis", B. M. J., Vol. 307, (1993).

Ramo, S & Whinnery, J, R, "*Fields and waves in modern radio*", 2nd edition, John Wiley and Sons, Inc., (1945).

Ring, E. F. J., "Quantitative thermography in arthritis using the AGA integrator", Arthritis and Rheumatism Council Research Group, 172-176.

Ring, E. F. J., "Thermography in rheumatology", Thermology, Vol. 1, 149-153, (1986).

Roberts, J. E & Cook, H. F, "Microwaves in medical and biological research", Brit. J. Appl. Phys., Vol. 3, 33-40, (1952).

Robillard, M. et al, "Microwave thermography - Characteristics of waveguide applicators and signatures of thermal structures", Journal of Microwave Power, Vol. 17, No. 2, (1982).

Rogers, J.A. et al, "The dielectric properties of normal and tumour mouse tissue between 50Mhz and 10Ghz", The British Journal of Radiology, 56, 335-338, (1983).

Rohlfs, K, "*Tools of radio astronomy*", Springer-Verlag, (1986).

Romanes, G. J (editor), "*Cunningham's manual of practical anatomy, volume 1, upper and lower limbs*", Oxford Medical Press, (1972).

Rubin. C. S et al, "Ultrasonic examination of the breast", Breast Disease, Marchant, D.J & Nyirjesy, (eds), (1979).

Rybicki, G. B & Lightman. A. P., "*Radiative processes in astrophysics*", John Wiley & sons, (1979).

Salisbury, R. S et al, "Heat distribution over normal and abnormal joints: Thermal pattern and quantification, Ann. Rheum. Dis., Vol. 42, 494-499, (1983).

Schepps, J. L & Foster, K. R.,"The UHF and microwave dielectric properties of normal and tumour Tissues: variation in dielectric properties with tissue water content", Phys. Med. Biol., Vol. 25, No,6, 1149-1159, (1980).

Schwan, H. P & Foster, K. R, "Microwave dielectric properties of tissue:·some comments on the rotational mobility of tissue water", Biophysical Journal, Vol. 17, (1977).

Schwan, H. P., "Electrical properties of tissue and cell suspensions", Adv. Biol. Med. Phys., 5, 147-209, (1957).

Schwan, H.P & Li, K, "Capacity and conductivity of body tissues at ultrahigh frequencies", Proc. IRE, 41, 1735-1740, (1953).

Senie, R. T et al, "Timing of breast cancer exision during the menstrual cycle influences duration of disease free survival", Annals. Internal Med., Vol. 115, No. 5, (1991).

Shitzer, A & Eberhart, R. C (editors), "Heat transfer in medicine and biology", Plenum Press, New York & London, (1985).

Slater, J. C , "*Microwave transmission*", 1st edition, McGraw-Hill, Inc., (1942).

Smyth, C. M et al, "Influence of the menstrual cycle on the concentrations of estrogen and progesterone receptors in primary breast cancer biopsies", British Cancer Research & Treatment, Vol. 11, 45-50, (1988).

Solsona, F., "The history of thermography", Acta Thermographica, Vol. 3, 83-85, (1978).

Spells, K. E, "The thermal conductivities of some biological fluids", Phys. Med. Biol., Vol. 5, 139-153, (1960).

Spencer, F , "*Introduction to human and molecular biology*", Butterworth & Co., (1970).

Spratt, J. S et al, "Breast cancer detection demonstration project data can determine whether the prognosis of breast cancer is affected by the time of surgery during the menstrual cycle", Journal of Surgical oncology, Vol. 53, No. 4-9, (1993).

Sterns, E. E & Zee, B., "Thermography as a predictor of prognosis in cancer of the breast", Cancer, Vol. 67, 1678-1680, (1991).

Stuchly, M. A, "Applications of time-varying magnetic fields in medicine", Critical Reviews in Biomedical Engineering, 18, 89-124, (1990).

Surowiec, A et al, "In vitro dielectric properties of human tissues at radiofrequencies", Phys. Med. Biol.,Vol. 32, No. 5, 615-621, (1987).

Teodoridis, V et al, "The reflection from an open-ended rectangular waveguide terminated by a layered dielectric medium", IEEE Trans. Microwave Theory & Techniques, Vol. 33, No. 5, (1985).

Valvano, J. W et al., "The simultaneous measurement of thermal conductivity, thermal diffusivity, and perfusion in small volumes of tissue", Trans. of the ASME, Vol. 106, (1994).

Vermey, G. F, "The simulation of skin temperature distributions by means of a relaxation method", Phys. Med. Biol., Vol.20, No. 3, 384-394, (1975).

Verzini, L et al, "Thermographic variations in the breast during the menstrual cycle", Acta Thermographica, Pt. 2, Vol. 3, 143-149, (1977).

Williams, L. W., "Thermography in breast cancer", Proc. British Institute of Radiology,Jan.,(1969).

APPENDIX B

B1

Experimental measurement of microwave and infra-red temperature data.

All temperature measurements were made in still-air environments at ambient temperatures of 19-23C, with the exception of some of the hand measurements (see conditions noted and discussed in Chapter 6, section 6.8). The environment was not temperature controlled, but typically changed by less than 0.5C over the scanning time for a subject. The area of the subject to be scanned was unclothed, the rest of the body was lightly clothed. For breast and knee scans the measurements were made with the subject lying still and comfortably on an examination couch with the head and torso raised at approximately 30° on a pillowed support. For the hand scans the subject sat still and comfortably at a small table with the hands resting on the table (see Chapter 6, section 6.8.1 for special scanning precautions for this case). The subject was in the scanning position for 10-15minutes prior to scanning.

The infra-red surface temperature measurements were made first using a commercial pyroelectric element hand-held infra-red thermometer. The scanning procedure being identical to the microwave measurements.

Microwave scanning was performed by holding the antenna (shown in Fig 4.3) in contact with the skin and moving it smoothly in a straight line at a rate of 1cm/2.5secs. The antenna is therefore only in contact with a particular area of the skin for at the most 5sec, thus avoiding significant disturbance of the tissue thermal pattern.

The above scanning procedures were standard throughout this period of research.

B2

Regulation of temperature within the body

The constancy of body temperature implies that a balance must be maintained between the metabolic heat generated in the body and the heat

lost to the environment. This is achieved mainly by controlling heat loss from the skin surface.

The principle method of physiological control of heat loss in comfortable temperatures is the regulation of the blood flow to the skin which may be made by vasodilation or vasoconstriction in order to increase or decrease the skin temperature and so increase and decrease heat loss.

In a very warm environment heatloss is increased by sweating and/or panting. Erection of hair on the surface of skin decreases the heatloss at the surface in a cold environment. At very low temperatures shivering can be used to increase heat production.

The measurement conditions given in B1 are chosen so as to avoid the need for the body to be adjusting its heat loss to accommodate any significant changes in environment.

B3

Patient selection

The subjects used in the hand study (Chapter 6, section 6.7) were outpatients attending a rheumatoid arthritis clinic at Glasgow Royal Infirmary. All outpatients were selected by the clinical staff and had a long-standing history of rheumatoid arthritis. Disease duration varied from approximately 3 to greater than 25 years.

No other selection criteria was applied.

B4

Statistical analysis of Figs. 7.16A, 7.18A, 7.20A, 7.22A & 7.26A.

The student t-test was used to determine whether the variation between phases of the menstrual cycle shown on the estimated blood perfusion and water content graphs given in Chapter 7 were significant. With reference to the above mentioned graphs and the results of the t-tests shown on the

graphs, it is reasonable to suggest that the phase variations observed are statistically significant.

B5

Do ambient temperature and posture changes have any affect on the microwave temperature?

During research into the use of microwave thermography for assessments in rheumatology Fraser, S and Land, D.V carried out an investigation into the effect of ambient temperature on the measured microwave temperature. They concluded that a change of ambient temperature was found to have negligible effect on the measured microwave temperature patterns. As the measurement conditions were very similar to the conditions throughout this research, the effect of limited ambient temperature change on the microwave temperature pattern relation was not considered to be an important factor.

al-Alousi et al, 1994 (discussed in Chapter 1, pge 13) also noted that "changes in the temperature of the environment had no significant effect on the readings of the probes.". They were considering the effect of ambient temperature on the equipment readings i.e. the ambient temperature does not affect the radiometer calibration. This is further evidence to suggest that the effect of ambient temperature is not significant to the research carried out in this thesis.

The effect of posture changes is not relevant, since posture was not changed during the investigations considered here. In general, however, posture changes may cause tissue perfusion changes and small changes to the surface heatloss coefficient.

B6

Reproducibility of Quadriceps/Patella scans

Figs 6.1A & 6.1B show that both the microwave and infra-red temperature scans for two 'normal' subjects. Fig 6.1A scans were taken 1 week apart; Fig 6.1B scans being taken 3 months apart. Normal subjects were chosen as they provide stable data i.e. there is no disease variation on the data. As the difference between microwave and surface temperatures is the particularly important quality for these studies, it is the variability of the difference that is most important to consider. Referring to Figs 6.1A & 6.1B it is seen that the form of the temperature scans remain very similar, as do the temperature differences, $(T_{MW} - T_{SUR})$. To confirm that there is no significant statistical difference between scans the difference between means for both subjects scans were considered. With reference to Figs 6.1A, it was calculated that the probability of the differences over the quadriceps/patella scans taken 1 week apart being similar was $0.50>P>0.317$ similarly, the probability that the scans taken 3 months apart shown in Fig 6.1B was calculated to be $0.317>P>0.10$. This suggests that it is unlikely that the two scans are significantly different. This result suggests that the reproducibility of observations is excellent.

B7

Calculated error values

The calculated errors in the water content and effective perfusion graphs shown in Chapter 7 are as follows:

% error in water content : 19%

% error in perfusion : 13%

It should be noted that these would be the typical errors for all the measurements made.